

Departament d'Enginyeria Tèxtil i Paperera



**UNIVERSITAT POLITÈCNICA
DE CATALUNYA**
BARCELONATECH

**TREATMENT OF TEXTILE SURFACES BY PLASMA
TECHNOLOGY FOR BIOMEDICAL APPLICATIONS**

Cédric Labay

May 2014

PhD. Thesis

Directors: Dra. C. Canal Barnils

Dr. J. M^a Canal Arias

ACKNOWLEDGMENTS

My first and sincere appreciation goes to my thesis supervisors. I would like to express my heartfelt gratitude to **Dra. Cristina Canal Barnils** and **Dr. José Maria Canal Arias** for taking a chance on me and giving me the opportunity to enable this PhD., as well as for their guidance, encouragement, patience and support in all stages of my doctoral thesis. I also express them my deepest gratitude to facilitate the access to fellowships, the participation in conferences, abroad research stage accommodation and to patiently correcting my writing.

Moreover, I would like to express additional thanks to **Dr. Antonio Navarro** for enabling the access to his laboratory, allowing me the use of some equipment useful to perform the experimental part and also for his advice.

Also, I would like to thank the rest of the **SPPT group of the Technical University of Catalonia, UPC**, in particular to **Sra. Cristina Rodriguez** and **Sr. Gabriel Caballero** for giving me a lot of suggestions on my research.

I would like to express my very great appreciation to **Uroš Cvelbar** for receiving me in his research group of the **Jožef Stefan Institute** (Ljubljana, Slovenia), offering me access to pointer equipments that allowed to make significant progress in my thesis, and also for his valuable and constructive suggestions during my research stage. I would also like to extend my thanks to the technicians, PhD. students and the staff of the laboratory, especially to **Martina Modic**, **Tatiana Filipič**, **Nina Recek** and **Gregor Filipič** for their help in offering me the resources in running my investigation.

Advice and assistance provided at the beginning of my thesis by **Alejandro Patiño** were greatly appreciated. I am grateful to **Mercedes Escusa** for running the scanning electron microscopy and her help in the interpretation of the results. I would also like to thank Mr. **Jordi Lloveras** for the technical information, production and supply of the polyamide knitted fabric.

I am particularly grateful to the **Biomaterials, Biomechanics and Tissue Engineering Group** of the Materials Science and Metallurgy Dept. of the Polytechnical University of Catalonia, UPC, and **Prof. F. Javier Gil Mur** and **Prof. M^a Pau Ginebra Molins** for providing me the access to the laboratory installation and equipments that allow me to go deeper in my researches.

I would also like to thank **Prof. María Antonia Arbós Via** and **Prof. María Teresa Quiles Pérez**, and their research group of **General Surgery of the Research Institute of the Vall d'Hebron (VHIR)** for performing the biological studies on the plasma-treated surgical meshes.

Financial support by the **Spanish Ministry of Science and Innovation** through the MAT2010-12022-E project and the CTQ 2008-06892-C03-02/PPQ project is also acknowledged.

I wish to thank **my parents**, for their constant support, encouragement and help throughout my studies. I am also very much indebted to **my family**, who always supported me in every possible way, although I have not been very present and I could not see them as much as I wanted during these recent years to undertake my studies aboard.

I would like to offer my special thanks to my supportive friends. I want to thank those who, besides friendship, gave me in some moment scientific support or advice, like **Iñigo Martin, Aurora Dols, Josep Rebled, Ferran Roig, David Pastorino, Aurélie Josselin** as well as those who have no direct connection with my thesis but who helped me to make good advances and to progress in the best way, or just who have been supporting me since I was a young boy, such as **Béatrice, Céline, Christine, Frédéric, Pierre**.

Finally, I am concerned that I might forget to mention someone and, because the list of people to whom I am grateful is literally too long to be fully inclusive, I also extend my sincerest gratitude to those not expressly mentioned here.

For any errors, mistakes, omissions and other shortcomings I could have made in this work, of course, the responsibility is entirely of my own.

"Knowledge is in the end based on acknowledgement." - Ludwig Wittgenstein

AGRADECIMIENTOS

Mi primer y sincero agradecimiento va dirigido a mis directores de tesis. Me gustaría expresar mi más sincero agradecimiento a la **Dra. Cristina Canal Barnils** y al **Dr. José María Canal Arias** por confiar en mí y darme la oportunidad de cursar esta tesis doctoral, así como por su guía, ánimo, paciencia y apoyo en todas las etapas de esta tesis. También quiero expresar mi más profunda gratitud por facilitarme el acceso a becas, a la participación en conferencias, a las estancias de investigación en el extranjero y por corregir pacientemente mi escritura.

Por otra parte, me gustaría dar las gracias al **Dr. Antonio Navarro** por permitir el acceso a su laboratorio, y permitirme el uso de algunos equipos importantes para llevar a cabo la parte experimental de esta investigación, así como por sus consejos.

Además, me gustaría dar las gracias al resto del grupo SPPT de la Universidad Politécnica de Cataluña, UPC, en particular, a la **Sra. Cristina Rodríguez** y el **Sr. Gabriel Caballero** por sus sugerencias que ayudaron en el desarrollo de mi investigación.

Me gustaría expresar mi gran agradecimiento al **Dr. Uroš Cvelbar** por recibirme en su grupo de investigación del Instituto Stefan Jožef (Ljubljana, Eslovenia), ofreciéndome el acceso a equipos punteros que permitieron hacer progresos significativos en mi tesis, y también por sus valiosos y constructivos consejos durante mi etapa de investigación. Me gustaría expresar también mi agradecimiento a los técnicos, los doctorandos y al personal del laboratorio, especialmente a **Martina Modic, Tatiana Filipič, Nina Recek** y **Gregor Filipič** por su ayuda y por ofrecerme los recursos en la gestión de mi investigación.

El asesoramiento y la asistencia en el inicio de mi tesis por parte de **Alejandro Patiño** fueron de agradecer. Por igual, estoy muy agradecido a **Mercedes Escusa** por su

experto trabajo en microscopía electrónica de barrido y su ayuda en la interpretación de los resultados. También me gustaría dar las gracias al **Sr. Jordi Lloveras** por la información técnica, la producción y el suministro del tejido de punto de poliamida.

Estoy especialmente agradecido al **Grupo de Biomateriales, Biomecánica e Ingeniería de Tejidos** del Departamento de Ciencia de los Materiales e Ingeniería Metalúrgica de la Universidad Politécnica de Cataluña, UPC, y a sus responsables el **Prof. F. Javier Gil Mur** y la **Prof^a. M^a Pau Ginebra Molins** por darme el acceso a las excelentes instalaciones de laboratorios y equipos que permitieron que pudiera ir más profundo en mi investigación.

Me gustaría también agradecer a la **Prof^a. María Antonia Arbós Vía** y a la **Prof^a. María Teresa Quiles Pérez**, y a su grupo de investigación de **Cirugía General del Instituto de Recerca del Vall d'Hebron (VHIR)** para llevar a cabo el estudio sobre la adhesión celular de las mallas cirugías.

También se agradece el apoyo financiero del **Ministerio Español de Ciencia e Innovación** a través del proyecto MAT2010-12022-E y del proyecto CTQ 2008-06892-C03-02/PPQ.

Quiero dar las gracias a **mis padres**, por su constante apoyo, ánimo y ayuda a lo largo de mis estudios. Estoy agradecido también a **mi familia**, que siempre me ha apoyado en todo lo posible, aunque no he estado muy presente y no pude verlos tanto como yo quería en estos últimos años por llevar a cabo mis estudios en el extranjero.

Me gustaría ofrecer mi agradecimiento especial a algunos de mis amigos que me han ido apoyando a lo largo de los años. Quiero dar las gracias a los que, además de la amistad, me dieron en algún momento algo de consejo científico, de asesoramiento o de ayuda, como **Iñigo Martín, Aurora Dols, Josep Rebled, Ferran Roig, David**

Pastorino, Aurélie Josselin, así como aquellos que no tienen conexión directa con mi tesis pero que me ayudaron en su momento a hacer buenos progresos, o simplemente aquellos que me han estado apoyando desde niño, como **Béatrice, Céline, Christine, Frédéric, Pierre**.

Por último, me preocupa que me pueda olvidar de mencionar a alguien y, debido a que la lista de personas a las que estoy agradecido sería muy larga para estar totalmente completa, quiero expresar también mi más sincero agradecimiento a los no están mencionados expresamente aquí.

Para los errores, las equivocaciones, las omisiones y otras deficiencias que han podido y pueden suceder en este trabajo de tesis, por supuesto, la responsabilidad es enteramente mía.

"El conocimiento está al final basado en el reconocimiento." - Ludwig Wittgenstein

ABSTRACT

Medical applications of technical textiles are an expanding field of research. One of the added values of these new materials would be that they were suitable to contain and release pharmaceutical and cosmetic active compounds in a controlled and sustained manner.

Drug incorporation and release from synthetic fibers is related to the interaction of the drug with the polymer and greatly depends on the surface chemistry of the fiber. Plasma technology is a tool that enables to modify physical and chemical properties of the first nanometers of the surface of the fibres without affecting the bulk of the material. Applied to the medical textile field, plasma treatment of polymer fibres could lead to the design of new textile-based drug delivery systems.

The novelty of this PhD. Thesis rests upon the modification of the drug/fiber interactions by plasma treatment to allow the modulation of the loading and the release of active principles (pharmaceutics and cosmetics) from the textile-based drug delivery systems, without requiring the use of any further chemicals.

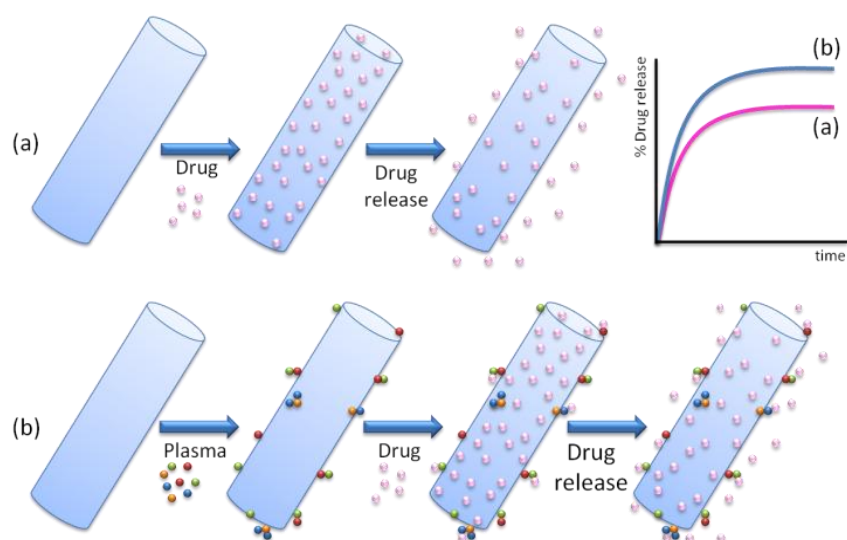


Figure 1: Proposed modulation of the drug release kinetics from synthetic fibers to an isotonic media using plasma treatment to modify chemical and topographical properties of the fibre surface previous to loading of active principles in the fibres.

This PhD. Thesis aims at the development of two families of textile-based drug delivery systems, based on a novel surface functionalization by plasma treatment, with suitable characteristics for topical use as medical devices, or for clinical application in soft tissue repair. It is therefore organized in two distinct parts.

In both parts of this thesis a general scheme has been followed: we have investigated the surface modification of textile materials with different types of plasmas (atmospheric and low pressure plasma), characterizing the surface modifications achieved by different complementary techniques. The effects of the plasma treatment have been evaluated on the subsequent incorporation of active pharmaceuticals or cosmetics. In the last step, the drug release has been studied by “in-vitro” dissolution assays.

The first part is focused on medical textiles for topical application. Therein, the surface modification of polyamide 66 elastic-compressive knitted fabrics has been studied by corona plasma and low pressure plasma. The experimental work has studied in parallel laboratory prepared fabrics and industrially finished fabrics, with views on the potential implementation of the proposed process in the textile industrial chain. Plasma treatment improved the release kinetics of anti-inflammatory pharmaceutical (ketoprofen) and of lipolytic cosmetic (caffeine) active principles, loaded in the plasma-treated polyamide 66 fabrics. A fundamental study comparing three different molecules of the same chemical family (caffeine, theobromine and pentoxifylline) has been performed measuring their loading to the textile material and the subsequent release of the drugs.

The second part focuses on textiles used as implants for soft tissue repair (e.g. hernia). The fiber surface of a polypropylene mesh, clinically approved for surgical use, has been modified by corona plasma and low-pressure plasma. The treatments evaluated had a major effect on the loading of antibiotic (ampicillin), presenting an important increase of the active principle loaded. Release kinetics of the ampicillin from the polypropylene meshes to an isotonic liquid media was very fast. The effect of coating the ampicillin-loaded polypropylene meshes by plasma polymerization with a biocompatible polymer was also investigated.

RESUMEN

Las aplicaciones médicas de los textiles técnicos son un campo de investigación en expansión. Uno de los valores añadidos de estos nuevos materiales puede ser su capacidad para contener y liberar principios activos farmacéuticos y cosméticos de una forma controlada y sostenida.

La incorporación de fármacos y su liberación a partir de fibras sintéticas está relacionada con la interacción del fármaco con el polímero y puede depender en gran medida de la química de superficie de la fibra. La tecnología de plasma es una herramienta que permite modificar las propiedades físicas y químicas de los primeros nanómetros de la superficie de las fibras sin afectar el interior del material. Aplicado al campo de los textiles médicos, el tratamiento con plasma de fibras poliméricas podría conducir al diseño de nuevos sistemas de liberación de fármacos basados en soportes textiles.

La novedad de esta Tesis Doctoral se basa en la modificación de las interacciones fármaco / fibra por tratamiento de plasma para permitir la modulación de la incorporación y la liberación de los principios activos (farmacéuticos y cosméticos) a partir de sistemas de administración de fármacos basados en material textil, sin requerir el uso de productos químicos adicionales.

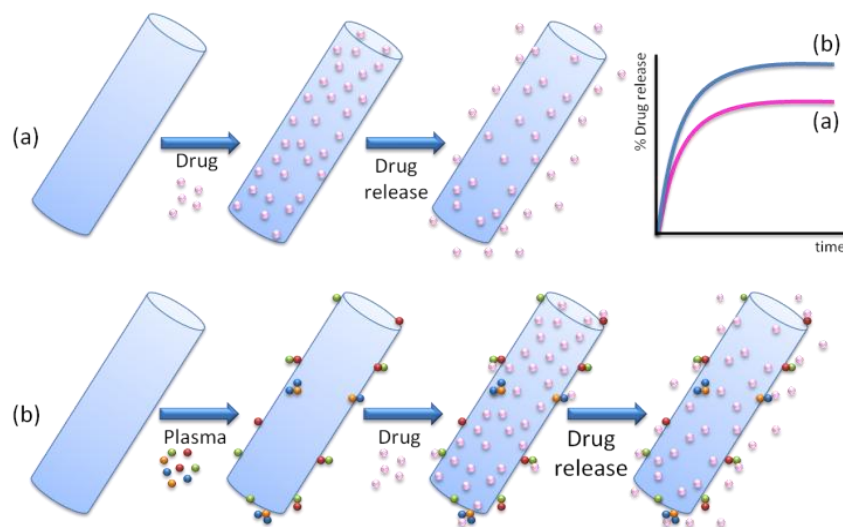


Figura 1: Propuesta de modulación de la cinética de liberación del fármaco a partir de fibras sintéticas a un medio isotónico usando tratamiento de plasma para modificar las propiedades químicas y topográficas de la superficie de la fibra antes de la incorporación del principio activo a la fibra.

Esta Tesis tiene como objetivo el desarrollo de dos familias de sistemas de liberación de fármacos basados en soportes textiles, por funcionalización de la superficie mediante tratamiento de plasma, con características adecuadas bien para uso tópico como dispositivos médicos, bien para aplicación clínica en la reparación de tejidos blandos. Por tanto, esta Tesis se organiza en dos partes bien diferenciadas.

En ambas partes de esta Tesis se ha seguido el siguiente esquema general: en primer lugar se ha investigado primero la modificación superficial de los materiales textiles con diferentes tipos de plasmas (plasma corona y plasma de presión atmosférica), caracterizando las modificaciones de la superficie obtenidas mediante diferentes técnicas instrumentales. Los efectos del tratamiento con plasma se han evaluado entonces sobre la incorporación de principios activos farmacéuticos o cosméticos. En el último paso, se ha estudiado la liberación del fármaco mediante ensayos de disolución "*in vitro*".

La primera parte de la Tesis Doctoral se centra en los textiles médicos para aplicación tópica. Para ello, se ha estudiado la modificación de la superficie de tejidos de punto elástico-compresivos de poliamida 66 con plasma corona y plasma de baja presión. En este trabajo experimental se han estudiado en paralelo tejidos preparados en laboratorio y tejidos industrialmente acabados, con vistas a la posible implementación del proceso propuesto en la cadena de producción industrial textil. Se ha observado que el tratamiento con plasma mejora la cinética de liberación de un fármaco antiinflamatorio (ketoprofeno) y de un principio activo cosmético lipolítico (cafeína), incorporados en los tejidos de poliamida 66 tratados con plasma. Se ha desarrollado un estudio fundamental comparando tres moléculas diferentes de la misma familia química (cafeína, teobromina y pentoxifilina) con respecto a la incorporación al material textil y a la liberación del principio activo.

La segunda parte se centra en los textiles utilizados como implantes para la reparación de tejidos blandos (por ejemplo, hernias abdominales). La superficie de la fibra de una malla de polipropileno aprobada para su uso clínico ha sido modificada por el plasma

corona y plasma de baja presión. Los tratamientos estudiados tuvieron un efecto importante sobre la carga de un antibiótico (ampicilina) mostrando un importante incremento del porcentaje de impregnación. La cinética de liberación in vitro del antibiótico de la malla de polipropileno a un medio líquido isotónico fue rápida. También se investigó la posibilidad de realizar un recubrimiento de la malla de polipropileno cargada con ampicilina mediante polimerización por plasma con un polímero biocompatible.

TABLE OF CONTENTS

1. INTRODUCTION	24
1.1. TECHNICAL TEXTILES	24
1.1.1. <i>Medical textiles</i>	25
1.1.2. <i>Cosmetotextiles</i>	27
1.1.3. <i>Textile materials for drug delivery systems</i>	31
1.1.3.1. <i>Non-implantable textile materials for topical and transdermal applications</i>	32
1.1.3.1.1. <i>Textile materials for non-implantable medical textiles</i>	34
1.1.3.1.2. <i>The skin: natural barrier for drug delivery</i>	36
1.1.3.1.3. <i>Considerations to take into account in the selection of drugs for topical applications</i>	40
1.1.3.2. <i>Implantable medical textiles</i>	42
1.1.3.2.1. <i>Hernia repair</i>	43
1.1.3.2.2. <i>Abdominal meshes and prosthetic devices</i>	46
1.2. CHEMICAL FIBERS OF SYNTHETIC POLYMER	52
1.2.1. <i>Polyamide</i>	52
1.2.1.1. <i>Structure and classification</i>	52
1.2.1.2. <i>Physical and chemical properties</i>	54
1.2.1.3. <i>Applications</i>	54
1.2.2. <i>Polypropylene</i>	54
1.2.2.1. <i>Structure and classification</i>	54
1.2.2.2. <i>Physical and chemical properties</i>	55
1.2.2.3. <i>Applications</i>	55
1.3. COSMETIC AND PHARMACEUTICAL ACTIVE PRINCIPLES	56
1.3.1. <i>Anti-inflammatory active principles for topical applications</i>	56
1.3.2. <i>Anti-lipidic active principles for topical cosmetic applications</i>	58
1.3.3. <i>Antibiotic-loaded fibres for implantable textiles</i>	62
1.4. MODIFICATION OF TEXTILE MATERIALS BY PLASMA TREATMENT	64
1.4.1. <i>Plasma definition</i>	65
1.4.2. <i>Plasma in nature and laboratory devices</i>	65
1.4.3. <i>Plasma reactors in research and at industrial level: Cold plasmas</i>	67
1.4.3.1. <i>Low-pressure plasmas</i>	68
1.4.3.2. <i>Atmospheric pressure plasmas</i>	69

1.4.4.	<i>Plasma applied to polymeric surfaces and fibers</i>	70
1.4.4.1.	<i>Etching and surface cleaning</i>	73
1.4.4.2.	<i>Surface activation</i>	74
1.4.4.3.	<i>Functionalization reactions</i>	75
1.4.4.4.	<i>Plasma polymerization</i>	78
1.4.4.5.	<i>Thin film deposition</i>	79
1.4.5.	<i>Plasma treatments in the textile field</i>	80
2.	MOTIVATION, OBJECTIVES AND STRUCTURE OF THE THESIS	106
2.1.	MOTIVATION	106
2.2.	PURPOSE OF THE INVESTIGATION	107
2.3.	MAIN OBJECTIVES	108
2.4.	STAGES TO REACH THE OBJECTIVES	110
2.5.	STRUCTURE OF THE THESIS	111
3.	EXPERIMENTAL PART	116
3.1.	MATERIAL	116
3.1.1.	<i>Textiles and polymer films</i>	116
3.1.2.	<i>Active principles</i>	117
3.1.2.1.	<i>Ketoprofen</i>	117
3.1.2.2.	<i>Metylxantines</i>	118
3.1.2.2.1.	<i>Caffeine</i>	118
3.1.2.2.2.	<i>Pentoxifylline</i>	119
3.1.2.2.3.	<i>Theobromine</i>	120
3.1.2.3.	<i>Ampicillin</i>	120
3.1.3.	<i>Chemicals</i>	121
3.2.	EXPERIMENTAL STRATEGIES	123
3.3.	METHODS AND TECHNIQUES	124

3.3.1.	<i>Washing processes of the fabrics</i>	124
3.3.2.	<i>Plasma treatments</i>	125
3.3.2.1.	<i>Corona plasma treatment</i>	125
3.3.2.2.	<i>Low pressure plasma treatment</i>	126
3.3.2.3.	<i>Low pressure pulsed-plasma polymerization</i>	128
3.3.3.	<i>Loading process of active principles into textile materials</i>	130
3.3.3.1.	<i>Polyamide fabric impregnation</i>	131
3.3.3.1.1.	<i>Ketoprofen loading of PA66 knitted fabrics</i>	131
3.3.3.1.2.	<i>Caffeine and methylxantines loading of PA66 knitted fabrics</i>	131
3.3.3.2.	<i>Polypropylene fabric impregnation</i>	132
3.3.4.	<i>In-vitro release assays</i>	133
3.3.5.	<i>Physical characterization techniques</i>	137
3.3.5.1.	<i>Scanning Electron Microscopy (SEM)</i>	137
3.3.5.2.	<i>Atomic Force Microscopy (AFM)</i>	139
3.3.5.3.	<i>X-ray Photoelectron Spectroscopy (XPS)</i>	141
3.3.5.4.	<i>Wetting properties</i>	143
3.3.5.4.1.	<i>Static contact angle</i>	143
3.3.5.4.2.	<i>Drop Test</i>	145
3.3.5.5.	<i>UV-Visible Spectroscopy</i>	145
3.3.5.6.	<i>High-Pressure Liquid Chromatography (HPLC)</i>	147
3.3.5.7.	<i>Antibacterial assays</i>	149
3.3.6.	<i>Data analysis</i>	150

4. RESULTS AND DISCUSSION..... 158

4.1. PART I – PLASMA-TREATED POLYAMIDE 6.6 AS DRUG DELIVERY SYSTEM FOR TOPICAL APPLICATION	159
4.1.1. <i>Influence of plasma treatment on wetting properties</i>	160
4.1.2. <i>Influence of plasma treatment on surface chemistry</i>	165
4.1.3. <i>Influence of plasma treatment on PA66 fiber topography</i>	175
4.1.4. <i>Ageing of plasma-treated PA66 fabrics</i>	178
4.1.5. <i>Influence of plasma treatment on the loading and release of the active principles</i>	181
4.1.5.1. <i>Ketoprofen</i>	181
4.1.5.1.1. <i>Loading</i>	181
4.1.5.1.2. <i>Release</i>	183
4.1.5.2. <i>Caffeine</i>	184
4.1.5.2.1. <i>Loading</i>	184
4.1.5.2.2. <i>Release</i>	187

4.1.5.3. Methylxantines.....	200
4.1.5.3.1. Loading.....	200
4.1.5.3.2. Release	202
4.2. PART II – PLASMA-TREATED POLYPROPYLENE MESHES AS DRUG-DELIVERY BODY IMPLANTS	
204	
4.2.1. <i>Influence of plasma treatment on wetting properties.....</i>	204
4.2.2. <i>Influence of plasma treatment on surface chemistry.....</i>	206
4.2.3. <i>Influence of plasma treatment on PP fiber topography</i>	211
4.2.4. <i>Influence of plasma treatment on the ampicillin loading.....</i>	217
4.2.5. <i>Influence of plasma treatment on the release of ampicillin from PP meshes</i>	221
4.2.6. <i>Plasma polymerization of PP meshes</i>	228
4.2.7. <i>Influence of plasma treatment on antibacterial effect of PP mesh.....</i>	243
5. CONCLUSIONS	260
6. FURTHER INVESTIGATION LINES.....	266
7. PUBLICATIONS AND ACTIVITIES DERIVED FROM THE PHD. THESIS	270
8. APPENDIX.....	277
8.1. LIST OF ABBREVIATIONS	277
8.2. INDEX OF FIGURES.....	278
8.3. INDEX OF TABLES	284
8.4. LIST OF TECHNIQUES USED IN THIS PHD. THESIS	286
8.5. GLOSSARY	287

INTRODUCTION

1. INTRODUCTION

1.1. Technical textiles

Technical textiles include all those textile-based products which are mainly used for their performance or functional characteristics rather than for their aesthetics, and that can be used for non-consumer (i.e. industrial) applications. The definition includes from finished products to textile components of other products. Thus, the definition does not depend on the textile material used (yarn or fibre), but on the end-use of the product itself.

An outstanding feature of the technical textiles industry is the range and diversity of raw materials, processes, products and applications. Indeed, the growth of the sector is closely linked to the development of science and research, which has allowed finding numerous new applications for textiles.

Technical textiles have been developed thanks to key innovations in new textile fibres, textile material processing, production processes and final products. Therefore, their diversity renders difficult to identify them as they are very often mixed with other materials, are part of a product or used as a semi-product, all of these in different economic sectors or activities. Technical textiles are today being used in a wide range of industries such as aeronautics, construction, automotive, agriculture, cosmetics, pharmaceuticals and even the sport industry.

According to the TECHTEXTIL classification, technical textiles are classified into 12 categories:

- AGROTECH (Textile products for agriculture, horticulture, aquaculture, forestry, gardening, landscaping, and forestry applications.)
- BUILDTECH (Textile products for architectural structures, and construction. Membrane construction, lightweight construction, solid and hydraulic earthworks, road construction.)

- CLOTHTECH (Textile products with technical components for footwear and clothing.)
- GEOTECH (Geotextiles and civil engineering textile materials. Used for Public Construction, construction of dikes or landfill construction.)
- HOMETECH (Technical components of tapestry, carpets, and home textiles.)
- INDUTECH (Textiles for industrial applications: filtration, conveyor belts, cleaning, etc.)
- **MEDTECH (Textile products for medical applications and hygiene.)**
- MOBILTECH (Textile products for automotive, boats, trains, planes and satellites.)
- OEKOTECH (Textiles for environmental protection applications, recycling and waste disposal.)
- PACKTECH (Textile Materials for packaging and transportation.)
- PROTECH (Textile products for personal and property protection.)
- SPORTTECH (Textile products for sports, leisure and entertainment industry.)

1.1.1. Medical textiles

Medical textiles are used in different areas of medicine and pharmaceutical technology as sanitary materials (bandages, dressings, surgical clothing, patches, etc.) or as implants. Materials used include monofilament and multifilament yarns, woven, knitted, and nonwoven fabrics, and composite structures. The number of applications is huge and diverse, ranging from a bio-absorbable single thread suture to the complex composite structures for bone replacement, and from a simple cleaning wipe for wound hygiene to advanced barrier fabrics used in operating rooms. These materials can be categorized into four separate and specialized areas of application as follows (Figure 2):

- Non-implantable materials: wound dressings, bandages, plasters, etc.
- Extracorporeal devices: artificial kidney, liver, and lung

- Implantable materials: sutures, vascular grafts, artificial ligaments, artificial joints, etc.
- Healthcare/hygiene products: bedding, clothing, surgical gowns, cloths, wipes, etc.

In this PhD. Thesis the study has been focused on two kinds of medical textile: non-implantable textile materials for topical application and implantable textile materials for hernia repair respectively.



Figure 2: Textile materials and products include non-implantable materials (a), implantable materials (b) and healthcare and hygiene products (c).

The MEDTECH market is forecasted to grow at 4.5 percent per year between 2011 and 2018, to reach \$455 billion, according to the EvaluateMedTech™ World Preview 2018, reported at the AdvaMed 2012 conference taking place in Boston, October 1-3 (Figure 3). This growth will outpace the global prescription drug market, which is expected to grow 2.5 percent per year between 2011 and 2018. Global worldwide MEDTECH R&D spends set also to grow by 3.9% to \$ 26.7 billion by 2018. In-vitro diagnostics is expected to be the largest MEDTECH segment in 2018, with sales of \$58.8 billion.

Medtech Industry Trends

By 2018:

Worldwide medtech sales forecast to be

\$455 billion

Compound Annual Growth Rate will be

4.5% between 2012 and 2018

Medtech R&D spend forecast to reach

\$26.7 billion

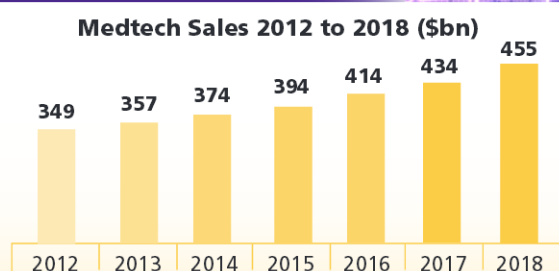


Figure 3: Medical textiles industry trends from the EvaluateMedTech™ World Preview 2018 report.

Therefore, this PhD. Thesis is focused on an area of interest not only from the scientific point of view but also from the applied market perspective.

1.1.2. Cosmetotextiles

Cosmetotextiles are a branch of the medical textiles (MEDTECH) and are also a growing trend in the world, with promising developments. A cosmetotextile, consequence of the fusion of cosmetics and the textile industry through various techniques, is a textile consumer article containing a durable cosmetic substrate which is released over a certain time. A cosmetotextile is a textile containing a cosmetic preparation mainly for dermatology applications such as moisturizing, anti-aging, anti-cellulite, or slimming, designed for aesthetic skin conditions. Cosmetotextiles can be considered as cosmetic textiles when the cosmetic ingredients linked onto the textiles have to be transferred to the wearer's skin, and the amounts transferred have to be enough to ensure that cosmetic benefits are possible (Singh, 2011).

Until today, commercialized cosmetotextiles are usually based on finished fabrics with microcapsules containing the cosmetic active principle. The preparation of such active nano- or micro-capsules is generally based on the encapsulation of active molecules by a polymer matrix (particles or capsules) and deposited or fixed on the fiber. The textile functionalization described in literature mainly rests upon the immobilization or impregnation of textile fibers by microcapsules containing drugs, or upon hollow fibres

containing microcapsules in the nano- or micro-channels, methods in which the release of the drug is then due to the physical degradation of the polymer matrix or via molecular diffusion processes (Singh, 2011). In this PhD. Thesis, the loading of the active ingredients in the fiber does not involve any encapsulation technique and the active molecules have been directly loaded to the textile fiber after previous modification of surface fibre by plasma treatment, being this process the novelty of the work.

Impregnated textiles and/or chemically grafted textiles allowing the release of active molecules have been developed since the 1990s'. The first cosmetotextiles include hygiene and/or maintenance wipes, bactericide and insecticide drapery and bedding containing essential oils, perfumes, etc. (Nelson, 2002; Kukovic, 1996). Applications combining clothes and cosmetics have been added to this list over the years to finally be used in a wide range of applications, for all functional dressings (belts, socks, pants, underwear) and for all purposes (slimming, anti-bacterial, anti-cellulite, anti-odor, moisture, ect.) (Nelson, 2002).

In 2002, FIRTEX L.L.C. (Firstex L.L.C., 2002) patented a technique for application of nanoparticles to textiles that can be occluded in the natural fibers. Nanoparticles were starch-based and had a helicoidal configuration with a nano- hydrophilic cavity and hydrophobic inner wall. It was claimed that such cavities can contain several types of active molecules. The nanoparticles were immobilized by covalent grafting on natural fibers by the use of epichlorohydrin, polycarboxylic acid, dimetilol dihydroxy etilenurea or other formaldehyde-free substances. In some cases, the immobilization was performed by adsorption or special binders.

In 2002, Combe filed a patent for textiles for clothing related to the loading of cosmetic, sanitary, a medical substances in textile fabrics for human or veterinary use. The impregnation process according to the invention consists in spraying on one or both sides of the fabric one or more substances in solution or dispersion in a liquid medium, so as to produce one continuous sprayed film which is accommodated in the meshes of the textile structure and thus fill the holes (Combe, 2002). The described solution or dispersion for the

impregnation of the textile fabric is compound by a drug, a binder and a gelling agent in liquid phase. According to Combe, the binder may be defined as a substance which facilitates immobilization of an active ingredient to the fiber to ensure that it remains fixed during at least 3 washing processes of the textile fabric. As binder it has been mentioned more particularly cellulose derivatives, soluble or dispersible in water, such as methylcellulose, ethylcellulose, β -hydroxyethyl cellulose, hydroxypropylcellulose, hydroxypropylmethylcellulose and similar products, as well as polymers of ethylene glycol or propylene glycol with an average molecular weight between 1,000 and 30,000. As gelling or thickening agent, it has been mentioned, in particular, polymers of acrylic acid or methacrylic acid, polymers of esters of methacrylic acid, polyacrylamides, or others cationic, anionic or amphoteric thickeners depending on the chemical nature of the fabric. Reloading of the textile article is possible and done by heating and moistening the fabric article before exposing the desired locations or the entire dressing under the same spraying conditions, with the same solution or suspension of active ingredient.

In 2008, Skin'up patented a process for textile fabric treatment with encapsulated nanoparticles. The synthetic fibers described are polyamides, polyesters, acrylics, and polyolefins, such as polypropylene or polyethylene, or polytetrafluoroethylene. The textile for which the monitoring and/or the following of the release of the active principle is intended can be an item of clothing, gloves, slippers, underwear, stockings or pantyhose, but also curtains, cushion or sofa covers, or else medical articles, such as bandages, splints or dressings but also compresses, head bandages or masks ([Patent WO 08/068418 2008](#)).

According to the patent, the incorporated molecules may be a colorant or an active principle in the form of nanoparticles, with a size of less than 300 nm, fullerenes, nanocrystals and nanoemulsions, nanocapsules, nanospheres, nanovesicles or spherulites. The active principle applied can be pharmaceutical or cosmetic active principles, deodorizing agents, insecticides, acaricides, slimming, refreshing or moisturizing active principles. Fat-soluble pharmaceutical active principles have been

described such as fluvastatin, ketoprofen, verapamil, atenolol, griseofulvin or ranitidine as well as hydrophilic active principles from aminoglycosides (gentamicin), antibiotics (β -lactam, sulbenicillin, cefotiam, cefmenoxime), peptide hormones (TRH, leuprolide, insulin), antiallergic, to antimycotic or cytostatic agents, anxiolytics, contraceptives, sedatives, mineral salts (calcium, chlorine, magnesium, phosphorus, potassium, sodium, sulfur), amino acids, peptides, proteins, etc. Textile fabrics were impregnated in an exhaustion bath or by spray. In addition to the compound of interest and/or active principle, the aqueous solution in which the dipping of the textile is carried out can comprise other additives, such as those chosen from preservatives and/or antibacterials, fillers, antifoaming agents, antistatic agents, stabilizers, antioxidants and/or UV screening agents. The aqueous solution can also comprise flame retardants, plasticizers, pigments and agents which make possible the formation of a protective sheath around the fibers of which the textile is composed, which protective sheath slowly disintegrates on contact with the subject wearing the textile. In parallel, the authors developed a monitoring technique to follow the drug release as a function of the number of washes, by using a labeled sample treated with a dye. (Patent WO 08/068418 2008). The concentration of the colour solution is adjusted depending on the drug release kinetics.

Numerous studies describe microparticles immobilized on textile or included in the textile fiber (Ying, 2004; Da Rocha Gomes, 2006; De Lucas Martinez, 2007; Da Silva Ribeiro, 2008; Mondal, 2008; Ripoll, 2010). A general problem of the cosmetotextiles is their low resistance to repeated washing. Currently, this resistance is improved with the development of new particles and new methods of fixation. The textile industry has also developed charging systems that increase the life of the product. These systems allow the recharging of the fibers with drugs, when these are used up. Recharging usually consists in the addition of a single dose in the final domestic wash stage.

As studied in this PhD. Thesis, **an alternative to the use of chemical binders or fibres containing microcapsules to achieve the release of cosmetic compounds from textile fabrics could be based on the modification of the interactions between the fiber and the active molecule by plasma treatment, as a way to attach the drug directly to the**

textile fibre surface and achieve an adequate release profile as a function of the application.

1.1.3. Textile materials for drug delivery systems

Drug delivery is a term that refers to the delivery of a pharmaceutical compound to humans or animals. Most common methods of delivery include the preferred non-invasive oral (through the mouth), nasal (inhalation), rectal, topical dermal and transdermal routes.

Current investigations in the area of drug delivery systems include the development of targeted delivery in which the drug is only active in the target area of the body and drug formulations which are released over a predetermined period of time in a sustained and controlled manner from a formulation. When these concepts are applied to textiles, innovative medical textiles can be designed.

Thus, textiles can be used as an interesting support for drug delivery systems, conferring an important added value to the primary function of such material. A wide number of wound dressings constitute good drug delivery systems and can own the ability to release active principles loaded into the fiber from different formulations (gels, foams, hydrogels...). Besides their added value, the main highlights for wound dressing-based drug delivery systems are the non-invasive administration way and the improved targeting of the disease or the dysfunction, due to the localized behavior of the application. Non-implantable textile materials eligible for topical and transdermal drug delivery and their requirements for this kind of application are reported in section 1.1.3.1.

This principle can be also transposed to some textile-based body implants. Antibiotic-loaded implants can be a solution to the device-associated infections that is the result of bacterial adhesion and subsequent bio-film formation at the implantation site (Zilberman, 2008), of a surgical mesh, for example. Textile-based surgical meshes

commercially available or described in literature for potential application are presented in section 1.1.3.2.

1.1.3.1. Non-implantable textile materials for topical and transdermal applications

Topical drug delivery is the term used for local treatment of the dermatological condition where the medication is not targeted for systemic delivery (Osborne, 2008); examples include treatment of dermatological conditions like eczema or psoriasis by application on the skin from a pharmaceutical dosage form such as gel, cream, ointment, powder, spray, liquid lotion, etc. Examples of drugs delivered topically include antifungals, antivirals, antibiotics, antiseptics, local anesthetics, and antineoplasics.

Transdermal drug delivery refers to the administration of active compounds in discrete dosage forms through the skin (at controlled rate and concentration) to the systemic circulation. The transdermal route has numerous advantages over the more traditional drug delivery routes. These include high bioavailability, absence of first pass hepatic metabolism, steady drug plasma concentrations, and the fact that therapy is non-invasive. The main obstacle to permeating drug molecules is the outermost layer of the skin, the stratum corneum.

Drug delivery systems based on textile materials and structures can improve the efficiency and the therapeutic benefits of compressive elastic knitwear and provide them with an additional value. **Therefore, in the first part of this PhD. Thesis we have used elastic-compressive fabrics where the incorporation of cosmetic or pharmaceutical compounds and their controlled release from such fabrics may be of interest.** For example, adding the advantages of compressive stockings (improved venous return) with the presence of an active principle (caffeine) with action on body lipids (cellulite), and is one of the investigation lines studied in this PhD. Thesis to improve the efficiency of such materials and to provide a textile-based cosmetic

product for topical application. In the same way, the loading of compressive stockings with non steroidal anti-inflammatory drugs (NSAIDs), like ketoprofen in this work, can provide improved results for the treatment of rheumatoid arthritis via transdermal route, which has been also studied in this PhD. Thesis.

However, in general if drugs are incorporated directly to the textiles without any additional agent or mechanism, the release is immediate. Therefore, in the way to uptake this major issue, different means have been studied to limit drug release with the elapse of time and achieve the release of an active ingredient to its topical therapeutic concentration for a predetermined time period, such as coating of the fibers with different biocompatible polymers, microcapsules, or even more complex approaches such as the use of:

- Hollow fibers as drug reservoirs (Okuda, 2010)
- Electrospun nanofibers with a high surface area to volume ratio (Yoo, 2009). A basic concept of electrospinning is to employ electrostatic repulsions of highly-charged polymer jets to produce randomly oriented or aligned nanofibers deposited on the collector surface. Upon applying an electric field, the polymeric solution with a moderate viscosity value forms the Taylor cone at the tip of an injecting device (Doshi, 1995). In order to apply electrospun nanofibers in biomedical uses, their surfaces have been chemically and physically modified with bioactive molecules and cell recognizable ligands after the electrospinning method; this subsequently provides bio-modulating or biomimetic microenvironments to contacting cells and tissues and for that reason, they have received much attention because of their potential applications for biomedical devices, tissue engineering scaffolds, and drug delivery carriers (Pham, 2006; Yoo, 2009).

Development of medical textiles for topical application needs to take into account different parameters such as the natural barrier of the skin, the diffusion mechanism of the active principle molecule from the fabrics through the skin, and the requirements of the fabric, as described in the following sections.

1.1.3.1.1. Textile materials for non-implantable medical textiles

Traditional wound dressings include mainly natural (principally cotton) or synthetic bandages and gauzes. Unlike the topical pharmaceutical formulations, these dressings are dry and do not provide a moist wound environment. They may be used as primary or secondary dressings, or be part of a composite of several dressings, each performing a specific function. Bandages are made from natural (cotton and cellulose) and synthetic (e.g. polyamide, polypropylene, etc.) fibres which perform different functions (Boateng, 2008). Non-implantable medical textiles for wound care and bandages can be classified as described in Table 1.

Table 1: Non-implantable medical textiles. Examples of non-implantable textiles, type of fiber and manufacture system (adapted from Bektaş, 2010).

Product application	Type of fibre	Manufacture system
Wound care		
Absorbent pad	Cotton, viscose	Nonwoven
Wound contact layer	Silk, polyamide, viscose, polyethylene	Knitting, weaving, nonwoven
Base material	Viscose, plastic film	Weaving, nonwoven
Bandages and elastic-compressive textiles		
Simple inelastic/ elastic	Cotton, viscose, polyamide, elastomeric yarns	Knitting, weaving, nonwovens
Light support	Cotton, viscose, elastomeric yarns	Knitting, weaving, nonwoven
Compression	Cotton, polyamide, elastomeric yarns	Knitting, weaving,
Orthopaedic	Cotton, viscose, polyester, Polypropylene, polyurethane foam	Weaving, nonwoven
	Viscous, plastic film, cotton, polyester, glass, polypropylene	Knitting, weaving, nonwoven
Plasters	Cotton, viscose	Weaving, nonwoven
Gauzes	Cotton	Weaving

A number of **wound dressings** are available for a variety of medical and surgical applications. The functions of these materials are to provide protection against

infection, absorb blood and exudates, promote healing and, in some instances, apply medication to the wound. The wound contact layer should prevent adherence of the dressing to the wound and be easily removed without disturbing new tissue growth. The base materials are normally coated with an acrylic adhesive to provide the means by which the dressing is applied to the wound. Developments in coating technology have led to pressure sensitive adhesive coatings that contribute to wound dressing performance by becoming tacky at room temperature but remain dry and solvent free. The use of collagen, alginate and chitin fibers has proved successful in many medical and surgical applications because they contribute significantly to the healing process. For instance, when alginate fibers are used for wound contact layers, the interaction between the alginate and the exuding wound creates a sodium alginate gel. The gel is hydrophilic, permeable to oxygen, impermeable to bacteria and contributes to the formation of new tissue.

Bandages and elastic-compressive textiles are designed to perform a whole variety of specific functions depending upon the final medical requirement. They can be woven, knitted, or nonwoven and possess either elastic or non elastic properties. The most common application for bandages is to hold dressing in place over wounds. Such bandages include lightweight knitted or simple open weave fabrics made from cotton or viscose that are cut into strips then scoured, bleached and sterilized. Elastic yarns are incorporated into the fabric structure to impart support and conforming characteristics. Knitted bandages can be produced in tubular form, as those employed in this work, in varying diameters on weft knitting machines. Woven light support bandages are used in the management of sprains or strains (ligaments) and the elastic properties are obtained for example by weaving cotton crepe yarns that have high twist content. Similar properties can also be achieved by weaving two warps together; one beam under a normal tension and the other under a high tension. When applied under sufficient tension, the stretch and recovery properties of the bandage provide support for the sprained limb. **Compression bandages are also used for the treatment and prevention of deep vein thrombosis, leg ulceration, and varicose veins and are designed to exert a required compression to different areas of the leg.** Compression bandages are classified by the degree of compression and can be either woven and

contain cotton and elastomeric yarns or wrap and weft knitted in both tubular and fully fashioned forms. Orthopedic cushion bandages are used under plaster casts and compression bandages to provide padding and comfort.

New MEDTECH products incorporate new reactive agents which have therapeutic value, and overcome some of the disadvantages associated with the use of topical pharmaceutical agents. The modern dressings used to deliver active agents to wounds include hydrocolloids, hydrogels, alginates, polyurethane foam/films, and silicone gels (Heenan, 1998). So, they often do not rely on the textile structure or the fibres themselves, but those are rather used as a support layer for other substances. The incorporated drugs play an active role in the wound healing process either directly or indirectly as cleansing or debriding agents for removing necrotic tissue, antimicrobials which prevent or treat infection or growth agents (factors) to aid tissue regeneration.

1.1.3.1.2. The skin: natural barrier for drug delivery

Numerous drugs have undesirable side effects for oral administration due to their low solubility and susceptibility to first pass metabolism in the liver. Drugs, such as non-steroidal anti-inflammatory drugs (NSAIDs), have patient related drawbacks, such as undesirable gastrointestinal side effects. For such drugs, alternative routes of administration are of interest, and practically every available body surface and entrance has been considered. Since the skin is readily accessible and has a large surface area, dermal and transdermal drug delivery has been the subject of a great interest in research and product development. In humans, skin is the largest organ of our body, which guards the underlying muscles, bones, ligaments and internal organs, and acts as a protective barrier against the entry of foreign material and possible invasion of pathogens. Its other functions are insulation, temperature regulation, sensation, and it also prevents the loss of excessive endogenous material such as water (Brown, 2006; Proksch, 2008).

The primary barrier layer of skin is the stratum corneum (Figure 4). The stratum corneum is the outermost layer of skin that forms the main barrier for diffusion of the permeants through the skin (Wertz, 1989). The stratum corneum consists of 18–21 layers of flat, roughly hexagonal cells called corneocytes that are constantly shed and renewed (Menon, 2002). These keratin-rich dead cells, measuring 20–40 μm in diameter, are interspersed within a crystalline lamellar lipid matrix to assume a “bricks and mortar” arrangement (Elias, 1983). The extracellular lipid contributes 10% of the dry weight of this layer, while 90% is the intracellular keratin. The barrier function of the skin can be attributed to the lamellar lipids that are synthesized in the granular layer and subsequently organized into the extracellular lipid bilayer domains of the stratum corneum (Landmann, 1986; Proksch, 2008).

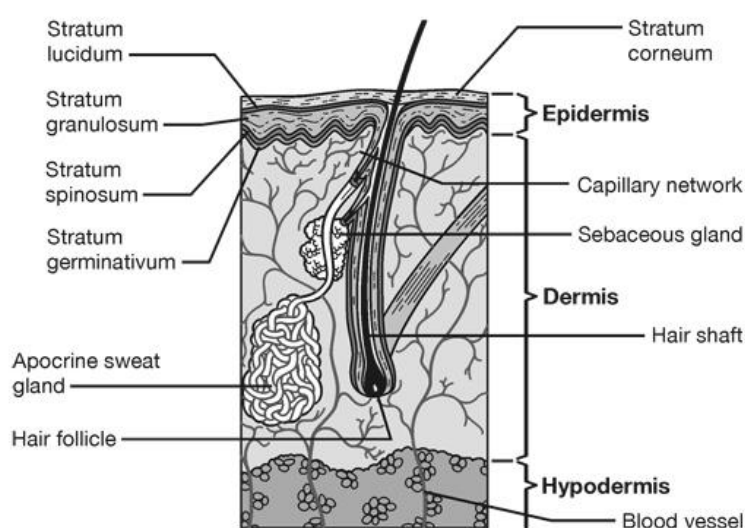


Figure 4: Cross-section representation of skin layers.

Lipophilic drugs can readily diffuse through the first skin layer at a rate that depends primarily on their molecular size and lipophilic properties. Low molecular-weight drugs enter also into the dead cells, and the lipid pathways for diffusion are marked by numerous detours.

After passing through the stratum corneum, drug encounters more hydrophilic layers: the epidermis and the dermis, which constitute the two main layers of the skin (Figure 4), before being absorbed in capillaries perfusing the dermis. The epidermis is

avascular in nature, consisting of several types of cells (keratinocytes, melanocytes, Langerhans cells, and Merkel cells) and a variety of catabolic enzymes (esterases, phosphatases, proteases, nucleotidases, and lipases) (Jansen, 1969; Mier, 1975). The stratified epidermis is about 100–150 μm thick and comprises four distinct layers, namely the stratum basale, stratum spinosum, stratum granulosum, and stratum corneum. The dermis that forms the bulk of the skin (1–2 mm thick) is made up of connective tissue elements. Dermis is highly vascular and filled with pilosebaceous units, sweat glands, adipose cells, mast cells, and infiltrating leukocytes (Menon, 2002).

Drug that is absorbed through the skin is not susceptible to first pass metabolism by intestine and liver, although some metabolism may occur in the skin itself.

While ointments, gels and creams are usually used for topical delivery to the skin, patches have been developed for controlled systemic delivery. Thus, patches are transdermal drug delivery systems consisting in self-contained discrete dosage forms designed to deliver a therapeutically effective amount of drug through intact skin (Wokovich, 2006). Most commercially available transdermal drug delivery systems are of three different types:

- Reservoir systems
- Matrix systems with drug-release rate-controlling membrane
- Matrix systems without drug-release rate-controlling membrane.

The reservoir system is made up of three major components, namely the drug reservoir, the rate-controlling membrane, and the adhesive. The active principle present in the reservoir, along with the other excipients, has to permeate through the rate-controlling membrane before reaching the skin. The adhesive that holds the system in place on the skin can completely cover the drug release area or only the perimeter around the non-adhering drug release surface.

In the matrix type, the drug may be embedded in the adhesive matrix. A rate controlling membrane may be present between the drug-loaded matrix and the

adhesive or sometimes the matrix itself can control the rate of release of the actives from the system (Murthy, 2010).

The simplest patch consists of an adhesive layer containing drug in a dissolved or in a finely divided solid form, and an impermeable backing layer. For such patches, delivery rate is controlled primarily by the permeability of the stratum corneum, which depends on the drug's partition coefficient between the patch material and the stratum corneum, the drug's diffusivity in the stratum corneum, and the thickness of the stratum corneum. Provided these parameters remain constant during application of the patch, and if drug activity in the patch remains constant by dissolution of solid drug into the adhesive, then zero order, constant rate delivery can be achieved (Siegel, 2012).

The simple adhesive patch design is best for drugs with a large therapeutic range, since skin permeability may vary across patients and between sites of application in an individual patient. When more precise control of drug concentration in blood is desired, it is useful to insert a rate controlling membrane between the drug reservoir and the adhesive layer. The membrane's permeability must be less than that of the skin in order to achieve a controlled release rate.

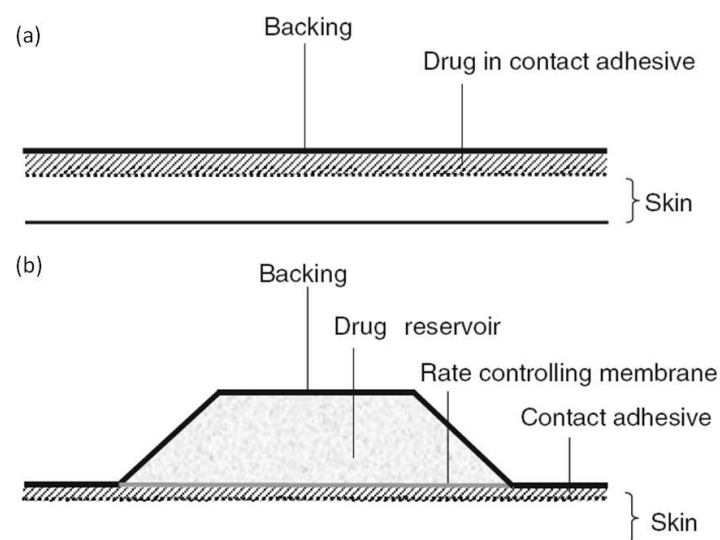


Figure 5: Conceptual design of transdermal commercial delivery patches based on (a) Skin permeability control and (b) membrane control adapted from Siegel, 2012.

There is a wide variety of research on the topical and transdermal delivery of active molecules based on dissolution assays, defined by Pharmacopeias, such as the *Farmacopea Española* employed as standard for the experiments designed in this PhD. Thesis. This variety is due to the numerous possibilities offered by the existing number of active molecules, combined with the use of different physical carriers and supports, and the different formulations that can be found (Ueda, 2009; Paudel, 2010; Siegel, 2012). However, every investigation has the skin properties as the common limitation to take into account in the selection of the drug, the formulation and the viability of the administration way for the specific application.

1.1.3.1.3. Considerations to take into account in the selection of drugs for topical applications

Passive methods of drug application for topical applications include carriers as ointments, creams, gels and patches. However, the amount of drug that can be delivered using these methods is still limited because the barrier properties of the skin essentially do not change.

Since the skin naturally acts as a natural barrier, only a limited number of drugs can penetrate and diffuse through it at an adequate rate. Generally, **a drug molecule should be sufficiently lipophilic to overpass the stratum corneum, but sufficiently hydrophilic to also cross the viable layers. Its molecular weight should be low to ensure adequate mobility in the stratum corneum, so the maximum molecular weight for a compound involved in this route of administration cannot exceed 500 g.mol⁻¹** (Bos, 2000; Brown, 2006). Finally, the concentration of the drug and its pharmacokinetic properties should be such that the delivery of the drug to the site of action places the drug concentration within the therapeutic range. While the rate of delivery can be increased by using larger patches, there are practical size limitations (Sieglar, 2012) which could be overcome using textiles as vehicle for drug delivery, as the contact area with the skin would be much larger. The drugs presented in the

market for transdermal application by means of patches include scopolamine, nitroglycerine, nicotine, clonidine, fentanyl, estradiol, testosterone, lidocaine, and oxybutinin (Langer, 2004).

Because the skin is so accessible, much effort has been devoted to expanding the spectrum of transdermally deliverable drugs by using more complex delivery systems. Drug delivery systems based on textile supports can be one way to improve the delivery of the drug, to maintain the continuous release along day and night for chronic disease or dysfunction or to treat diseases affecting directly the skin.

The following table (Table 2) presents a selection of benefits and limitations related to the dermal and transdermal release of active principles.

Table 2: Benefits and limitations associated with cutaneous release.

Benefits	Limitations
<ul style="list-style-type: none"> • Avoid the first pass metabolism and other variables associated with the gastrointestinal tract. • Allow a controlled sustained release over a prolonged period • Reduction of the side effects associated with systemic toxicity. • Improve the acceptance and patient compliance. • Direct access to the target (e.g. treatment of skin disorders such as psoriasis, eczema, fungal infections). • Easy to suspend the dosage in case of adverse systemic and local reaction. • Easy and painless administration. • The facility of use can reduce the overall costs of healthcare treatments. • Provide an alternative when it is not possible oral administration. 	<ul style="list-style-type: none"> • A molecular weight less than 500 g.mol⁻¹ is essential to ensure ease of diffusion through the stratum corneum, since the diffusivity of solute is inversely related to their size. • Sufficient solubility in water and oil. It is recommended (octanol / water) a partition coefficient value (Log P) between 1 and 3 for the permeant to cross the stratum corneum and to access the lower layers for systemic release. • Intra-and inter-variability related to the permeability of intact and diseased skin. This implies different absorption profiles, with different biological responses. • Pre-systemic metabolism: the presence of enzymes in the skin can metabolize the drug to an inactive form, reducing its effectiveness. • Irritation and skin sensitization.

Nowadays, patch-type products currently on the market are used to release a limited number of drugs, and although they do not overcome all the physicochemical restrictions mentioned above, which offer an improvement in controlling the dose, in the patient acceptance and the compliance, compared to formulations such as creams or gels. Similarly, **the incorporation of drugs to textile fabrics directly in contact with the skin can be an advantage from the viewpoint of improving the dose compliance and acceptance by the patient.**

1.1.3.2. *Implantable medical textiles*

Medical textiles can also be aimed for implantation in the body. Implantable textiles are used in effecting repair to the body whether it is wound closure (sutures) or replacement surgery. Table 3 illustrates the range of specific products employed within this category with the type of associated materials and their manufacture. Biocompatibility is of prime importance if the textile material has to be accepted by the body. Biocompatibility is defined as the ability of a biomaterial to perform its designed function with respect to a medical therapy, without eliciting any undesirable local or systemic effects in the host body and generating the most appropriate beneficial cellular or tissue response and optimizing the clinical performance of the therapy (Williams, 2008).

Polyamide has been used mainly for artificial ligaments, tendons and artificial joints, and recently for artificial hip prostheses and inguinal meshes (Wisniewski, 2002; Singhal, 2002; Shmack, 2006). Polypropylene (PP) is the least reactive polymer together with polytetrafluoroethylene (PTFE) and polyester (PES) and one of the most employed in abdominal repair surgery.

Table 3: Implantable medical textiles. Examples of implantable textiles, type of fiber and manufacture system.

Product application	Type of fibre	Manufacture system
Sutures		
Biodegradable	Collagen, polylactide, polyglycolide	Monofilament, strip, yarn
Non-Biodegradable	Polyamide, polyester, Teflon, polypropylene, polyethylene	Monofilament, strip, yarn
Soft tissue implants		
Artificial tendon	Teflon [®] , polyester, polyamide, polyethylene, silk	Braided, woven
Artificial ligaments	Polyester, carbon	Braided
Artificial cartilage	Low-density polyethylene	Nonwoven
Artificial skin	Chitin	Nonwoven
Eye contact lenses, artificial cornea	Polymethyl methacrylate, silicone, collagen	
Hernia repair mesh	Polypropylene, Teflon [®]	Nonwoven, knitting, polymer film
Orthopedic implants		
Artificial joints / bones	Silicon, polyacetal, polyethylene	
Cardiovascular implants		
Artificial blood vessels	Polyester, Teflon	Knitting, weaving
Heart valves	Polyester	Knitting, weaving

1.1.3.2.1. Hernia repair

A hernia is an abnormal protrusion of an organ or a part of it outside the body cavity which normally contains it. The opening through which organs bulge outside the body cavity is called the hernia gate or the hernia port. Most frequently, hernias occur in the

groin or the abdomen, and statistically in four cases of inguinal hernia there is one case of abdominal hernia (Ciechańska, 2012).

An abdominal wall defect or abdominal hernia is defined as a protrusion through the abdominal wall of intra-abdominal content with an intact lining of the sac. The only effective treatment for abdominal wall defects is surgery to restore integrity and maintain function of the abdominal wall and prevent incarceration and strangulation of intra-abdominal content (Engelsman, 2007). In the past, hernia surgery and abdominal wall reconstructions frequently have used tense sutures to approximate and close a hernial port or defect. This has led to wound dehiscence, recurrent hernias and non-healing of the wound due to tissue ischaemia, with the sutures cutting through the soft tissue (George, 1986).

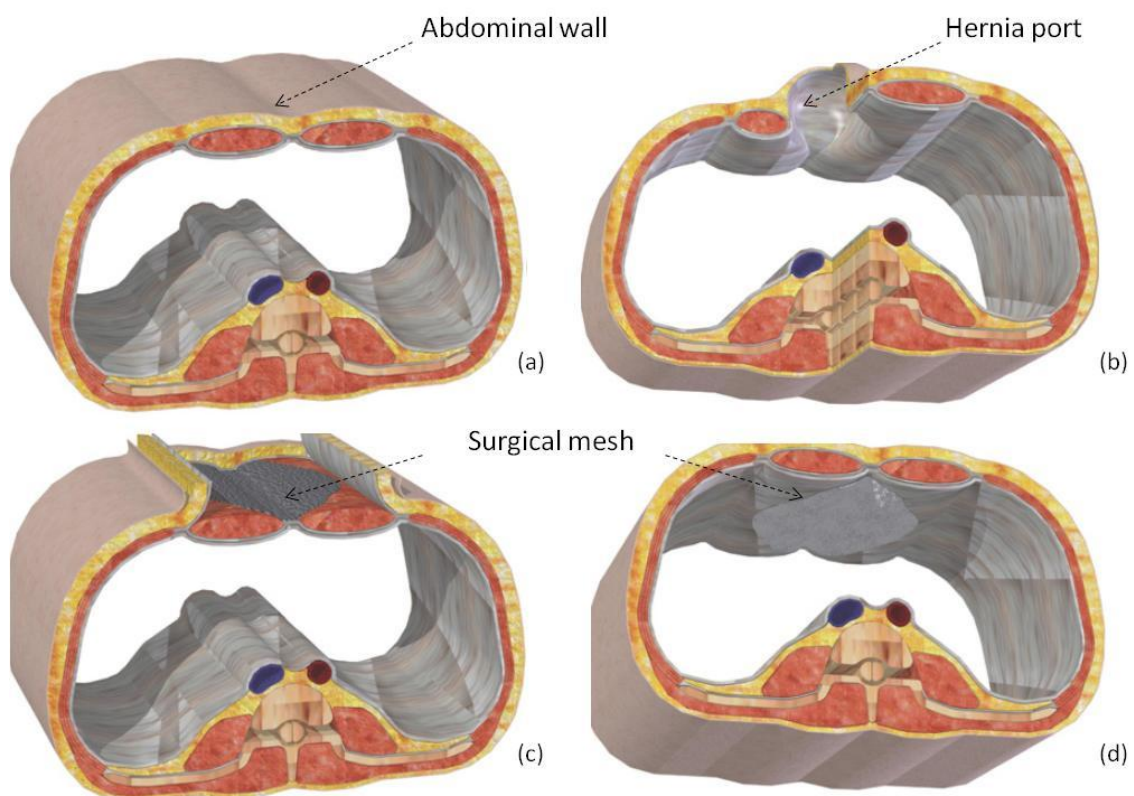


Figure 6: A schematic presentation of the normal anatomy of the abdominal wall (a), the mechanism of an abdominal wall defect (b) and the possibility of open (c) and laparoscopic (d) implantation of a surgical mesh. (Adapted from Engelsman, 2007)

Nowadays, the methods by which hernia repairs are performed can be divided into two general categories:

- Tension methods, which involve an approximation of tissue edges and stitching them together to close the hernia gate. In this type of repair, stitches or sutures exert tension on the body tissues on each side of the hernia gate in order to keep it closed.
- Tension-free methods, which involve an implantation of prosthesis, which is to complement the defect in the fascia and close the hernia gate without exercising a tension in the surrounding tissue.

Figure 6a illustrates the normal anatomical situation with the peritoneum covering the entire abdominal cavity. Also, the relation between the main anatomical structures such as the abdominal cavity, abdominal muscles and fasciae, aorta and spine is shown. Figure 6b demonstrates a midline abdominal wall defect due to detachment of the bilateral rectus abdominal muscles. A hernia sac lined with peritoneum protrudes (arrow) through the hernial port of the abdominal fascia and muscles and is bilaterally enclosed by the rectus abdominal muscle. A protrusion can occur when the abdominal wall is exposed to chronically elevate intra-abdominal pressure (Figure 7).

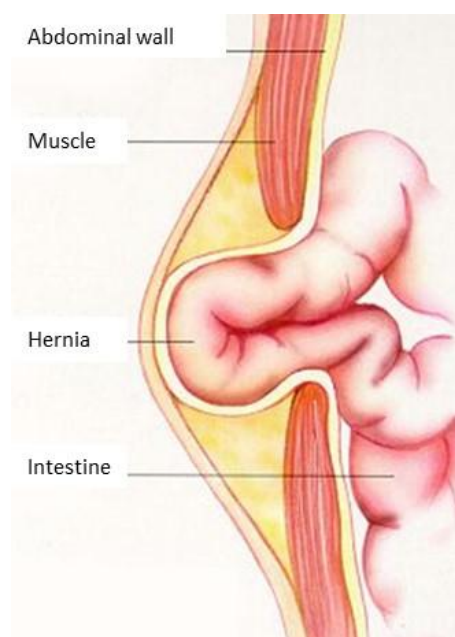


Figure 7: Protrusion formation to an elevate intra-abdominal pressure in case of a midline abdominal wall defect.

A tension-free closure may be accomplished by the placement of a surgical mesh to relieve tension from tissue surrounding the hernial port (Amid, 1992). To allow the placement of the mesh between the external facial layer and the rectus abdominal muscles, the abdominal wall has to be opened. Two surgical methods for hernia repair are commonly used and differ by the placement of the surgical mesh (Lichtenstein, 1989; Awad, 2004; Gray, 2008):

- Open hernia repair surgery consists in a single long incision which is made in the groin. If the hernia is bulging out of the abdominal wall (a direct hernia), the bulge is pushed back into place. If the hernia is going down the inguinal canal (indirect), the hernia sac is either pushed back or tied off and removed. After reducing the hernial sac into the abdominal cavity, the defect is covered with a surgical mesh (Figure 6c).
- Laparoscopic hernia repair consists in a small incision made in or just below the navel. The abdomen is inflated with air so that the surgeon can see the abdominal organs. A thin, lighted scope called a laparoscope is inserted through the incision. The instruments to repair the hernia are inserted through other small incisions in the lower abdomen. The mesh is then placed over the defect to reinforce the abdominal wall. Figure 6d illustrates the placement of an intra-abdominally placed mesh by means of laparoscopic surgery covering the internal hernial port (Engelsman, 2007).

1.1.3.2.2. Abdominal meshes and prosthetic devices

Polypropylene (PP), polyester and expanded polytetrafluoroethylene are nowadays the most common polymers used for medical meshes (Orenstein, 2012), with PP meshes being one of the most frequent materials used in hernia repair. PP meshes are produced with mono or multifilaments and are currently preferred over biological and synthetic absorbable meshes (Figure 8).

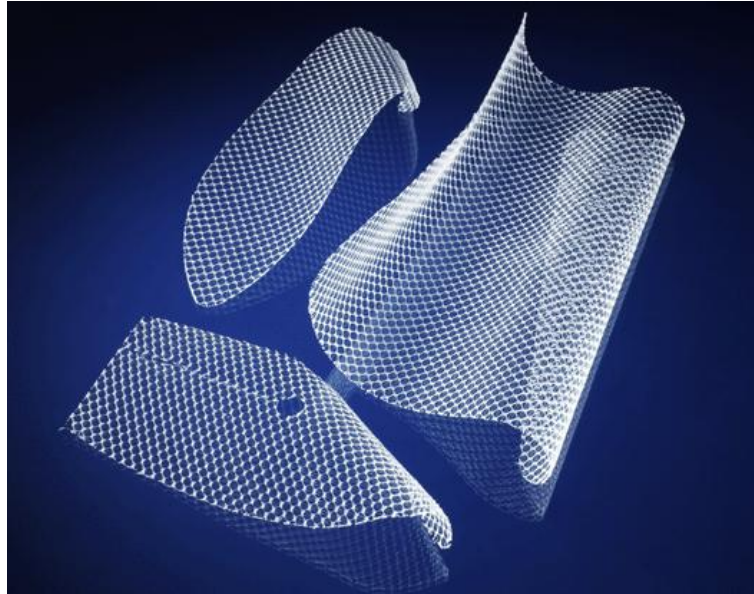


Figure 8: Multifilament PP meshes currently used in hernia repair.

The use of prosthetic material for abdominal wall surgery dates back more than one century. Around 1900, the first prosthesis used for the treatment of inguinal hernia was an inoxidable steel metallic mesh, later abandoned because of its rigidity, responsible for sequellar pain. The modern era started in 1958 with the introduction by Usher et al. of polypropylene mesh implants (Usher, 1958; Usher, 1962), and popularized later by Lichtenstein (Lichtenstein, 1986). The positive effects of the use of a mesh on recurrence of the hernia stimulated the search for an optimal mesh with high biocompatibility, low adhesion formation and low infection rates. The aim of the first studies was focused on the PP mesh closure of the complicated abdominal wound (Fansler, 1995), on the integration, adhesion formation and resistance to traction of PP prostheses used in the partial or total repair of abdominal wall defects (Bellón, 1998), the functional and morphological evaluation of different PP mesh modifications for abdominal wall repair (Klosterhalfen, 1998) and/or the influence of polyglactin-coating on functional and morphological parameters of polypropylene-mesh modifications for abdominal wall repair (Klinge, 1999). Engelsman et al., in 2007, reviewed the clinical background for abdominal wall reconstruction, the different types of surgical meshes employed and known mechanisms of infection. It has been shown that there are major physico-chemical differences between available meshes, which, in combination with

the location of the mesh, the surgical technique applied and hernia type involved influence the infection potential (Engelsman, 2007).

A large number of clinical trials have been published to compare the different types of polymeric meshes, emphasizing on tissue adhesion (Van't Riet, 2003), recurrence (Luijendijk, 2000) and infection (Leber, 1998). Studies on heavy weight, mid-weight, and light weight PP mesh in a porcine ventral hernia model have been described (Cobb, 2006) as well as comparative analysis of histopathologic effects in mice of synthetic meshes as a function of the material used (PP, PE, PTFE), the weight, and the pore size of the mesh (Orenstein, 2012), which bring out the importance of the biocompatibility on the mesh performances. Advanced polymeric meshes have also been studied *in vivo* as drug delivery systems. An antibiotic-releasing polyester mesh to reduce prosthetic sepsis has been designed by Harth et al., loading the antibiotic (vancomycin) into the coated polymer mesh placed in aqueous solution of vancomycin (VM) (5 mL of 25 wt%) for 4 days at room temperature (Harth, 2010). Using an *in vivo* wound infection model, the drug delivery polymer mesh was able to effectively prevent a *Staphylococcus aureus* mesh infection with efficacy demonstrated at 2 and 4 weeks.

In the past decade, PP mesh has been used as prosthetic biomaterial not only to buttress the defect of incisional hernias, abdominal or inguinal, creating a tension-free repair (Matthews, 2003; Engelsman, 2007; Wong, 2011; Deeken, 2011) but also for the treatment of stress urinary incontinence (Hung, 2004), for vaginal prolapse (Siniscalchi, 2011) or to prevent prosthetic device infection (Harth, 2010).

Surgical operations for soft tissue reinforcement are common procedures in medical field and every year require at least one million prostheses (Rutkow, 2009) and surgery for inguinal hernia is one of the most common techniques performed in a general surgical service. Even if this type of surgery is considered clean and the meshes used on prolapsed pelvic organs or on abdominal wall hernia decrease postoperative complications, reoperation rates are still significant (Bako, 2009; Diwadkar, 2009). Mesh-related infection is one of the limitations on the use of synthetic prostheses, and

generally occurs in 1–2% of cases for laparoscopic ventral and incisional hernia repair (Condon, 1991; Page, 1993; Dellinger, 1994; Woods, 1998; Heniford, 2000; Kirshtein, 2002; Heniford, 2003; Engelsman, 2007) and up to 8% for open incisional hernia repair (Petersen, 2001; Cobb, 2003; Falagas, 2004).

Infection complications can appear after the mesh implantation and may generate patient's health risks in the post-operative period (Baessler, 2005; Saihi, 2005). Sources for infectious bacteria include the ambient atmosphere of the operating room, surgical equipment, clothing worn by medical professionals, resident bacteria on the patient's skin and bacteria already in the body (An, 1996; Zilberman, 2008). **Prosthetic device infection is a broad problem that can occur at varied stages of the materials lifespan and can be acute or delayed in their presentation. The nature of device infections requires both preventive and therapeutical strategies.**

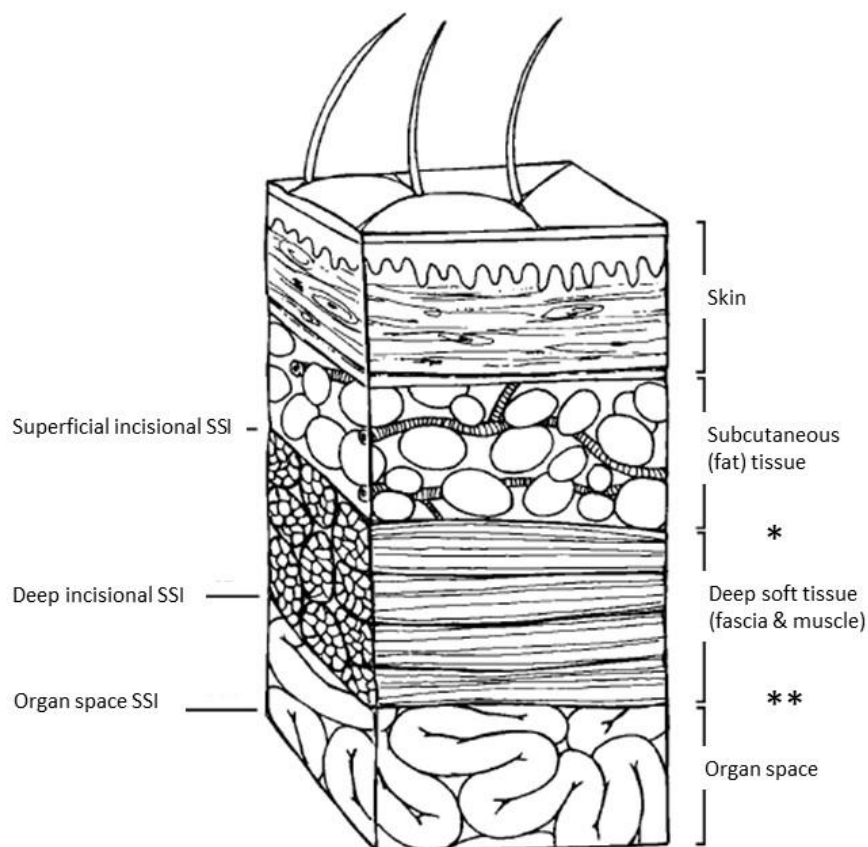


Figure 9: Cross-section of abdominal wall with classification of surgical site of infection (Adapted from Horan, 1992) with positioning of the surgical mesh in case of and of open implantation (*) and laparoscopic abdominal repair ().**

Incisional surgical site infections (SSIs) resulting from abdominal wall implant are divided into superficial incisional (only involves skin and subcutaneous tissue) and deep incisional (involves deeper soft tissue, including fascia and muscle layers), as shown in Figure 9. Despite improvements in operating room practices, instrument sterilization methods, better surgical technique and the best efforts of infection prevention practitioners, surgical site infections remain a major cause of nosocomial infections—and rates are increasing globally (Alvarado 2000).

One of the current approaches to prevention of infection includes the administration of prophylactic antibiotics systemically. This approach should achieve adequate local tissue antimicrobial levels to fight the infection but comes at the risk of systemic secondary effects to the antibiotic exposure (Harth, 2010). A common solution to avoid bacterial contamination of a wound is the systemic treatment of the patient with antibiotics (ABs), but it requires large doses of administered drugs are necessary because only a small part of it reaches the target zone (Avtan, 1997).

As alternative to avoid systemic treatment of the patient with antibiotics, some investigations were performed to obtain an antimicrobial implant by using a silver coating (Kumar, 2002; Kumar, 2005; Monteiro, 2009). This metal is well-known for its broad-spectrum antimicrobial activity against gram-positive and gram-negative bacteria, fungi, protozoa and certain viruses (Balazs, 2004), including antibiotic-resistant strains (Melaiye, 2005; Stobie, 2008), and used to reduce infections, to prevent bacterial colonisation on medical devices as well as in textile fabrics (Taylor, 2005; Panáček, 2006; Ip, 2006).

Another alternative consists of local antibiotic delivery by the immersion of the implant in an antibiotic solution prior to its use. Antibiotic-loaded implants present a straightforward approach for the prevention of implant-associated infections. They can provide an immediate response to the threat of implant contamination and do not necessitate the use of an additional carrier for the antibacterial agent other than the implant itself (Zilberman, 2008).

Most biomaterials present only a low affinity towards drugs, which are subsequently adsorbed onto the medical device in only small amounts, and are then released with a too short delay to produce the expected benefits to the patient. In 2008, El Ghouli et al. proposed an improvement in the sorption and release rates of the antibiotic after chemical modifications of the biomaterial surface by means of functionalization with cyclodextrins (CDs). Recently, improved surgical meshes have been developed with some finishing agents such as cyclodextrin and maltodextrin for the prolonged release of ciprofloxacin from a PP artificial abdominal wall implant (Laurent, 2011), and improved surgical mesh with a degradable polymer coating as a carrier for the sustained release of the antibiotic, ofloxacin, with an in-vitro evaluation of the mesh preparation and antimicrobial efficacy to minimize the risk of post-implantation infection (Guillaume, 2012a; Guillaume, 2012b). In this work, Guillaume et al. designed a new antibiotic-eluting mesh from pre-existing polypropylene prostheses using an airbrush spraying technology. An anti-infective drug (e.g. ofloxacin) is incorporated into a poly(lactic acid) (PLA) or a poly(ϵ -caprolactone) (PCL) coating, presenting a homogeneous, regular and smooth shell around the polypropylene filaments of the mesh. The *in vitro* release kinetics of the antibiotic from the modified meshes to a phosphate buffer saline (PBS) present a limited burst effect followed by sustained drug diffusion for several days as a function of the thickness of the coated polymer, with a longer sustain release for PLA coating.

A recent study about plasma pre-treated PP meshes deals with the physico-chemical characterization of polypropylene fibers for prosthetic applications, pre-treated by atmospheric pressure plasma in a dielectric barrier discharge apparatus (APP-DBD) and later functionalized with chitosan, known for its antibacterial properties (Nisticò, 2012). Unlike this work, **the purpose of the PhD. Thesis is to design an antibiotic delivery system in which the modification of fibre surface for the attachment of the active principle and the modulation of the release is the result of dry processes, using plasma treatments.**

In this PhD. Thesis, the study on implantable medical textile and its modification by plasma treatment has been focused on the polypropylene, currently used as implant mesh for abdominal hernia repair due to its long-lived nature and its biocompatibility, as described before. The aim of the present work is to investigate the effects of plasma treatment on the PP meshes with regard to antibiotic incorporation and release.

1.2. Chemical fibers of synthetic polymer

In this PhD. Thesis two types of chemical fibers have been used: polyamide 6.6 (PA66) and polypropylene (PP). First, an elastic-compressive knitted polyamide 6.6 fabric designed as compressive stockings has been selected as textile-based drug release system for topical applications, in views of studying how the modification of fibre surface properties achieved by plasma treatment influences the loading and the release of selected drugs from the fibres. Then, a polypropylene surgical mesh, made from a homopolymer polypropylene monofilament has been chosen as implantable medical textile to study how the fibre surface properties modification achieved by plasma treatment influences the loading and the release of an antibiotic from the fibres.

1.2.1. Polyamide

1.2.1.1. Structure and classification

Polyamide fibres (or nylon fibres) are defined by the ISO standards as chemical fibres formed from a polymer of synthetic linear macromolecules in which the chain is a succession of amide groups, with a minimum of 85% of them linked to alifatic or cycloalifatic groups (Gacén, 1991). Polyamides are semi crystalline polymers typically produced by the condensation of a diacid and a diamine. Depending on the number of carbon atoms in the monomers or intermediate products used in the synthesis, a specific polyamide is obtained. There are several types of polyamides and each type is often described by a number, such as polyamide 6, 11, 12, 4.6, 6.10, 6.12... or

polyamide 6.6 (PA66) used in this investigation. The numeric suffixes refer to the number of carbon atoms present in the molecular structures of the amine and acid, respectively (or a single suffix if the amine and acid groups are part of the same molecule). The most common fibres are polyamide 6 and 6.6 and are very similar in properties. The general synthesis reaction for polyamides is shown in Figure 10.

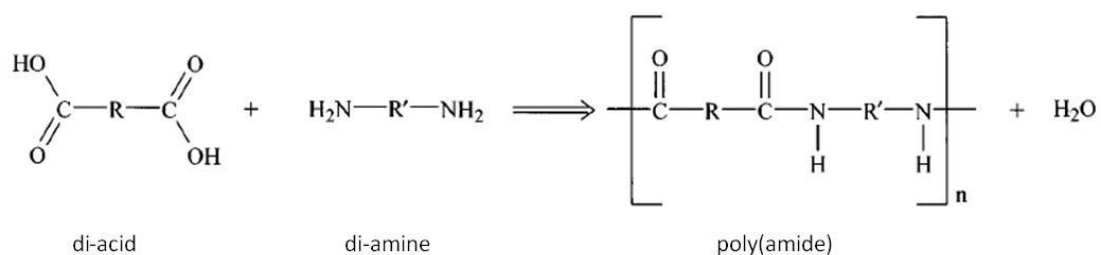


Figure 10: General polyamide polycondensation reaction.

The -COOH acid group reacts with the -NH₂ amine group to form an amide. A molecule of water is given off as the nylon polymer is formed. The properties of the polymer are determined by the R and R' groups in the monomers and the average degree of polymerization. Following Figure 10, in polyamide 6.6, R' =6C and R =4C alkanes, but one has to also include the two carboxyl carbons in the diacid.

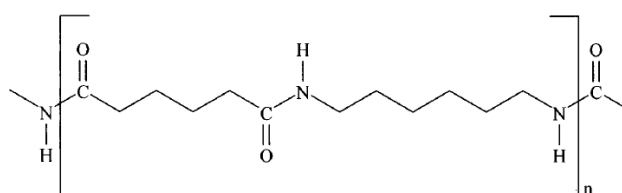


Figure 11: Chemical structure of polyamide 6.6.

Polyamide 6.6 (Figure 11) is prepared by step growth polymerization of hexamethylene diamine and adipic acid. After drying, polyamide 6.6 is melt spun into fibres at 280 °C – 290 °C and drawn to mechanically orient the filaments followed by processes such as thermal stabilization, cutting, spinning, etc.

1.2.1.2. *Physical and chemical properties*

Polyamide 6.6 presents a specific weight of 1.14 g/cm^3 , a glass point transition of $245 \text{ }^\circ\text{C}$ and a melting point of $255 \text{ }^\circ\text{C}$. PA66 is known and usually used for its outstanding balance of mechanical properties, toughness in equilibrium moisture content, chemical resistance and oil resistance, wear and abrasion resistance, long-term heat resistance (at a long-term, continuous, maximum temperature ranging between $80 \text{ }^\circ\text{C}$ and $150 \text{ }^\circ\text{C}$). PA66 also offers high water absorption and outstanding gas barrier properties (Rouette, 2002)

1.2.1.3. *Applications*

Conventional polyamide fibres are usually rodlike with a smooth surface. Polyamides are extensively used in hosiery, lingerie, underwear, sweaters, and other knitted goods such as carpets, tie cord, parachutes, sails, ropes, thread, and outdoor wear.

In this work, a polyamide 6.6 knitted fabric designed as finished elastic-compressive socking was used.

1.2.2. Polypropylene

1.2.2.1. *Structure and classification*

Polypropylene (PP) is the generic name of fibres constituted by linear macromolecules of saturated alifatic hydrocarbons, in which one of every two atoms has a methyl ramification, usually in isotactic configuration $(-\text{CH}_2-\text{CH}(\text{CH}_3)-)_n$ (Figure 12) (Gacén, 1991). It is a thermoplastic polymer synthesized by polymerization of propylene monomers $[(\text{CH}_2=\text{CH}-\text{CH}_3)]$. The relative orientation of each methyl group relative to

the methyl groups on neighboring monomers has a strong effect on the finished polymer's properties.

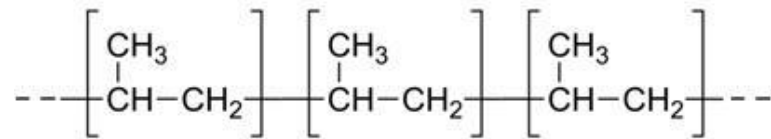


Figure 12: Chemical structure of polypropylene in isotactic configuration.

The polymer is melt, spun into filaments and drawn to orient them. PP enters in a wide range of applications such as packaging, technical textiles, automotive components or in plastic parts of various types.

1.2.2.2. *Physical and chemical properties*

Polypropylene, manufactured according to the melt-spin process and drawn began in 1959. They are important as monofilaments and multifilaments. Polypropylene filaments are strong fibers with good elongation and recovery properties. They present a breaking strength between 2.5–6 cN/dtex with an elongation to break between 15 % and 30% and the fibers recover well from stress, with 95% recovery at 10% elongation. Moisture does not affect these properties, since polypropylene is hydrophobic and has a moisture regain of 0%. They present a softening range of 149–160 °C and a melting point range of 163 –170 °C (Rouette, 2000). The polypropylene is extremely inert and resistant to chemical attack. It is unaffected by chemical and biological agents under normal conditions. Polypropylene fiber only slowly undergoes oxidative decomposition at its melting point (Needles, 1986).

1.2.2.3. *Applications*

Polypropylene is becoming increasingly employed in the textile industry in the form of filaments and fibres. PP is known as a versatile and valuable fibre-forming polymer material. Due to the improvement of their water absorbency and dyeability, the original fields of application (technical textiles, geotextiles, carpet primary backing fabrics, nonwovens) has been expanded, and now, for example, furnishing and decorative materials or swimming costumes and knitgoods are manufactured from texturized polypropylene. (Rouette, 2000). PP is widely used for the production of medical and hygienic products, carpets and floor coverings, apparel and household textiles, filtering media, agro-textiles, automotive interior and many other technical textiles. The wide range of goods comprises a variety of products including mono- and multifilaments, staple fibres, tapes and fibrillated fibres as well as spun-bonded and melt-blown nonwovens. As described in section 1.1.3.2.2, polypropylene has also been implanted in the medical textile field for its biocompatibility and low-degradability and is well established as implantable mesh for abdominal wall and hernia repair or as prosthetic device.

1.3. Cosmetic and pharmaceutical active principles

In this PhD. Thesis different active principles are applied to textiles:

- In the first part, where PA66 elastic-compressive fabrics are concerned, two families of drugs have been selected: Non-Steroidal Anti-Inflammatory Drugs (NSAIDs) for rheumatoid arthritis, where ketoprofen has been chosen, and different methylxantines, in particular caffeine as cosmetic active principle for the treatment of a dermal disorder such as cellulite.
- In the second part, with views on the prevention of surgery-derived infections, an antibiotic, ampicillin, was selected for application in PP meshes.

1.3.1. Anti-inflammatory active principles for topical applications

Drug products topically administered via the skin fall into two general categories, those applied for local action and those for systemic effects. Local actions include those at or

on the surface of the skin, those that exert their actions on the stratum corneum, and those that modulate the function of the epidermis and/or the dermis. Common products in the former category include creams, gels, ointments, pastes, suspensions, lotions, foams, sprays, aerosols, and solutions. Creams, ointments, and gels generally are referred to as semisolid dosage forms (Ueda, 2009). Topical dosage forms include solutions (for which release testing is not indicated), collodion, suspensions, emulsions (e.g., lotions), semisolids (e.g., foams, ointments, pastes, creams, and gels), solids (e.g., powders and aerosols), and sprays. The physical characteristics of these dosage forms vary widely.

The most common drug products applied to the skin for systemic effects are referred to as self-adhering transdermal drug delivery systems (TDS) or transdermal patches. TDS or transdermal patches are physical devices applied to the skin and vary in their composition and method of fabrication. Therefore, they release their active ingredients by different mechanisms. **In the local use, most commercial NSAID patches are frequently applied to the elbows and knees for the remedy of inflammation and joint pains; therefore, flexibility becomes the most important condition for the backing materials of these dosage forms to enable the skin to move in a natural way (Ueda, 2009; Vanniasinghe, 2008). To avoid these constraints, woven and non-woven fabrics, that are the materials on which is focused this PhD. Thesis, could be one way for the use of drug delivery system for local topical applications on the skin.**

Many of the current drugs used for the management of rheumatic disorders and other inflammatory arthritis are nonsteroidal anti-inflammatory drugs (NSAIDs) and corticosteroids (Vanniasinghe, 2008). Recent studies highlight glucocorticoids' (GC) effectiveness in reducing inflammation and slowing joint damage, especially when patients are treated at an early stage of disease propagation (Goekoop-Ruiterman, 2007). However, the toxicity associated with these drugs is also well documented particularly with long-term use and administration (Boers, 2004). For this reason NSAIDs are the most commonly used drugs to reduce pain and inflammation in topical application (Escribano, 2003; Baboota, 2007; Vanniasinghe, 2008).

Oral therapy of NSAIDs is very effective, but its clinical use is often limited because of adverse side effects, such as irritation and ulceration of the gastro-intestinal mucosa. Topical administration of these agents can prevent these side effects associated with oral use and may help to maintain consistent blood plasma levels for long-term therapy from a single dose (Beetge, 2000; Jantharaprapap, 2007; Okur, 2011). Common traditional NSAIDs are: aspirin and ibuprofen which are the most used NSAIDs molecules in oral administration for general anti-inflammatory application (Swarbrick, 2007). Ketoprofen, naproxen (Okur, 2011), diclofenac, etc. are currently used for the treatment of rheumatoid arthritis, osteoarthritis and traumatic contusions in gel dosage form. Two commercial examples include *Voltaren*[®] diclofenac 1% and ketoprofen Powergel[®] 2.5% w/w topical gels.

1.3.2. Anti-lipidic active principles for topical cosmetic applications

Cellulite is the unsightly skin dimpling that is frequently found on the thighs and buttocks of women, and its appearance is often described as resembling the surface of an orange peel. Approximately 85% of post-adolescent women have some degree of cellulite (Draelos, 1997; Sainio, 2000). Many successful cosmetic and medical treatments show little effect in improving cellulite, and none of them has been shown to cause its complete disappearance. The anatomy and pathophysiology of cellulite are poorly understood. A review of the literature demonstrates a lack of studies to validate currently popular theories and treatments. The condition is best described by Goldman as a normal physiologic state in post-adolescent women, which maximizes adipose retention to ensure adequate caloric availability for pregnancy and lactation (Goldman, 2002). Adipose tissue is also essential for nutrition, energy, support, protection, and thermal insulation (Querleux, 2002).

When using topical treatments to reduce the appearance of cellulite, the concentration and pharmacokinetics of the active drugs as well as the nature of the vehicle must be considered. Vehicles can be in the form of gels, ointments, foams,

creams, and lotions, all of which aim to efficiently deliver active product to the skin. Factors that affect the clinical response to treatment are: (i) the interaction of the drug with the vehicle and the skin, (ii) the method by which the drug is applied, and (iii) other biological and environmental factors (Addicks, 1989; Hadgraft, 1993; Riviere, 1993). The main barrier to drug penetration is the stratum corneum, the cornified outermost layer of the epidermis. Formulations for topical use may include “skin enhancers,” which significantly increase cutaneous penetration when included in the formulation. Skin enhancers can be common solvents (water, alcohol, and methyl alkyl sulphoxide) or surfactants. They may also be phospholipid molecules called phytosomes, which, when attached to the active drug, increase their lipid solubility. Also percutaneous delivery systems utilize liposomes, which are specially designed lipid vesicles that are filled with active medication (Zatz, 1993; Seiller, 1994). Topical anticellulite preparations can be divided into four major groups according to their proposed mechanism of action (Hexler, 2006):

1. Agents that increase microvascular flow.

This includes most of the active ingredients in cellulite treatments. They are included to increase microvascular flow and lymphatic drainage, which is thought to play a role in cellulite pathogenesis.

2. Agents that reduce lipogenesis and promote lipolysis.

With the goal of reducing the size and volume of adipocytes, decreased tension on surrounding connective tissue is thought to decrease the clinical appearance of puckering.

3. Agents that restore the normal structure of the dermal and subcutaneous tissue.

By thickening the dermis or preventing fat herniation into superficial tissue, the appearance of cellulite may be reduced.

4. Agents that prevent or destroy free-radical formation.

It is believed that free radicals modify free fatty acids by peroxidation, contributing to the availability of lipids for cellulite formation. Free radicals may also damage elements of the microcirculation, further assisting cellulite development.

Table 4: Topical therapies for cellulite based on the proposed mechanism of action, from Hexsler, 2006.

Topical Therapies for Cellulite

Agents that increase microvascular flow

- Ivy
- Indian or horse chestnut (*Aesculus hippocastanum*)
- Ginkgo biloba
- Rutin
- Pentoxifylline
- Butcher's broom (*Ruscus aculeatus*)
- Asiatic centella
- Silicium
- Chofitol or artichoke (*Cynara scolymus*)
- Common ivy (*Hedera helix*)
- Ground ivy (*Glechoma hederaceae*)
- Sweet clover (*Melilotus officinalis*)
- Red grapes (*Vitis vinifera*)
- Papaya (*Carica papaya*)
- Pineapple (*Ananas sativus*, *Ananas comosus*)

Agents that reduce lipogenesis and promote lipolysis

- Methylxanthines (theobromine, caffeine, aminophylline, theophylline)
- Beta-adrenergic agonists (isoproterenol, adrenaline)
- Alpha-adrenergic antagonists (yohimbine, piperoxan, phentolamine, dihydroergotamine)

Agents that restore the normal structure of the dermal and subcutaneous tissue

- Retinol (vitamin A)
- Ascorbic acid (vitamin C)
- Bladderwrack (*Fucus vesiculosus*)

Agents that prevent or destroy free-radical formation

- Alpha-tocopherol (vitamin E)
- Ascorbic acid (vitamin C)
- Ginkgo biloba
- Red grapes (*Vitis vinifera*)

In this PhD. Thesis, the research will be focused on caffeine and other compounds of the methylxantine family (caffeine, theobromine and theophylline) that act on the reduction of lipogenesis and promote lipolysis. These act through phosphodiesterase inhibition and are the most common active ingredients in commercial anticellulite formulations (Collis, 1999). **The most useful and safest methylxanthine is caffeine, normally used at a concentration of 1% to 2% in topical gel forms.** Whereas the solubility of caffeine in water is 2.2%, commercially available topical creams prepared with co-solvent systems can reach 3% caffeine content (Dias, 1999; Amnuakit, 2008; Amnuakit, 2011).

Beside its widely known pharmacological effects on the central system and others (Ritchie, 1975), caffeine has been correlated with reduced adiposity through stimulation of lipolysis by increased expression of adiponectin and lipid oxidizing enzymes (Yun, 2008). This methylxantine has an important first-step metabolism (Liguori, 1997), which has justified investigation on topical treatment (Batchelder, 2004). The combination of both parameters is related to its use as active principle in cosmetic formulations with views on treating cellulite (Bolzinger, 2008). **Caffeine offers good skin penetration and is therefore rapidly absorbed, leading to rapid action. It acts directly on adipocytes, promoting lipolysis through the inhibition of phosphodiesterase (Portad, 1999). All methylxanthines activate the enzyme triglyceride lipase and transform triglycerides into free acids and glycerol. Caffeine also has a stimulating effect on the cutaneous microcirculation (Hexsler, 2006).** Therefore, caffeine is found in a number of commercial preparations, mostly as a hydrophilic gel, for the treatment of skin disorder (e.g. *Somatoline Cosmetic*[®] gel), or for the reduction of puffy-eyes, applying around the eyes since it can provide clear appearance, cooling effect and non-greasy feeling (Dias, 1999; Dreher, 2002; Boonme, 2007; Amnuakit, 2008; Amnuakit, 2011).

In literature, different products can also be found products which are based on the combination of different active agents to reduce cellulite. Bertin et al. described a product combining retinol with a microencapsulated time-release mechanism to treat

cellulite. The compound contains **caffeine** to stimulate the lipolysis and prevent fat accumulation, esculoside to improve local microcirculation, asiatic centella as an anti-inflammatory agent, and l-carnitine to stimulate free fatty acid transport and breakdown (Bertin, 2001). Efficacy parameters included cellulite appearance before and after treatment, histology, cutaneous flowmetry, and skin mechanical characteristics. The product also contains ruscogenine, which inhibits elastase activity, allowing recovery of extracellular matrix integrity that contributes to the thickening of the dermis and the masking of cellulite.

In this PhD. Thesis, caffeine and other methylxantines molecules (theobromine and pentoxifylline) are directly loaded into the polyamide 6.6 fibres from an aqueous solution, and low temperature plasma is used to modulate the interaction between the drug and the textile support.

1.3.3. Antibiotic-loaded fibres for implantable textiles

The use of antibiotics for textile-based drug delivery systems is oriented for implantable meshes. Postoperative antibiotic-based infection prophylaxis is usually administered following mesh implantation. But, even after decades of routine use, its capacity to minimize mesh-related infection is still a matter of debate (Aufenacker, 2004; Hedrick, 2007; Taylor, 1997). Because management of infections associated with surgical implants can be both difficult and costly, prevention of such infections remains a priority. Preventive strategies comprise systemic perioperative administration of antibiotics and local application of antimicrobial agents (antibiotics or antiseptics). Local antimicrobial prophylaxis can be provided in various forms and aims to prevent implant-associated infections by impeding bacterial adherence to the implant surface and/or reducing the concentration of bacteria in the immediate vicinity of the implant (Darouiche, 2003).

One of the new trends in biomedical research is to deliver active compounds directly into the surgical site from the medical device (Shukla, 2010; Wu, 2006). The main

objective of these new active prostheses is not only to restore a damaged function, but to also prompt tissue integration (Chen, 2005; Maciver, 2011; Steigerwald, 2009), avoid periprosthetic inflammation (Chen, 2003; Junge, 2005a) and prevent surface contamination (Blanchemain, 2008; Gomez-Alonsa, 2007; Junge, 2005b) (Guillaume, 2012).

There is a need for a system including antibiotics directly to the mesh, or via some antibiotic encapsulated-based nano-carrier (Fu-Giles, 2013), to treat and alleviate post surgical and post-transplantation infections, particularly in reaction to body implants. This approach provides a novel therapeutic approach, more efficient, with effective doses for the prevention and treatment of bacterial, fungal and viral infections that are often associated with implants. This design of such specific targeting drug delivery system also aims to reduce undesired side effects. It also eliminates the time that otherwise is needed for the drugs to be processed by the liver. Therefore, a reduced amount of the drug will produce comparable beneficiary effects compared to the amount of drug usually required for intravenous or oral administration. Furthermore, such kinds of delivery systems can be customized based on the needs of the patient by varying the entrapped antibiotics/drugs.

Depending on the body implant, suitable antibiotics reported in literature include rifampicin, chloramphenicol, novobiocin, spectinomycin, trimethoprim, erythromycin, doxycycline, minocycline, vancomycin, acyclovir, amphotericin B, gentamicin, gentamicin sulfate, tobramycin, **ampicillin**, penicillin, ethambutol, clindamycin, and cephalosporins including pharmacologically acceptable salts and acids thereof (Fu-Giles, 2013).

In this PhD. Thesis, ampicillin, a β -lactam antibiotic that is active against both gram-positive and gram-negative bacteria widely used clinically for the for the treatment of a broad range of bacterial infections (Mandell, 1990; Queiroz, 2001; Carafa, 2004) has been used as antibiotic for its application in implantable PP meshes.

1.4. Modification of textile materials by plasma treatment

Synthetic polymer textile fibers have a lot of advantages such as high chemical stability, good mechanical properties, etc. However, despite these advantages, polymers have limitations. In general, special surface properties with regard to chemical composition, adhesion, hydrophilicity, roughness or conductivity are required for successful application of polymers in such wide fields as adhesion, coatings, thin-film technology, biomaterials, and so on. Unfortunately, polymers very often do not possess the surface properties needed for these applications. In fact, polymer fibers that are mechanically strong, chemically stable, and easy to process usually will have inert surfaces both chemically and biologically. Due to this dilemma, surface modification of the polymer fibers with low-temperature plasma without altering the bulk properties has been a classical research topic during the last years, and is still extensively studied as new applications of polymeric materials emerge, especially in the fields of biotechnology, bioengineering, and in nanotechnology.

The main hypothesis of this PhD. Thesis regards the drug incorporation and release from the surface of the polymer fibers, which is related to the interaction of the drug with the polymer and probably greatly depends on the surface chemistry of the fiber. Plasma technology is a tool that allows modifying physical and chemical properties of a material's surface such as the textile fibers. The novelty of this investigation rests upon the implementation of plasma technology to medical and sanitary textiles aimed at constituting new drug delivery systems. **The treatment of the textile material by plasma technology fits the aim of modifying the interactions drug/fiber and modulating its incorporation to the fibre and the release of the antibiotic from the fiber of the textile-based drug delivery systems.** In the following sections, low-temperature plasma is described, and the state of the art regarding the modification of textiles is reviewed.

1.4.1. Plasma definition

The physical definition of a “plasma” is a state of mixed ions, free radicals, electrons, excited molecules, UV and visible radiation that preserves electrical neutrality. Plasmas can exist over an extremely wide range of temperature and pressure. Atmospheric pressure plasmas (APP) or low-temperature plasmas (LTP), used in this research work, are generated by gaseous electric discharges, they provide a source of high-energy electrons without excessive heating and are highly reactive chemically (Ward, 1982; Inagaki, 1996). The interactions of the electrically charged particles with each other, with the neutral gas and with contact surfaces produce the unique physical and chemical properties of the plasma environment. This environment is distinct from that found in solids, liquids or gases; hence plasmas are usually called the 4th state of the matter.

1.4.2. Plasma in nature and laboratory devices

Although some phenomena related with plasma had already been described before, plasma was first defined by W. Cookes in 1879 as electrically charged gas molecules or ions. However, it was Langmuir in 1923 who gave the name plasma to the 4th state that occurred when a gas at low pressure was submitted to an electric field. Since then, many efforts have been done in order to understand better the plasma state but also in order to use plasma as a tool for processing technology.

Much of the visible matter in the universe is in the plasma state. This is true because stars, as well as all visible interstellar matter, are in the plasma state. As described in Figure 13, plasmas are classified as a function of their electron number density and their generation temperature.

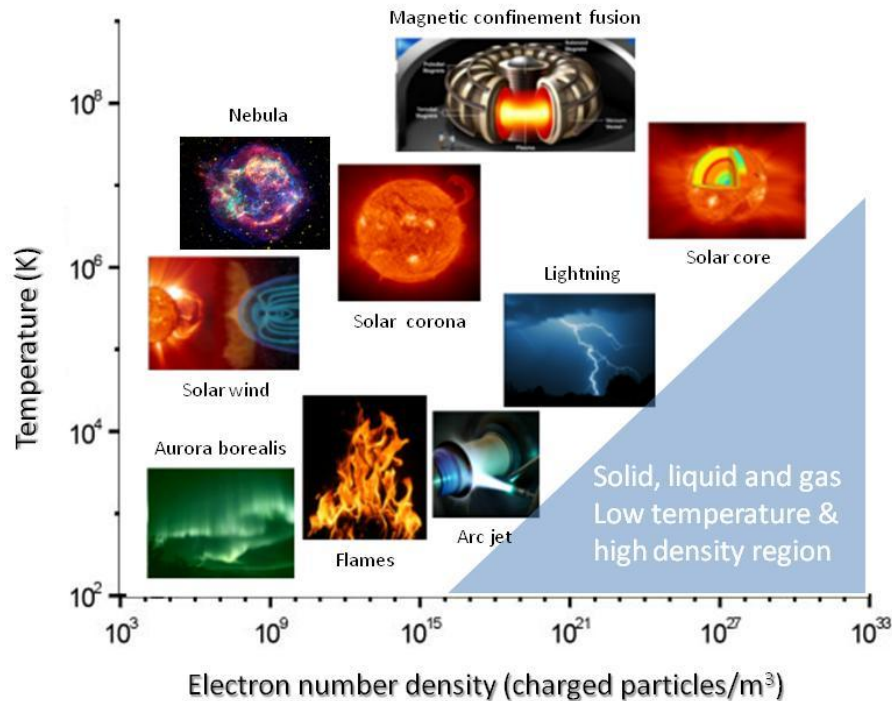


Figure 13: Classification of plasmas in nature as a function of generation temperature and electron number density.

Besides the astro-plasmas, which are omnipresent in the universe, two main groups of plasmas can also be distinguished, i.e. the high-temperature or fusion plasmas, and the so-called low-temperature plasmas or cold plasmas (Bogaerts, 2002). Cold plasmas are divided in thermal plasmas, which regroup arc plasmas or plasma torches, and non-thermal plasmas, which include laboratory plasmas such as corona plasma, glow discharge, dielectric barrier discharge, low-pressure plasmas, etc. (Figure 14). The latter group of plasmas is the one that includes the plasmas used for this investigation.

Cold plasmas can be obtained at an experimental level, from a gaseous media combined with an adequate power source. A gas is normally an electric insulator. However, when a sufficiently large voltage is applied across a gap containing a gas or gas mixture, it will break down and conduct electricity. The reason is that the electrically neutral atoms or molecules of the gas have been ionized, i.e. split into negatively charged electrons and positively charged ions.

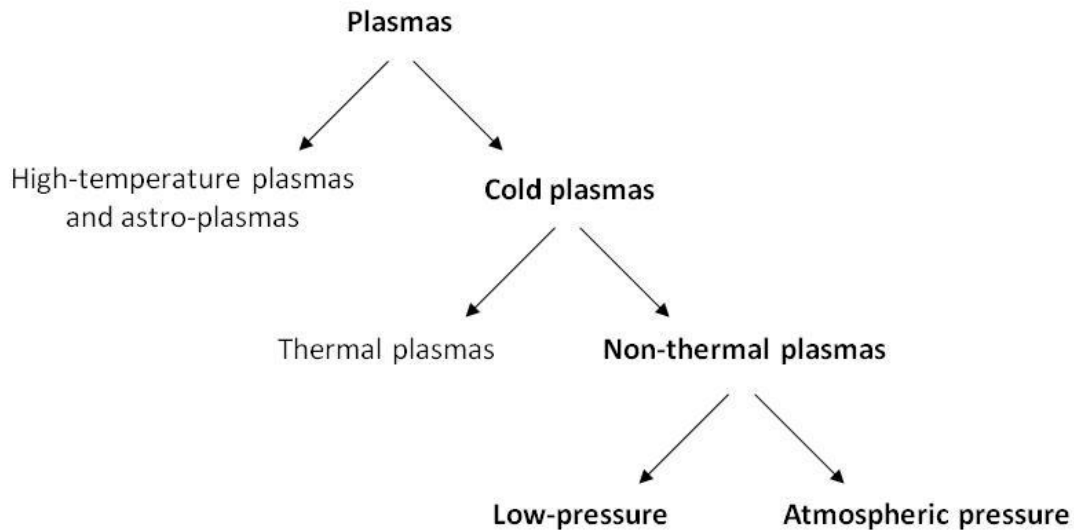


Figure 14: General classification of plasmas.

The nature of the breakdown and the voltage at which this occurs varies with the gas species, gas pressure (from low pressure to atmospheric pressure), gas flow rate, the materials and the geometry, nature and separation of the electrodes across which the voltage is sustained, the separation distance of the electrodes, the nature of the high voltage supply and the actual electrical circuitry. The resulting ionized gas is often called a discharge, low-temperature or cold plasma. The main effects of cold plasmas on a material's surface in the first nanometers on the material surface (described in details in section 1.4.4) are:

- Functionalization (covalent bonding of new chemical moieties)
- Etching (elimination of material from the surface)
- Thin film deposition (deposition of thin layers)

1.4.3. Plasma reactors in research and at industrial level: Cold plasmas

Cold plasmas can be used for various surface treatments such as: cleaning, surface activation, functionalization, plasma polymerization (gaseous monomers); grafting; deposition of polymers, chemicals and metal particles by suitable selection of gas and process parameters. They are commonly used for their low temperature ensuring the

preservation of the treated material and for being a dry process without the use of any chemical, avoiding the generation of wastewaters, to achieve the desired physical and chemical modification of a surface.

Plasma reactors can be classified as a function of their power supply and applied frequency in:

- Low-frequency reactors between 50 and 450 kHz,
- Radio-frequency reactors at 13.56 MHz or 27.12 MHz,
- Microwave reactors when the frequency achieves 915 MHz or 2.45 GHz.

The power required may range from 10 to 5000 watts, depending on the size of the reactor and the desired treatment (Shishoo, 2007). In these types of generators, plasmas are produced when energy is transferred by an electric field to free electrons within a low-pressure environment (Lichtenberg, 1994).

Plasmas can also be classified as a function of the working pressure into low-pressure plasma or atmospheric pressure plasma.

1.4.3.1. Low-pressure plasmas

On the one hand, in low pressure plasmas, a vacuum chamber (or vessel) is pumped down to a pressure in the range of 10^{-2} to 10^{-3} mbar (or below) with the use of high vacuum pumps. The gas which is then introduced in the chamber is ionized with the help of a high frequency generator or an AC power supply. The advantage of the low-pressure plasma method is that it is a well-controlled and reproducible technique (Shishoo, 2007). This kind of plasma has been used in this PhD. Thesis. Cold plasmas are a mature technology originally developed for the microelectronics industry but now applied to a wide variety of fields. However, low-pressure plasma systems require an expensive and complicated vacuum environment (Liston, 1993).

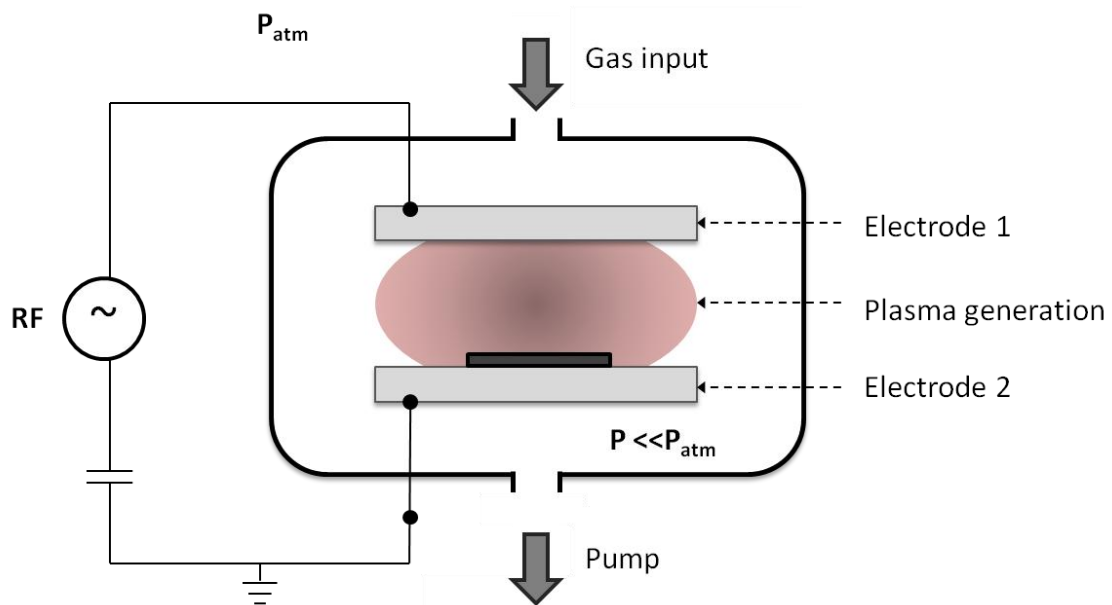


Figure 15: Scheme of a low-pressure plasma reactor.

1.4.3.2. Atmospheric pressure plasmas

On the other hand, atmospheric pressure plasmas regroup corona plasmas and dielectric barrier plasmas. Atmospheric pressure plasma devices have been developed to overcome the drawbacks of low pressure plasma treatment in which a vacuum system is required. Typical atmospheric pressure plasma systems are corona discharges, dielectric barrier discharges (DBD) and plasma torches (Jeong, 1998; Jeong, 1999; Shishoo, 2007).

Corona treatment

Corona discharge is characterized by sharp bright filaments extending towards the substrate, due to the high-voltage between two electrodes. Corona treatment is the longest established and most widely used plasma process; it has the advantage of operating at atmospheric pressure, the reagent gas usually being the ambient air (Shishoo, 2007). Corona systems have the manufacturing requirements for the textile industry (width, speed, etc.), even if in this type of plasma the spectrum of surface

functionalization of materials is not as broad as the low-pressure plasmas. Corona systems also rely upon very small inter-electrode spacing (millimeter scale) and accurate web positioning, which are incompatible with ‘thick’ materials (Figure 16). This type of plasma has been used in this PhD. Thesis for the treatment of polyamide and polypropylene fibres.

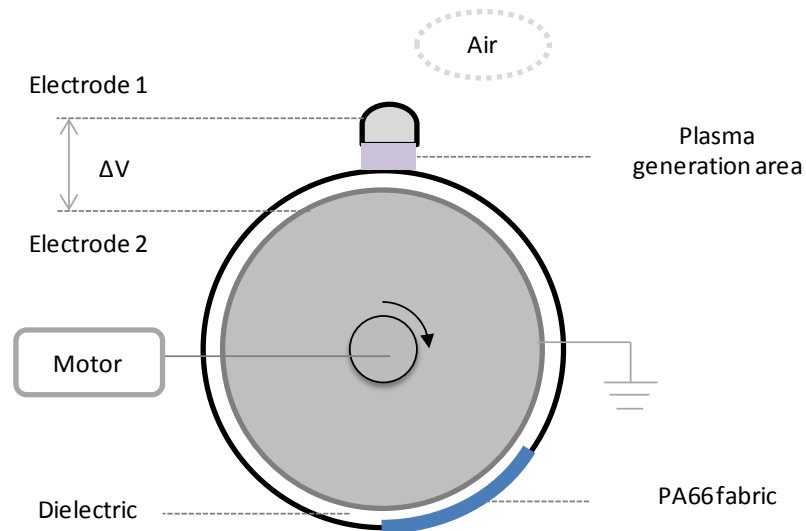


Figure 16: Scheme of an atmospheric plasma reactor: corona system of potential use in the textile industry.

Dielectric barrier discharge (DBD)

Dielectric barrier discharge is a broad class of plasma source that has an insulating (dielectric) cover over one or both of the electrodes and operates with high voltage power ranging from low frequency to 100 kHz. This results in a non-thermal plasma and a multitude of random, numerous arcs form between the electrodes. However, these micro-discharges are non-uniform and have potential to cause uneven treatment.

1.4.4. Plasma applied to polymeric surfaces and fibers

The surface modification of polymers using plasma technology has increasingly attracted attention in the recent years. Plasma treatments are an effective way to modify the wettability (or hydrophilicity) and the topography of the first nanometers of a polymer surface without affecting the bulk properties (Qui, 1993; Qiu, 2002a; Qiu, 2002b; Okuno, 1992, Wakida, 1993; Wakida, 1998; Holländer, 1999; Liu, 2006; Ren, 2007). The goal of surface treatment is to modify the interactions between the material and the environment. Surface properties of polymers and textiles can be modified by atmospheric or low-pressure plasma. Physical and chemical properties of a solid surface significantly affect adhesion, wetting, friction, anticorrosion and light reflection. Low-pressure and atmospheric plasma treatments are attractive for several reasons: they allow modification of the surface layers up to a depth of several nanometers of the substrate while maintaining its bulk properties, they can achieve the desired surface polarities, their low temperature avoids sample damage, they are of a dry, environmentally friendly nature (Shishoo, 1996) and they offer new research areas, in particular in material sciences.

Atmospheric plasma technology is well established in different industrial applications. In the last decades, the plasma technology has been studied in the textile industry as well. Fields of application are desizing, functionalizing, and modification of fabric surface properties for different applications, among others, such as textile digital printing, functional finishes, etc. Applied to the textile field, plasma technology is suitable to modify the surface chemistry as well as the topography of the surface of the fibres. Therefore, plasma treatment on textiles can be used to give hydrophilic properties to a hydrophobic surface. This increased wettability can enable a better incorporation of chemical components into the fabrics. Modified wettability is one of the most apparent results of plasma treatment. Plasma-produced polar groups increase the surface free energy (γ) of the fibre and decrease the contact angle (θ), usually correlating with better bonding of adhesives; θ has often been used as an approximation to evaluate adhesion and wetting behavior (Shishoo, 2007).

Literature reports different treatment times used for surface modification of polymers ranging from milliseconds (Borcia, 2003; Borcia, 2004) to several minutes. A millisecond treatment often causes oxidation and removal of surface contaminants which is often sufficient to improve surface wettability. A further treatment usually causes chemical bonding of oxygen atoms at active sites on the polymer surface, leading to formation of various functional groups that modify the surface wettability. With prolonged treatment time excessive chain scission may appear leading to a layer of low-molecular-weight fragments on the surface (Strobel, 1994). Also, prolonged treatment often causes chemical etching of polymer materials, increased sample temperature and eventual irreversible damage of the bulk properties. In many cases, the longer exposure of the surface, not only of polymers, leads to creation of various nanostructures (Cvelbar, 2003; Chen, 2008; Mozetič, 2005; Ostrikov, 2007; Tam, 2006; Xu, 2005, Vessel, 2009).

The type of gas and working parameters of the plasma treatment (time, power, pressure, etc.), as well as the fabric pre-treatment and its initial state, condition the effects obtained on the sample. This enables a variety of generic surface processes and effects such as surface activation by bond breaking to create reactive sites, grafting of chemical moieties and functional groups, material volatilization and removal (etching), dissociation of surface contaminants/layers (cleaning) and deposition of thin layers.

Gases usually used for plasma treatments can be:

- Chemically inert (e.g. helium and argon)
- Reactive and non-polymerisable (e.g. ammonia, air, nitrogen, oxygen)
- Reactive and polymerisable (e.g. tetrafluoroethylene, hexamethyldisiloxane).

In the course of this PhD. Thesis, the three different kinds of gases are employed.

The interaction of cold plasmas with polymer surfaces involves both gas and surface reaction mechanisms. The gas-phase reactions in the discharge volume leads to the production of species including atoms, molecules, free radicals, ions of both polarities, electrons, photons and excited species in different electronic, vibrational and

rotational states. Depending on the energy and the reactivity of the plasma-created species with respect to each other and with respect to the polymer surface, recombination on the surface, deposition process or etching of the polymer take place (D'Agostino, 2008).

Polymer materials subject to plasma treatments undergo major chemical and physical (China, 2012) and both surface chemistry and surface topography may be affected, and the specific surface area of fibres can be significantly increased. The main effects that can be produced by plasmas are described in the following sections.

1.4.4.1. Etching and surface cleaning

Plasmas create a high density of free radicals by dissociating molecules through electron collisions and photochemical processes. This causes the disruption of the chemical bonds in the fibre polymer surface which results in the cleaning of the material surface and in the formation of new chemical species.

Plasma etching or ablation is essentially used to remove material from a surface. It can be conducted with a variety of discharge sources, such as direct current glow discharges or RF discharge. The three important parameters for etching are: etched rate uniformity, anisotropy and selectivity. Usually, surface etching reactions are carried out to improve wettability of material surface and favor the formation of weak boundary layers.

One can take advantage of this ablation effect of plasmas to eliminate deposited materials or contaminant layers often existing on the surface of polymers (Figure 17). This layer could be due to polymer processing products and finishing additives such as antistatic agents, lubricants (mineral oil, polyolefin waxes, fatty acid esters, etc.), antioxidants (phenols, amines, mercaptans, etc.), and light-protecting agents. Furthermore, the large molecular weight polydispersity of the polymer chains is also a

problem, and the presence of remnants of the initial monomers, oligomers, and solvents can never be excluded. Such compounds can be present over a thickness of 1 to 10 nm and can constitute a weak boundary layer responsible for a great number of adhesion failures in different polymer assemblies with other materials (Bikerman, 1961; Bikerman, 1968).

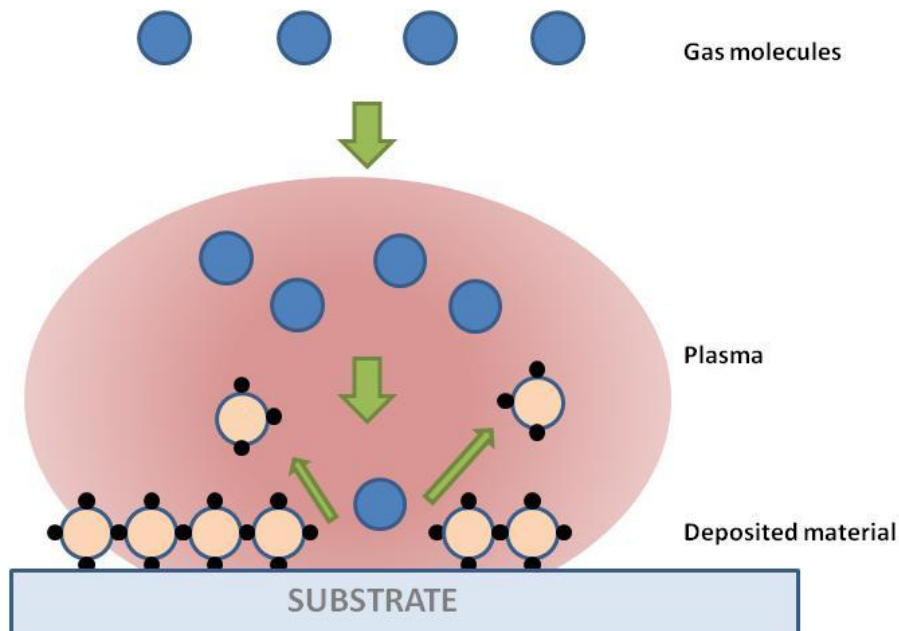


Figure 17: Scheme of plasma etching of materials from the polymer surface.

Plasma cleaning is an economical process if the build up of the contamination layer is not too massive, i.e. well below 1 mm. Depending on the type of contamination (oxidized surface, deposited material, etc.), different plasmas have been proposed: inert gases such as Ar to remove different contamination layers by sputtering, oxygen plasmas to oxidize organic contaminants, and hydrogen plasmas to reduce inorganic contaminants such as oxides or sulfides (Krüger, 1999).

1.4.4.2. Surface activation

The reaction of the polymer with the plasma-created species leads to bond cleavages of the polymer backbone, i.e. C–C and/or C–H bonds which results in the formation of

radicals in a process known as surface activation. Since all surfaces exposed to a plasma establish a negative potential (Grill, 1993; Lichtenberg, 1994), the positive ions in the plasma play a significant role in such processes. The ultraviolet radiations also contribute to the production of free radicals (Holländer, 1999). The activation step is shown below in the case of the simplest polyolefins, i.e. polyethylene giving rise to alkyl radicals:

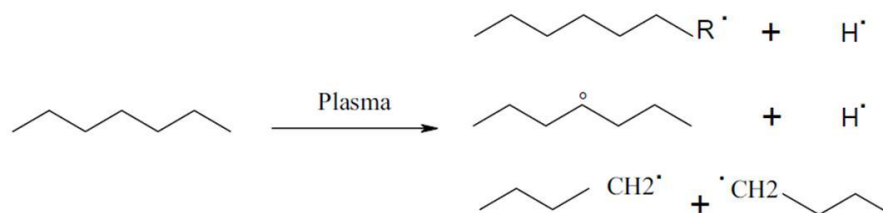


Figure 18: Activation step in the case of the polyethylene giving rise to alkyl radicals.

These free radicals which are characterized by short lifetimes (Kuzuya, 1998) can then go through various chemical reactions involving plasma species (grafting or functionalization) in situ, result in cross-linking of the polymer layer (D'Agostino, 2008), or react with air in the gas extraction from the plasma reactor.

The activation stands for the formation of polar functional groups on the polymer surface. Standard polar functional groups formed on a polymer surface after surface activation are C–O, C=O, O–C O, i.e. oxygen is bonded to carbon atoms, (partially) substituting hydrogen originally bonded to carbon atoms (Occhiello, 1991; Hody, 2006). Oxygen may also break double bonds C=C to form the functional groups. In any case, the appearance of functional groups and resulting modification of surface properties of polymer materials are usually due to interaction of oxygen with surface carbon radicals (Cvelbar, 2007).

1.4.4.3. Functionalization reactions

Surface functionalization by plasma processes can be defined as the grafting of new chemical moieties to the surface substrate by covalent bonding. The selection of the

type of gas for plasma generation depends on the subsequent application of the treated material and the type of bond desired.

Functionalization of polymer surfaces by plasma treatment can be of two types (Figure 19):

- A specific functionalization, being a process leading to the formation of functional groups, by bromination, fluorination, etc.
- An unspecific functionalization, as the formation of different oxygen-containing groups by exposure to air or oxygen plasma, like the plasma treatments using air as gas for plasma generation performed in this PhD. Thesis.

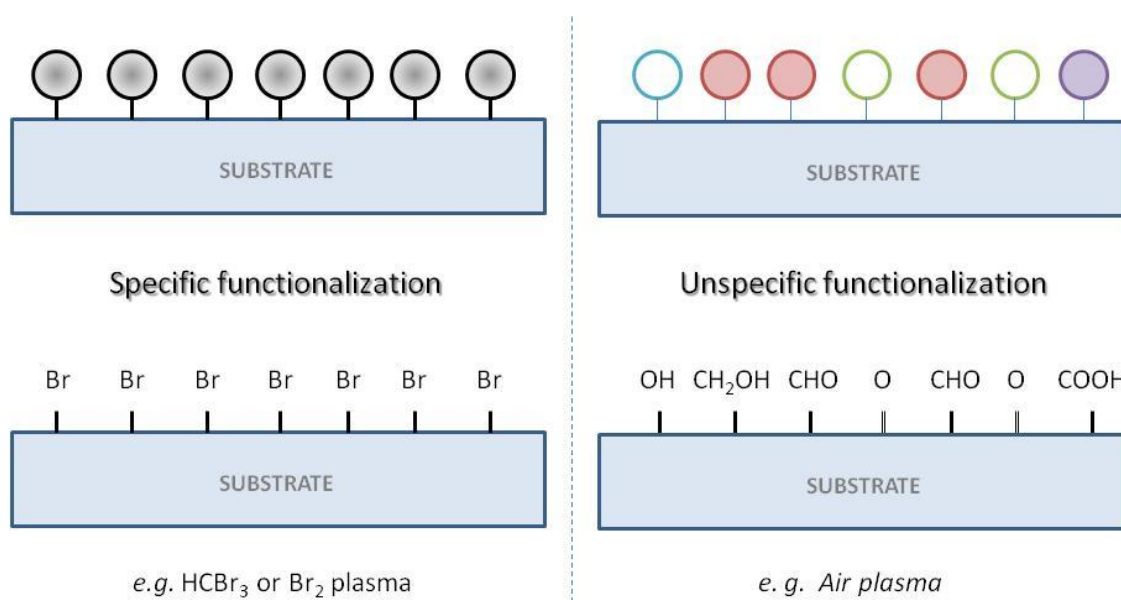


Figure 19: Concept of specific functionalization and unspecific functionalization of a polymeric surface by plasma treatment.

Even for specific functionalization, that can show a selectivity >85%, it should be noted that plasma treatment usually does not produce only one type of a functional group on a polymer surface. Typically, several different functional groups appear on the surface of polymer during plasma treatment. It is therefore necessary to apply such plasma that facilitates formation of the functional groups that are most important for a given application and to attempt to shift the distribution in favor of a specific functionality by changing plasma parameters (Gerenser, 1996).

The surface tension (also called surface energy) of many polymers is rather low due to the lack of polar functional groups in the material. A broad range of surface energy can be achieved by using appropriate plasma for polymer treatment, from extreme hydrophilicity to significant hydrophobicity. **The type of gas used for plasma generation and plasma working conditions influence the type of functionalization, enabling a variety of generic surface wettability for a same polymer.** Increased hydrophobicity is usually achieved by application of plasma rich with fluorine (Yasuda, 1984), while hydrophilicity is often achieved using oxygen plasma. In some applications, especially to increase the biological compatibility of organic materials, nitrogen or ammonia plasma gives better results (Meyer-Plath, 2003).

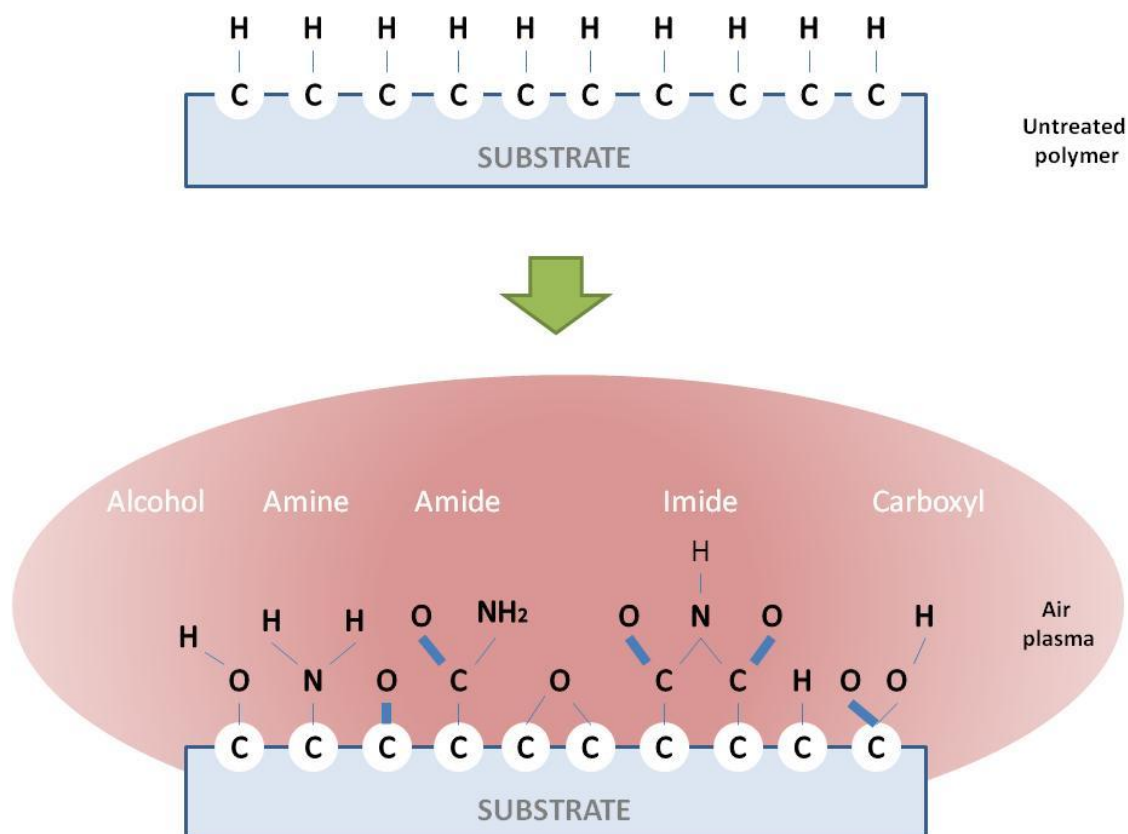


Figure 20: Scheme of polymer surface functionalization by plasma processes using air as gas for plasma generation.

Oxygen and air plasma treatments usually lead to the formation of different functional groups such as C-O, C=O, O=C-O. Sometimes, other groups can be produced on the surface of some polymers, like imides, amines, amides, etc. (Gerenser, 1996; Strobel,

1994) (Figure 20) due to the presence of N₂ in the air. Reactive particles created in oxygen or air plasma react with organic materials at certain rates. The rates depend on the type of polymer and particle as well as the sample temperature and particles kinetic temperature. High oxidation selectivity for different types of organic materials can only be obtained with cold plasmas (Vessel, 2009).

1.4.4.4. Plasma polymerization

Besides the surface activation, the introduction of functional groups or the etching of the polymer fibers surface, plasma can be used for the deposition of thin polymer films by the so-called plasma polymerization. Coating by plasma polymerization is defined as the formation of polymer materials, on a surface, under the influence of plasma conditions. It refers to the deposition of polymer films due to the excitation of an organic monomer in gas state and subsequent deposition and polymerization of the excited species on the surface of a substrate. Polymers formed by plasma polymerization are, in most cases, highly branched and highly cross-linked. The deposition of solid polymer coatings under plasma conditions has been well studied since the 1960s, with a very wide range of materials now accessible (Yasuda, 1985).

Before plasma polymerization, a previous surface activation step by plasma reaction is generally carried out to remove contaminants or finishing agents from the surface and to generate surface radicals which may then react with the precursor monomers and generate a stronger bond on the surface. In the plasma polymerization process, a monomer gas is pumped into a vacuum chamber where it is polymerized by a plasma to form a thin film on the surface. The monomer, which starts out from a liquid fed into an external recipient, is converted to a gas in an evaporator or dragged by bubbling with an inert gas, and is pumped into the vacuum chamber. A glow discharge initiates the polymerization. The excited electrons created in the glow discharge ionize the monomer molecules. The monomer molecules break apart creating free electrons, ions, excited molecules and radicals. The radicals absorb or react with the previously activated surface, condense, and polymerize on the substrate. The electrons and ions

crosslink, or create a chemical bond, with the already deposited molecules to form a polymer (Figure 21).

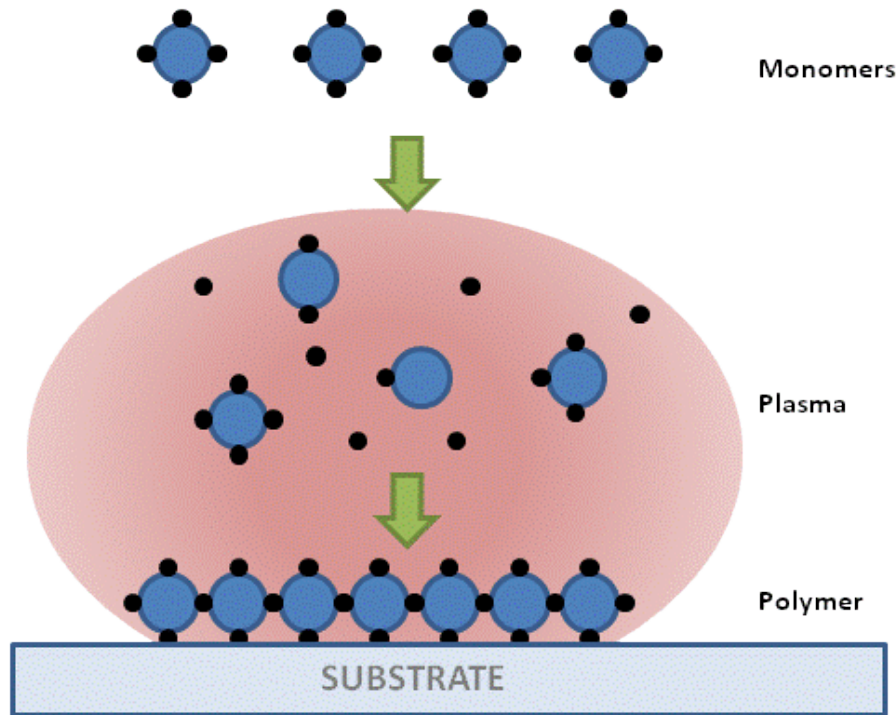


Figure 21: Scheme of plasma polymerization process.

The selection of monomers for plasma polymerization will determine the polymers produced on the surface. For biomedical applications, the monomer selected should yield biocompatible plasma polymers. In the present work, we have investigated the possibility of applying a biocompatible polymer to the surface of polypropylene meshes.

1.4.4.5. *Thin film deposition*

Plasma technology can also be used for thin film deposition. Using Physical Vapor Deposition (PVD), a film can be formed by atoms directly transported from a source to the substrate through gas phase by evaporation (thermal evaporation or e-beam evaporation), sputtering or reactive PVD. Another way to obtain plasma-assisted thin

film deposition is by Chemical Vapor Deposition (CVD), in particular Plasma-Enhanced CVD (PECVD), in which the film is formed by chemical reaction on the surface substrate.

Both types of techniques are widely used to performed metallization of surfaces and are broadly develop in microelectronic industry. The last years, plasma assisted-PVD and CVD have also found attraction in textile investigation (Gulrajani, 2011). Ultra thin layers on textile can be developed by using plasma either in PVD or PECVD. For example, PVD has been used for Indium-Tin-Oxide coating of nonwoven fabrics (Wei, 2010) or for the coating with copper to produce an antimicrobial finish on cotton textiles of a 60-70 nm thickness (Vihodceva, 2011) while PECVD has been used to obtain thin uniform coating of poly(allyl alcohol) on silk, wool and cotton fibres (Malkov, 2010), or PECVD of TiO₂ films on cotton knits has been reported for photocatalytic applications (Szymanowski, 2005).

1.4.5. Plasma treatments in the textile field

As shown in the previous section, the main effects of plasma treatment using gas for plasma generation as unique reactive on polymer surfaces usually results in the formation of new functional groups (such as —OH,—C=O, —COOH in the case of oxygen-containing plasma gas) combined with the elimination of surface contaminants, which affect fabric wettability as well as facilitate graft polymerization. All these effects, combined with the advantages of being a dry technology which avoids the use of chemicals and does not produce any wastewaters, have lead plasma technology to be incrementally implemented in the recent years in the textile industrial field to create new technical textiles, to modulate the wettability of natural and synthetic fibres, to improve the adhesion or shrink resistance of fabrics or to improve textile manufacture processes.

Until today, plasma technology has been studied in the textile field for specific applications. The first studies to modify textile fibres were carried out in the 1960's by

Anderson et al. who used ionic bombardment ablation to prepare synthetic fibres for electron microscopy studies (Anderson, 1960). The first experiment in which low-pressure plasmas were applied to textiles was in the 1970's. By using Ar and volatile monomers, thin films were deposited on polyester, polyamide 6.6 and wool fabrics (Byrne, 1972).

Since these initial experiments, a wide range of plasma applications for modification of textile fibres properties have been investigated. It was applied in particular to increase color depth of dyestuffs on wool, silk (Ryu, 1991), polyamide (Ryu, 1992) and aramide (Kobayashi, 1995) fabrics, to increase the wettability of wool fabrics (Kan, 1998a; Kan, 1998b; Rouette, 2001; Kim, 2002), or to improve their shrink resistance (Zuchairah, 1997; Erra, 1999). It has also been studied to produce water repellent fabrics by means of CF₄ plasma (Yasuda 1984) or to improve the adhesive properties of both natural and synthetic fabrics (Rakowski, 1982; Wakida, 1996a); in dyeing processes to increase the color intensity of the fibres (Hirano, 1984) or the dyeing kinetics (Wakida, 1996b; Wakida, 1998; Yip, 2002a; Yip, 2002b). However, until now, investigation on plasma technology has been mostly applied to textiles for conventional textile applications but, to our knowledge, never to incorporate active principles in textile materials.

One of the first works on polypropylene fibers describing low temperature plasma treatments, was a study of the modification of the topography and the roughness of RF plasma treated polypropylene with several gases and at different treatment times and RF-potentials (Collaud Coen, 1996). Plasma treatments with reactive gases (N₂, O₂) lead to the incorporation of new chemical species on the PP surface, whereas plasma treatments with noble gases (He, Ar, Xe) induced the desorption of hydrogen and a graphitization (Collaud Coen, 2003).

The influence of cold plasma parameters on wettability and adhesion of polymeric surfaces has also been investigated, focusing on the nature of the relationship between wettability and adhesion (Carrino, 2002). Surface characterization of plasma-treated PP fibers has also been studied with a low pressure plasma with O₂ as plasma activation gas (Wei, 2004; Wei, 2006) or with a vertical cold gas plasma (Huang, 2006)

with special emphasis on the influence of the plasma treatment on the dynamic contact angles of the PP fibers. Induced super hydrophilicity due to surface modification of PP membrane treated by O₂ radio frequency glow discharge plasma was also reported (Jaleh, 2010).

Plasma treatment of PP fabrics by means of atmospheric dielectric barrier discharge (DBD), has also been studied for improved dyeability with a textile dyestuff (Yaman, 2009). The impact of plasma treatment parameters on the surface morphology, physical-chemical, and dyeing properties of PP using anionic and cationic dyestuffs were investigated. Argon plasma treatment was used to activate PP fabric surfaces. Plasma activation of nonwoven PP using two different ambient air plasma sources: volume dielectric barrier discharge (DBD) and diffuse coplanar surface barrier discharge (DCSBD) has also been described for its subsequent functionalization by silver ion deposition (Radić, 2012).

Medical textiles are a field of increasing interest and growing applications, which include implantable and non-implantable textiles. To confer them with added value, various approaches to use the medical textiles as drug delivery systems have been described in literature, usually based on encapsulation techniques, hollow fibres, biodegradable fibres or the use of chemical linkers. However, to our knowledge, there is not any technique or drug delivery system in which the attachment of the pharmaceutical and/or cosmetic active principle is directly achieved as a result of the modification of the interface drug/fibers by a physical dry process such as plasma, well known and set in surface science as an efficient tool for polymer surface modification.

REFERENCES

- W. J. Addicks, N. D. Weiner, R. L. Curl, G. L. Flynn, Drug delivery from topical formulations: theoretical prediction and experimental assessment. In: "Transdermal drug delivery: Developmental issues and research initiatives", J. Hadgraft, R. H. Guy Eds., Marcel Dekker, New York, NY, **1989**, pp. 221.
- C. J. Alvarado, The science of hand hygiene: A self-study monograph. University of Wisconsin Medical School and Sci-Health Communications, **2000**.
- P. K. Amid, A. G. Shulman, I. L. Lichtenstein, Selecting synthetic mesh for the repair of groin hernia, *Postgrad. Gen. Surg.*, **1992**, 4, 150.
- T. Amnuaikit, S. Ingkatawornwong, D. Maneenuan, K. Worachotekamjorn, Caffeine topical gel formulation, *Isan. J. Pharm. Sci.*, **2008**, 4, 16.
- T. Amnuaikit, D. Maneenuan, P. Boonme, Evaluation of caffeine gels on physicochemical characteristics and in vivo efficacy in reducing puffy eyes, *J. Appl. Pharm. Sci.*, **2011**, 01, 56.
- Y. H. An, R. J. Friedman, Prevention of sepsis in total joint arthroplasty, *J. Hosp. Infect.*, **1996**, 33, 93.
- F. R. Anderson, V. F. Holland, Ion-bombardment etching of synthetic fibers, *J. Applied Physics*, **1960**, 31, 1516.
- T. J. Aufenacker, D. van Geldere, T. van Mesdag, A. N. Bossers, B. Dekker, E. Scheijde, R. van Nieuwenhuizen, E. Hiemstra, J. H. Maduro, J. W. Juttman, D. Hofstede, C. T. van Der Linden, D. J. Gouma, M. P. Simons, The role of antibiotic prophylaxis in prevention of wound infection after Lichtenstein open mesh repair of primary inguinal hernia: a multicenter double-blind randomized controlled trial, *Ann. Surg.*, **2004**, 240, 955.
- L. Avtan, C. Avci, T. Bulut, G. Fourtanier, Mesh infections after laparoscopic inguinal hernia repair, *Surg. Laparosc. Endosc.*, **1997**, 7, 192.
- S. S. Awad, S. P. Fagan, Current approaches to inguinal hernia repair, *Am. J. Surg.*, **2004**, 188, 9.

- S. Baboota, F. Shakeel, A. Ahuja, J. Ali, S. Shaafiq, Desing, development and evaluation of novel nanoemulsion formulations for transdermal potential of celecoxib, *Acta Pharmaceut.*, **2007**, 57, 315.
- K. Baessler, A. D. Hewson, R. Tunn, B. Schuessler, Severe mesh complications following intravaginal slingplasty, *Obstet. Gynecol.*, **2005**, 10, 713.
- A. Bako, R. Dhar, Review of synthetic mesh-related complications in pelvic floor reconstructive surgery, *Int. Urogynecol. J. Pelvic Floor Dysfunct.*, **2009**, 20, 103.
- D. J. Balazs, K. Triandafillu, P. Wood, Y. Chevolut, C. van Delben, H. Harms, Inhibition of bacterial adhesion on PVC endotracheal tubes by RF-oxygen glow discharge, sodium hydroxide and silver nitrate treatments. *Biomaterials*, **2004**, 25, 2139.
- R. J. Batchelder, R. J. Calder, C. P. Thomas, C. M. Heard, In vitro transdermal delivery of the major catechins and caffeine from extract of *Camellia sinensis*, *Int. J. Pharm.*, **2004**, 283, 45.
- S. Bauer, P. Schmuki, K. von der Mark, J. Park, Engineering biocompatible implant surfaces: Part I: Materials and surfaces, *Prog. Mater. Sci.*, **2013**, 58, 261.
- E. Beetge, J. Plessis, D. G. Müller, C. Goosen, F. J. Rensburg, The influence of the physicochemical characteristics and pharmacokinetic properties of selected NSAIDs on their transdermal absorption, *Int. J. Pharm.*, **2000**, 193, 261.
- J. M. Bellón, L. A. Contreras, J. Buján, D. Palomares, A. Carrera-San Martín, Tissue response to polypropylene meshes used in the repair of abdominal wall defects, *Biomaterials*, **1998**, 19, 669.
- C. Bertin, H. Zunino, J. C. Pittet, A double-blind evaluation of the activity of an anti-cellulite product containing retinol, caffeine, and ruscogenine by a combination of several non-invasive methods, *J. Cosmet. Sci.*, **2001**, 52, 199.
- J. J. Bikerman, *The science of adhesive joints*, 2nd Ed., Academic Press, New York, **1968**.
- J. J. Bikerman, Effect of impurities on polyethylene adhesion, *J. Appl. Chem.*, **1961**, 11, 81.

N. Blanchemain, T. Laurent, F. Chai, C. Neut, S. Haulon, V. Krump-Konvalinkova, M. Morcellet, B. Martel, C. J. Kirkpatrick, H. F. Hildebrand, Polyester vascular prostheses coated with a cyclodextrin polymer and activated with antibiotics: Cytotoxicity and microbiological evaluation, *Acta Biomater.*, **2008**, 4, 1725.

M. Boers, Glucocorticoids in rheumatoid arthritis: A senescent research agenda on the brink of rejuvenation?, *Best. Pract. Res. Clin. Rheumatol.*, **2004**, 18, 21.

A. Bogaerts, E. Neyts, R. Gijbels, J. van der Mullen, Gas discharge plasmas and their applications, *Spectrochimica Acta Part B*, **2002**, 57, 609.

M. A. Bolzinger, S. Briançon, J. Pelletier, H. Fessi, Y. Chevalier, Percutaneous release of caffeine from microemulsion, emulsion and gel dosage forms, *Eur. J. Pharm. Biopharm.*, **2008**, 68, 446.

P. Boonme, H. Boontawee, W. Pichayakorn, Physical properties of various gels containing high hydroalcoholic solvent. Proceedings of the 33rd Congress on Science and Technology of Thailand (STT. 33), **2007**.

G. Borcia, C. A. Anderson, N. M. D. Brown, Dielectric barrier discharge for surface treatment: application to selected polymers in film and fibre form, *Plasma Sources Sci. Technol.*, **2003**, 12, 335.

G. Borcia, C. A. Anderson, N. M. D. Brown, The surface oxidation of selected polymers using an atmospheric pressure air dielectric barrier discharge. Part II, *Appl. Surf. Sci.*, **2004**, 225, 186.

J. D. Bos, M. M. Meinardi, The 500 Dalton rule for the skin penetration of chemical compounds and drugs, *Exp. Dermatol.*, **2000**, 9, 165.

M. B. Brown, G. P. Martin, S. A. Jones, F. K. Akomeah, Dermal and transdermal drug delivery systems: current and future prospects, *Drug Deliv.*, **2006**, 13, 175.

G. A. Byrne, K. C. Brown, Modifications of textiles by glow-discharge reactions, *J. Soc. Dyers Colour.*, **1972**, 88, 113.

- M. Carafa, C. Marianecchi, G. Lucania, E. Marchei, E. Santucci, New vesicular ampicillin-loaded delivery systems for topical application: Characterization, in vitro permeation experiments and antimicrobial activity, *J. Control. Release*, **2004**, 95, 67.
- L. Carrino, G. Moroni, W. Polini, Cold plasma treatment of polypropylene surface: a study on wettability and adhesion, *J. Mater. Process. Technol.*, **2002**, 121, 373.
- M. Chen, P. O. Zamora, P. Som, L. A. Pena, S. Osaki, Cell attachment and biocompatibility of polytetrafluoroethylene (PTFE) treated with glow-discharge plasma of mixed ammonia and oxygen, *J. Biomater. Sci. Polym.*, **2003**, 14, 917.
- M. C. Chen, H. F. Liang, Y. L. Chiu, Y. Chang, H. J. Wei, H. W. Sung, A novel drug-eluting stent spray-coated with multi-layers of collagen and sirolimus, *J. Control. Release*, **2005**, 108, 178.
- Z. Chen, U. Cvelbar, M. Mozetič, J. He, M. K. Sunkara, Long-range ordering of oxygen-vacancy planes in α -Fe₂O₃ nanowires and nanobelts, *Chem. Mater.*, **2008**, 20, 3224.
- D. Ciechańska, J. Kazimierczak, J. Wietecha, M. Rom, Surface biomodification of surgical meshes intended for hernia repair, *Fibres Text. East. Eur.*, **2012**, 20, 107.
- W. S. Cobb, J. B. Harris, J. S. Lokey, E. S. McGill, K. L. Klove, Incisional herniorrhaphy with intraperitoneal composite mesh: a report of 95 cases, *Am. Surg.*, **2003**, 69, 784.
- W. S. Cobb, J. M. Burns, R. D. Peindl, A. M. Carbonell, B. D. Matthews, K. W. Kercher, B. T. Heniford, Textile analysis of heavy weight, mid-weight, and light weight polypropylene mesh in a porcine ventral hernia model, *J. Surg. Res.*, **2006**, 136, 1.
- M. Collaud Coen, G. Dietler, S. Kasas, P. Griining, AFM measurements of the topography and the roughness of ECR plasma treated polypropylene, *Appl. Surf. Sci.*, **1996**, 103, 27.
- M. Collaud Coen, R. Lehmann, P. Groening, L. Schlapbach, Modification of the micro- and nanotopography of several polymers by plasma treatments, *Appl. Surf. Sci.*, **2003**, 207, 276.

N. Collis, L. A. Elliot, C. Sharpe, D. Sharpe, Cellulite treatment: a myth of reality: a prospective randomized, controlled trial of two therapies, endermologie and aminophylline cream, *Plast. Reconstr. Surg.*, **1999**, 104, 1110.

R. E. Condon, D. H. Wittmann, The use of antibiotics in general surgery, *Curr. Probl. Surg.*, **1991**, 28, 803.

P. Combe, G. Gutierrez, Impregnated textile materials and method of making them, Patent EP 1353002 A2, **2002**.

U. Cvelbar, S. Pejovnik, M. Mozetič, A. Zalar, Increased surface roughness by oxygen plasma treatment of graphite/polymer composite, *Appl. Surf. Sci.*, **2003**, 210, 255.

U. Cvelbar, M. Mozetič, I. Junkar, A. Vesel, J. Kovač, A. Drenik, T. Vrlinič, N. Hauptman, M. Klanjšek-Gunde, B. Markoli, N. Krstulović, S. Milošević, F. Gaboriau, T. Belmonte, Oxygen plasma functionalization of poly(p-phenylene sulphide), *Appl. Surf. Sci.*, **2007**, 253, 8669.

R. D'Agostino, P. Favia, Y. Kawai, H. Ikegami, N. Sato, F. Arefi-Khonsari, *Advanced Plasma Technology*, Wiley-VCH, Weinheim, Germany, **2008**, pp. 139.

J. N. Da Rocha Gomes, Double walled microcapsules with an outer thermoplastic wall and application process thereof, Patent US 2006/0188582, **2006**.

A. F. Da Silva Ribeiro, R. M. Magalhaes Vaz Vieira, J. I. Naylor Rocha Gomes, S. Pinto Cerqueira Barros, Agglomerates of microcapsules of phase change materials (pcm), processes for their formation and application in fibrous or porous polymeric materials, Patent WO 2008/041191 A3, **2008**.

A. De Lucas Martinez , J. F. Rodriguez Romero , P. Sanchez Paredes , M. L. Sanchez Silva , M. L. Torres Barreto, Process for microencapsulation of phase change materials, microcapsules obtained and uses thereof, Patent WO 2007/107171 A1, **2007**.

C. R. Deeken, M. S. Abdo, M. M. Frisella, B. D. Matthews, Physico-mechanical evaluation of polypropylene, polyester, and polytetrafluoroethylene meshes for inguinal hernia repair, *J. Am. Coll. Surg.*, **2011**, 212, 68.

E. P. Dellinger, P. A. Gross, T. L. Barrett, P. J. Krause, W. J. Martone, J. E. McGowan, Quality standard for antimicrobial prophylaxis in surgical procedures, *Clin. Infect. Dis.*, **1994**, 18, 422.

M. Dias, A. Farinha, E. Faustino, J. Hadgraft, J. Pais, C. Toscano, Topical delivery of caffeine from some commercial formulations, *Int. J. Pharm.*, **1999**, 182, 41.

G. B. Diwadkar, M. D. Barber, B. Feiner, C. Maher, J. E. Jelovsek, Complication and reoperation rates after apical vaginal prolapse surgical repair: a systematic review, *Obstet. Gynecol.*, **2009**, 113, 367.

J. Doshi, D. H. Reneker, Electrospinning process and applications of electrospun fibers, *J. Electrostat.*, **1995**, 35, 151.

Z. D. Draelos, K. D. Marenus, Cellulite—Etiology and purported treatment, *Dermatol. Surg.*, **1997**, 23, 1177.

F. Dreher, F. Fouchard, C. Patouillet, M. Andrian, J. T. Simonnet, F. Benech-Kieffer, Comparison of cutaneous bioavailability of cosmetic preparations containing caffeine or alpha-tocopherol applied on human skin models or human skin ex vivo at finite doses, *Skin Pharmacol. Appl. Skin Physiol.*, **2002**, 15, 40.

Y. El Ghouli, N. Blanchemain, T. Laurent, C. Campagne, A. El Achari, S. Roudesli, M. Morcellet, B. Martel, H. F. Hildebrand, Chemical, biological and microbiological evaluation of cyclodextrin finished polyamide inguinal meshes, *Acta Biomaterialia*, **2008**, 4, 1392.

P. M. Elias, Epidermal lipids, barrier function and desquamation, *J. Invest. Dermatol.*, **1983**, 80, 44.

A. F. Engelsman, H. C. van der Mei, R. J. Ploeg, H. J. Busscher, The phenomenon of infection with abdominal wall reconstruction, *Biomaterials*, **2007**, 28, 2314.

P. Erra, R. Molina, D. Jovic, M. R. Julia, A. Cuesta, J. M. D. Tascon, Shrinkage properties of wool treated with low temperature plasma and chitosan biopolymer, *Text. Res. J.*, **1999**, 69, 811.

E. Escribano, A. C. Calpena, J. Queralt, R. Obach, J. Domenech, Assessment of diclofenac permeation with different formulations: Anti-inflammatory study of a selected formula, *Eur. J. Pharm. Sci.*, **2003**, 19, 203.

M. E. Falagas, S. K. Kasiakou, Mesh-related infections after hernia repair surgery, *Clin Microbiol. Infect.*, **2005**, 11, 3.

R. F. Fansler, P. Taheri, C. Cullinane, B. Sabates, L. M. Flint, Polypropylene mesh closure of the complicated abdominal wound, *Am. J. Surg.*, **1995**, 170, 15.

Firstex L.L.C., J. Zhang, L. Zhu, L. Xu, Functional treatment of textile materials, Patent WO 2002/084017 A1, **2002**.

P. Fu-Giles, Sustained drug release from body implants using nanoparticle-embedded polymeric coating materials, Patent US 2013/0004651 A1, **2013**.

J. Gacén, Fibras de Poliamida, Universidad Politècnica de Catalunya, Terrassa, Spain, **1991**.

S. J. Gallagher, L. Trottet, C. M. Heard, Ketoprofen: release from, permeation across and rheology of simple gel formulations that simulate increasing dryness, *Int. J. Pharm.*, **2003**, 268, 37.

C. D. George, H. Ellis, The results of incisional hernia repair: a twelve year review, *Ann. Roy. Coll. Surg. Eng.*, **1986**, 68, 185.

L. J. Gerenser, Surface chemistry of plasma-treated polymers. In: "Handbook of thin film process technology", Eds. D. A. Glocker and S. I. Shah, IOP, Bristol, **1996**.

Y. P. Goekoop-Ruiterman, J. K. de Vries-Bouwstra, C. F. Allaart, D. van Zeben, P. J. S. M. Kerstens, J. M. W. Hazes, Comparison of treatment strategies in early rheumatoid arthritis: a randomized trial, *Ann. Intern. Med.*, **2007**, 146, 406.

M. P. Goldman, Cellulite: a review of current treatments, *Cosmet. Dermatol.*, **2002**, 15, 17.

A. Gomez-Alonso, F. J. Garcia-Criado, F. C. Parreno-Manchado, J. E. Garcia-Sanchez, E. Garcia-Sanchez, A. Parreno-Manchado, Y. Zambrano-Cuadrado, Study of the efficacy of

Coated VICRYL Plus Antibacterial suture (coated Polyglactin 910 suture with Triclosan) in two animal models of general surgery, *J. Infect.*, **2007**, 54, 82.

S. H. Gray, M. T. Hawn, K. M. Itani, Surgical progress in inguinal and ventral incisional hernia repair, *Surg. Clin. North. Am.*, **2008**, 88, 17.

A. Grill, *Cold Plasma in materials fabrication*, IEEE Press, New York, **1993**.

O. Guillaume, X. Garric, J.-P. Lavigne, H. Van Den Berghe, J. Coudane, Multilayer, degradable coating as a carrier for the sustained release of antibiotics: Preparation and antimicrobial efficacy in vitro, *J. Control. Release*, **2012**, 162, 492.

M. L. Gulrajani, D. Gupta, Emerging techniques for functional finishing of textiles, *Indian Journal of Fibre & Textile Research*, **2011**, 36, 388.

J. Hadgraft, Skin penetration enhancement. In: "Predication of percutaneous penetration", J. Hadgraft, K. A. Walters Eds., Marcel Dekker, New York, NY, **1993**, pp. 138.

K. C. Harth, M. J. Rosen, T. R. Thatiparti, M. R. Jacobs, I. Halaweish, S. Bajaksouzian, J. Furlan, H. A. von Recum, Antibiotic-releasing mesh coating to reduce prosthetic sepsis: an in-vivo study, *J. Control. Release*, **2010**, 163, 337.

C. M. Heard, S. Johnson, G. Moss, C. P. Thomas, In vitro transdermal delivery of caffeine, theobromine, theophylline and catechin from extract of guarana, *Paullinia Cupana*, *Int. J. Pharm.*, **2006**, 317, 26.

T. L. Hedrick, P. W. Smith, L. M. Gazoni, R. G. Sawyer, The appropriate use of antibiotics in surgery: a review of surgical infections, *Curr. Probl. Surg.*, **2007**, 44, 635.

A. Heenan, Dressings on the drug tariff, Surgical material testing laboratory, *Worldwide Wounds*. 4th Ed., Wales, UK, **1998**.

B. T. Heniford, A. Park, B. J. Ramshaw, G. Voeller, Laparoscopic ventral and incisional hernia repair in 407 patients, *J. Am. Coll. Surg.*, **2000**, 190, 645.

B. T. Heniford, A. Park, B. J. Ramshaw, G. Voeller, Laparoscopic repair of ventral hernias: nine years' experience with 850 consecutive hernias, *Ann. Surg.*, **2003**, 238, 391.

D. Hexsel, D. Zechmeister do Prado, J. Rao, M. P. Goldman, Topical management of cellulite. In: "Cellulite - Pathophysiology and treatment", Mitchel P. Goldman Eds., Taylor & Francis Group, New York, NY, **2006**.

Y. Hirano, Improved polyesters and their dye affinity — Polyester fibers for deep and vivid color dyeing, J. Text. Mach. Soc. of Japan, **1984**, 37(3), 11.

V. Hody, T. Belmonte, T. Czerwiec, G. Henrion, J.M. Thiebaut, Oxygen grafting and etching of hexatriacontane in late N₂-O₂ post-discharges, Thin Solid Films, **2006**, 506, 212.

N. Ahmad, N. Saad, Effects of antibiotics on dental implants: A review, J. Clin. Med. Res., **2012**, 4, 1.

A. Holländer, R. Wilken, J. Behnisch, Subsurface chemistry in the plasma treatment of polymers, Surf. Coat. Technol., **1999**, 116, 788.

T. C. Horan, R. P. Gaynes, W. J. Martone, W. R. Jarvis, T. G. Emori, CDC definitions of nosocomial surgical site infections: a modification of CDC definitions of surgical wound infections, Infect. Control. Hosp. Epidemiol., **1992**, 13(10), 606.

F. Huang, Q. Wei, X. Wang, W. Xu, Dynamic contact angles and morphology of PP fibres treated with plasma, Polym. Test., **2006**, 25, 27.

M. J. Hung, F. S. Liu, P. S. Shen, G. D. Chen, L. Y. Lin, E. S. C. Ho, Analysis of two sling procedures using polypropylene mesh for treatment of stress urinary incontinence, Inter. J. Gynec. Obstetrics, **2004**, 84, 133.

N. Inagaki, Plasma Surface Modification and Plasma Polymerization, N. Inagaki, Technomic Publishing, Lancaster, PA, **1996**.

M. Ip, S. L. Lui, V. K. M. Poom, I. Lung, A. Burd, Antimicrobial activities of silver dressings: an in vitro comparison. J. Med. Microbiol., **2006**, 55, 59.

B. Jaleh, P. Parvin, P. Wanichapichart, A. Pourakbar Saffar, A. Reyhani, Induced super hydrophilicity due to surface modification of polypropylene membrane treated by O₂ plasma, Appl. Surf. Sci., **2010**, 257, 1655.

C. J. Jansen, V. K. Hopsu-Havu, Proteolytic enzymes in the skin. Studies on the extractability, stability and modifier characteristics of the caseinolytic enzymes in the rat skin, *Acta Derm-Venereol.*, **1969**, 49, 525.

R. Jantharaprapap, G. Stagni, Effects of penetration enhancers on in vitro permeability of meloxicam gels, *Int. J. Pharm.*, **2007**, 343, 26.

J. Y. Jeong, S. E. Babayan, A. Schutze, V. J. Tu, J. Park, I. Henins, G. S. Selwyn, R. F. Hicks, Etching polyimide with a nonequilibrium atmospheric-pressure plasma jet, *J. Vac. Sci. Technol. A*, **1999**, 17, 2581.

J. Y. Jeong, S. E. Babayan, V. J. Tu, Etching materials with an atmospheric pressure plasma jet, *Plasma Sources Sci. Technol.*, **1998**, 7, 282.

K. Junge, R. Rosch, U. Klinge, M. Saklak, B. Klosterhalfen, C. Peiper, V. Schumpelick, Titanium coating of a polypropylene mesh for hernia repair: Effect on biocompatibility, *Hernia*, **2005a**, 9, 115.

K. Junge, R. Rosch, U. Klinge, C. Krones, B. Klosterhalfen, P. R. Mertens, P. Lynen, D. Kunz, A. Preiss, H. Peltroche-Llacsahuanga, V. Schumpelick, Gentamicin supplementation of polyvinylidene fluoride mesh materials for infection prophylaxis, *Biomaterials*, **2005b**, 26, 787.

C. W. Kan, K. Chan, C. W. M. Yuen, M. H. Miao, The effect of low temperature plasma on chrome dyeing of wool fibres, *J. Mat. Proc. Tech.*, **1998a**, 82, 122.

C. W. Kan, K. Chan, C. W. M. Yuen, M. H. Miao, Surface properties of low temperature plasma treated wool fabrics, *J. Mat. Proc. Tech.*, **1998b**, 83, 180.

M. S. Kim, T. J. Kang, Dimensional and surface properties of plasma and silicone treated wool fabric, *Text. Res. J.*, **2002**, 72, 113.

B. Kirshtein, L. Lantsberg, E. Avinoach, M. Bayme, S. Mizrahi, Laparoscopic repair of large incisional hernias, *Surg. Endosc.*, **2002**, 16, 1717.

U. Klinge, B. Klosterhalfen, M. Müller, M. Anurov, A. Öttinger, V. Schumpelick, Influence of polyglactin-coating on functional and morphological parameters of

polypropylene-mesh modifications for abdominal wall repair, *Biomaterials*, **1999**, 20, 613.

B. Klosterhalfen, U. Klinge, V. Schumpelick, Functional and morphological evaluation of different polypropylene-mesh modifications for abdominal wall repair, *Biomaterials*, **1998**, 19, 2235.

S. Kobayashi, T. Wakida, S. Niu, S. Hazama, T. Ito, Y. Sasaki, The effect of sputter etching on the surface characteristics of dyed aramid fabrics. *J. Soc. Dyers Colour.*, **1995**, 111, 72.

P. Krüger, R. Knes, J. Friedrich, Surface cleaning by plasma-enhanced desorption of contaminants, *Surf. Coat. Technol.*, **1999**, 112, 240.

M. Kukovic, E. Knez, Process for preparing carriers saturated or coated with microencapsulated scents, Patent WO 96/09114, **1996**.

R. Kumar, H. Münstedt, Silver ion release from antimicrobial polyamide/silver composites, *Biomaterials*, **2002**, 23, 1139.

R. Kumar, S. Howdle, H. Münstedt, Polyamide/silver antimicrobials: Effect of filler types on the silver ion release, *Biomaterials*, **2005**, 26, 2081.

M. Kuzuya, S. I. Kondo, M. Sugito, T. Yamashiro, Peroxy radical formation from plasma-induced surface radicals of polyethylene as studied by electron spin resonance, *Macromolecules*, **1998**, 31, 3230.

L. Landmann, Epidermal permeability barrier transformation of lamellar granule-disks into intercellular sheets by a membrane-fusion process, a freeze fracture study, *J. Invest. Dermatol.*, **1986**, 87, 202.

R. Langer, Transdermal drug delivery: Past present, current status and future prospects, *Adv. Drug Deliv. Rev.*, **2004**, 56, 557.

T. Laurent, I. Kacem, N. Blanchemain, F. Cazaux, C. Neut, H. F. Hildebrand, B. Martel, Cyclodextrin and maltodextrin finishing of a polypropylene abdominal wall implant for the prolonged delivery of ciprofloxacin, *Acta Biomaterialia*, **2011**, 7, 3141.

G. E. Leber, J. L. Garb, A. I. Alexander, W. P. Reed, Long-term complications associated with prosthetic repair of incisional hernias, *Arch. Surg.*, **1998**, 133, 378.

M. A. Lichtenberg, A. J. Lieberman, Principles of plasma physics and materials processing, Wiley, New York, **1994**.

I. L. Lichtenstein, Hernia repair without disability. 2nd Ed. St. Louis: Ishiyaku EuroAmerica, Inc., **1986**.

I. L. Lichtenstein, A. G. Shulman, P. K. Amid, M. M. Montllor, The tension-free hernioplasty, *Am. J. Surg.*, **1989**, 157, 188.

A. Liguori, Absorption and subjective effects of caffeine from coffee, cola and capsules, *Pharm. Bioc. Behavior*, **1997**, 58, 721.

E. M. Liston, L. Martinu, M. R. Wertheimer, Plasma surface modification of polymers for improved adhesion: a critical review, *J. Adhes. Sci. Technol.*, **1993**, 7, 1091.

L. Liu, Q. Jiang, T. Zhu, X. Guo, Y. Sun, Y. Guan, Y. Qiu, Influence of aramid fiber moisture regain during atmospheric plasma treatment on aging of treatment effects on surface wettability and bonding strength to epoxy, *J. Appl. Polym. Sci.*, **2006**, 102, 242.

R. W. Luijendijk, W. C. J. Hop, M. P. Van den Tol, D. C. D De Lange, M. M. J. Braaksma, J. N. M. Ijzermans, R. U. Boelhouwer, B. C. de Vries, M. K. Salu, J. C. Wereldsma, C. M. Bruijninx, J. A. Jeekel, A comparison of suture repair with mesh repair for incisional hernia, *N. Engl. J. Med.*, **2000**, 343(6), 392.

A. H. Maciver, M. D. McCall, R. L. Edgar, A. L. Thiesen, D. L. Bigam, T. A. Churchill, A. M. J. Shapiro, Sirolimus drug-eluting, hydrogel-impregnated polypropylene mesh reduces intra-abdominal adhesion formation in a mouse model, *Surgery*, **2011**, 150, 907.

G. S. Malkov, E. R. Fisher, Pulsed Plasma Enhanced Chemical Vapor Deposition of poly(allyl alcohol) onto natural fibers, *Plasma Process. Polym.*, **2010**, 7, 695.

G. L. Mandell, R. C. Douglas, J. I. Bennet, Principles and practice of infection disease, 3rd Ed., Churchill Livingstone, Edinburgh, **1990**, pp. 240.

B. D. Matthews, B. L. Pratt, H. S. Pollinger, C. L. Backus, K. W. Kercher, R. F. Sing, B. T. Heniford, Assessment of adhesion formation to intra-abdominal polypropylene mesh and polytetrafluoroethylene mesh, *J. Surg. Res.*, **2003**, 114, 126.

A. Melaiye, W. J. Youngs, Silver and its application as an antimicrobial agent, *Expert. Opin. Ther. Pat.*, **2005**, 15, 125.

G. K. Menon, New insights into skin structure: scratching the surface. *Adv. Drug Deliv. Rev.*, **2002**, 54, 3.

A. A. Meyer-Plath, K. Schröder, B. Finke, A. Ohl, *Vacuum*, **2003**, 71, 391.

P. Mier, J. van den Hurk, Lysosomal hydrolases of the epidermis, *Br. J. Dermatol.*, **1975**, 93, 509.

S. Mondal, Phase change materials for smart textiles – An overview, *Appl. Therm. Eng.*, **2008**, 28, 1536.

D. R. Monteiro, L. Fernando Gorup, A. Satie Takamiya, A. Colla Ruvollo-Filho, E. Rodrigues de Camargo, D. Barros Barbosa, The growing importance of materials that prevent microbial adhesion: Antimicrobial effect of medical devices containing silver, *Int. J. Antimicrob. Agents*, **2009**, 34, 103.

R. Morent, N. De Geyter, C. Leys, L. Gengembre, E. Payen, Study of the ageing behaviour of polymer films treated with a dielectric barrier discharge in air, helium and argon at medium pressure, *Surf. Coat. Technol.*, **2007**, 201, 7847.

N. Morosoff, An introduction to plasma polymerization. In: "Plasma deposition, treatment, and etching of polymers", R. d'Agostino Eds., Elsevier Inc., **1990**.

M. Morra, E. Occhiello, F. Garbassi, Contact angle hysteresis in oxygen plasma treated poly(tetrafluoroethylene), *Langmuir*, **1989**, 5, 872.

M. Mozetič, U. Cvelbar, M. K. Sunkara, S. Vaddiraju, A method for the rapid synthesis of large quantities of metal oxide nanowires at low temperatures, *Adv. Mater.*, **2005**, 17, 2138.

S. N. Murthy, H. N. Shivakumar, Topical and transdermal drug delivery. In: "Handbook of non-invasive drug delivery systems: Science and technology", Eds., Elsevier Inc., **2010**, pp. 4.

H. L. Needles, Textile fibers, dyes, finishes, and processes, Noyes Publication, Park Ridge, New Jersey, U.S.A, **1986**.

G. Nelson, Application of microencapsulation in textiles, *Int. J. Pharm.*, **2002**, 242, 55.

R. Nisticò, M. G. Faga, G. Gautier, G. Magnacca, D. D'Angelo, E. Ciancio, G. Piacenza, R. Lamberti, S. Martorana, Physico-chemical characterization of functionalized polypropylenic fibers for prosthetic applications, *Appl. Surf. Sci.*, **2012**, 258, 7889.

E. Occhiello, M. Morra, G. Morini, F. Garbassi, P. Humphrey, Oxygen-plasma-treated polypropylene interfaces with air, water, and epoxy resins: Part I. Air and Water, *J. Appl. Polym. Sci.*, **1991**, 42, 551.

T. Okuda, K. Tominaga, S. Kidoaki, Time-programmed dual release formulation by multilayered drug-loaded nanofiber meshes, *J. Control. Release*, **2010**, 143, 258.

T. Okuno, T. Yasuda, H. Yasuda, Effect of crystallinity of PET and nylon 66 fibers on plasma etching and dyeability characteristics, *Text. Res. J.*, **1992**, 62, 474.

N. Ü. Okur, S. Apaydın, N. Ü. Karabay Yavaşoğlu, A. Yavaşoğlu, H. Y. Karasulua, Evaluation of skin permeation and anti-inflammatory and analgesic effects of new naproxen microemulsion formulations, *Int. J. Pharm.*, **2011**, 416, 136.

S. B. Orenstein, E. R. Saberski, D.L. Kreutzer, Y.W. Novitsky, Comparative analysis of histopathologic effects of synthetic meshes based on material, weight, and pore size in mice, *J. Surg. Res.*, **2012**, 176, 423.

D. W. Osborne, Review of changes in topical drug classification, *Pharm. Tech.*, **2008**, 32, 66.

K. Ostrikov, A. B. Murphy, Plasma-aided nanofabrication: where is the cutting edge?, *J. Phys. D: Appl. Phys.*, **2007**, 40, 2223.

- C. P. Page, J. M. A. Bohnen, J. R. Fletcher, A. T. MacManus, J. S. Solomkin, D. H. Wittmann, Antimicrobial prophylaxis for surgical wounds. Guidelines for clinical care, *Arch. Surg.*, **1993**, 128, 79.
- A. Panáček, L. Kvítek, R. Pucek, M. Kolár, R. Vecerová, N. Pizúrová, Silver colloid nanoparticles: synthesis, characterization, and their antibacterial activity, *J. Phys. Chem. B*, **2006**, 110, 16248.
- K. S. Paudel, M. Milewski, C. L. Swadley, N. K. Brogden, P. Ghosh, A. L. Stinchcomb, Challenges and opportunities in dermal/transdermal delivery, *Ther. Deliv.*, **2010**, 1, 109.
- S. Petersen, G. Henke, M. Freitag, A. Faulhaber, K. Ludwig, Deep prosthesis infection in incisional hernia repair: predictive factors and clinical outcome, *Eur. J. Surg.*, **2001**, 167, 453.
- Q. P. Pham, U. Sharma, A. G. Mikos, Electrospinning of polymeric nanofibers for tissue engineering applications: a review, *Tissue Eng.*, **2006**, 12, 1197.
- G. Portad, C. Laugel, A. Baillet, H. Schaefer, J. P. Marty, Quantitative HPLC analysis of sunscreens and caffeine during in vitro percutaneous penetration studies, *Int. J. Pharm.*, **1999**, 189, 249.
- E. Proksch, J. M. Brandner, J.-M. Jensen, The skin: an indispensable barrier, *Exp. Dermatol.*, **2008**, 17, 1063.
- Y. Qiu, C. Zhang, Y. J. Hwang, B. L. Bure, M. McCord, Atmospheric pressure helium + oxygen plasma treatment of ultrahigh modulus polyethylene fibers, *J. Adhes. Sci. Technol.*, **2002a**, 16, 449.
- Y. Qiu, Y. J. Hwang, C. Zhang, B. L. Bure, M. McCord, The effect of atmospheric pressure helium plasma treatment on the surface and mechanical properties of ultrahigh-modulus polyethylene fibers, *J. Adhes. Sci. Technol.*, **2002b**, 16, 99.
- Y. Qiu, S. Deflon, P. Schwartz, Plasma surface treatment of poly (p-phenylenebenzobisthiazol) fibers, *J. Adhes. Sci. Technol.*, **1993**, 7, 1041.
- A. C. Queiroz, J. D. Santos, F. J. Monteiro, I. R. Gibson, J. C. Knowles, Adsorption and release studies of sodium ampicillin from hydroxyapatite and glass-reinforced hydroxyapatite composites, *Biomaterials*, **2001**, 22, 1393.

- B. Querleux, C. Cornillon, O. Jolivet, J. Bittoun, Anatomy and physiology of subcutaneous adipose tissue by in vivo magnetic resonance imaging and spectroscopy: Relationships with sex and presence of cellulite, *Skin Res. Technol.*, **2002**, 8, 118.
- N. Radić, B. M. Obradović, M. Kostić, B. Dojčinović, M. M. Kuraica, M. Černák, Deposition of silver ions onto DBD and DCSBD plasma treated nonwoven polypropylene, *Surf. Coat. Technol.*, **2012**, 206, 5006.
- W. Rakowski, M. Okoniewski, K. Bartos, J. Zawadzki, Plasma treatment of textiles - Potential applications and future prospects, *Melliand Textilber*, **1982**, 11, 301.
- Y. Ren, C. Wang, Y. Qiu, Influence of aramid fiber moisture regain during atmospheric plasma treatment on aging of treatment effects on surface wettability and bonding strength to epoxy, *Appl. Surf. Sci.*, **2007**, 253, 9283.
- L. Ripoll, C. Bordes, S. Etheve, A. Elaissari, H. Fessi, Cosmeto-textile from formulation to characterization: an overview, *e-Polymers*, **2010**, 40, 1.
- J. M. Ritchie, The xanthines. The pharmacological basis of therapeutics, 5th Eds., Mac Millan, New York, **1975**, p. 367.
- J. E. Riviere, Biological factors in absorption and permeation. In: "Skin permeation: fundamentals and application", J. L. Zatz Eds., Wheaton: Allured Publishing Corporation, **1993**, pp. 113.
- H. K. Rouette, *Encyclopedia of Textile Finishing*, Springer, **2002**.
- I. M. Rutkow, Surgical operations in the United States. Then (1983) and now (1994), *Arch. Surg.*, **1997**, 132, 983.
- J. Ryu, T. Wakida, T. Takagishi, Increase of color depth of black-dyed wool and silk fabrics by low temperature plasma treatment, *Sen-I Gakkaishi*, **1991**, 47, 612.
- J. Ryu, J. Dai, K. Koo, T. Wakida T, The effect of sputter etching on the surface characteristics of black-dyed polyamide fabrics. *J. Soc. Dyers Color.*, **1992**, 108, 278.
- D. Saihi, A. El-Achari, I. Vroman, A. Périchaud, Antibacterial activity of modified polyamide fibers, *J. Appl. Polym. Sci.*, **2005**, 98, 997.

E. L. Sainio, T. Rantanen, L. Kanerva, Ingredients and safety of cellulite creams, *Eur. J. Dermatol.*, **2000**, 10, 596.

L. Sanchez, P. Sanchez, A. De Lucas, Microencapsulation of PCMs with a polystyrene shell, *Colloid Polym. Sci.*, **2007**, 285, 1377.

M. Seiller, A. M. Orecchioni, C. Vaution, Vesicular systems and multiple emulsions in cosmetology. In: "Cosmetic Dermatology", R. Baran, H. I. Maibach Eds., Williams and Wilkins, Baltimore, US, **1994**, pp. 27.

R. Shishoo, Plasma technologies for textiles, R. Shishoo, Eds., 1st Ed. Woodhead Publishing Limited, Cambridge, **2007**.

R. L. Shishoo, Proc. 6th Int. Conf. Text. Coat. & Lam., Dusseldorf, Germany, **1996**.

G. Shmack, V. Dutschk, E. Pisanova, Modification of polyamide fibres to improve their biocompatibility, *Fibre Chem.*, **2006**, 32, 48.

A. Shukla, S. N. Avadhany, J. C. Fang, P. T. Hammond, Tunable vancomycin releasing surfaces for biomedical applications, *Small*, **2010**, 6, 2392.

J. P. Singhal, A. R. Ray, Synthesis of blood compatible polyamide block copolymers, *Biomaterials*, **2002**, 23, 1139.

R. Siniscalchi, P. Palma, C. Riccetto, L. C. Maciel, G. Ens, I. del Fabbro, Biomechanical effects of the inclusion of holes to facilitate the integration in monofilament polypropylene meshes: An experimental study, *Actas Urol. Esp.*, **2011**, 35(10), 599.

R. A. Siegel, M. J. Rathbone, Overview of controlled release mechanisms. In: "Fundamentals and applications of controlled release drug delivery, Advances in delivery science and technology", J. Siepmann et al. Eds., Controlled Release Society, **2012**.

M. K. Singh, V. K. Varun, B. K. Behera, Cosmetotextiles: State of art, *Fibres Text. East. Eur.*, **2011**, 19, 27.

Skin'Up, S. Beauge Duguet, Textile and/or fiber processing method using an active ingredient composed of nanoparticles, Patent WO 2008/068418 A3, **2008**.

K. Steigerwald, S. Merl, A. Kastrati, A. Wieczorek, M. Vorpahl, R. Mannhold, M. Vogeser, J. Hausleiter, M. Joner, A. Schomig, R. Wessely, The pre-clinical assessment of rapamycin-eluting, durable polymer-free stent coating concepts, *Biomaterials*, **2009**, 30, 632.

N. Stobie, B. Duffy, D. E. McCormack, J. Colreavy, M. Hidalgo, P. McHale P, Prevention of *Staphylococcus epidermidis* biofilm formation using a low-temperature processed silver-doped phenyltriethoxysilane sol-gel coating, *Biomaterials*, **2008**, 29, 963.

M. Strobel, C. S. Lyons, K. L. Mittal, Plasma surface modification of polymers: Relevance to adhesion, VSP, Utrecht, **1994**.

J. Swarbrick, Encyclopedia of Pharmaceutical Technology, 3rd Edition, Vol. 1, PharmaceuTech Inc., Pinehurst, North Carolina, USA, **2007**.

H. Szymanowski, A. Sobczyk, M. Gazicki-Lipman, W. Jakubowski, L. Klimek, Plasma Enhanced CVD deposition of titanium oxide for biomedical applications, *Surf. Coat. Technol.*, **2005**, 200, 1036.

E. Tam, I. Levchenko, K. Ostrikov, Deterministic shape control in plasma-aided nanotip assembly, *J. Appl. Phys.*, **2006**, 100, 036104.

E. W. Taylor, D. J. Byrne, D. J. Leaper, S. J. Karran, M. K. Browne, K. J. Mitchell, Antibiotic prophylaxis and open groin hernia repair, *World J. Surg.*, **1997**, 21, 811.

P. L. Taylor, A. L. Ussher, R. E. Burrell, Impact of heat on nanocrystalline silver dressings, Part I: Chemical and biological properties, *Biomaterials*, **2005**, 26, 7221.

C. T. Ueda, V. P. Shah, K. Derdzinski, G. Ewing, G. Flynn, H. Maibach, M. Marques, H. Rytting, S. Shaw, K. Thakker, A. Yacobi, Topical and Transdermal Drug Products, *Pharmacopeial Forum*, **2009**, 35, 750.

F. C. Usher, J. Ochsner, L. L. Tuttle Jr., Use of marlex mesh in the repair of incisional hernias, *Am. Surg.*, **1958**, 24, 74.

F. C. Uscher, Hernia repair with marlex mesh, *Arch. Surg.*, **1962**, 84, 325.

M. Van't Riet, P. J. De Vos van Steenwijk, F. Bonthuis, R. L. Marquet, E. W. Steyerberg, J. Jeekel, Prevention of adhesion to prosthetic mesh: Comparison of different barriers using an incisional hernia model, *Ann. Surg.*, **2003**, 237, 123.

A. S. Vanniasinghe, V. Bender, N. Manolios, The potential of liposomal drug delivery for the Treatment of inflammatory arthritis, *Semin. Arthritis Rheum.*, **2009**, 39, 182.

A. Vesel, M. Mozetič, Surface functionalization of organic materials by weakly ionized highly dissociated oxygen plasma, *J. Phys. Conf. Ser.*, **2009**, 162, 012015.

S. Vihodceva, S. Kukle, J. Barloti, Nanolevel functionalization of natural fiber textiles, *IOP Conf. Series: Mate. Sci. Eng.*, **2011**, 23, 012037.

T. Wakida, M. Lee, Y. Sato, S. Ogasawara, Y. Ge, S. Niu, Dyeing properties of oxygen low-temperature plasma-treated wool and nylon 6 fibres with acid and basic dyes, *J. Soc. Dyers Colour.*, **1996**, 112, 233.

T. Wakida, S. Tokino, *Indian J. Fiber. Text.*, **1996**, 21, 69.

T. Wakida, S. Tokino, S. Niu, H. Kawamura, Y. Sato, M. Lee, H. Uchiyama, H. Inagaki, Surface characteristics of wool and Poly(Ethylene-Teraphthalate) fabrics and film treated with low-temperature plasma under atmospheric pressure, *Textile Res. J.*, **1993**, 63, 433.

T. Wakida, S. Cho, S. Choi, S. Tokino, M. Lee, *Text. Res. J.*, **1998**, 68, 848.

T. L. Ward, R. R. Benerito, *Text. Res. J.*, **1982**, 52, 256.

Q. F. Wei, Surface characterization of plasma-treated polypropylene fibers, *Mater. Charact.*, **2004**, 52, 231.

Q. Wei, Q. Lia, X. Wang, F. Huang, W. Gao, Dynamic water adsorption behaviour of plasma-treated polypropylene nonwovens, *Polym. Test.*, **2006**, 25, 717.

Q. Wei, H. Wang, B. Deng, Y. Xu, Surface and interface investigation of Indium-Tin-Oxide (ITO) coated nonwoven fabrics, *J. Adhes. Sci. Technol.*, **2010**, 24, 135.

P. W. Wertz, D. T. Downing, Stratum corneum: biological and biochemical considerations. In: "Transdermal drug delivery", J. Hadgraft, R. H. Guy Eds., Marcel Dekker, New York, pp. 1–17, **1989**.

D. F. Williams, On the mechanisms of biocompatibility, *Biomaterials*, **2008**, 29, 2941.

A. Wisniewski, N. Rajamand, U. Adamsson, P. E. Lins, W. M. Reichert, B. Klitzman, Analyte flux through chronically implanted subcutaneous polyamide membranes differs in humans and rats, *Am. Physiol. Soc.*, **2002**, 10, 152.

A. M. Wokovich, S. Prodduturi, W. H. Doub, A. S. Hussain, L. F. Buhse, Transdermal drug delivery system (TDDS) adhesion as a safe and quality attribute, *Eur. J. Pharm. Biopharm.*, **2006**, 64, 1.

R. K. Woods, E. P. Dellinger, Current guidelines for antibiotic prophylaxis of surgical wounds, *Am. Fam. Physician.*, **1998**, 58, 2731.

J.-U. Wong, T.-H. Leung, C.-C. Huang, C.-S. Huang, Comparing chronic pain between fibrin sealant and suture fixation for bilayer polypropylene mesh inguinal hernioplasty: a randomized clinical trial, *Am. J. Surg.*, **2011**, 202, 34.

P. Wu, D. W. Grainger, Drug/device combinations for local drug therapies and infection prophylaxis, *Biomaterials*, **2006**, 27, 2450.

S. Y. Xu, J. D. Long, L. N. Sim, RF plasma sputtering deposition of hydroxyapatite bioceramics: Synthesis, performance and biocompatibility, *Plasma Process. Polym.*, **2005**, 2, 373.

N. Yaman, E. Özdoğan, N. Seventekin, H. Ayhan, Plasma treatment of polypropylene fabric for improved dyeability with soluble textile dyestuff, *Appl. Surf. Sci.*, **2009**, 255, 6764.

T. Yasuda, M. Gazicki, H. Tasuda, *J. Appl. Polym. Sci.*, **1984**, 38, 201.

H. Yasuda, *Plasma polymerization*, Academic Press Inc., Orlando, FL, **1985**.

B. Ying, Y. Kwok, Y. Li, Q. Zhu, C. Yeung, Assessing the performance of textiles incorporating phase change materials, *Polym. Test.*, **2004**, 23, 541.

J. Yip, K. Chan, M. K. Sin, K. S. Lau, Low temperature plasma-treated nylon fabrics, *J. Mater. Process. Tech.*, **2002a**, 123, 5.

J. Yip, K. Chan, M. K. Sin, K. S. Lau, Study of physico-chemical surface treatments on dyeing properties of polyamides. Part 1: Effect of tetrafluoromethane low temperature plasma, *Coloration Technol.*, **2002b**, 118, 26.

H. S. Yoo, T. G. Kim, T. G. Park, Surface-functionalized electrospun nanofibers for tissue engineering and drug delivery, *Adv. Drug Delivery Rev.*, **2009**, 61, 1033.

J.-W. Yun, E.-S. Shin, S.-Y. Cho, S.-H. Kim, C.-W. Kim, T.-R. Lee, B.-H. Kim, The effects of BADGE and caffeine on the time-course response of adiponectin and lipid oxidative enzymes in high fat diet-fed C57BL/6J mice: correlation with reduced adiposity and steatosis, *Exp. Anim.*, **2008**, 57, 461.

J. L. Zatz, Modification of skin permeation by solvents and surfactants. In: "Skin permeation: fundamentals and application", J. L. Zatz Eds., Wheaton: Allured Publishing Corporation, **1993**, pp. 127.

M. Zilberman, J. J. Elsner, Antibiotic-eluting medical devices for various applications, *J. Control. Release*, **2008**, 130, 202.

I. M. Zuchairah, M. T. Pailthorpe, S. K. David, Effect of glow discharge-polymer treatments on the shrinkage behavior and physical properties of wool fabric, *Text. Res. J.*, **1997**, 67, 69.

OBJECTIVES

2. MOTIVATION, OBJECTIVES AND STRUCTURE OF THE THESIS

2.1. Motivation

Medical textiles (MEDTECH) constitute an expanding field within the technical textiles. MEDTECHs include healing and suture materials, elastic-compressive products, materials of protection and hygiene, and body implants. **One of the added values of these materials can be the capacity to contain and release an active principle.**

Currently, R&D in the development of drug delivery systems is oriented in achieving controlled release of active agents over a predetermined lapse of time, in order to avoid the administration of several doses of drugs or cosmetic products and improve the therapy compliance by the patient. Nowadays, there are drug delivery systems based on textile fibres, which are used as drug reservoirs, (e.g. hollow fibers), as resorbable fibers, or with hydrogels or other polymeric coatings.

The main investigation line of this PhD. Thesis is focused on textile-based drug delivery systems where pharmaceutical and cosmetic active principles are loaded into synthetic textile fibres, whose surface has been suitably modified chemically and/or topographically, at the nanoscale, using plasma technology. Therefore, the influence of the surface modification of the polymer fibres by plasma treatment has to be evaluated on the drug loading and latter release from the fibres to a suitable receptor media, in views of their biomedical applications as delivery systems for active substances. The use of plasma technology to modulate the drug incorporation and release is an innovative and original contribution of this thesis. By modifying the chemical bonds on the surface of textile fibers through the use of plasma, we foresee to improve the release kinetics of the active principles from the synthetic fibres, and the improvement of the therapeutic efficiency.

The subject investigated in this PhD. is Thesis framed in the field of Textile Engineering, Biomaterials, Nanotechnology and Health, and therefore has an undoubted interdisciplinary component. **One of the milestones associated with this thesis is to**

bring innovative applications and high added value for textile-based materials in the field of biomaterials and on drug delivery systems.

The application of nanotechnology in the fields of biotechnology and human health presents promising expectations in the field of materials science for biomedical applications. In this context, an emerging technology such as low-temperature plasma, which can modify the first nanometers of the surface of the material and which has been studied extensively for the modification of textile materials, can open the doors to new applications.

2.2. Purpose of the investigation

The PhD. Thesis will investigate if the controlled modification of the surface of two chemical fibers of synthetic polymer by means of two kinds of plasma systems modifies the quantity of pharmaceuticals and cosmetics active principles that can be incorporated into these fibres and the “in vitro” release kinetics of the drug from the fibres to an isotonic liquid receptor. In this way, the surface modification of textile materials will be performed by atmospheric and low pressure plasmas, and the changes of surface chemistry and topography will be evaluated to determine how the subsequent incorporation of active pharmaceuticals and cosmetics to the fabric and the early release to the standard medium are affected by these surface modifications. The aim of this investigation is to determine if the plasma treatments of the fabrics can modulate the loading to the textile fibre and the release of the drugs from them, and in which way they bring this modulation (modification of the drug loaded in the fibres, modification of the release amount of drug and/or the release kinetics, etc.).

In this thesis, two types of textile materials will be studied:

- An elastic-compressive PA66 knitted fabric, loaded with pharmaceutical and cosmetic active principles and aimed for a release in topical applications.

- A polypropylene mesh, loaded with antibiotics, and aimed to prevent infection and noseucomial disease after hernia repair surgery by releasing the antibiotic directly in the surgical site.

2.3. Main objectives

The main objective consists in designing drug delivery systems based on a new-loading technology using textile materials (fibers, yarns, fabrics) as supports, in which modulation of the release of the active principles is guided by the surface modification achieved by plasma treatment. By monitoring the parameters of plasma treatments, the objective is to determine the mechanisms by which low-temperature plasmas influence the loading of drugs in the fibre and their release for two types of applications of the textile-based drug delivery system:

Modification of textile materials by plasma treatment for topical applications

A first investigation line is focused on the evaluation of corona plasma and low temperature plasma in the modification of the incorporation and release of an anti-inflammatory drug (ketoprofen) and an anti-lipidic active principle (caffeine) from PA66 knitted elastic-compressive fabrics. Theobromine and pentoxifylline, belonging to the methylxantines' family as well as caffeine, have also been studied for a fundamental study to support the results obtained with caffeine. In this way, the objectives of this first part of the PhD. Thesis are the following:

- **To determine** the effects of atmospheric and low-pressure plasma treatments, using air as gas for plasma generation on the surface chemistry and the topography of the PA66 fibres. The most relevant parameters of the plasma treatment (pressure, power supply, gas flow, etc.) leading this surface modification have thus to be determined to **select the optimal conditions** of

plasma treatment of the PA66 fabrics for subsequent loading of active molecules to the fibres.

- **To evaluate** if the plasma treatment leads to an improvement of the loading of the active principle, and its relationship with the surface modifications on the PA66 fibres achieved by plasma treatment.
- With views on industrial applications, it is an aim of this work **to evaluate potential differences** between industrially finished fabrics and laboratory washed PA66 fabrics.
- **To determine** if air atmospheric and low-pressure plasma treatments on PA66 fabrics are able of modifying the release kinetics of the active principles, and to which extend depending on the conditions employed during the plasma treatments. It should also **be verified** that the modified release of the active principle from the plasma-treated PA66 fabrics is comprised within the therapeutic range of the active principle.

Modification of textile materials by plasma treatment for implants

The second part of this PhD. Thesis is focused on the evaluation of the potential of plasmas (both non- and polymerizing) with regards to the incorporation and release of an antibiotic (ampicillin) from PP meshes aimed as body implant for hernia repair, in views to confer an added value to the surgical mesh in order to prevent and avoid post-surgical infections. Thus, the main aims of the second part of the work are:

- **To determine** how both atmospheric and low-pressure plasma treatments modify the surface chemistry and the topography of the PP fibres and select the optimal conditions for treatment.

- **To study** if the surface modification produced reverts in a modification of the loading of an antibiotic (ampicillin) on the polymer fibres.
- **To determine** the influence of plasma treatments of the PP meshes with non-polymering gases on the release properties of ampicillin.
- Given the relevance of surface adhesion in biological properties, its modification **will be investigated** through plasma polymerization treatments.
- **To verify** the conservation of the antibacterial activity of the drug loaded in the plasma-treated PP surgical meshes.

2.4. Stages to reach the objectives

To achieve the main objective of designing new delivery systems for active principles using textile materials as supports in which the modulation of the release of the active principles is the consequence of the surface modification by plasma treatment, the following strategies and stages have been stated:

- Characterize the textile materials
- Study the modification of the surface properties (physical, chemical and topographical) of plasma treated textiles.
- Study the impregnation and release of various active ingredients from the untreated fabrics.
- Study the impact of plasma modification of textile products on the impregnation and the release kinetics of the active pharmaceutical and cosmetic molecules selected.
- Study the influence of the initial state and preparation of the textile fibres.

- Determine the plasma working parameters directly influencing the modulation of the release of the active principles (gas flow rate, power, processing time, pressure, etc.).
- Find pharmacokinetics models that can adjust the release profiles according to the treatment plasma applied.

2.5. Structure of the thesis

After the introduction dedicated to the state of the art in the fields of medical textiles, chemical fibres, cosmetic and pharmaceutical active principles and plasma treatment of polymers and textile materials, and the exposition of the objectives presented in this section, the textile materials, experimental protocols, strategies and techniques used for the development of this Thesis are presented in the following experimental part.

Afterwards, the results and discussion have been organized in two differentiated parts. The **first part** aims at the study of the influence of plasma treatment on the physical, chemical and topographical properties of a polyamide 6.6 knitted fibres, and its consequences on the loading of ketoprofen and methylxantines compounds into the fabric and on the subsequent release of such active principles from the fibres to an isotonic liquid media, in view to an application of the polyamide fabric as drug delivery system for topical application.

The **second part** aims at the influence of plasma treatment on physical, chemical and topographical properties of a polypropylene mesh and its consequences on the loading of the ampicillin into the mesh and on the subsequent release of such antibiotics from the fibres to an isotonic liquid media, in view to an application of the polypropylene fabric as drug delivery system as implantable textile. Antibacterial properties of plasma-treated PP mesh has also been studied, as well as a subsequent polyethylene glycol coating by plasma polymerization of the ampicillin-loaded PP mesh to support the modulation of the antibiotic release from the PP fibres.

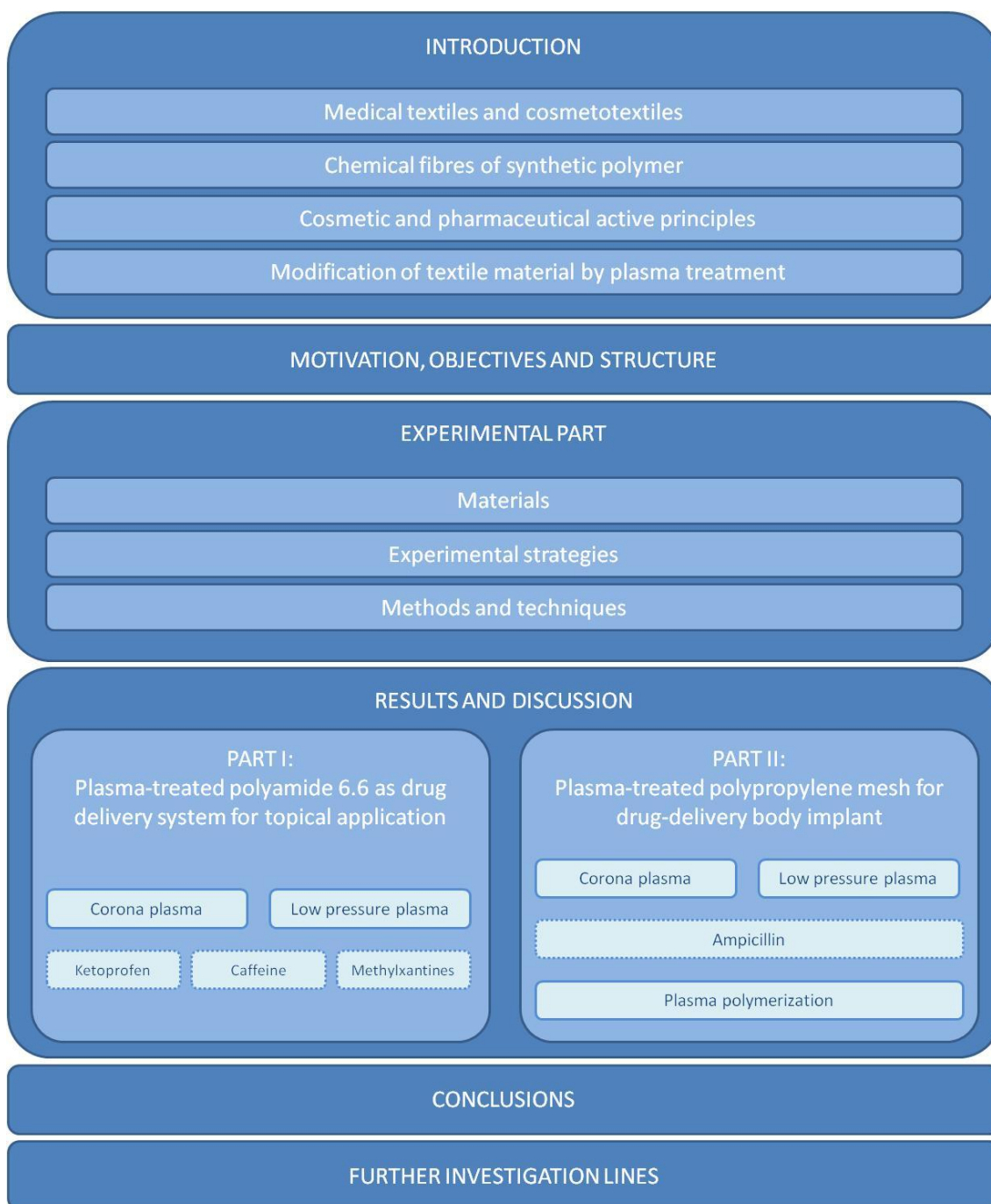


Figure 22: Structure of the PhD. Thesis.

This PhD. Thesis will conclude with a final chapter in which the most relevant results will be recapitulated, leading to an opening regarding the further investigation lines. Therefore, the structure of the Thesis can be schematized as described in Figure 22.

EXPERIMENTAL PART

3. EXPERIMENTAL PART

3.1. Material

3.1.1. Textiles and polymer films

For this research, two different fabrics have been employed:

- A polyamide 6.6. (PA66) elastic-compressive knitted fabric, undyed, kindly provided by *Tejidos Elásticos Lloveras S.A.* (Spain) with a density of $132 \text{ g}\cdot\text{m}^{-2}$ has been used as medical textile support for topical applications (Figure 23). It is made by textured multifilaments of PA66 and multifilament of elastane (Lycra) fully covered with circular-section PA66 multifilaments, being only the polyamide filaments directly exposed to the surface.

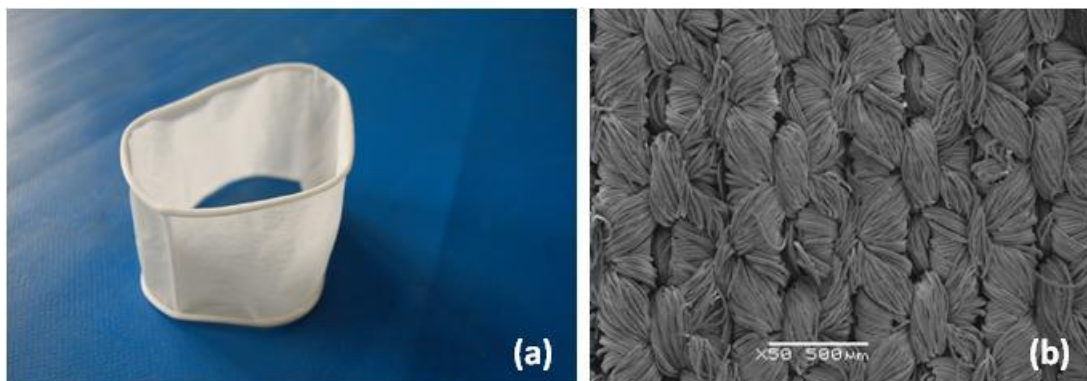


Figure 23: PA66 elastic-compressive knitted fabric (a) macroscopic image and (b) SEM image used as textile supports in this PhD. Thesis.

- A polypropylene surgical mesh, made from a 0.15 mm diameter monofilament, with $1.3 \times 1.0 \text{ mm}$ pore size and $97 \pm 2.0 \text{ g/m}^2$ weight, provided by *SurgicalMesh™* (USA) has been selected for this research (Figure 24). This PP mesh presents a $0.53 \pm 0.10 \text{ mm}$ thickness and a MD/CMD (Machine Direction/Cross Machine Direction) grab strength of 313 and 419 N/2.5 cm

(ASTM D-5034 standard). The fabric has been manufactured from homopolymer polypropylene monofilament. According to the supplier, the PP mesh fabric has been found to meet ISO-10993 (specially parts 4, 5 and 10) for biocompatibility with respect to hemolysis, cytotoxicity and intercutaneous reactivity.

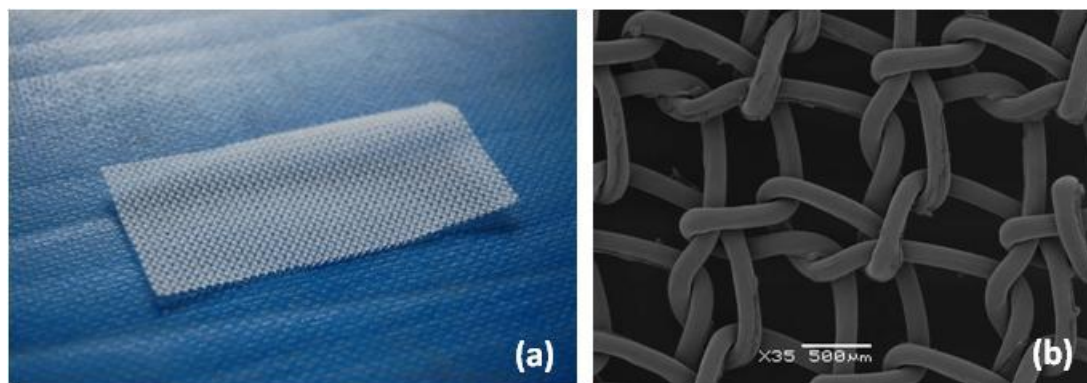


Figure 24: (a) PP mesh macroscopic image and (b) Scanning Electron Micrograph of the structure of the PP mesh.

A homopolymer PP film (*Goodfellow*, England) with a 79.2 g.m^{-2} and 0.27 mm thickness has been used as a model surface for contact angle measurements in the study of the modification of polypropylene surface by plasma treatment.

3.1.2. Active principles

3.1.2.1. Ketoprofen

Ketoprofen (2-(3-benzoylphenyl propionic acid)) (KP), is a nonsteroidal anti-inflammatory drug (NSAID) with analgesic and antipyretic properties. Ketoprofen is poorly soluble in water and its molecular weight is 254.3 g.mol^{-1} . Like other NSAIDs, KP has undesirable gastrointestinal side effects after oral administration. Among the efforts that have been made, topical and transdermal administration is one of the ways to overcome these side effects (Cordero, 1997). NSAIDs are widely used in the

treatment of rheumatoid arthritis, osteoarthritis, as well as mild remedy to moderate pain (Garcia, 2001).

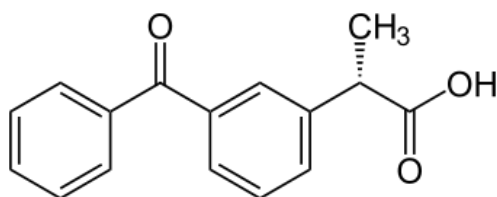


Figure 25: Chemical structure of ketoprofen.

Ketoprofen (C₁₆H₁₄O₃) (Figure 25), (KP), used as a model drug, has been purchased from *Roig Farma, S.A., Spain*, with a 99.8% purity.

3.1.2.2. Methylxantines

Three molecules from the same chemical family (methylxantines) have been employed in this work:

- Caffeine
- Pentoxifylline
- Theobromine

As explained in the following sections, caffeine has been used for its cosmetic properties while pentoxifylline and theobromine have been used in the fundamental study of the interactions between the plasma-modified surface and the active principles.

3.1.2.2.1. Caffeine

Caffeine (1,3,7-trimethylxanthine), with molecular structure shown in Figure 26, is a natural white crystalline xanthine alkaloid, occurring in coffee, cocoa beans, cola nuts

and tea leaves. It is mildly stimulating and is also used as a therapeutic agent. Caffeine has pharmacological effects on the central nervous system, heart, peripheral and central vasculature, renal, gastrointestinal and respiratory system (Ritchie, 1975).

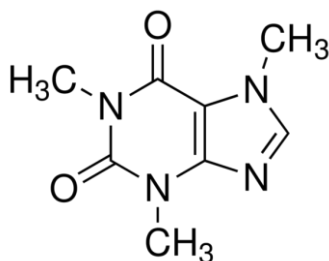


Figure 26: Chemical structure of caffeine.

However, in this work caffeine is employed as a cosmetic active principle for the treatment of cellulite. For cosmetic purposes, caffeine is reported to be used as an active compound in anti-cellulite products (Bertin, 2001), as described in section 1.3.2. Caffeine (*Fagron Iberica S.A*, 99.0%) was used in aqueous solution.

3.1.2.2.2. Pentoxifylline

Pentoxifylline (1-(5-oxohexyl)-3,7-dimethylxanthine), also known as Pentopak, Pentoxil, and Trental, is a xanthine derivative haemorrhheological agent (Figure 27). Pentoxifylline reduces the viscosity of blood by increasing the flexibility of erythrocytes, encouraging migration of white cells, inhibition of aggregation of platelets, and lowering of the viscosity of plasma, actions that might correct microcirculatory disorders (Ward, 1987).

Pentoxifylline has been purchased by *Sigma Aldrich*[®] with a purity grade ≥ 99.0 %. It presents a molecular weight of 278.31 g/mol and a limit of solubility in water at 20 °C of 517 mg/L.

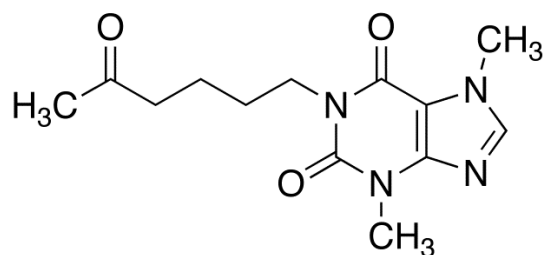


Figure 27: Chemical structure of pentoxifylline.

3.1.2.2.3. Theobromine

Theobromine (3,7-dimethylxanthine) is a crystalline powder with a colour listed as either white or colorless, such as caffeine and pentoxifylline (Figure 28). It has a similar, but lesser, effect than caffeine on the human nervous system as well as on vascular disease, making it a lesser homologue. The only molecular difference with caffeine is that the N-H group of theobromine is an N-CH₃ group. Theobromine (C₇H₈N₄O₂) has been purchased by *Sigma Aldrich*[®] with a purity grade ≥ 99.0 %. It presents a molecular weight of 180.164 g/mol and a slightly water-solubility of 330 mg/L at 20 °C.

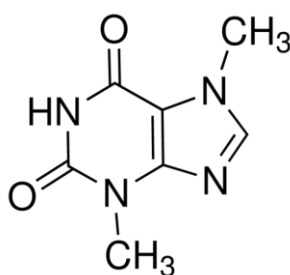


Figure 28: Chemical structure of theobromine.

3.1.2.3. Ampicillin

Ampicillin is a β -lactam antibiotic that is active against both gram-positive and gram-negative bacteria and is widely used for the treatment of infections (Farang, 1998; Queiroz, 2001). Ampicillin (C₁₆H₁₈N₃NaO₄S) possesses an amino group side chain

attached to the penicillin structure (Figure 29). This penicillin derivative inhibits bacterial cell-wall synthesis by inactivating transpeptidases on the inner surface of the bacterial cell membrane. Ampicillin sodium salt (371.39 g/mol), provided by *Sigma Aldrich*[®] in white powder, presents a water solubility of 50 mg/mL .

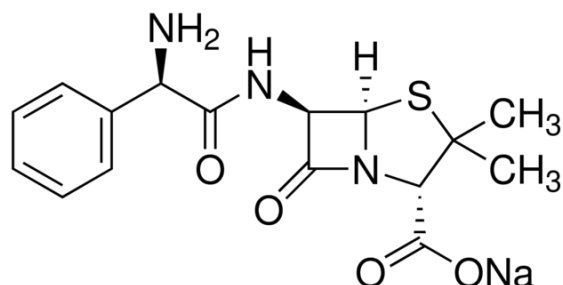


Figure 29: Chemical structure of ampicillin sodium salt.

In this PhD. Thesis, ampicillin was the drug selected for incorporation in PP mesh for the treatment of surgical infections.

3.1.3. Chemicals

- ECE standard detergent without brightening agent provided by *SDC* (Bradford, England) has been used for the laboratory washing of the PA66 and PP fabrics according to ISO 105:C06.
- Phosphate buffer saline (PBS), pH 7.4, was prepared from KH_2PO_4 (*Fagron Iberica S.A.V*, Spain), Na_2HPO_4 (*Probus S.A*, Spain), NaCl (*Acofarma*[®], Spain), and Milli-Q[®] deionized water. All these chemicals were of analytical grade.
- Orthophosphoric acid (H_3PO_4), 85% purity, from *Scharlab S.L.* (Spain) was used to adjust the pH value of the phosphate buffer solution.

- Ethanol (*Fagron Iberica S.A.V*, Spain) with 99.8% purity was used to prepare the hydro-alcoholic solution of ketoprofen.
- Ambient air was used as reactive gas for corona plasma generation and low pressure plasma generation
- Argon (Ar) (*Air Liquide S.A.*, France), was employed as initiator gas during the surface activation process by pulsed-plasma, previous to the plasma polymerization of poly(ethylene glycol) (PEG) on the polypropylene fibres.
- Tetraethylene glycol dimethyl ether ($\text{CH}_3\text{O}(\text{CH}_2\text{CH}_2\text{O})_4\text{CH}_3$), also called tetraglyme with purity $\geq 99\%$ (*Sigma-Aldrich*), was employed as precursor in liquid form for the plasma polymerization to obtain coatings of PEG in the surface of PP fibres.
- Agar bacteriological (*Scharlau S.A.*, 07-004, 500 g, lot 100921) and Brain Heart Infusion Broth (BHI Broth) (*Scharlau S.A.*, 02-599, 500 g, lot 10227) have been used to prepare the bacteriological culture media of *Staphylococcus aureus*.
- Milli-Q water (*Millipore Corp.*)

3.2. Experimental strategies

The research performed has been conducted in three main parts, as shown in Figure 25:

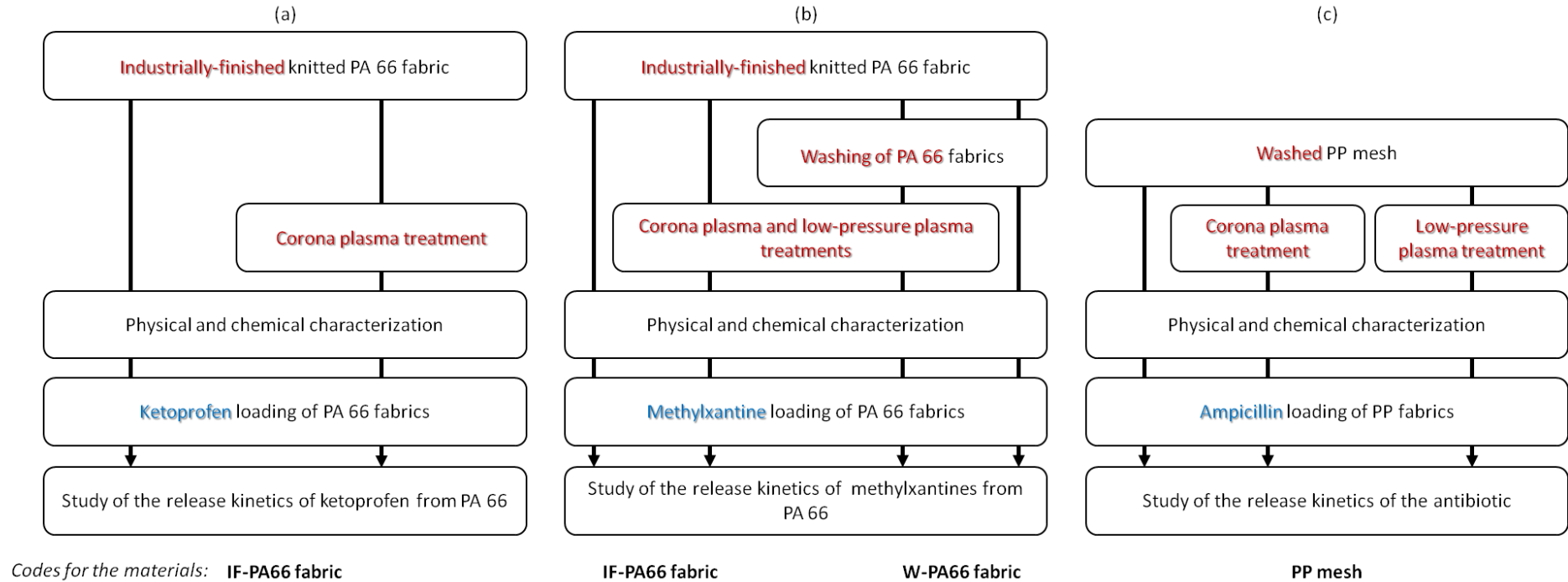


Figure 30: Experimental scheme followed for (a) ketoprofen loading of industrially-finished PA66 knitted fabrics for pharmaceutical topical applications, (b) for the study of the influence of plasma treatment and initial preparation of the PA66 fabrics on the loading and the release of methylxantines, and (c) for obtaining plasma-treated ampicillin-loaded PP meshes to study of the influence of the plasma on the PP meshes for the loading and the release of ampicillin from the PP fibers.

3.3. Methods and techniques

3.3.1. Washing processes of the fabrics

Given that the polyamide fibers (IF-PA66) contain additives coming from industrial processing such as mineral oils, antistatic products, paraffin oils and/or silicone, a laboratory washing was carried out to obtain washed PA66 (W-PA66) and to study the influence of the surface state (and of these additives) on the plasma treatments and also on the subsequent impregnation and release of active principle from the fibers. All the PP mesh samples have been used after washing.

Washing of both PA66 and PP was carried out using an *Ahiba Polymat* equipment with bath ratio of 1/10 and 5% v/v ECE standard detergent (ISO105:C06). Working conditions were maintained constant (60 °C, 40 r.p.m.) during the 30 minutes of the process. Samples were rinsed five times under the same working conditions in distilled water. Finally they were dried at 60 °C during 12 h followed by over-drying at 105 °C during 15 min before their storage, in a desiccator (Figure 31).



Figure 31: Storage of PP fabrics in a desiccator to avoid humidity absorption.

Two types of nomenclatures for polyamide 6.6 fabrics appear, corresponding to the initial preparation of the fabric, as the influence of the initial state of the PA66 fabrics has also been evaluated and compared between industrially-finished PA66 (I-PA66) and laboratory washed PA66 (W-PA66).

3.3.2. Plasma treatments

In this research work, three different commercial plasma reactors have been employed: a corona plasma for treatments at atmospheric pressure and two low-pressure plasma reactors. Surface activation and functionalization of fiber surfaces have been performed by corona plasma and low-pressure while coating by plasma polymerization has been carried out only with low pressure plasma.

3.3.2.1. Corona plasma treatment

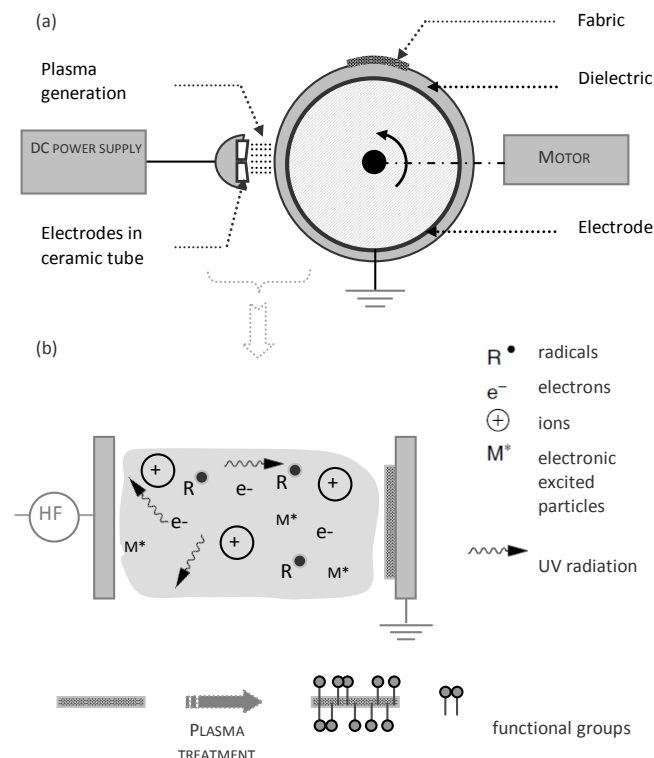


Figure 32: (a) Scheme of the corona plasma used to treat the textile samples. (b) Scheme of different reactive species present in the plasma generation zone.

Corona plasma treatments were carried out by means of an *Ahlbrandt FG-2* (Germany) equipment, using air as gas for plasma generation. Distance between the electrode and the fabric was adjusted to 20 mm. Upper electrode size was of (400 × 20) mm. During the treatments, power, speed and incident current were kept constant at 380 W, 15 r.p.m. and 1.90 A respectively. In these optimized conditions, each passage of the textile material between both electrodes corresponds to a 0.35 s plasma treatment for any point of the fabric.

Fabrics were treated for 1, 3, 5, 10 or 20 plasma sequences, corresponding to 0.35 s, 1.05 s, 1.75 s, 3.5 s and 7.0 s of contact between plasma and fabric surface. Textile samples were laid flat on the roll, attached at their ends with a piece of tape.

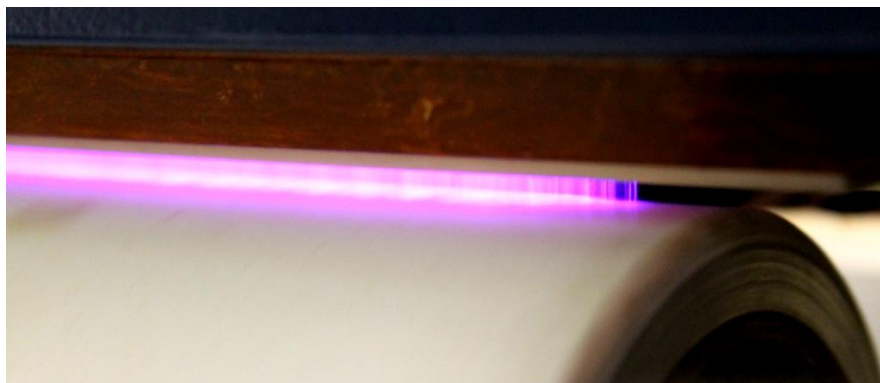


Figure 33: Plasma generation with ambient air using an *Ahlbrandt FG-2* corona plasma equipment.

3.3.2.2. *Low pressure plasma treatment*

Low pressure plasma treatment was carried out by an *Europlasma Junior Advanced PLC* (Belgium) equipment. Plasma treatment of the fabrics has been carried out with the textile samples laid flat, without mechanical tension, on a glass support between both electrodes in the plasma chamber, as presented in Figure 34c.



Figure 34: Europlasma Junior Advanced PLC low-pressure plasma equipment using with air as gas for plasma generation (a). Focus of the panel control screen (b) and the inside of the chamber (c).

Power supply was kept constant at 100 W while gas flow was studied in the range between 5 and 15 L/min, plasma treatment time between 30 s and 300 s, and gas pressure between 0.13 and 0.40 mbar. PA66 fabrics were laid flat on the ground of the reactor, as shown in Figure 35, so that only one side of the sample was directly exposed to the plasma treatment, although it can be considered that the plasma species may penetrate through the loose knit fabrics structure and modify both sides of the material (Poll, 2001).

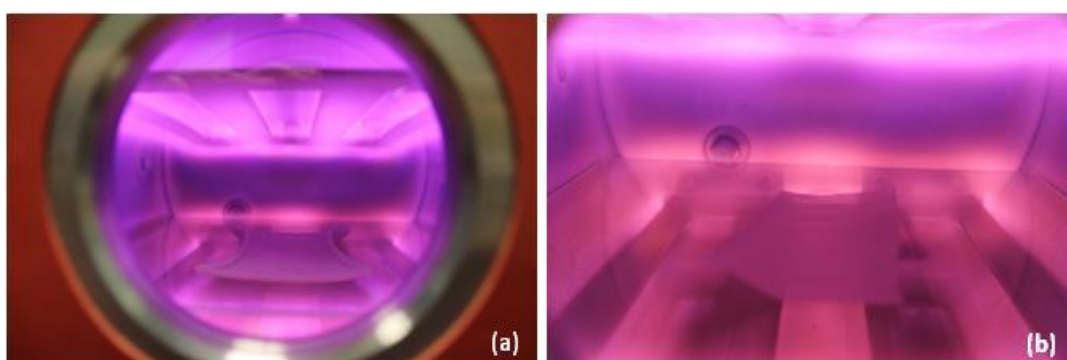


Figure 35: Picture of the low pressure plasma reactor used in this PhD. Thesis for the treatment of PA66 (a) and PP (b) fabrics with air as plasma generation gas.

Low-pressure plasma treatment consists of the following stages:

- Introduction of the textile samples in the chamber

- Initial vacuum of the chamber to a value < 0.40 mbar.
- Entry of air for 30 s until keeping constant the pressure.
- Plasma treatment between 30 s and 300 s at constant power of 100 W and gas flow range between 5 and 15 L/min, as a function of the studied working conditions.

3.3.2.3. Low pressure pulsed-plasma polymerization

Plasma polymerization was carried out with an equipment of low-pressure radio-frequency plasma (13.56 MHz) (*Standard Femto Plasma System*, Diener, Germany) (Figure 36), equipped with mass controllers for the gas inlet and a bubbler system for the introduction of monomer.

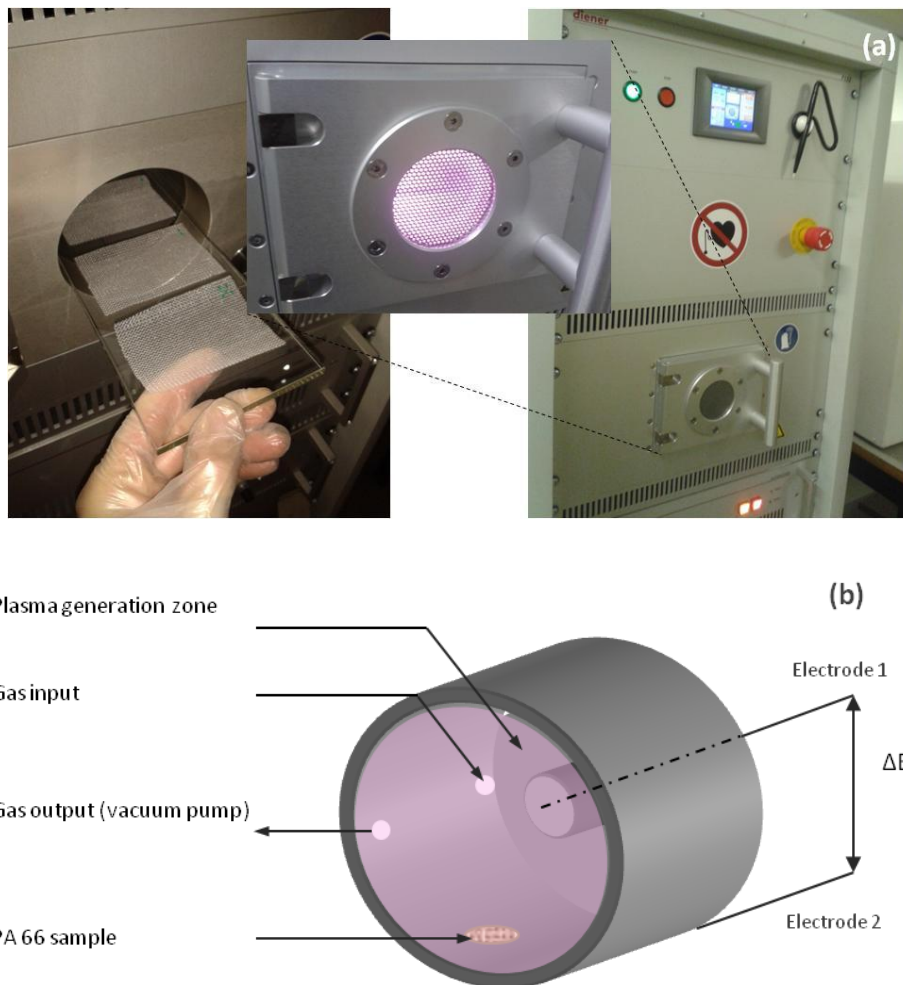


Figure 36: Standard pulsed-plasma equipment used for polymerization (a). Schematic cross-section of the reactor (b).

In this work, plasma polymerization has been used to create a deposited biocompatible (PEG) film after active principle impregnation of PP fabrics to modulate its release and preserve a low cellular adhesion to the PP fibre, since polyethylene glycol is a well-known non-fouling material used for protein adsorption and cellular adhesion. To obtain coatings of PEG by plasma polymerization, it starts from a precursor with four repeating units, the tetraglyme, with molecular formula $\text{CH}_3\text{O}(\text{CH}_2\text{CH}_2\text{O})_4\text{CH}_3$ as presented in Figure 37.

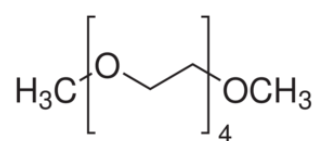


Figure 37: Tetraglyme molecule used as precursor for plasma polymerization.

The plasma polymerization consists in introducing tetraglyme in the plasma chamber by bubbling liquid tetraglyme with a carrier gas, in the setup argon. Before the polymerization, a surface activation is carried out with argon. Activation plasma consists of the following stages:

- Introduction of the textile samples in the chamber (maximum 3 samples by plasma treatment) as shown in Figure 36.
- Initial vacuum of the chamber to a value of 0.20 mbar.
- Entry of argon gas for 1 min, keeping the pressure at 0.40 mbar.
- Plasma treatment during 30 s and a power of 100 W.

The plasma polymerization was carried out in pulsed mode, with plasma pulses of 20 μs spaced of 20 ms (values set by the manufacturer) and consists of the following stages:

- Initial vacuum chamber to a value of 0.20 mbar, right after the end of the activation step.

- Introduction of tetraglyme monomer in the chamber for 1 min by bubbling tetraglyme in liquid phase with argon gas.
- Plasma pulses of 20 μ s spaced of 20 ms with a power of 200 W during 30, 60 or 120 minutes to study the influence of treatment time.

To minimize the ageing process of all plasma-treated samples, analysis and post-treatments like fabric impregnation and surface analysis were carried out right after plasma treatment of the fabrics (Boyd, 1997; Canal, 2004; Canal, 2008).

3.3.3. Loading process of active principles into textile materials

As described in Table 5, ketoprofen was been used as pharmaceutical active principle for the impregnation of PA66 fabrics aimed as topical application. PA66 was been used as textile support for the release of caffeine, theobromine and pentoxifylline, used as cosmetic active principles in the treatment of lipids and cellulite, also for topical application. Finally, antibiotic loading of PP meshes for body implant applications was done with ampicillin.

Table 5: Classification of the active principles used with their corresponding textile fabrics as used in this PhD. Thesis.

Polyamide 6.6 knitted fabric	Polypropylene mesh
<p>Anti-inflammatory model drug</p> <ul style="list-style-type: none"> • Ketoprofen <p>Anti-cellulitic model drugs</p> <ul style="list-style-type: none"> • Caffeine • Theobromine • Pentoxifylline 	<p>Antibiotic</p> <ul style="list-style-type: none"> • Ampicillin

Different active principles have been used, and the loading methods have been optimized in each case as described in the following sections.

3.3.3.1. Polyamide fabric impregnation

3.3.3.1.1. Ketoprofen loading of PA66 knitted fabrics

PA66 knitted fabrics were cut into discs of 2.5 cm diameter and impregnated dropwise with 150 μL of a 1% ketoprofen solution in $\text{H}_2\text{O}/\text{EtOH}$ (1:1 wt%). Samples were dried in an oven for 24 hours at 50 °C. The samples were weighed again to calculate the amount of ketoprofen absorbed by the fibres.

Impregnation of the fabrics previously treated by plasma was carried out right after the plasma treatment, on the plasma-treated side of the samples.

3.3.3.1.2. Caffeine and methylxantines loading of PA66 knitted fabrics

PA66 knitted fabrics were cut into rectangular samples of 11.6×6.0 cm, weighing about 1.90 g. Impregnation of the PA66 samples was carried out by immersion in 50 mL of a 1% caffeine solution in distilled water, during 10 min, with continuous shaking at 90 r.p.m. at 20 °C.

Subsequently, PA66 samples were submitted to a double padding process under 1.0 kg/cm^2 pneumatic pressure and 1 m/min speed working conditions in a laboratory pneumatic padder (*Tepa*, Spain) (Figure 38) to guarantee an uniform distribution of the product on the textile fabric sample. Samples were finally dried in an oven during 24 hours at 37 °C.



Figure 38: Padding equipment used for homogenization of the active principle on the PA or PP sample after impregnation process.

Impregnation of the plasma-treated fabrics was carried out 10 min after plasma treatment to avoid ageing process of the sample and a loss of the wetting properties achieved with plasma treatment, as observed in previous works (Canal, 2004).

Both for ketoprofen as well as for caffeine and methylxantines loading, the PA66 samples were weighed before and after the impregnation process to calculate the amount of caffeine in the fibers and the impregnation ratio (%), following the Equation (1).

$$\% I = \frac{W_f - W_i}{W_i} \times 100 \quad (1)$$

where W_f is the final weight of the wet sample after impregnation and double padding process and W_i the initial weight of the fabric. Samples were kept in a dessicator until constant weight.

3.3.3.2. Polypropylene fabric impregnation

Polypropylene meshes were cut into rectangular samples of (7.0×5.0) cm, weighing about 0.32 g. Impregnation of the PP samples was carried out by immersion of 6 PP

samples in 20 mL of a 4% ampicillin solution in distilled water, during 24 h with continuous shaking at 160 r.p.m. at 20 °C. This setting corresponds to a bath to fabric ratio of 1/10 (2 g of fibers in 20 mL solution). Subsequently, PP samples were submitted to a double padding process under 1 kg/cm² pneumatic pressure and 1 m/min speed working conditions. Samples were finally dried in an oven during 24 hours at 37 °C. The samples were weighed before and after the impregnation process to calculate the amount of ampicillin in the fibers and the impregnation ratio, according to Equation (1).

As for PA66 samples, the impregnation of the plasma-treated PP fabrics was carried out 10 min after plasma treatment to avoid ageing of the wetting properties achieved with plasma treatment. Samples were dried until constant weight and stored in a dessicator.

3.3.4. In-vitro release assays

The drug release assays, adapted from the dissolution experiments for solid pharmaceutical dosage forms of *Farmacopea Española*, were performed using untreated and plasma treated PA and PP fabrics impregnated with specific active principles to determine the rate of release and the yielded concentration of such molecules to an isotonic liquid medium. For the drug release study, five thermo-stabilized vessels were used to have replicates of the measurements. They were filled with 300 mL of PBS (pH 7.4) and stirring and temperature were maintained constant at 25 r.p.m. and 37 °C respectively, during the 8 or 24 hours of the release experiment (Figure 39). It has been estimated that an average time of wearing a garment may be around the time interval, justifying this timeframe selection. The different textile samples, with the specific geometry described in the section 3.3.3, were placed on a vertical stainless steel holder that ensures uniform and continuous optimum contact between the textile materials and the buffer solution. 1 mL samples were withdrawn from the receptor compartment for latter spectroscopy analysis that allowed determining the quantity of drug that was released from the textile materials. After each sample withdrawal, the same volume of fresh PBS was added to the receptor

medium. Sink conditions were kept constant in the receptor solution during the experiment (Washington, 1990). To obtain the release profile of each type of fabrics, 4 replicates of each drug-loaded textile material have been studied, together with a non-loaded fabric used as a reference.



Figure 39: Active principle release experiment.

For the analysis of the concentration of the active principles, UV-Vis spectrophotometry was used at fixed wavelength depending on the maximum absorption of the determined active principle, as described in section 3.3.5.5.

For ketoprofen concentration determination, the detection wavelength used was 233 nm, corresponding to the wavelength of maximum peak of absorption. Maximum peak absorption has been detected at a wavelength of 273 nm for caffeine, of 264 nm for pentoxifylline, of 254 nm for theobromine and of 206 nm for ampicillin. In some experiments, for untreated and corona plasma-treated IF-PA66, caffeine concentration has also been determined by High-Pressure Liquid Chromatography as described in section 3.3.5.6.

To obtain the percentage of drug released, the following calculations and corrections were made: Two volume corrections were taken into account to determine precisely the drug concentration in the trial compartment at each moment t : (i) A total volume correction due to evaporation and (ii) a step to step correction due to sample collection.

➤ Total volume correction

This correction is due to the weak evaporation of liquid medium during the experiment so that the final volume is not the same than the initial one. Assuming a constant evaporation during the study, a linear correction is carried out taking into account initial and final volumes:

$$v^t_{cor} = v_i - \left(\frac{v_i - v_f}{t_f} \right) \cdot t \quad (2)$$

with v^t_{cor} : corrected volume at the sampling time t (mL)

t : duration of experiment (min)

v_i : initial volume (mL)

v_f : final volume (mL)

t_f : sampling time (min)

So, from the volume correction, a first correction of the drug concentration in the release media is done at each timepoint t by the following equation:

$$c^t_{cor} = \frac{c_i}{v_i} \cdot v^t_{cor} \quad (3)$$

with c^t_{cor} : corrected drug concentration at the sampling time t (mg/L)

c_i : drug concentration as obtained from the reading of the spectrophotometer (mg/L)

v_i : initial volume (mL)

➤ Step to step correction due to sampling :

This correction is due to the withdrawal of the liquid sample from the release compartment. At each timepoint t, a certain volume of sample (1 mL) is withdrawn and the same volume of PBS is added. Therefore, a little variation of drug concentration

(slight dilution) after each withdrawal that has to be taken into account. The real concentration of drug at time t of the experiment is calculated the following equation:

$$C_{real}^t = \frac{(v_{cor}^t \cdot C_{cor}^t + v_s \cdot C_{cor}^{t-1})}{(v_{cor}^{t-1} + v_s)} \quad (4)$$

with C_{real}^t : real released concentration of active principle (mg/L) at instant t

C_{cor}^t : drug concentration at instant t, already corrected for evaporation

C_{cor}^{t-1} : drug concentration at instant (t-1), already corrected for evaporation

v_{cor}^t : corrected volume (mL)

v_s : withdrawn sample volume (mL)

The values obtained from Equations (3) and (4) are used in all the subsequent calculations. The released percentage of drug in the isotonic liquid media at a determined instant t of the experiment (R^t %) is obtained from C_{real}^t , the corrected volume v_{cor}^t and the weight of loaded-active principle in the fibres before the release experiment Δ_m , following the equation:

$$R^t \% = \frac{(C_{real}^t \cdot v_{cor}^t) \cdot 10^{-3}}{W} \times 100 \quad (5)$$

with R^t : drug released percentage in the isotonic liquid media at instant t (%)

C_{real}^t : corrected concentration of drug in the isotonic liquid media at instant t (mg/L)

v_{cor}^t : corrected volume at instant t (mL)

W : weight of active principle loaded in the fibres before release experiment (mg)

From the values of drug release percentage R% at determined instant t of the assay, the drug release kinetics $R\% = f(t)$ have been plotted and the comparison of the drug release kinetics profiles from the different plasma-treated PA66 and PP fabrics has

been performed to evaluate the influence of the kind of plasma treatment and the plasma working conditions on the release kinetics of the drug.

3.3.5. Physical characterization techniques

Different characterization methods have been used to investigate the influence of plasma treatment on the physical properties (topography, morphology) and the surface chemistry (wetting behavior and functional groups on the fibre surface) of such fibres. These characterization techniques are reported in Table 6 and are described in details in the following sections.

Table 6: Experimental techniques used for the physical characterization and the surface chemistry analysis of the elastic-compressive PA66 fabrics knitted fabric and the PP mesh.

Experimental techniques used for the characterization of the fabrics	
Elastic-compressive polyamide 6.6 knitted fabric	Polypropylene mesh
<ul style="list-style-type: none"> • Static contact angle • Drop test • X- ray Photoelectron Spectroscopy • Scanning Electron Microscopy 	<ul style="list-style-type: none"> • Static contact angle on PP film • X- ray Photoelectron Spectroscopy • Scanning Electron Microscopy • Atomic Force Microscopy • Antibacterial assays

3.3.5.1. Scanning Electron Microscopy (SEM)

A Scanning Electron Microscope (SEM) allows to produce image of objects in the micro to nanometer range with relatively lower diffraction effects. The optical wavelengths from deep UV to IR are in range of hundreds of nanometers while electron beams of energy in keV have wavelengths in fractions of nanometers. Using a SEM to produce

proper topographic image of a surface requires a judicious choice of beam energy, intensity, width and proper preparation of the sample being studied. Nowadays, the electron beam in a SEM is generated using a field emission filament that uses ideas of quantum tunneling. The deflection of an electron beam of a certain energy E is accomplished by means of electromagnetic lenses. Typical E values for conventional SEM can range from as low as 2-5 keV to 20-40 keV.

A basic SEM consists of an electron gun (field emission type or others) that produces the electron beams, electromagnetic optics guide the beam and focus it. The detectors collect the electrons that come from the sample (either direct scattering or emitted from the sample) and the energy of the detected electron together with their intensity (number density) and location of emission is used and processed to put together image. Nowadays some SEM equipments also offer energy dispersive photon detectors that provide analysis of X-rays that are emitted from the specimen due to the interactions of incident electrons with the atoms of the sample.

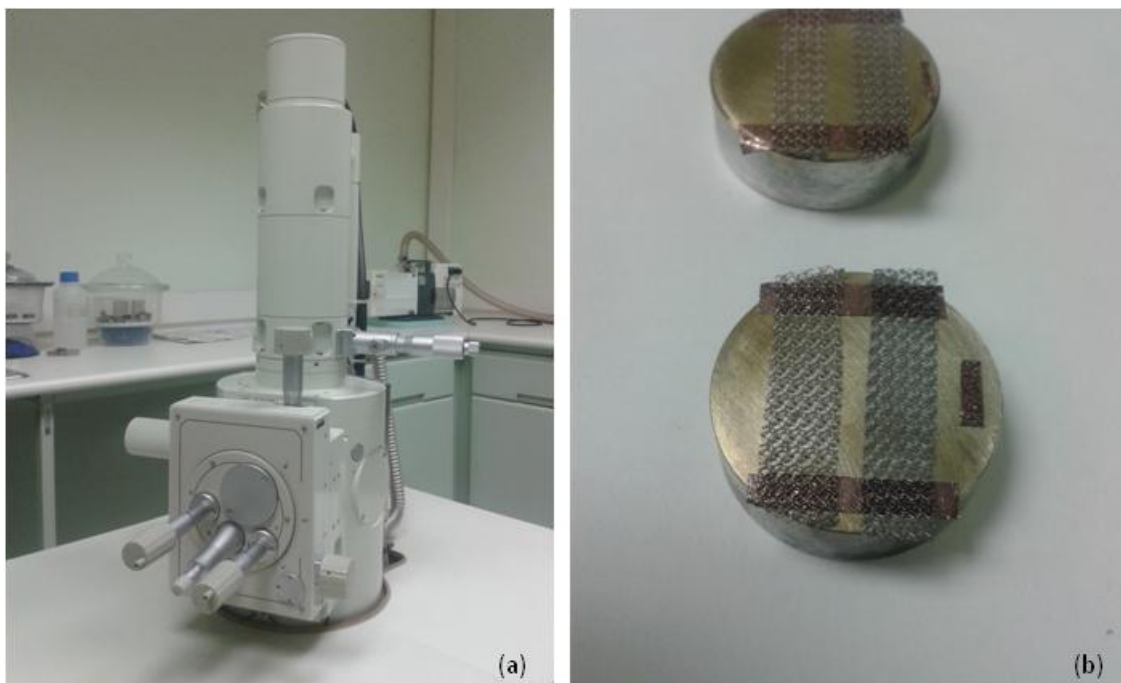


Figure 40: (a) *Jeol JSM-5000/5610* SEM Field-Emission Scanning Electron Microscopy. (b) Au-coated PP mesh fabrics prior to SEM observation (UPC, Terrassa, Spain).

In this work, two different SEM were used:

Topography of PP and PA66 fibres was studied by Field- Emission Scanning Electron Microscopy using a *Hitachi S-2300 SEM*. All samples were C coated prior to SEM observation with a sputter coater. Observations were carried out at 10 kV working voltage.

Topography of PA66 fibers was studied by Field-Emission Scanning Electron Microscopy using a *Jeol JSM-5000/5610 SEM* (Figure 40). Samples were Au-coated before SEM observation with a *Baltec SCD 005* sputter coater. Observations were carried out at 10 kV working voltage.

3.3.5.2. Atomic Force Microscopy (AFM)

Atomic force microscopy (AFM) is a powerful characterization tool for polymer science, capable of revealing surface structures with superior spatial resolution (Cohen, 1994). AFM is a modern technique for generating high resolution surface topography images and it can capture many orders of magnitude below the optical diffraction limit. It uses principally a similar to the one used by the phonograph developed by Thomas Edison. Essentially, the phonograph has a sharp object which is dragged across a moving surface, the tip is deformed by the features it encounters and the signal is converted in another one (acoustic signal in this case) (Frewin, 2012). AFM rests upon the same principle, with a more complex and precise feedback system.

An AFM consists of a probe, a scanner, a controller, and a signal processing unit-computer. AFM works by scanning a sharp probe across the surface to obtain a three-dimensional surface topographic picture. As the probe rasters, it feels the highs and lows of surface topography through complex mechanisms of tip-surface interactions. The forces between the tip and the sample are measured during scanning, by monitoring the deflection of the cantilever (Cohen, 1994). These signals are sent back via a laser reflected back from the probe surface to a photo-detector. The photo-detector through a feedback control loop, keeps the tip at constant height or constant

force from the surface (Figure 41a). The feedback signals are sent to a signal processing software, which generates a three-dimensional topographic image of the surface. Further interactions arising between the tip and the sample can be used to investigate other characteristics of the sample, the tip, or the medium in-between (Butt, 2005). AFM has developed into a multifunctional technique suitable for characterization of topography, adhesion, mechanical, and other properties on scales from tens of microns to nanometers (Sitterberg, 2010).

Considering the versatility of types of samples, several modes have been developed and adapted to scope with the demand of the specific research field. The operating modes of AFM can be divided into *static (DC) mode* – the probe does not vibrate during imaging, and *dynamic (AC) mode* – the cantilever is excited to vibrate at (or off) its resonant frequency. In dynamic mode the character of repulsive forces between the tip and the sample enables examination of even single polymer molecules without disturbance of their integrity (Kocun, 2011).

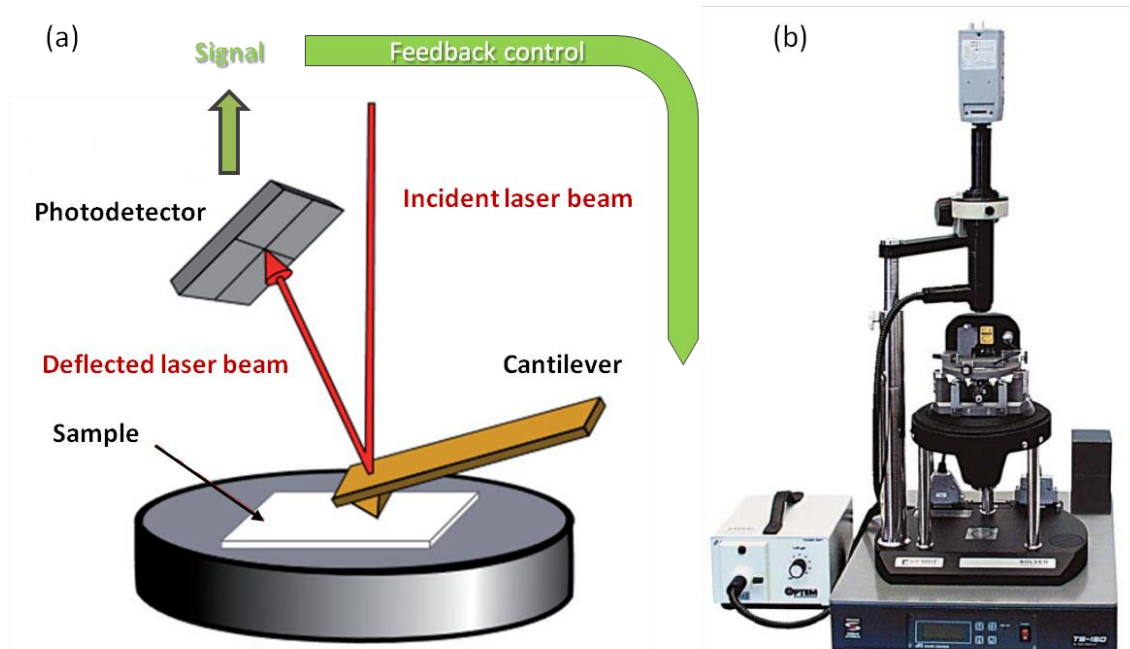


Figure 41: Schematic functioning principle of an Atomic Force Microscope (a). Picture of the Solver Pro NT-MDT Atomic Force Microscope used in this work (IJS Center, Ljubljana, Slovenia) (b).

Surface topography of the PP and PA fibres was investigated by Atomic Force Microscopy with a *Solver Pro NT-MDT* equipment (Figure 41b) in air environment, with manufacturer specific software. Oscillating semi-contact mode with Si cantilever was used for surface imaging over range (1×1) to (20×20) μm. Surface roughness R_a was calculated after subtraction of the background from the image, using the following relation:

$$R_a = \frac{1}{N} \times \sum_i (z_i - \mu) \quad (6)$$

where N is the total number of height data per image, z_i is the heightvalue of data point i and μ is the average height of the samplesurface after plane subtraction.

3.3.5.3. X-ray Photoelectron Spectroscopy (XPS)

XPS is an instrumental technique used to obtain chemical information from the first nanometers of the surface of a material. From the XPS spectra information is obtained on the surface chemical composition and chemical bonds. During the XPS analysis, a sample is illuminated with a monochromatic X-ray light in the spectrophotometer and the energy of emitted photoelectrons from the sample is analyzed. In the photoelectron spectrum, which represents the distribution of emitted photoelectrons as a function of their binding energy, peaks can be observed which are characteristic of the different element sfrom the sample surface until 6 nm in depth. In this PhD. Thesis, 2 different XPS were used:

(1) Surface chemistry of PA66 and PP samples was analyzed with a *PHI ESCA-5500 Multitechnique System (Physical Electronics)* (Figure 42) with a monochromatic X-ray source (Al K_{α} line of 1486.6 eV energy and 350 W), placed perpendicular to the analyzer axis and calibrated using the $3d_{5/2}$ line of Ag with a full width at half maximum (FWHM) of 0.8 eV. The analized area was a circle of 0.8 mm diameter, and the selected resolution for the spectra was 187.5 eV of pass energy and 0.8 eV/step for the general spectra and 23.5 eV of pass energy and 0.1 eV/step for the spectra of the different

elements. All measurements were made in an ultra high vacuum chamber pressure between 6.7×10^{-9} and 2.7×10^{-8} mbar.



Figure 42: PHI ESCA-5500 Multitechnique System (*Physical Electronics*) equipment (IJS Center, Ljubljana, Slovenia).

(2) XPS analysis of PA66 samples aimed for ketoprofen loading was performed in XPS Spectrophotometer *TFA XPS model*, by *Physical Electronics Inc.* An Al monochromatic source of X-ray light with a power of 250 W was used. During the analysis, two types of spectra were recorded.

First, a general spectrum was performed through a wide energy range. In this spectrum, the elements present in sample surface were identified and their relative concentrations were calculated by taking into account the relative sensitivity factors of each one provided by the XPS spectrophotometer manufacturer. The results were normalized to 100%. The relative error on the calculation of surface composition for XPS method sensitivity is about 0.5%. Each sample was analyzed at two different places and the average composition is calculated. The C_{1s} peak was referred to the C-C bond energy of 285.0 eV (Brack, 1999). In addition to the wide energy range spectra,

high-energy resolution spectra of characteristic peaks of C_{1s} element were recorded through a narrow energy range.

Afterwards, C_{1s} peaks were deconvoluted into subpeaks centered in characteristic energies that correspond to determined bondings with carbon atoms. This data processing allows identifying the predominant carbon bonds in polymer surface. In this PhD. Thesis, the deconvolution of C_{1s} peak has been performed using *Multipak* and *Origin* softwares.

3.3.5.4. Wetting properties

3.3.5.4.1. Static contact angle

Water static contact angle determines surface wettability by measuring the extent of spreading of a droplet on a surface. The sessile drop technique is used for the characterization of solid surface energies. The method consists in placing a droplet of liquid of known surface energy on a solid surface and then by measuring the contact angle it establishes with the solid surface, the surface energy of the material can be determined. The theoretical description of contact angle arises from the consideration of a thermodynamic equilibrium between the three phases: the liquid phase, the solid (S), and the gas phase (G). The shape of a liquid/vapor interface is determined by the Young–Laplace equation, with the contact angle playing the role of a boundary condition following the Young's Equation:

$$\gamma_{SG} - \gamma_{SL} - \gamma_{LG} \times \cos \theta = 0 \quad (7)$$

where γ_{SG} corresponds to the solid–vapor interface energy, γ_{SL} to the solid–liquid interfacial energy, γ_{LG} to the liquid–vapor interfacial energy (i.e. the surface tension) and θ the contact angle, as described in Figure 43.

Water can be used as a test liquid to establish whether a surface is hydrophilic (angle $<45^\circ$), hydrophobic (angle $>90^\circ$) or somewhere in-between (angle of 45° to 90°) (ASTM Standard D7334). The lower the contact angle, the more hydrophilic the surface. As a surface becomes more oxidized, or has more ionizable groups introduced to it, hydrogen bonding with water becomes easier and the droplet spreads along the hydrophilic surface, resulting in a lower contact angle (Mittal, 2002).

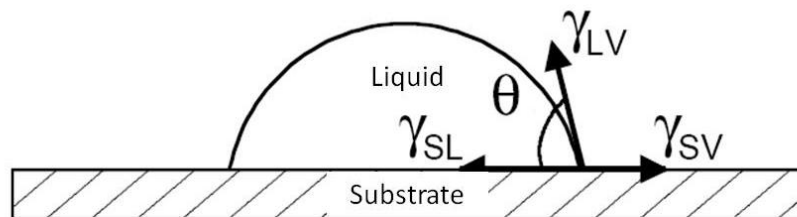


Figure 43: Schematic representation of the contact angle of a liquid drop on a solid surface.

In this work, the determination of the wetting properties of PA66 fabrics with and without plasma treatment was done by static contact angle measurements. Contact angles were measured by means of a *Krüss DSA100* goniometer equipped with a CCD camera, coupled with *DSA3* software fitting a mathematical expression to the shape of the drop and then calculating the slope of the tangent to the drop at the liquid-solid-vapor (LSV) interface line (Figure 44). PA66 textile samples were laid flat on a glass support without mechanical tension and 10 μL water droplets were laid on the fabrics. Measurements were carried out on the plasma-treated side of the samples. At least 4 replicates of each measurement were carried out. Given the open structure of PP meshes, a PP film was used as model surface for the determination of contact angle.

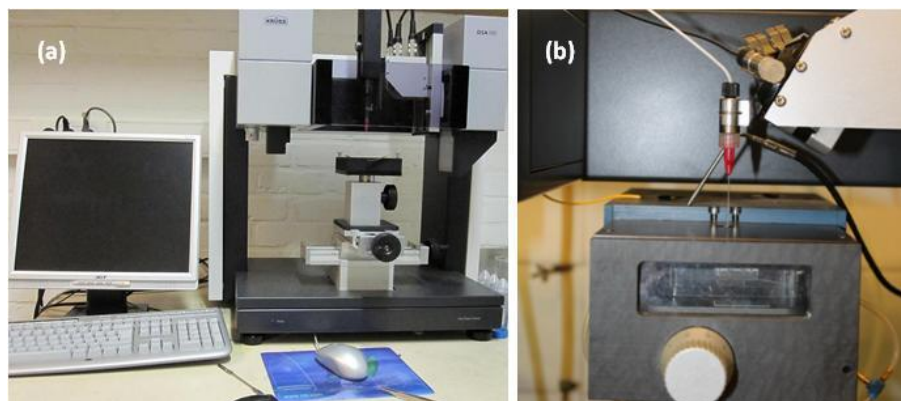


Figure 44: Krüss DSA100 goniometer (a) with detail of the sample support and the needle for deposition of the droplets (b).

3.3.5.4.2. Drop Test

Hydrophilicity of PA66 fabrics was evaluated according to the AATCC Test Method 39-1980 by determining the wetting time in seconds using the drop test. The test schematically consists of laying down a droplet of water of constant volume on the surface of the fabric and measuring the time required for its complete absorption. Results are the average of at least four measurements.

Drop test has also been used to follow the ageing of plasma-treated fabrics. The ageing of plasma-modified polymer surfaces is defined by the evolution of wettability with the elapse of storage time after plasma treatment (Canal, 2008). Therefore, an improved understanding of the ageing of modified surfaces during storage is required to optimize the processing conditions leading to interfacial properties that are controlled and predictable at the time of use. After plasma treatment of the textile materials, the samples were stored in an ambient closed environment and measurements of the plasma-treated fabrics are repeated at different time points. Evolution of the static contact angle or water absorption time of 10 μL droplet is represented as functions of time to quantify this ageing. Also, measurements of untreated fabrics were carried out as control.

3.3.5.5. UV-Visible Spectroscopy

Many molecules absorb ultraviolet (below 400 nm) or visible light (between 400 and 800 nm). When a molecule is placed in solution between a light source and a spectrometer, the substance absorbs certain part of the spectrum. An absorption spectrum shows a number of absorption bands corresponding to specific structural groups of a molecule and which are directly associated to the excitation state of outer electrons. When sample molecules are exposed to light having an energy that matches a possible electronic transition within the molecule, some of the light energy is absorbed as the electron is promoted to a higher energy orbital. An optical spectrometer records the wavelengths at which absorption occurs, together with the degree of absorption at each wavelength. The resulting spectrum is presented as a graph of absorbance (A) versus wavelength λ . Absorbance usually ranges from 0 (no absorption) to 2 (99% absorption), and is precisely defined by spectrometer working range. The absorption spectrum, registered by the spectrophotometer on the all range of wavelengths of the equipment, is specific to a given molecule. The specific absorption spectrum of each molecule allows identifying and quantifying a given molecule. Absorbance follows the Beer's Law:

$$A = \epsilon \times b \times c \quad (8)$$

Where A is absorbance (no units)

ϵ is a constant of proportionality, called the molar absorptivity, in $\text{L}\cdot\text{mol}^{-1}\cdot\text{cm}^{-1}$

b is the path length of the sample - that is to say the path length of the cuvette in which the sample is contained, expressed in cm.

c is the concentration of the compound in solution, expressed in $\text{mol}\cdot\text{L}^{-1}$.

Therefore, the absorbance of a solution, at a determined wavelength, increases with the increasing of the concentration of the molecule, and UV-visible spectroscopy allows correlating the absorbance with the concentration of some compound in solution. From the general absorption spectrum, the wavelength of the peak with the

maximum absorbance intensity is chosen for the quantification of the concentration of the molecule in aqueous solution.

UV-visible spectrometers used for this work were double-beam spectrophotometers which can determine the concentration of a determined molecule in solution comparing the absorbance of such solution (sample cell) with a reference cell containing the dispersive liquid media only, as described in Figure 45.

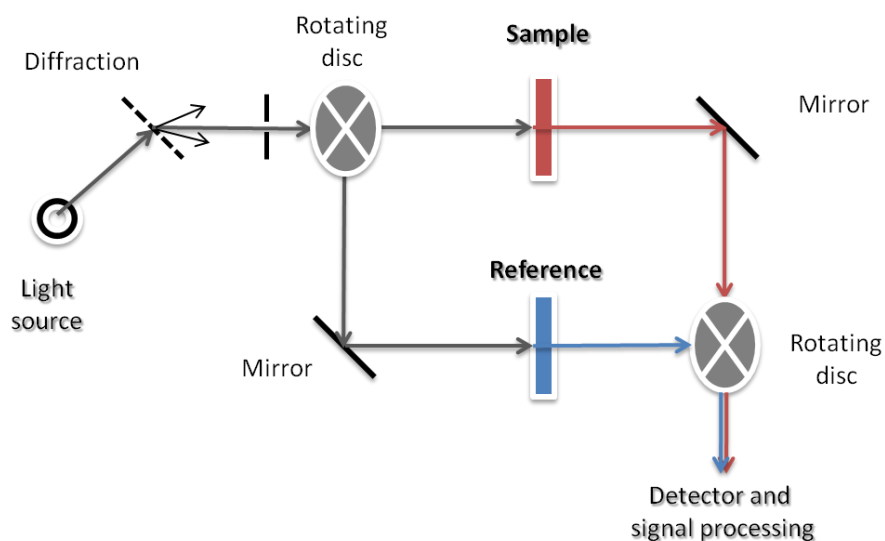


Figure 45: Schematic of the working principle of a double beam UV-visible spectrophotometer.

For the quantification of drug released, a *ThermoSpectronic - Helios β* spectrophotometer was used for ketoprofen studies, while a *Shimadzu UV-1800* spectrophotometer model of *Thermo Fisher Scientific Inc.* with *UV Probe* software was used for methylxantines and ampicillin studies.

3.3.5.6. High-Pressure Liquid Chromatography (HPLC)

High pressure liquid chromatography (HPLC) is a chromatographic method that is used in analytical chemistry and biochemistry to separate a mixture into individual compounds for their identification, quantification or purification. This can be achieved by using the different interactions between compounds in solution and a stationary

phase. By selecting a particular combination of mobile and stationary phase, the mode of separation can be chosen and optimized. It provides dynamic retention of compounds possessing hydrophobic and organic functionality. Components in a mixture are separated on a column packed with silica-based particles (referred to as stationary phase) by pumping a solvent (referred to as mobile phase) through the column. Depending on the unique affinity of each compound (referred to as the analyte) between the mobile phase and the stationary phase, each compound migrates along the column at different speeds and emerges from the column at different times, thus establishing a separation of the mixture. Analytes with higher affinity for the mobile phase migrate faster down the column, whereas those with higher affinity for the stationary phase migrate slower. This migration time (referred to as retention time) is unique for each analyte and can be used in its identification. With the appropriate use of a detection method after the column, each compound can also be quantified for analysis.



Figure 46: Agilent 1100 series HPLC equipment used in this PhD. Thesis.

For detection, even if UV-visible spectrometry is a sensitive detection method, not every compound exhibits UV-visible absorption, and usually a mass-spectrometer can be used as secondary detector. Quantification of the compounds can be performed by calculating the area under the curve of the peaks in the chromatogram.

In this work, the caffeine concentration after release experiments from corona plasma treated PA66 was determined by HPLC (*Agilent 1100 series*) equipment using a *Kromasil® 100-5C18* column (4.6×250 mm) with Methanol/Water/Acetic acid 40:59:1 v/v (pH 2.8) as mobile phase (Figure 46). Retention time of caffeine in PBS (pH 7.4) was found to be 4.9 min at a flow rate of 1 mL.min⁻¹ and at 25 °C. Detection of caffeine was done with a UV-Vis detector at $\lambda=272$ nm using an injection volume of 20 μ L.

3.3.5.7. Antibacterial assays

The antibacterial activity was studied on untreated and plasma-treated PP meshes with ampicillin. Influence of plasma treatment conditions of PP samples loaded with ampicillin on antibacterial properties has been evaluated for corona plasma and low-pressure plasma treatment, with special regard on the treatment time for both types of plasma and gas flow rate for low-pressure plasma. The activity of the treated meshes was tested against *Staphylococcus Aureus* (gram positive bacterium) and *Escherichia Coli* (gram negative bacterium).

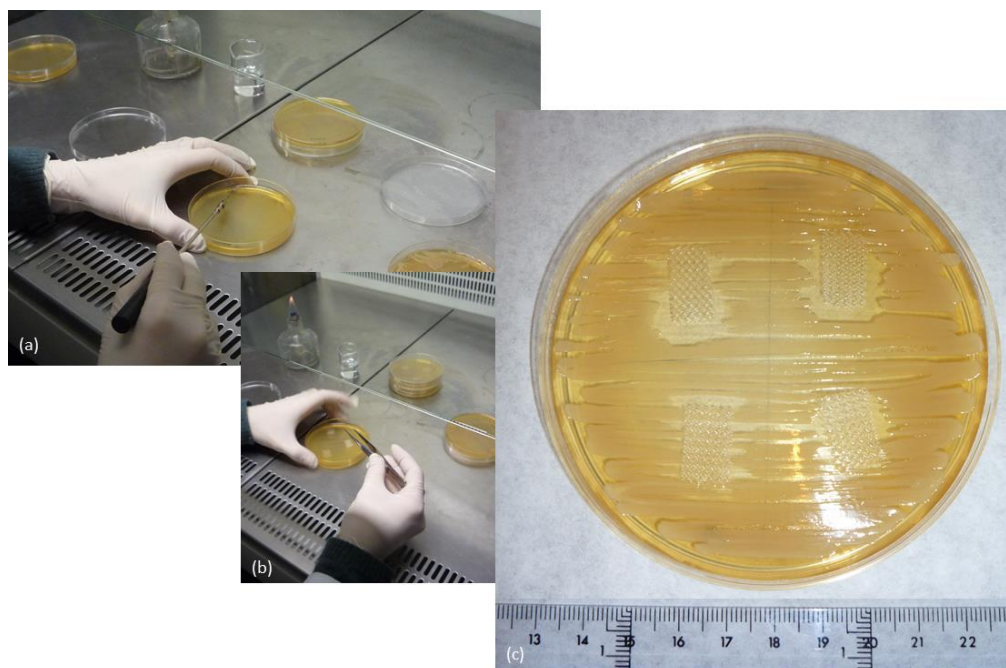


Figure 47: Antibacterial assays. (a) Preparation of the *Staphylococcus aureus* culture media. (b) Placement of treated textile materials. (c) Measurement of the inhibition areas.

To qualitatively determine the antibacterial activity on the treated textile materials the Parallel Streak Method AATCC Test Method 147-2004 was used. This method allows a relatively quick and easy qualitative method to determine antibacterial activity of diffusible antimicrobial agents on treated textile materials (Canal, 2009; Pinho, 2011). It consists in placing several parallel streaks in a standard Petri dish with the appropriate culture media for the bacteria tested (Figure 47). Bacteriological culture media of *Staphylococcus Aureus* and *E. Coli*. was prepared from Agar Bacteriological (Scharlau S.A., 07-004, 500 g, lot 100921) at concentration of 15.0 g.L^{-1} and Brain Heart Infusion Broth (BHI Broth) (Scharlau S.A., 02-599, 500 g, lot 10227) at $[\text{BHI}] = 37.0 \text{ g.L}^{-1}$. The treated side of the samples was put in contact with the culture media and incubated at $37 \text{ }^\circ\text{C}$ for 24 h in an autoclave. Image treatment of the Petri dishes after 24 h to determine the inhibition areas of the antibiotic-loaded PP meshes has been performed with Image J software, image processing program developed at the National Institutes of Health for this type of applications.

3.3.6. Data analysis

Statistical differences were determined using one-way ANOVA a 95% confidence with Tukey's post-tests using Minitab 16 software (Minitab, Inc., State College, Pennsylvania, U.S.). Statistical significance was noted when $p < 0.05$. In this work, different symbols (*, **, ***) indicate statistically significant differences.

REFERENCES

R. Arenas, C. Atoche, Post-thrombotic leg ulcers: Safety and efficacy of treatment with pentoxifylline (double-blind study in 30 patients), *Dermatologia Rev. Mexicana Segunda Epoca*, **1988**, 32, 34.

A. Arnez, The use of pentoxifylline in venous disease, *Venous Review*, **2011**, 4(3), 2.

M. Balat-Pichelin, A. Vesel, Neutral oxygen atom density in the MESOX air plasma solar furnace facility, *Chem. Phys.*, **2006**, 327, 112.

ASTM Standard D7334 – 08 (2013), "Standard practice for surface wettability of coatings, substrates and pigments by advancing contact angle measurement", ASTM International, West Conshohocken, PA, **2013**, DOI: 10.1520/D7334.

C. Barbarino, Pentoxifylline in the treatment of venous leg ulcers, *Curr. Med. Res. Opin.*, **1992**, 12, 547.

C. Bertin, H. Zunino, J. C. Pittet, P. Beau, P. Pineau, M. Massonneau, C. Robert, J. Hopkins, A double-blind evaluation of the activity of an anti-cellulite product containing retinol, caffeine, and ruscogenine by a combination of several non-invasive methods, *J. Cosmet. Sci.*, **2001**, 52, 199.

H. Biederman, *Plasma polymer films*, Imperial College Press, London, **2004**.

M. A. Bolzinger, S. Briançon, J. Pelletier, H. Fessi, Y. Chevalier, Percutaneous release of caffeine from microemulsion, emulsion and gel dosage forms, *Eur. J. Pharm. Biopharm.*, **2008**, 68, 446.

G. Borcia, C. A. Anderson, N. M. D. Brown, The surface oxidation of selected polymers using an atmospheric pressure air dielectric barrier discharge. Part II, *Appl. Surface Sci.*, **2004**, 225, 186.

R.D. Boyd, A. M. Kenwright, J. P. S. Badyal, D. Briggs, Atmospheric nonequilibrium plasma treatment of biaxially oriented polypropylene, *Macromolecules*, **1997**, 30, 5429.

- N. Brack, R. Lamb, D. Pham, P. Turner, Effect of water at elevated temperatures on wool fibre surface, *Surf. Interface Anal.*, **1999**, 27, 1050.
- H.-J. Butt, B. Cappella, M. Kappl, Force measurements with the atomic force microscope: Technique, interpretation and applications, *Surf. Sci. Rep.*, **2005**, 59, 1.
- C. Canal, R. Molina, E. Bertran, P. Erra, Wettability, ageing and recovery process of plasma treated polyamide 6, *J. Adhesion Sci. Technol.*, **2004**, 18, 1077.
- C. Canal, R. Molina, E. Bertran, A. Navarro, P. Erra, Effects of low temperature plasma on wool and wool/nylon blend dyed fabrics, *Fiber. Polym.*, **2008a**, 9 (3), 293.
- C. Canal, R. Molina, E. Bertran, P. Erra, Study of the influence of scouring on the wettability of keratin fibers before plasma treatment, *Fiber. Polym.*, **2008b**, 9, 444.
- C. Canal, F. Gaboriau, S. Villegier, U. Cvelbar, A. Ricard, Studies on antibacterial dressings obtained by fluorinated post-discharge plasma, *Int. J. Pharm.*, **2009**, 367, 155.
- S. K. Chinta, S. M. Landage, S. Kumar, Plasma technology & its application in textile wet processing, *Int. J. Eng. Res. Technol.*, **2012**, 1, 5.
- S. H. Cohen, M. T. Bray, M. L. Lightbody, Atomic force microscopy/scanning tunneling Microscopy, Plenum Press, New York, **1994**, pp. 453.
- P. D. Coleridge Smith, Pathogenesis of chronic venous insufficiency and possible effects of compression and pentoxifylline, *Yale J. Biol. Med.*, **1993**, 66, 47.
- M. P. Colgan, J. A. Dormandy, P. W. Jones, I. G. Schraibman, D. G. Shanik, R. A. L. Young, Oxpentifylline treatment of venous ulcers of the leg, *BMJ*, **1990**, 300, 972.
- J. A. Cordero, L. Alarcon, E. Escribano, R. Obach, J. Domenech, A comparative study of the transdermal penetration of a series of nonsteroidal antiinflammatory drugs, *J. Pharm. Sci.*, **1997**, 86, 503.

- J. Dale, C. Ruckley, D. Harper, B. Gibson, E. Nelson, R. Prescott, Randomised, double blind placebo controlled trial of pentoxifylline in the treatment of venous leg ulcers, *BMJ*, **1999**, 319, 875.
- V. Falanga, R. M. Fujitani, C. Diaz, Systemic treatment of venous leg ulcers with high doses of pentoxifylline; Efficacy in a randomized, placebo-controlled trial, *Wound Repair Regen.*, **1999**, 7, 208.
- S. A. Farag, Simultaneous liquid chromatographic analysis of the β -lactam antibiotics cefazolin, cefadroxil, cepalexin, ampicillin, and cephadrine in solution, *J. AOAC Int.*, **1998**, 81, 381.
- C. L. Frewin, Atomic Force Microscopy investigations into biology – From cell to protein, Christopher L. Frewin Eds., **2012**.
- M. T. J. Garcia, J. M. Marchetti, M. V. L. B. Bentley, Determination by HPLC of ketoprofen in aqueous medium used for in vitro skin permeation studies, *Anal. Lett.*, **2001**, 34, 1865.
- A. Jull, J. Waters, B. Arroll, Pentoxifylline for treatment of venous leg ulcers: a systematic review, *Lancet*, **2002**, 359, 1550.
- M. Kocun, M. Grandbois, L. A. Cuccia, Single molecule atomic force microscopy and force spectroscopy of chitosan, *Colloids and Surfaces B: Biointerfaces*, **2011**, 82(2), 470.
- F. Leroux, A. Perwuelz, C. Campagne, N. Behary, Atmospheric air plasma treatments of polyester textile structures, *J. Adhesion Sci. Technol.*, **2006**, 20(9), 939.
- K. L. Mittal, Contact angle, wettability and adhesion, Volume 2, VSP, **2002**.
- I. Novak, S. Florian, Investigation of long-term hydrophobic recovery of plasma modified polypropylene, *J. Material Sci.*, **2004**, 39(6), 2033.
- E. Pinho, L. Magalhães, M. Henriques, R. Oliveira, Antimicrobial activity assessment of textiles: standard methods comparison, *Ann. Microbiol.*, **2011**, 61, 493.

H. U. Poll, U. Schladitz, S. Schreiter, Penetration of plasma effects into textile structures, *Surf. Coat. Technol.*, **2001**, 142, 489-493.

A. C. Queiroz, J. D. Santos, F. J. Monteiro, I. R. Gibson, J. C. Knowles, Adsorption and release studies of sodium ampicillin from hydroxyapatite and glass-reinforced hydroxyapatite composites, *Biomaterials*, **2001**, 22, 1393.

J. M. Ritchie, *The xanthines. The pharmacological basis of therapeutics*, 5th Ed., Mac Millan, New York, USA, **1975**.

C. Roudit, "AFM figures", www.freesbi.ch. Creative Commons Attribution, **2010**.

S. Shanmugham, J. W. Jeong, A. Alkhateeb, D. E. Aston, Polymer nanowire elastic moduli measured with digital pulsed force mode AFM, *Langmuir*, **2005**, 21(22), 10214.

J. Sitterberg, A. Ozcetin, C. Ehrhardt, U. Bakowsky, Utilising atomic force microscopy for the characterisation of nanoscale drug delivery systems, *Eur. J. Pharm. Biopharm.*, **2010**, 74(1), 2.

A. Vesel, M. Mozetič, M. Balat-Pichelin, Oxygen atom density in microwave oxygen plasma, *Vacuum*, **2007**, 81, 1088.

A. Ward, S. P. Clissold, Pentoxifylline: A review of its pharmacodynamic and pharmacokinetic properties, and its therapeutic efficacy, *Drugs*, **1987**, 34, 50.

C. Washington, Drug release from microdisperse systems: a critical review, *Int. J. Pharm.*, **1990**, 58, 1.

H. Weitgasser, The use of pentoxifylline (Trental 400) in the treatment of leg ulcers: Results of a double-blind trial, *Pharmatherapeutica*, **1983**, 3, 143.

R. Zaplotnik, A. Vesel, M. Mozetič, Transition from E to H mode in inductively coupled oxygen plasma: Hysteresis and the behaviour of oxygen atom density, *EPL*, **2011**, 95, 55001.

RESULTS AND DISCUSSION

4. RESULTS AND DISCUSSION

The presentation of the results obtained in this PhD. Thesis is done in two main parts corresponding to the kind of textile material used (polyamide 6.6 and polypropylene) and the application that they aimed for (topical applications and implants for hernia repair, respectively).

The first part presents the experimental results for elastic-compressive polyamide 6.6 fabrics intended for use in topical applications. It emphasizes the influence of the initial state of PA66 on the effects produced by corona plasma and low-pressure plasma treatments on the physical and chemical surface properties of the fibers, as well as on the subsequent loading and release of ketoprofen and methylxantines from the PA66 fibres.

The second part focuses on polypropylene meshes aimed for implants for hernia repair. The influence of both types of plasmas has been studied on the physical and chemical surface properties of the fibers, as well as on the subsequent loading and release of ampicillin from the PP fibres and their microbiological behavior. Subsequently, plasma polymerization of polyethylene glycol (PEG) of the ampicillin-loaded PP fibres previously modified with low-pressure pulsed plasma has also been studied to evaluate its influence in the modulation of adhesion of the PP fibres.

4.1. Part I – Plasma-treated polyamide 6.6 as drug delivery system for topical application

The elastic-compressive PA66 fabrics used in this PhD. Thesis are aimed for a use as therapeutic compressive stockings, knee socks or socks, and for this, the loading of nonsteroidal anti-inflammatory drugs (NSAIDs) or of lipolitic active principles can be of interest to confer them an added therapeutic or cosmetic value, respectively. Modification of the surface of the PA66 fibres by plasma treatments is evaluated in this work to study how it may influence the loading and release of drugs from the PA66 fibres, as it is the hypothesis of this work that they can greatly depend on the modification of the interactions between drug and fibre.

Surface characterization of PA66 fabrics has been performed to study the effects of corona plasma and low-pressure plasma treatments, both using air as gas for plasma generation, on the surface properties of the fiber. In the following sections, the results obtained with both types of plasmas are presented, beginning with corona plasma results, and followed by those obtained with low-pressure plasma.

Once the plasma-treated PA66 fabrics have been characterized, the influence of these modifications of the PA66 surface properties is studied on the loading of an active principle and its subsequent release from the PA66 fibres to an isotonic liquid media.

Industrially finished fabrics were selected for this work in order to be closer to a potential insertion of the plasma technology in the textile chain and are thus compared to laboratory-washed PA66 fabrics. Therefore, in the presentation of the results, the nomenclature IF-PA66 refers to industrially-finished polyamide 6.6 fabrics, while the nomenclature W-PA66 refers to the same fabrics washed and dried, as described in section 3.3.1. This study of the influence of the initial state of preparation of the PA66 fabrics on the effects of plasma treatment has been limited to the studies with corona plasma.

4.1.1. Influence of plasma treatment on wetting properties

Corona plasma

In order to study the wetting properties of PA66 fabrics, static contact angle determinations were carried out on untreated and corona plasma-treated samples. It is important to underline that contact angle was measured on the side of the fabric that had been directly exposed to the plasma treatment. Measurements were performed right after plasma treatment of the PA66 fabrics to avoid ageing of the samples, as previous studies (Nakamatsu, 1999; Molina, 2003; Canal, 2004; Canal, 2008; Morent, 2008) on different natural and synthetic polymers and textiles indicated that surface modifications by plasma are not permanent and can progressively vary and therefore, subsequent processes have to be performed as soon as possible.

Table 7 shows that both untreated PA66 fabrics are hydrophobic ($> 90^\circ$), with IF-PA66 fabric presenting the highest value of $123.0 \pm 2.6^\circ$, thus being much more hydrophobic than PA6 rods presented in a previous work (Canal, 2004) that show a contact angle of 71.4° . It can be observed that the values of the static contact angle of the untreated IF-PA66 fabrics are 34° higher than those of W-PA66 fabrics, reflecting the presence of hydrophobic finishing products used in the fabrication process of the fabrics, which influences the wetting properties of the fibers.

Table 7: Water static contact angle of corona plasma-treated PA66 fabrics.

Polyamide samples	t_{plasma} (s)	θ_s ($^\circ$)			
		0 s	1.05 s	1.75 s	3.5 s
IF-PA66		$123.0 \pm 2.6^\circ$	$122.4 \pm 2.7^\circ$	$108.7 \pm 3.7^\circ$	$102.2 \pm 4.6^\circ$
W-PA66		$89.0 \pm 2.1^\circ$	Not measurable Very fast water absorption by W-PA66		

Regarding the influence of corona plasma treatment time on IF-PA66 samples, a progressive decrease of the static contact angle is observed with longer plasma treatment times, up to a final difference of -20.83° between the untreated fabric and the 3.5 seconds-plasma treated fabric.

After any corona plasma treatment (even at short times) on the W-PA66 sample, fabrics become highly hydrophilic and contact angle could not be measured due to the too fast absorption of water droplet by the fibers. It is widely known that these increased hydrophilic properties can be attributed to the introduction of oxygen-containing functional groups on the surface and/or to a cleaning process of the surface (Berg, 1993), as will be shown in the following section 1.4.4. Therefore, the highest wettability improvement recorded in W-PA66 samples with regard to IF-PA66 ones has to be related to the surface being already prepared; in untreated IF-PA66, the plasma exerts a cleaning effect of the surface which is probably avoided in the already cleaner surface of W-PA66 and all plasma species reacting on the surface can be devoted to functionalization or etching processes. Even if it was not quantifiable, it could be perceived that absorption time was shortened at longer treatment times, so in this case plasma treatment also progressively increases the wetting properties of washed samples.

Table 8: Water absorption time of corona plasma-treated PA66 fabrics as a function of plasma treatment time.

Corona plasma treatment time (s)	t_{abs} (s)	
	IF-PA66	W-PA66
0	18.5 ± 0.5	7.5 ± 0.5
1.05	19.0 ± 1.0	< 1.0
1.75	15.5 ± 0.5	< 1.0
3.5	9.5 ± 1.0	< 1.0
7	9.5 ± 1.5	< 1.0

As observed with the static contact angle of corona plasma treated PA66 fabrics, Table 8 shows that corona plasma improved the wettability by reducing the absorption times of both W-PA66 and IF-PA66 fabrics. In Table 8, the correlation between static contact angle and drop test can be remarked, since the decrease of static contact angle corresponds to a decrease of the water absorption time, and the maximum difference in both cases is observed at 3.5 s corona plasma treatment. So, for the rest of surface characterization of PA66 fibres, 3.5 s plasma treatment has been used as the extreme condition of the treatment time.

Untreated IF-PA66 presents a hydrophilic behavior. With a decrease of 34.0 ° observed in static contact angle measurements, the washing of the PA66 fabrics greatly improves the wetting properties of the PA66 fabrics. Corona plasma treatment also achieves an improvement of the hydrophilic behavior of the IF-PA66, with a decrease of 21.8 ° of the contact angle, in short treatment times. Moreover, when plasma treatment is combined with a previous washing of the polyamide fabrics, it has been shown that the contact angle further decreases, so that corona plasma treatment produces a better improvement of the wettability of PA66 fibres after the washing process.

Low pressure plasma

Regarding low pressure plasma-treated PA66 fabrics, drop test (AATCC Test Method 39-1980) has been carried out to evaluate the wetting properties of the fabrics. This test allows a quick and reliable evaluation of the plasma effects on textiles and is closely related to contact angle (Canal, 2008).

In order to select which parameters are relevant in the modification of polymer fibre surface, preliminary studies have been performed. By fixing plasma treatment time

and gas flow rate at 180 s and 5 L/min respectively, it has been shown that power supplies between 75 W and 150 W do not lead to significant differences in wettability, as measured through the drop test by water absorption and presented in Table 9.

Table 9: Absorption time (t_{abs}) of a 10 μ L water droplet (in seconds) of low pressure plasma-treated IF-PA66 as a function of plasma power supply. Plasma treatment time of 180 s and gas flow rate of 5 L/min.

Power supply (W)	t_{abs} (s)		
	75	100	150
IF-PA66	46.8 \pm 2.4	48.6 \pm 3.9	45.0 \pm 2.6

It has therefore been decided to fix the power supply of the plasma generator at 100 W for the subsequent experiments.

The pressure of the reaction chamber is closely linked to the gas flow rate supplied to the chamber during the plasma treatment. For example, with a gas flow of 5 L/min, the pressure inside the chamber oscillates around 100 mT, while with a gas flow of 15 L/min the pressure rises to 300 mT. Thus, the study of the effects of low pressure plasma treatment on the PA66 fibres has been focused on the influence of plasma treatment time and gas flow rate on the surface modification of the PA66 fibres.

Therefore, water absorption time measurements by drop test of untreated and fabrics previously treated by low pressure plasma have been performed under different conditions of gas flow (air) and treatment time, and the results are reported in Table 10.

With a water absorption time of 19.0 \pm 1.0 s, which corresponds to a static contact angle above 123 ° (Table 7), untreated IF-PA66 fabrics are hydrophobic. In the textile industry, wettabilities above 3 seconds (or contact angles above 90 °) are related to poor wettability. Usually, plasma treatments with oxygen-containing gases such as air

are related to surface wettability increase. However, according to Table 10, wettability of most of the plasma-treated PA66 fabrics studied is poorer than for untreated fabrics. Nevertheless, it can be observed, that wettability of plasma treated fabrics improved at higher flow rate.

Table 10: Absorption time (t_{abs}) of a 10 μ L water droplet (in seconds) of low pressure plasma-treated IF-PA66 as a function of plasma treatment time and gas flow rate (air). Power supply of 100 W.

		t_{abs} (s)			
		0	60	180	300
Gas flow (L/min)	Plasma treatment time (s)				
0	0	19.0 \pm 1.0			
	5		39.2 \pm 3.4	104.0 \pm 19.5	276.2 \pm 16.8
	10		23.8 \pm 1.7	48.6 \pm 3.9	76.7 \pm 9.0
	15		16.2 \pm 1.3	27.7 \pm 1.7	35.2 \pm 1.5

At constant plasma treatment time, between the plasma-treated samples, the increase of the gas flow rate improves the wettability of the IF-PA66 fabric, as it can be observed with the decrease water absorption time. In contrast, at constant gas flow rate, the increase of plasma treatment time leads to an increase of the water absorption time. Usually, in literature (Friedrich, 2012), it has been shown that the improvement of wetting properties of polymer material is related to the functionalization of the surface with polar groups. To deepen in the possible causes of the observed behavior, XPS analysis have been performed and presented in the following section, since wetting behavior used for the evaluation of the superficial changes experienced by the polyamide fibers is closely linked with chemical changes of the fiber surface (Berg, 1993).

Combination of short plasma treatment time and higher flow rates yield improved wettability. Indeed, even if the evolution of water absorption time as a function of gas

flow rate followed the same decreasing tendency on fabrics treated either at 60, 180 or 300 seconds as plasma treatment times, sustained plasma treatment time deteriorates wetting properties of the fabrics.

The analysis of W-PA66 has not been possible due to the fast or the instantaneous water absorption ($t < 3$ s) observed for the low-pressure plasma treated W-PA66 for all the studied conditions of plasma treatment. However this behavior allows confirming the trend observed with corona plasma treatment, since W-PA66 for all conditions studied shows improved wetting properties with respect to the IF-PA66.

4.1.2. Influence of plasma treatment on surface chemistry

Corona plasma

In general, plasma treatment proceeds by free-radical introduction of a wide variety of oxygen-containing functional groups on the surface of the treated polymer. These oxidized functional groups may include C–OH, C=O, COOH, C–O–C, etc. To investigate the proportion of these functional groups on the fiber surface and its evolution with corona plasma treatment time, X-Ray photoelectron-spectroscopy (XPS) was performed on the IF-PA66 and W-PA66 fabrics, and the results, obtained from the general spectra presented in Figure 48 and Figure 49, are respectively reported in Table 11 and Table 12.

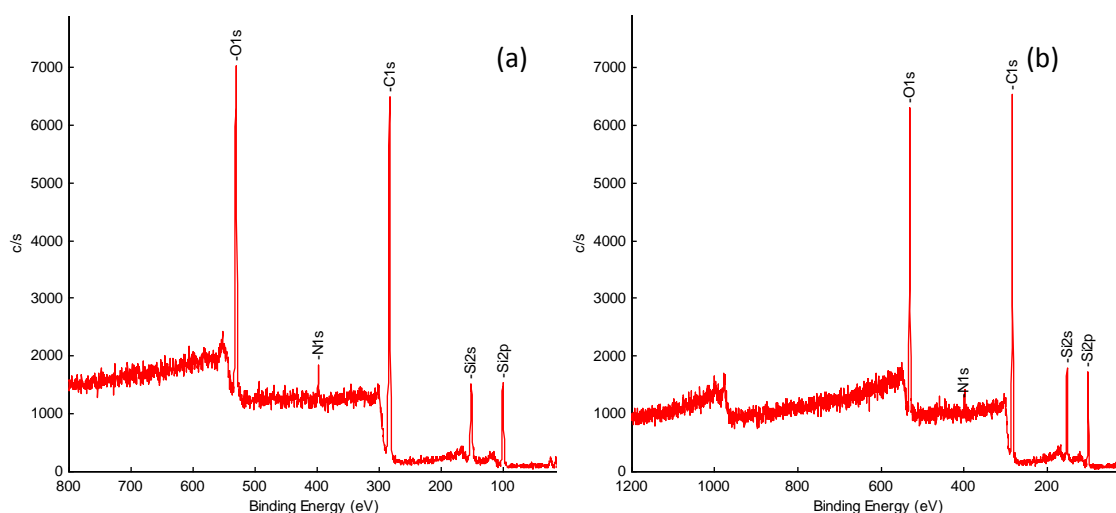


Figure 48: XPS general spectra of untreated IF-PA66 (a) and W-PA66 (b).

The general spectra of untreated PA66 fabrics, either industrially finished or washed, reveals the presence of O_{1s} , C_{1s} as main peaks, and N_{1s} and Si_{2s} and Si_{2p} in minor quantities (Figure 48).

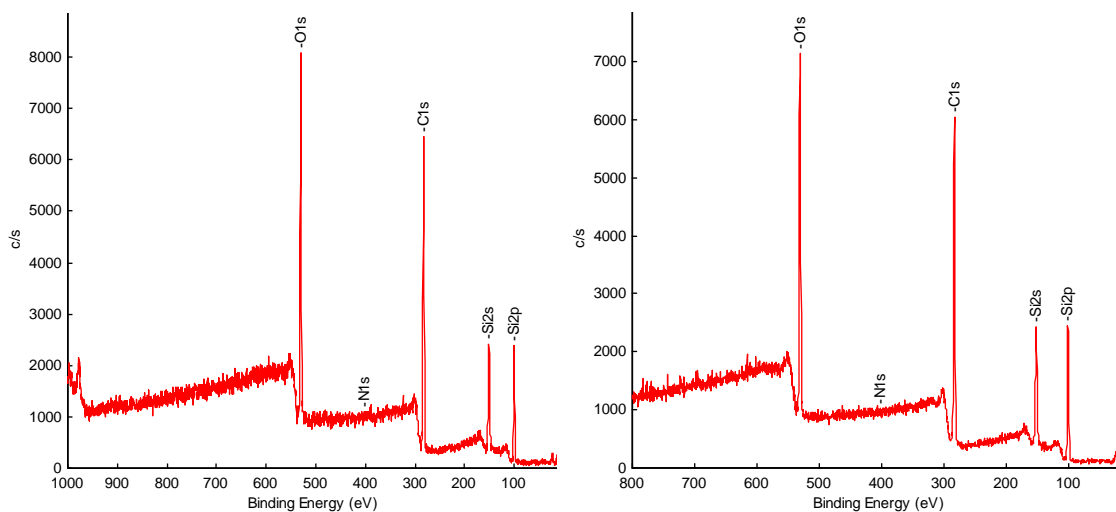


Figure 49: XPS general spectra of 1.75 s corona plasma-treated (a) and 3.5 s corona plasma-treated IF-PA66 (b).

The general spectra of air corona plasma-treated IF-PA66 fabrics (Figure 49), for different times, show that the main species present on the fibre surface are the same

than in the untreated samples. Details on the chemical composition are given in the following tables.

Table 11: Surface elemental composition and atomic ratios of untreated and corona-plasma treated IF-PA66 fabrics.

t_{plasma} (s)	Elemental composition (%)				Atomic ratios	
	C _{1s}	N _{1s}	O _{1s}	Si _{2p}	O/C	N/C
0	59.9	0.7	22.2	17.2	0.37	0.012
1.75	46.0	0.3	31.5	22.2	0.69	0.007
3.5	48.4	0.1	28.4	23.1	0.59	0.002

The untreated sample consists of about 60 at.% of carbon, 22 at.% of oxygen, 17 at.% of silicon and 1 at.% of nitrogen. For pure PA66 one would expect 75.0 % of carbon, 12.5 % of oxygen and 12.5 % of nitrogen. This difference can be explained taking into account that the fabrics used have been industrially finished with polydimethylsiloxane softeners (PDMS) of general formula $\text{CH}_3[\text{Si}(\text{CH}_3)_2\text{O}]_n\text{-Si}(\text{CH}_3)_3$. Therefore, Si and O are mainly due to the PDMS used in the finishing of IF-PA66 which covers the surface and explains also the low percentage of nitrogen observed coming from polyamide 66. Thus, the presence of these silicone-based finishing agents on the surface of the IF-PA66 fibers also explains the high percentages of Si observed on the surface of the IF-PA66 fabrics (17.2%), and the high O/C ratio (0.37) with respect to the theoretical value (0.17).

Surprisingly, plasma treatment increased the percentage of atomic Si on the surface of the fibres. This could be interpreted as an effect of thermomigration to the surface due to plasma: the local increase in temperature on the surface of the fibres due to the surface recombination of atomic species from the plasma phase and to the high temperature of the sparks of corona plasma may lead to migration of silicone compounds from the bulk of the fibre to the surface. It is coherent to expect higher

local surface temperatures on the more energetic corona plasma treatment than in a low pressure treatment, as will be shown in the next section, in part due to the corona being a filamentary discharge, with higher temperatures in the region of the sparks.

Additionally, the fibre surface was functionalized by O-containing moieties from the corona plasma phase, as indicated by the 63% increase in the O/C ratio between untreated and longest plasma treatment time (3.5 s plasma treatment). Increase of O concentration in the IF-PA66 surface can possibly due to the contribution of both functionalization and surface thermomigrated silicones.

The general spectra of air corona plasma-treated W-PA66 fabrics for 1.75 s and 3.5 s treatment time are shown in Figure 50 and the results of the main species present on the fibre surface are presented in Table 12 to study the influence of the corona plasma treatment on the elemental composition of the fibre surface and to be compared with the IF-PA66.

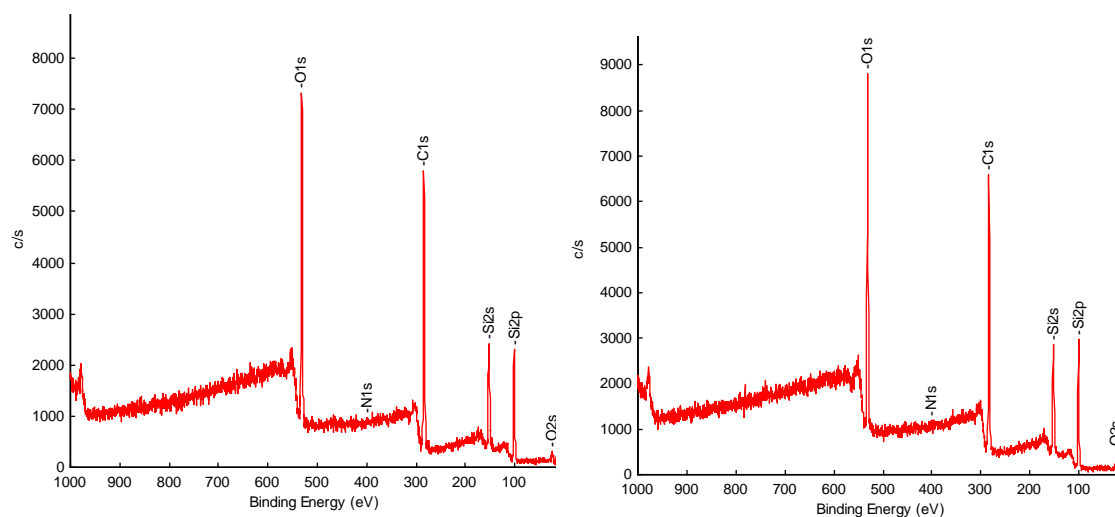


Figure 50: XPS general spectra of 1.75 s corona plasma-treated (a) and 3.5 s corona plasma-treated W-PA66 (b).

The higher amount of nitrogen in W-PA66 indicates that the washing process reduced the polysiloxane layer with respect to IF-PA66, so the N atoms from the polyamide structure are visible for the XPS. Even if the surface of untreated W-PA66 presents less Si atoms with respect to IF-PA66, corona plasma treatment of the W-PA66, as

observed for IF-PA66, leads to the increase of Si and O, which could be attributed to the combined effects of a O-based functionalization with a thermomigration of Si atoms from the bulk to the surface of the fibres, as described previously.

Table 12: Surface elemental composition and atomic ratios of of untreated and corona-plasma treated W-PA66 fabrics.

t_{plasma} (s)	Elemental composition (%)				Atomic ratios	
	C _{1s}	N _{1s}	O _{1s}	Si _{2p}	O/C	N/C
0	62.0	3.5	21.0	13.5	0.34	0.056
1.75	45.6	1.2	30.3	22.9	0.66	0.026
3.5	45.4	< 0.1	30.6	24.0	0.67	<0.002

As indicated by the general elemental compositions of the IF-PA66 and W-PA66 (Tables 11 and 12), no significant differences are found between the two corona plasma treatment times evaluated (1.75 s and 3.5 s).

Deconvolution analysis of C_{1s} peaks was performed for IF-PA66 (Table 13) and W-PA66 (Table 14) to estimate the new surface functional groups introduced on the surface, considering three main binding moieties: C–C and C–H bonds at a binding energy of 285.0 eV, C–O bonds at 286.5 eV, and C=O groups 288.2 eV. Corona plasma treatment of IF-PA66 for 3.5 s shows an increase of 1.7% of C-O groups on the IF-PA66 surface, the most relevant effect observed being the introduction of carboxylic groups (C=O) that progressively increase from 3.6% for untreated IF-PA66 to 11.0% for 3.5 s corona plasma treatment.

Table 13: Fraction of carbon functional groups from high-resolution C_{1s} XPS peaks of corona plasma treated IF-PA66 fabrics.

<i>t</i> _{plasma} (s)	Relative chemical bonds (%)		
	C ₁ : 285.0 eV <i>C-C, C-H</i>	C ₂ : 286.5 eV <i>C-O</i>	C ₃ : 288.2 eV <i>C=O</i>
0	85.6	10.8	3.6
1.75	78.8	12.1	9.1
3.5	76.5	12.5	11.0

The increase of new oxygenated groups grafted with corona plasma on the W-PA66 surface (Table 14) was comparable to the results obtained with IF-PA66, with the most significant increase registered being in C=O groups. In both cases (IF-PA66 and W-PA66) the proportion of C-O groups does not vary between 1.75 s and 3.5 s corona plasma treatment, while the proportion of carboxylic groups still increases for a longer plasma treatment time (3.5 s).

Table 14: Fraction of carbon functional groups from high-resolution C_{1s} XPS peaks of corona plasma treated W-PA66 fabrics.

<i>t</i> _{plasma} (s)	Relative chemical bonds (%)		
	C ₁ : 285.0 eV <i>C-C, C-H</i>	C ₂ : 286.5 eV <i>C-O</i>	C ₃ : 288.2 eV <i>C=O</i>
0	83.8	12.2	4.0
1.75	74.2	15.3	10.5
3.5	73.8	15.1	12.1

The results of the XPS analysis indicate a significant change in the surface chemistry of both IF-PA66 and W-PA66 with corona plasma treatment, as functionalization with O-containing groups, through C-O and mainly C=O bonds, leads to an increase of the possible bonding sites for the subsequent attachment of active molecules. This grafting

of O-containing groups on the PA66 fibre surface also explains the increase of wettability observed with corona plasma treatment in the previous section.

Low pressure plasma

XPS spectra were carried out on IF-PA66 fabrics exposed to different gas flow conditions in the plasma chamber (Figure 51). The relative atomic surface composition of the textiles before and after different plasma treatments is shown in Table 15.

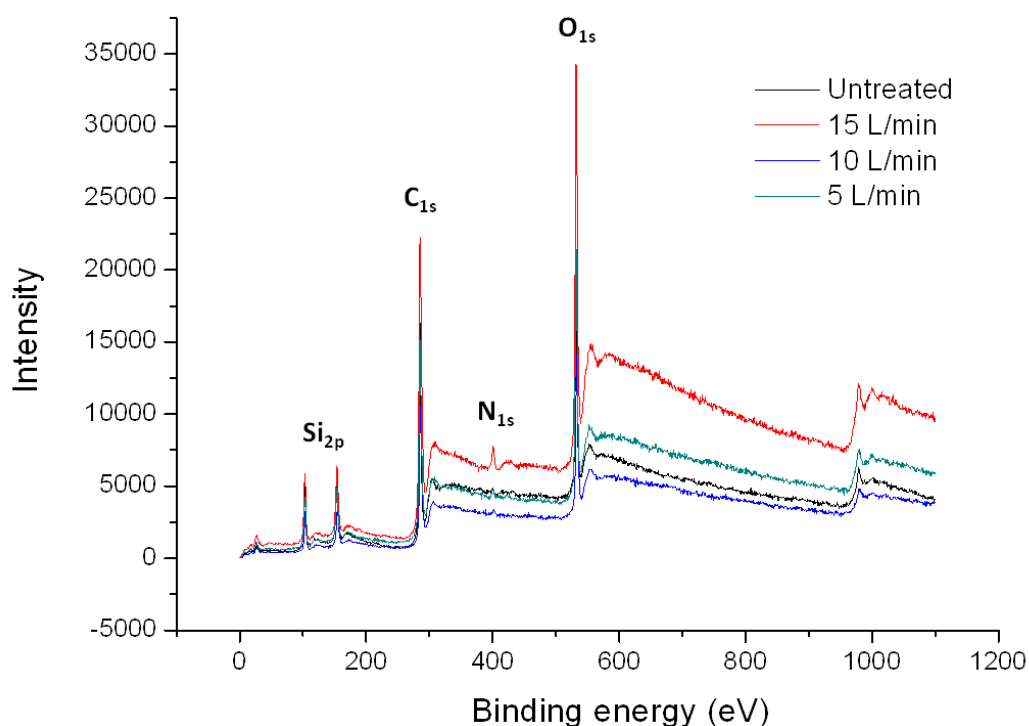


Figure 51: XPS general spectra of untreated and low pressure plasma treated IF-PA66 for 5, 10 and 15 L/min as gas flow.

As shown in Table 15, low-pressure plasma treatments modify the surface chemical composition of IF-PA66 by increasing N and O in parallel to decreasing carbon and silicon concentration with the increasing gas flow rate in the plasma chamber. This indicates an effective etching process of the PDMS on the surface of PA66, as confirmed by the Si/N ratio decrease with the increasing flow rate, which reflects the

elimination of PDMS chains which render N from amide bonds of polyamide more visible for the XPS.

Table 15: Surface elemental composition and atomic ratios of low pressure plasma treated IF-PA66 as a function of gas flow.

Gas flow (L/min)	Elemental composition (%)				Atomic ratios		
	C _{1s}	N _{1s}	O _{1s}	Si _{2p}	O/C	C/N	Si/N
0	59.9	0.7	22.2	17.2	0.37	85.51	24.57
5	56.9	1.1	28.0	14.0	0.49	50.77	12.53
10	58.8	1.0	25.7	14.5	0.44	58.23	14.34
15	56.4	2.3	29.3	12.1	0.52	24.96	5.34

The increase of O_{1s} percentage with the increase of gas flow rate into the plasma chamber may indicate an additional functionalization process of the fiber surface. This simultaneous etching and functionalization processes by low temperature plasma were previously observed in fibers with different finishing processes (Canal, 2007). This coupled effect can be explained by the fact that, in low-pressure plasma treatment, the increase of the gas flow or the pressure - since the pressure depends on the gas flow - possibly leads to increased density of active species in the reactor, as described in other works (Cvelbar, 2008).

The results obtained with low pressure plasma contrast with those observed in the previous section where corona plasma treatment produced an increase of silicon moieties, attributed to a thermomigration process from the bulk to the surface of the PA66 fibers. In this case, regarding silicon compounds, low pressure plasma treatment achieves principally a cleaning of the surface silicone-based agents. Due to the fact that corona plasma is a filamentary discharge, it is coherent to expect such results since the more energetic corona plasma treatment allows reaching higher local surface temperatures (with higher temperatures in the region of the sparks) than the low pressure plasma, and therefore allows the initiation of the thermomigration of these compounds.

In order to investigate the changes of functional groups in the surface of low pressure plasma-treated PA66 fabrics, deconvolution analysis of the high-resolution C_{1s} peaks was carried out. The original peak of each PA66 fabric showed three components (Figure 52a) with binding energies of at 285.00 eV, 286.53 eV and 288.21 eV which may be assigned to the presence of aliphatic C-C (or C-H), C-O (or C-N) and C=O bonds in the chain (Dorris, 1978; Brack, 1999), respectively.

Table 16: Fraction of carbon functional groups from high-resolution C_{1s} XPS peaks.

Gas flow (L/min)	Relative chemical bonds (%)		
	C_1 : 285.0 eV <i>C-C, C-H</i>	C_2 : 286.5 eV <i>C-O, C-N</i>	C_3 : 288.2 eV <i>C=O</i>
Untreated	83.5	12.4	4.1
5	75.9	12.0	11.8
10	76.5	12.5	11.0
15	72.2	12.0	15.8

Table 16 shows the results of the deconvolution analysis for the C_{1s} peak (Figure 52), showing a decrease of C–C, C–H content after the plasma treatment while C–O remain constant and C=O groups increase. It can be remarked that the progressive increase in C=O bonds with higher gas flow, reflect the functionalization process of PA66 fibers by carbonyl groups. Previous work on PA 6 films or fabrics also showed incorporation of C=O groups on the surface by low pressure plasma (Gao, 2009) or post discharges (Canal, 2007), respectively.

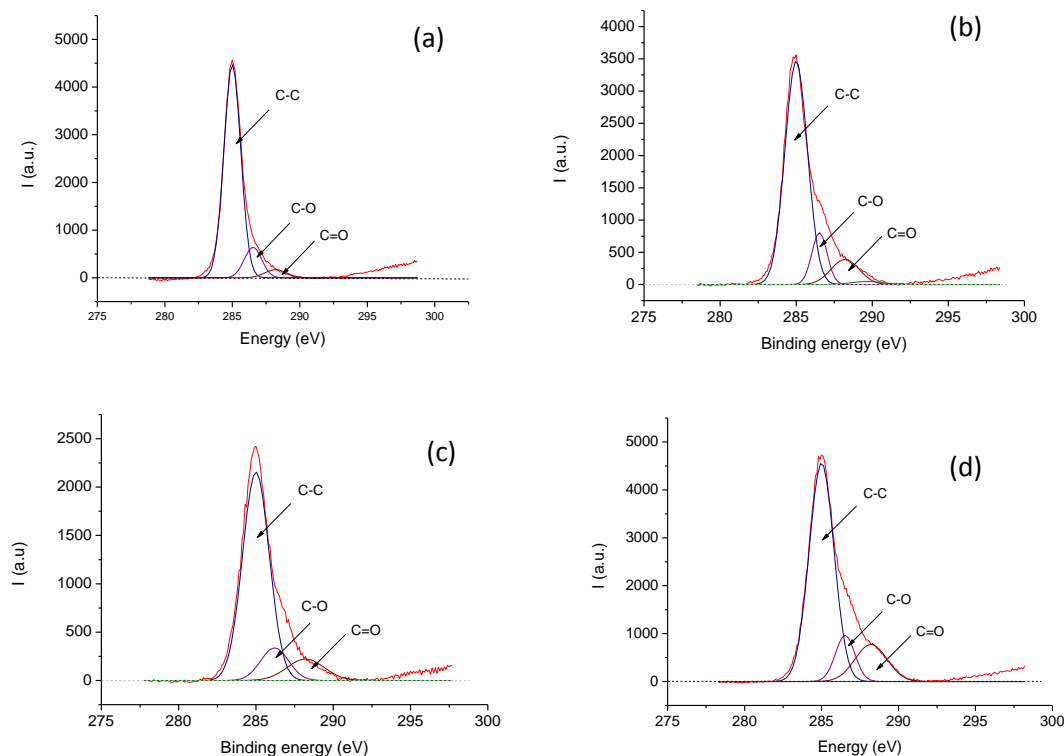


Figure 52: Deconvolution of C_{1s} peaks for untreated IF-PA66 sample (a) and plasma-treated PA66 under 5 (b), 10 (c) and 15 (d) L/min gas flow rate.

Surface functionalization of polymer fibers with oxygen moieties from low temperature plasmas is associated with improved wettability (Canal, 2004; Canal, 2007; Canal, 2008), while the presence of PDMS softeners on the surface of textiles is related to low wettability (Canal, 2007). Variations in superficial chemistry of the fibers are closely linked with the wetting properties.

It has been shown by XPS that PDMS were etched by the low-pressure plasma treatment, although they were not completely removed from the fiber surface. The higher wetting times recorded in section 4.1.1. for increasing times of plasma treatment may indicate redeposition of part of the etched material (i.e. hydrocarbons originating from the etched methyl groups which increase hydrophobic properties) or PDMS chain reticulation, while the progressive decrease in water absorption times obtained at increased flow rates have to be related to the etching of PMDS and functionalization with oxygenated moieties observed by XPS.

4.1.3. Influence of plasma treatment on PA66 fiber topography

Corona plasma

Figure 53 shows the surface of untreated IF-PA66 and W-PA66 fabrics. On the one hand, imaging of untreated IF-PA66 fibers by SEM shows highly uniform and regular fibers of 12–15 μm diameter arranged in yarns as corresponds to man-made fibers. It can be observed that IF-PA66 presents some irregularities on the surface which can be attributed to silicone aggregates.

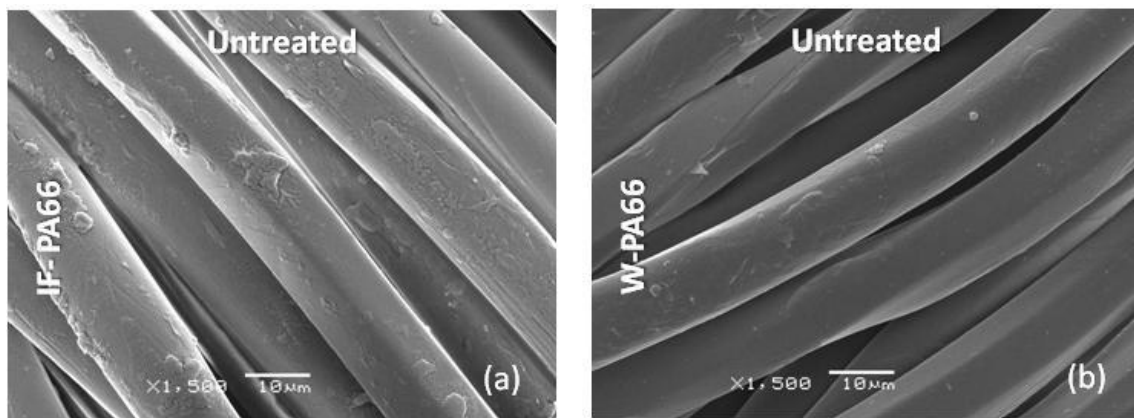


Figure 53: SEM micrographs of untreated IF-PA66 (a) and W-PA66 (b) fabrics.

Corona plasma treatment improved homogeneity of the surface topography by removal of the aggregates of the silicone-finishes present on untreated IF-PA66 fibers, as can be observed in Figure 54(a) and (c).

On the other hand, a smooth fiber surface can be observed in untreated W-PA66 due to the elimination of the finishing products by aqueous washing. No relevant topographic modifications at short plasma treatment times were detected in the W-PA66 fabrics (Figure 54(b) and (d)). In both kinds of samples, at the longest corona plasma exposure studied (after 3.5 s), some melt polymer or localized creasing of the

fibres can be randomly observed in some isolate regions of the surface due to the sparks of the corona plasma, although no generalized etching effects can be observed on the materials surface.

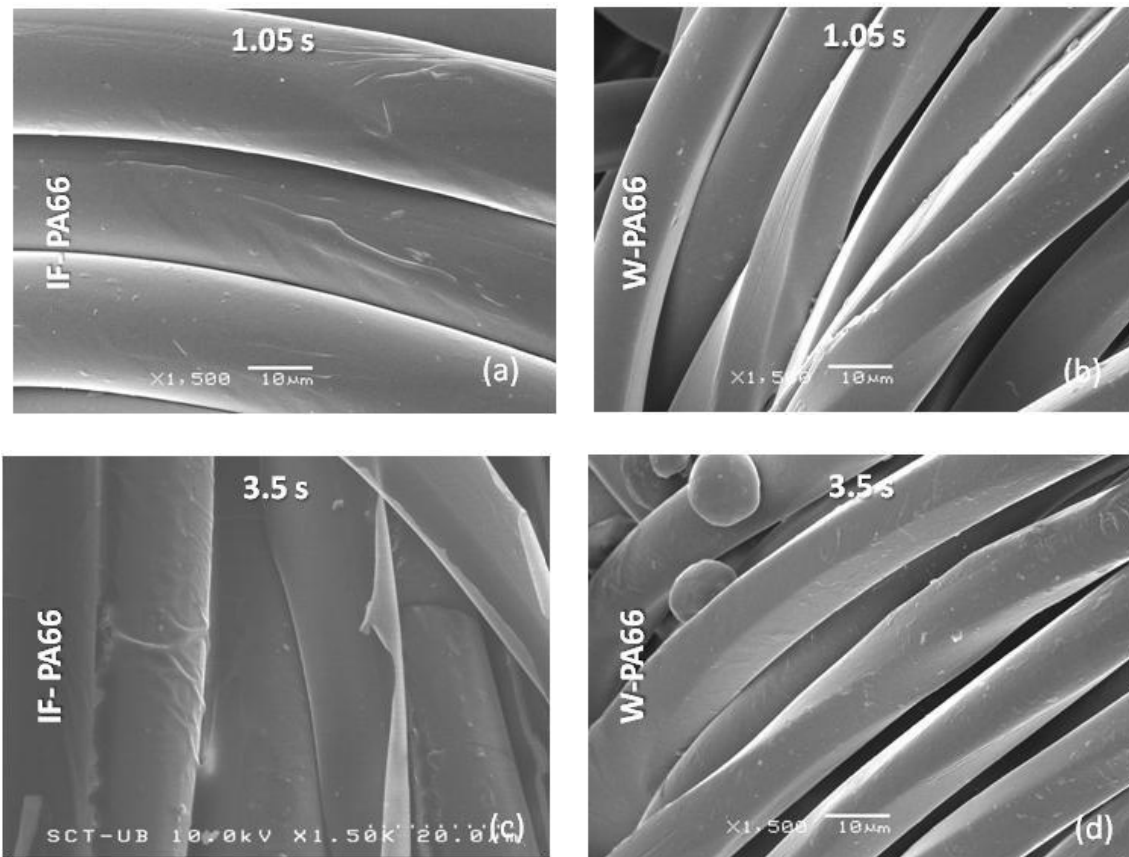


Figure 54: Influence of plasma treatment on PA66 fiber topography. SEM micrographs of 1.05 s corona plasma-treated IF-PA66 (a) and W-PA66 (b) fabrics, and 3.5 s corona plasma-treated IF-PA66 (c) and W-PA66 (d) fabrics.

Low pressure plasma

Scanning electron microscopy has also been used to study the influence of low pressure plasma treatment on the topography of PA66 fibers. As previously remarked, the presence of the PDMS finishing products can be also observed on the surface of the untreated IF-PA66 fibers as agglomerates in some regions of the fibers, and binding between some fibers. Etching effects by plasma pointed out by XPS can be confirmed by SEM in Figure 55b, where the cleaning effect by plasma treatment removed PDMS agglomerates leaving a clean and homogeneous fiber surface.

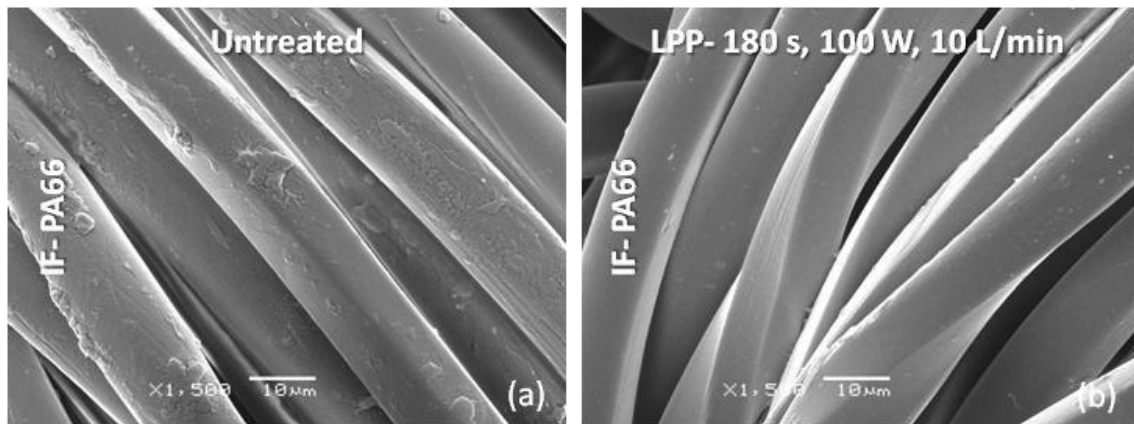


Figure 55: SEM images for (a) untreated IF-PA66 fibers and (b) low pressure plasma-treated PA66 fibers at 100 W, 180 s, 10 L/min.

SEM was carried out on IF-PA66 fabrics treated under different gas flow rate conditions and are presented in Figure 56. As observed for untreated fabrics, the surface of plasma-treated PA66 fibers is regular and the only roughness observed can be attributed to the presence of PDMS. In other works (Canal, 2007), the presence of PDMS on the surface of wool fibres was also detected by SEM as aggregates on the fibre surface. Except for the cleaning effect of the PDMS of the surface, low pressure plasma treatment did not produce remarkable changes on the topography of PA66 fibers.

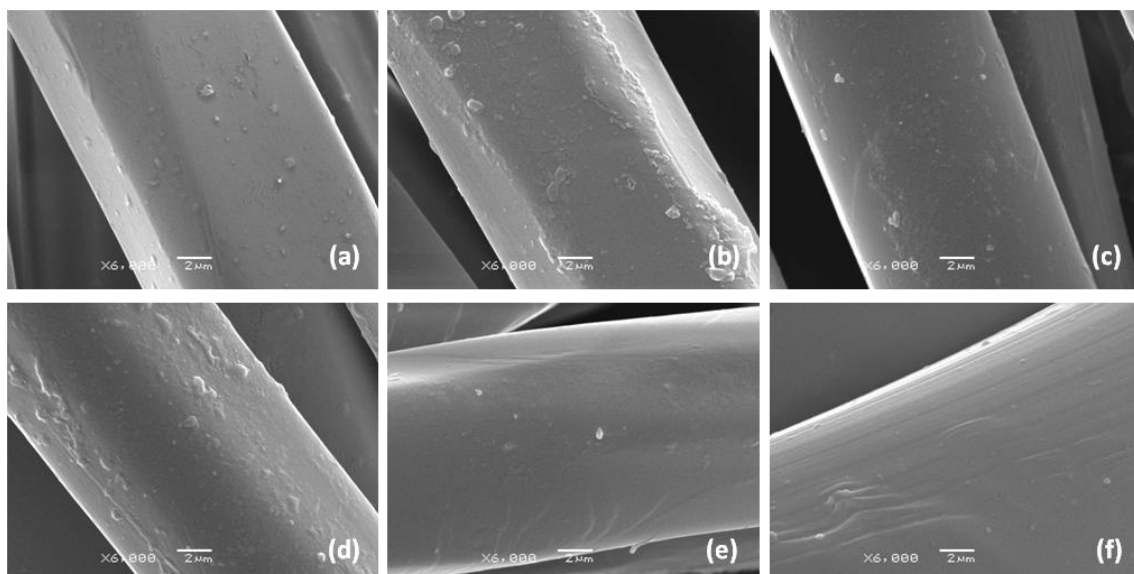


Figure 56: SEM images for untreated (a) and plasma-treated IF-PA66 fabrics with various treatment times and gas flow conditions at 1.33 mbar pressure and 100 W power supply as fixed working parameters. Effect of 60 s (b) and 300 s (c) minutes plasma treatment time on fiber topography for 5 L/min gas flow rate and effect of 5 (d), 10 (e), 15 (f) L/min gas flow on PA66 topography for 180 s plasma treatment time.

Regarding the cleaning of the PDMS, it can be also underlined that the increase of gas flow or treatment time allows a more effective elimination of these products (Figure 56(e) and (f)). It is interesting to remark that this type of plasma treatment is milder for the fiber than the corona plasma treatment shown in previous section where the presence of sparks in the plasma, locally increasing the temperature, provoked the apparition of creasing of the outer polymer layer of some corona plasma-treated PA66 fibres. In spite of a long exposure time, in this work, melt material, alteration of the fibers or creation of microcraters were not observed. While corona plasma treatment on IF-PA66 has as the advantage of improving the wetting properties of the fabrics with shorter times of treatment, the low pressure plasma treatment used does not alter fiber topography and is able to improve wettability at higher flow rates.

4.1.4. Ageing of plasma-treated PA66 fabrics

In this section the ageing, or evolution of the surface chemistry of the plasma-treated fabrics as a function of storage time, is studied on IF-PA66 fabrics by measuring the changes of the wetting behavior of the fibres by means of drop test.

Corona plasma

It has often been observed that the properties imparted by plasma treatment change with time. This phenomenon is commonly called as ageing. Previous studies (Morent, 2008; Canal, 2004; Canal, 2008; Molina, 2002; Molina, 2003; Nakamatsu, 1999; Borgia, 2004; Krump, 2005), on different natural and synthetic polymers indicated that surface modifications achieved by plasma treatment are not permanent and can progressively vary depending on the storage conditions of the sample and time.

The ageing effects observed depend on the nature of the polymeric materials, structure, crystallinity, (Novak, 2004) porosity etc. Additionally, it has been reported (Leroux, 2006), that the fabric porosity which depends on the fabric structure (e.g.

woven, nonwoven, knitted) influences the ageing of air-atmospheric plasma treated fabrics subjected to humidity at room temperature and pressure. It was also shown that for a low porosity-(high density) woven fabrics, oxidized species formed at the fabric surface are more easily removed by simple washing than for high porosity textile structure.

In the present study, the hydrophobic recovery of corona-plasma treated IF-PA66 fabrics has been measured up to 9 days, and is presented in Figure 57. The results obtained on the IF-PA66 samples show clearly that the improvement of the wetting properties of IF-PA66 fabrics is not permanent. The water absorption time of plasma-treated IF-PA66 increases, and therefore its hydrophobicity, in the course of one week storage. However, after that period of time, the drop test of either of the samples has not achieved the value of the untreated ones, so their wetting properties remain improved.

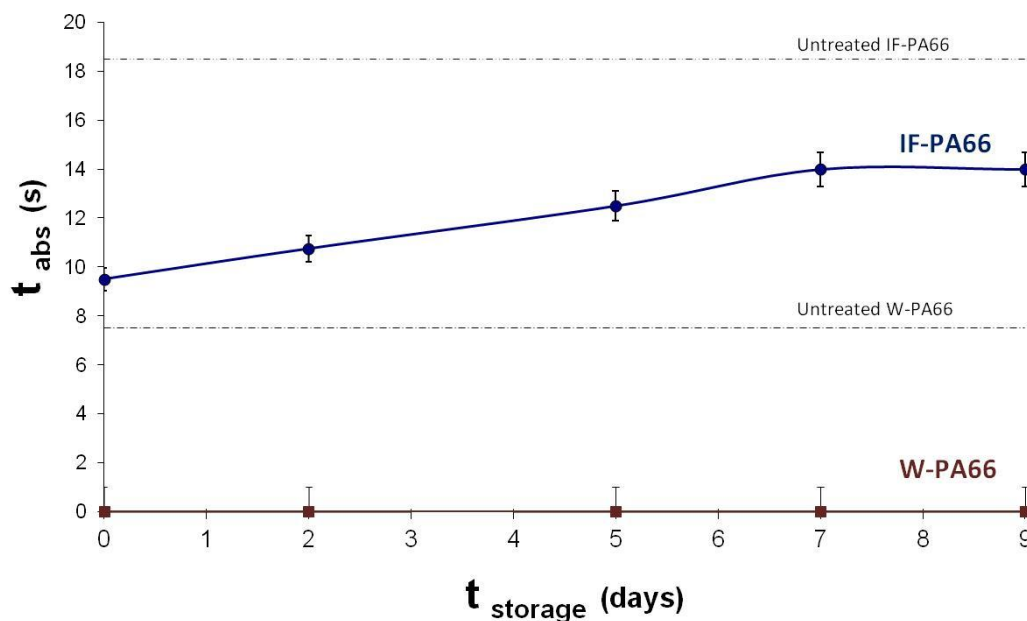


Figure 57: Evolution of water absorption time of 3.5 s corona-plasma treated IF-PA66 fabrics as a function of storage time, during 9 days.

Compared to the values obtained in previous papers for other textile fibres (Canal, 2004; Canal, 2008), where contact angles of PA6 rods treated by low pressure plasma

with air (100 Pa, 100 W, 13.56 MHz, 120 s) increased from 39 ° to 44 ° after 9 days of storage (Canal, 2004), the evolution observed in this work for IF-PA66 fabrics reveals a moderate degradation process of the wetting properties. As suggested in these previous studies, the increase in hydrophobicity of the plasma treated fabrics as a function of storage time indicates that the concentration of hydrophilic groups on the surface decreases, which has been attributed to the reorientation or the reorganization of these groups toward the bulk phase of PA during their storage in air environment. Some results suggest the existence of different mechanisms of hydrophobic recovery during the storage of plasma-treated fabrics: water adsorption, migration (through rotation or translation) of the amide groups, migration and/or rotation of the hydrophilic groups generated by the plasma towards the outer surface, surface contamination, blooming of additives, or absorption of ubiquitous contaminants (Morra, 1989; Boyd, 1997; Novak, 1999; Novak, 2001; Bhat, 2003; Canal, 2004; Pandiyaraj, 2009; Morent, 2008; Molina, 2002; Molina, 2003; Nakamatsu, 1999; Borcia, 2004; Krump, 2005). For this PhD. Thesis, a maximum lapse of 30 minutes has been fixed to perform any subsequent treatment on the plasma-treated materials.

Nevertheless, even though the water absorption time values increase, the corona plasma treated PA66 fabrics do not reach the contact angle values of the untreated fibres, even after 90 days of storage (16.0 ± 1.5 s), so the wetting properties still remain improved, as it could be observed in the work of Canal et al. in 2004, where contact angle of low pressure plasma-treated PA6 rods reached 58 ° after 77 days, far from the 71.8 ° of the untreated PA6 rod sample, demonstrating that the wetting properties also remained improved. Another study using XPS to follow the ageing process of Polypropylene films (Boyd, 1997) also revealed the gradual reduction of the O-containing groups achieved by atmospheric plasma treatment, through the decrease in the O/C ratio with time, pointing out that the time between plasma treatment and a subsequent bonding is a critical parameter.

It has been confirmed that the surface modifications achieved by corona plasma treatment are not permanent and that a hydrophobic recovery of a corona-plasma treated IF-PA66 fabrics progressively happens with the storage of the IF-PA66 in air environment. This wettability decrease necessarily influences the adsorption of chemicals and active principles on the treated fabrics, so in any case, it is advisable to carry out any subsequent treatment—in this case impregnation of the plasma treated fabrics with the active principle—as soon as possible after corona plasma treatment. Nevertheless the corona plasma treated PA66 fabrics does not reach the contact angle values of the untreated fibres after 3 months of storage, still showing improved wetting properties.

Regarding the W-PA66 samples and the low-pressure plasma IF-PA66 and W-PA66, the quick absorption time of the water droplet by the plasma-treated fibres, as observed in the previous section 4.1.1., did not allow following the evolution of the wetting properties with the time of storage of the samples, using either drop test or static contact angle.

4.1.5. Influence of plasma treatment on the loading and release of the active principles

Once characterized the surface effects of corona plasma and low pressure plasma treatments on PA66 fabrics that they have provoked, in the following sections their influence on the loading of drug molecules such as ketoprofen and methylxantine compounds is analyzed.

4.1.5.1. *Ketoprofen*

4.1.5.1.1. Loading

As mentioned in the introduction, ketoprofen was used in this work as an NSAID for the treatment of rheumatoid arthritis that, taking advantage of the compressive effect of the PA66 knitted fabrics used, could be used for the local treatment of the ankle and knee joints. Ketoprofen was incorporated from a hydro-alcoholic solution to IF-PA66 fabrics, as described in section 3.3.3.1.1. Ketoprofen impregnation of PA66 fibres has just been evaluated with corona plasma-treated IF-PA66 fabrics, focusing the study on the influence of the corona plasma treatment treatment time. Monitoring of the ketoprofen loading was carried out by measuring the dry weight of the materials before and after impregnation of the IF-PA66 fabrics, and the results are presented normalized in Figure 58 in grams of ketoprofen loaded in the fabrics for 1 g of IF-PA66.

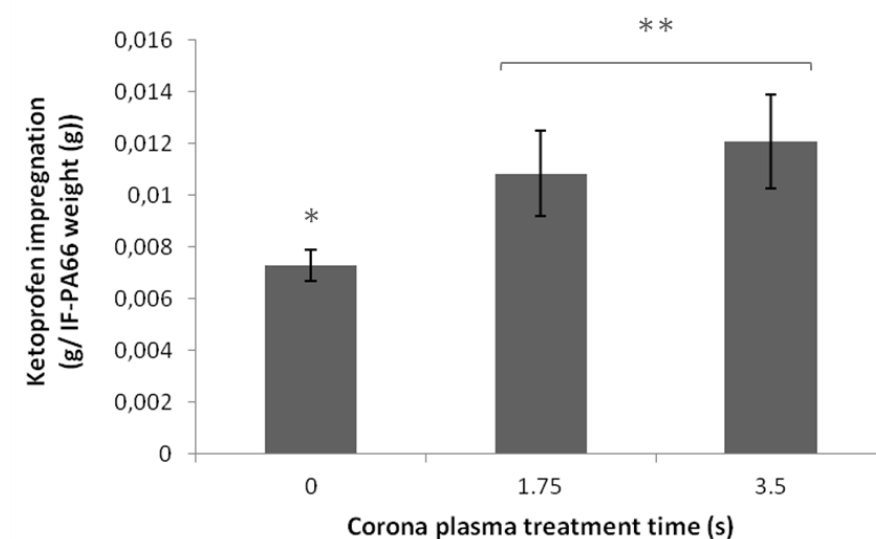


Figure 58: Ketoprofen impregnation for corona plasma-treated IF-PA66 for 1.75 s and 3.5 plasma treatment. Weight of ketoprofen loaded in the IF-PA66 for 1 g of IF-PA66 fabric.

Untreated IF-PA66 samples present a ketoprofen loading of 0.0073 ± 0.0006 g for 1 g of PA66 fibres, which is enhanced by corona plasma treatment which leads to an increase of the ketoprofen loading up to 0.0108 ± 0.0016 g and 0.0121 ± 0.0018 g, for 1.75 s and 3.5 s treatment time, respectively. While this improvement of the loading is significant at the shortest corona plasma treatment time, no significant difference is observed between the two time conditions studied.

4.1.5.1.2. Release

In order to determine if the amount of ketoprofen released from a PA66 fabric could be modified by plasma treatment, release experiments were performed from untreated and

corona plasma treated PA66 fabrics.

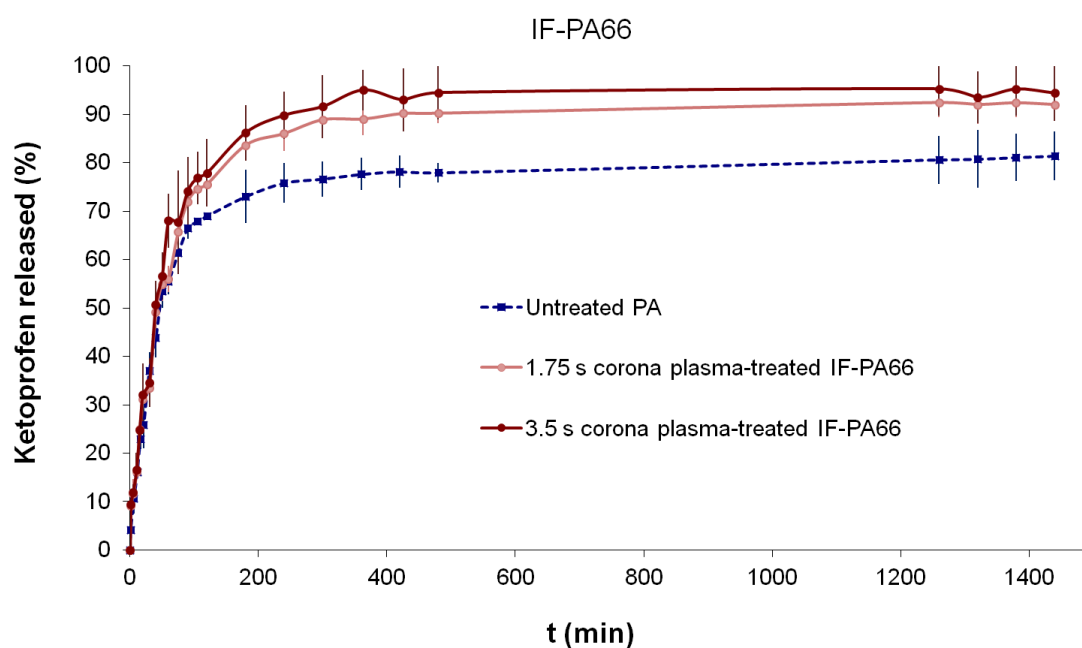


Figure 59: Accumulated ketoprofen release percentage from untreated, 1.75 s and 3.5 s corona plasma-treated IF-PA66 fabrics.

Figure 59 shows the release profiles obtained. The maximum amount of ketoprofen released is achieved after 5-6 hours, for both untreated and corona plasma-treated PA66 fabrics. The maximum ketoprofen released has been observed around 80% after 24 h. In plasma treated fabrics, the amount of ketoprofen released is higher than without treatment. The effects of plasma on release of ketoprofen from PA66 fabrics can be clearly observed in Figure 59. The atmospheric plasma treatment carried out increases the percentage of ketoprofen released up to 90%. This 10% increase in the ketoprofen released after 24 h could be explained by the fact that the plasma treated fabrics can be easily wetted by the aqueous receptor solution.

4.1.5.2. Caffeine

4.1.5.2.1. Loading

Caffeine is widely used in cosmetics as an active substance because of its action on lipids (Bolzinger, 2008) and, due to its low molecular weight ($194.2 \text{ g}\cdot\text{mol}^{-1}$), is found in a number of commercial cosmetic formulations for topical applications as gels, creams or patches. It presents a 2.2 g/L solubility in water at $20 \text{ }^\circ\text{C}$. Microemulsions and emulsions are also described as vehicles for percutaneous penetration through the skin in literature (Bolzinger, 2008), but direct loading of caffeine in the fibers, coupled with the use of plasma technology as described in this work, is a novel vector for transdermal applications.

Caffeine was selected as cosmetic active principle of interest for the treatment of cellulite by taking advantage of the improved venous return in the legs thanks to the compressive effect of the fabrics studied. The design of the tubular fabrics would allow focusing on the local treatment of thighs and calf, where the cellulite affection is particularly found.

First, impregnation studies of both IF-PA66 and W-PA66 fibres was done using caffeine as active principle to evaluate how the corona plasma and the low pressure plasma treatments affect its loading on the fibres. These studies have been mainly focused on the influence of plasma treatment time in the case of corona plasma treatment, and on the influence of chamber pressure, gas flow rate, plasma treatment time and power supply using low pressure plasma on the caffeine loading.

To deepen the fundamental study regarding the interactions established between plasma treated surface and drug, a panel of experiments has been designed using different molecules from the family of methylxantines, with distinct polarities.

Corona plasma

Figure 60 shows the caffeine impregnation weight percentage for IF-PA66 and W-PA66 fabrics as a function of the corona plasma treatment time applied.

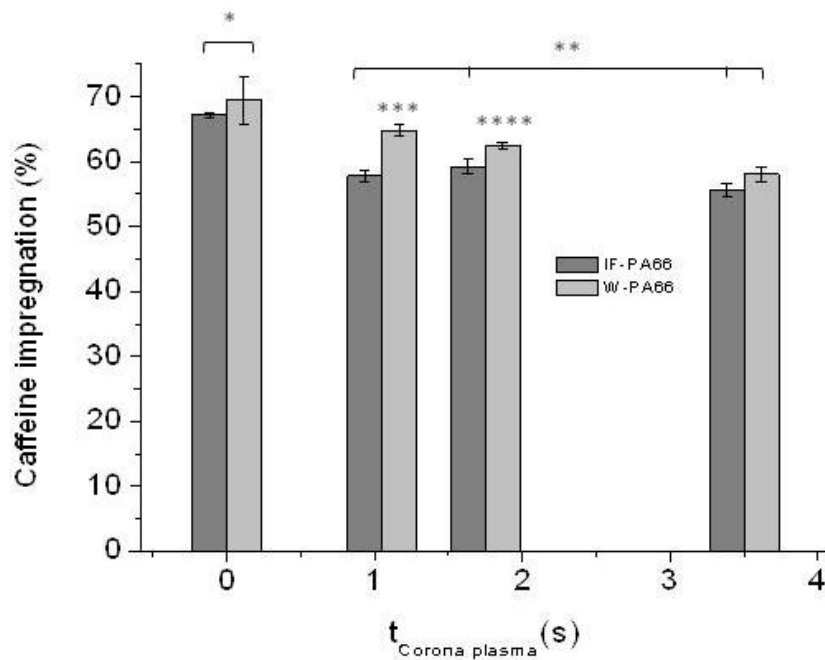


Figure 60: Caffeine impregnation percentage for IF-PA66 and W-PA66 fabrics as a function of corona plasma treatment time.

Around 70% weight percentage of caffeine was incorporated to the untreated fabrics from the 1% solution of caffeine employed. W-PA66 fabrics incorporate slightly more active principle than IF-PA66 samples (although no statistically significant differences were recorded), essentially due to the absence of oil and polysiloxane-based finishing products on the surface of the W-PA66 fibers, which is related to better wettability of the fabrics and thus improved contact with the impregnation solution. This trend is followed in the plasma-treated fabrics. For both types of PA66 fabrics, longer plasma treatment times tend to progressively reduce the percentage of caffeine impregnated on the fabrics, diminishing about 11% between untreated and 3.5 s-plasma treated fabrics.

So, while the plasma treatment improves the wetting properties of polyamide fabrics, it does not revert in an increase of the incorporation of active principle into the fiber. Although caffeine is a polar molecule, with a dipolar moment of 3.64D, given its relatively large molecular size, the charges are distributed over a large distance, making the molecule less polar than water. Thus, after plasma treatment, the new oxygen moieties on the plasma-treated fiber surface lead to increased surface electronegativity, so if the surface is more polar, it is expected that interaction with caffeine may be hampered, possibly justifying this tendency to lower drug incorporation.

Low pressure plasma

The effects of low pressure plasma treatment were evaluated on the caffeine loading of IF-PA66 fabrics, using a 1% caffeine aqueous solution, and the results are reported in Table 17. It can be observed that impregnation of plasma-treated fabrics with low flow rate (5 L/min) and short plasma treatment time (60 s) presents a percentage of impregnation similar to that of untreated fabrics. Further increase of the flow rate and treatment time of the plasma treatment of IF-PA66 leads to a decrease of the quantity of drug loaded in the fabric. This behavior can be related with the decrease of wettability of the low-pressure plasma treated samples with respect to the untreated one as observed in section 4.1.1. This could be explained by the scheme proposed in Figure 61. Plasma treatment at high flow rates reduces the thickness of the PDMS layer (as shown by XPS and SEM) and increases surface functionalization by oxygen moieties. In views of the chemical structure of caffeine, binding to the fiber can be expected to take place mainly by hydrogen bonds.

Table 17: Caffeine impregnation percentage of untreated and low-pressure plasma-treated IF-PA66 fabrics as a function of the gas flow (air) and treatment time.

IF-PA 66						
Gas flow (L/min)	0	5		10	15	
t_{plasma} (s)	0	60	180	300	180	180
Caffeine impregnation (%)	67.2 ± 0.4	66.2 ± 0.5	42.2 ± 0.2	47.5 ± 1.0	44.6 ± 0.6	44.9 ± 0.3

The presence of the PDMS layer offers higher number of hydrogen bonding sites, so its progressive elimination with plasma treatment somehow reduces the capacity of the material to incorporate the drug. The proposed mechanism of Figure 61 also explains the effects of increasing treatment times with corona plasma treatment on the amount of caffeine incorporated to the IF-PA66 fibres.

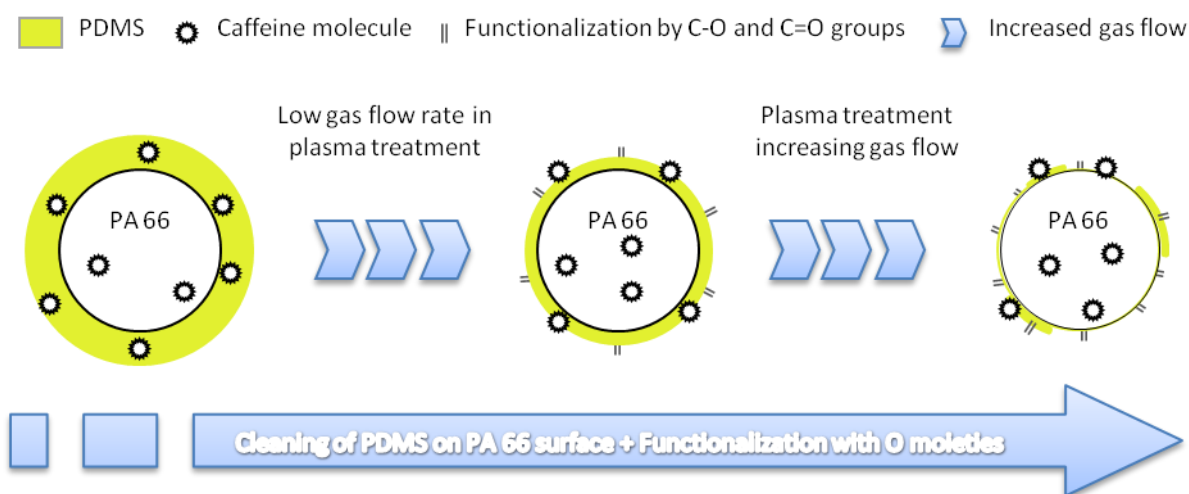


Figure 61: Proposed mechanism of PDMS layer reduction with the increase of gas flow in plasma treatment and its relationship with caffeine incorporation to the fibre.

4.1.5.2.2. Release

Corona plasma

In the present work, in vitro release experiments of caffeine-loaded samples were performed on both IF-PA66 and W-PA66 fabrics with and without plasma treatment.

Release kinetics are shown in Figure 62.

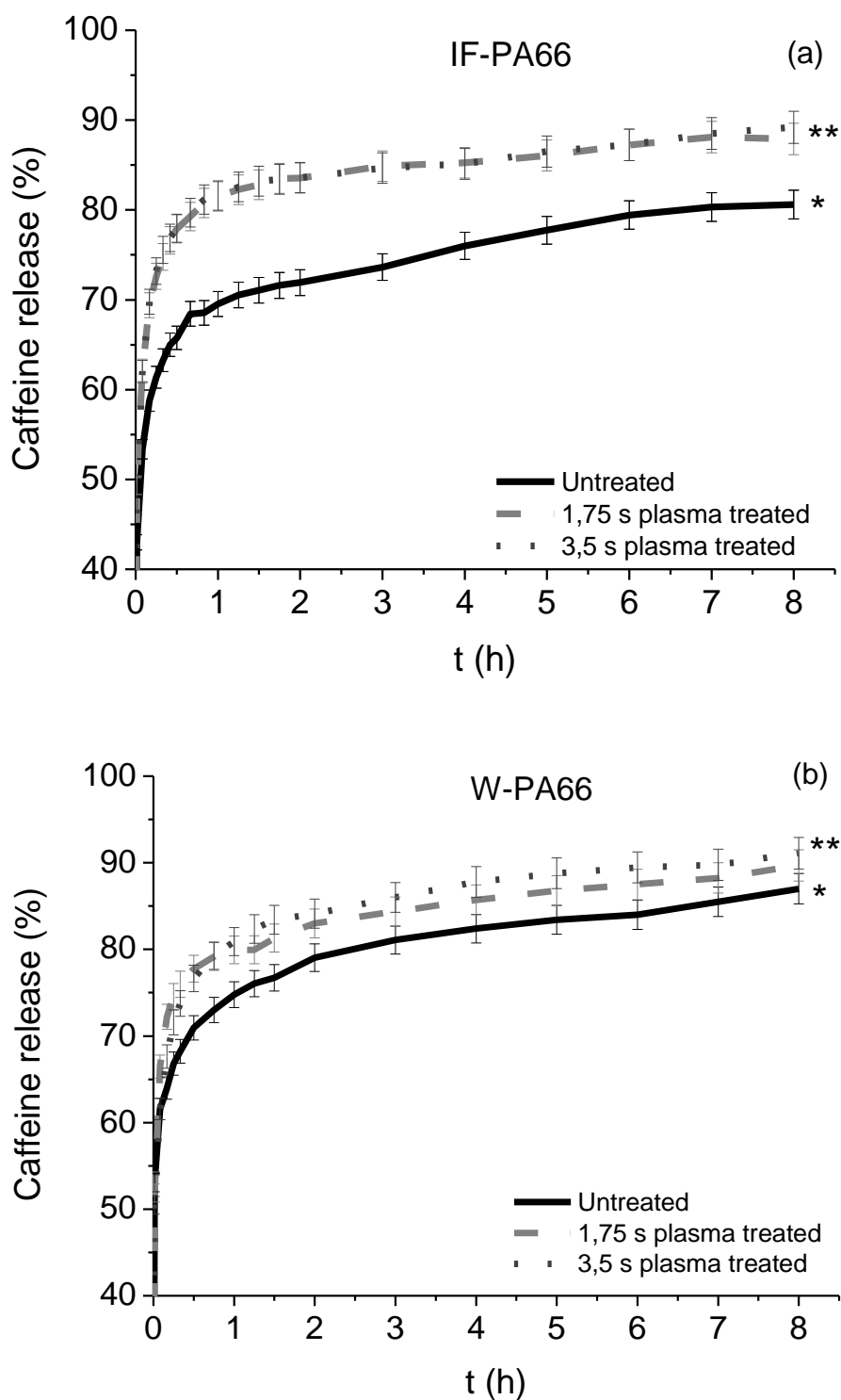


Figure 62: Accumulated caffeine release percentage from W-PA66 (a) and IF-PA66 (b) fabrics. Influence of corona plasma treatment on caffeine release kinetics. * and ** indicate statistically significant differences.

For both kinds of fabrics, two different stages can be distinguished: an initial fast release phase and a second stage of slower release. In both IF-PA66 and W-PA66 materials, plasma treated samples show higher release percentages, with no significant differences between the two different corona plasma treatment times evaluated. In all cases, burst release is recorded, up to 70% and 83% in the first hour for untreated and plasma-treated materials, respectively. This stage is followed by a slower release up to 8 hours, without reaching the stationary stage in any of the samples, and thus, with potential for longer release.

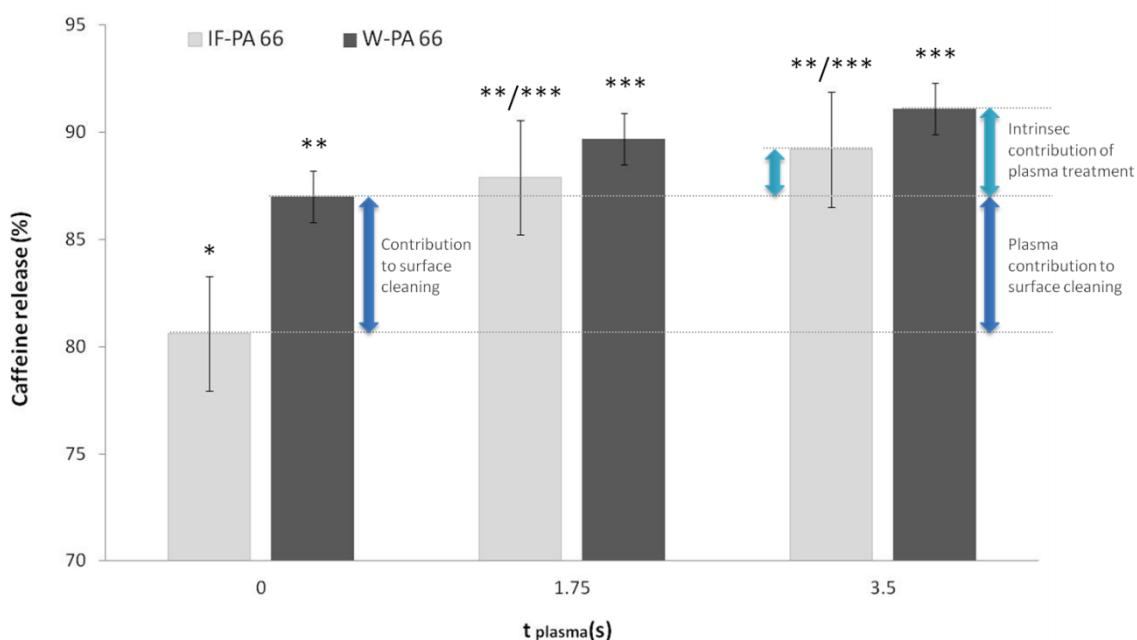


Figure 63: Caffeine release percentages at the end of 8 hour release assay, for untreated, 1.75 s and 3.5 s corona plasma-treated IF-PA66 and W-PA66 fabrics, with details of the dominant plasma contribution.

While previous laboratory washing of untreated PA66 leads to a final caffeine release +7.0 % higher with respect to the untreated IF-PA66, no significant difference is observed between W-PA66 and IF-PA66 for corona plasma-treated fabrics for all the plasma treatment times studied. This behavior indicates that the cleaning of the PA66 surface achieved by the plasma allows reaching a cleaning as good as for the washing of the PA66 fabrics by wet process.

In particular, the difference between the untreated IF-PA66 and W-PA66 samples indicates the specific effect of the washing process on the release percentage of caffeine (Figure 63). Plasma-treated IF-PA66 samples present final caffeine release percentages around 89%, improving around 9% with respect to the untreated sample. Untreated W-PA66 already has a higher release of 87% with respect to untreated IF-PA66, indicating that the cleaning effect of plasma or the washing process carried out prepare the surface of PA66 industrial fabrics in a similar way. This has allowed distinguishing between the contribution of plasma to the preparation of the surface (cleaning effect) and the intrinsic contribution of plasma functionalization, with regard to the drug release.

Comparative study with topical therapeutic level of commercial products

As shown in Table 18, the accumulated percentage released in the different samples after 8 hours corresponds to a caffeine dose between 496.6 and 540.9 mg/ 100 g for IF-PA66 fabrics, and between 560.6 and 620.4 mg/ 100 g for W-PA66 fabrics.

Table 18: Effect of low-pressure plasma treatment time on the release percentage of caffeine and the released quantity of caffeine from IF-PA66 and W-PA66 fabrics.

	IF-PA66 fabrics				W-PA66 fabrics			
	0	1.05	1.75	3.5	0	1.05	1.75	3.5
t_{plasma} (s)								
%R (after 8 h)	80.6 ± 3.3	89.1 ± 2.0	87.9 ± 2.6	89.2 ± 1.0	87.0 ± 0.8	88.1 ± 1.4	89.7 ± 0.2	91.1 ± 0.8
Released caffeine after 8 h (mg/100 g PA66)	540.9 ± 22.1	514.7 ± 11.6	520.6 ± 15.4	496.6 ± 5.6	604.5 ± 5.6	570.9 ± 9.1	560.6 ± 1.2	620.4 ± 5.4

Taking into account that the PA66 samples used for this research have a weight by square meter of 272 g/m², 100 g of fabric correspond to an area of 3678.9 cm².

Considering elastic-compressive leggings covering the legs from the hip to the knees, with an upper part of 112 cm of diameter and 44 cm of diameter in the lower part of each leg, the quantity of active compound which will be released by such PA66 mesh can be calculated. With a total surface area of 3500 cm², caffeine release after 8 hours would be between 472.4 mg and 590.2 mg. Compared to other caffeine-containing commercial formulations such as gels, which usually contain between 4% and 5% of caffeine (e.g. *Somatoline CosmeticTM*), a dose of 10-15 g of the formulation applied on the skin corresponds to between 400 and 750 mg of caffeine.

Therefore, the caffeine dose released from plasma-treated PA66 is comparable to the commercial ones and could be proposed as a novel alternative for anticelulitic therapy. Furthermore the homogeneity of distribution of an active compound in gel form applied by the user does not ensure uniform topical doses on the skin, while this type of textile support may avoid this issue. Also the efficacy of the compressive effect of such polyamide textile fabric on the treated skin can contribute to improve the mentioned therapeutic/cosmetic effects.

It could be speculated that the use of the compressive PA66 fabrics could also be combined with gel formulation treatments, alternating day/night treatments, to provide an optimal efficacy of the anti-cellulitic treatment during 24 hours.

Release kinetics modeling

The modeling of drug release from delivery systems is important for the understanding and the elucidation of the transport mechanisms. To compare the release profiles of the samples with different treatments, several models were tested, including Korsmeyer-Peppas, Higuchi, Zero order, First order, Hixson-Crowell and Weibull (Higuchi 1961, Higuchi 1963; Gibaldi and Feldman, 1967; Wagner, 1969; Hixson and Crowell, 1931; Langenbucher, 1972; Goldsmith et al., 1978).

In spite of the complexity of the phenomena involved in drug release mechanisms, the mathematical expressions used in pharmaceuticals to describe the kinetics of drug release from a large variety of devices are rather simple, and they can be summarized briefly in three basic laws. Basically, the mathematical expressions used to describe the kinetics of drug release and the discernment of the release mechanisms are the Higuchi law (Higuchi, 1961), the Peppas equation or the so-called power law (Ritger, 1987; Siepmann, 2001) and the Weibull equation.

For the simplest geometry of thin films with negligible edge effects, Higuchi published the famous square root of time relationship between the amount of drug released from a thin ointment film with a large excess of drug (initial drug concentration drug solubility in the carrier material) in 1961 (Higuchi, 1961). The first approach of Higuchi relies on Equation (11), which indicates that the fraction of drug released is proportional to the square root of time:

$$\frac{M_t}{A} = \sqrt{D(2c_o - c_s)t} \quad (9)$$

where M_t is the cumulative amount of drug released at time t , A is the surface area of the controlled release device exposed to the release medium, D is the drug diffusivity, and c_o and c_s are the initial drug concentration and the drug solubility, respectively. This law is valid for systems where the drug concentration is much higher than the drug solubility.

An important advantage of this equation is its simplicity. However, when applying it to controlled drug delivery systems, Higuchi based his equation on assumptions that must be all fulfilled, including:

- The initial drug concentration in the system must be much higher than drug solubility.
- The device geometry is that of a thin film with negligible edge effects.
- The size of the drug particles is much smaller than the thickness of the film.

- The carrier material does not swell or dissolve.
- The diffusivity of the drug is constant (not dependent on time or position).
- Perfect sink conditions are maintained throughout the experiment.

Unfortunately, Higuchi equation is often misused and applied to controlled drug delivery systems which do not fulfill all these assumptions.

The second approach, the Korsmeyer-Peppas equation is based on the semi-empirical Equation (11):

$$\frac{M_t}{M_\infty} = k \cdot t^n \quad (10)$$

where M_t and M_∞ are the absolute cumulative amount of drug released at time t and infinite time, respectively; k is a constant incorporating structural and geometric characteristics of the system, and n is the release exponent, which might be indicative of the mechanism of drug release, being n the exponent which is used to describe the kinetics beyond the release (Ritger, 1987) (Table 19).

Table 19: Ritger-Peppas diffusion exponent and mechanism of diffusional release from various non-swelling controlled release systems.

Diffusion exponent, n			Drug release mechanism
Thin film	Cylindrical sample	Spherical sample	
0.50	0.45	0.43	Fickian diffusion
0.50 < n < 1.0	0.45 < n < 1.0	0.43 < n < 1.0	Non-fickian diffusion
1.0	1.0	1.0	Zero-order release

Nicholas Peppas was the first to introduce this equation in the field of drug delivery (Peppas, 1984; Peppas, 1985; Korsmeyer, 1986a,b). When pure Fickian diffusion is the controlling release mechanism, $n = 0.5$ for a thin film, and Equation (10) collapses to Equation (9). Both Equation (9) and (10) are short time approximations (Siepmann,

2001; Kosmidis, 2003a) of complex exact relationships and therefore their use is confined for the description of the first 60% of the release curve.

Another alternative for the description of release profiles is based on the empirical use of the Weibull function:

$$\frac{M_t}{M_\infty} = 1 - \exp(-at^b) \quad (11)$$

where a and b are constants. Although this function is frequently applied to the analysis of dissolution and release studies (Van Vooren, 2001; Adams, 2002; Koester, 2004; Varma, 2005), its empirical use has been criticized (Costa, 2001a). The criticism is focused on: (i) the lack of a kinetic basis for its use and (ii) the non-physical nature of its parameters (Costa, 2001b). Besides, various attempts have been made to improve its performance and validate its use (Macheras, 2000; Elkoshi, 1997; Lansky, 2003).

Recently, Monte Carlo simulation techniques were used for the study of Fickian diffusion of drug release both in Euclidian and fractal spaces (Kosmidis, 2003b,c). It was found that Equation (10) describes nicely in both cases the entire drug release curve when the drug release mechanism is Fickian diffusion. In the case of release from Euclidian matrices studied by Kosmidis, 2003b, the value of the exponent b was found to be in the range 0.69–0.75. In the case of release from the two-dimensional percolation fractal (Kosmidis, 2003c) the values of b ranged from 0.35 to 0.39. It was shown that the Weibull function arises from the creation of a concentration gradient near the releasing boundaries of the Euclidian matrix (Kosmidis, 2003b) or because of the “fractal kinetics” behavior associated with the fractal geometry of the environment (Kosmidis, 2003c). The lower value of b in the percolation cluster reflects the slowing down of the diffusion process in the disordered medium. These Monte Carlo simulation results are apparently pointing to a universal law since the Weibull model provides a simple physical connection between the model parameters and the system geometry (Papadopoulou, 2006).

Korsmeyer-Peppas and Higuchi models are only valid for the first 60% of release, and the former showed good fitting to that part of the curve $M_t / M_\infty = k \times t^n$.

In Table 20, a summary of the release percentage and the corresponding quantity is shown for the samples of IF-PA66 and W-PA66 treated with corona air plasma at different times. Additionally, the fitting parameters to Korsmeyer-Peppas model are shown. The other model evaluated did not show adequate fitting so they are not presented here.

Table 20: Impregnated and released caffeine (in mg) from 100 g of corona plasma treated PA66 fabrics.

	IF-PA66 fabrics				W-PA66 fabrics				
	0	1.05	1.75	3.5	0	1.05	1.75	3.5	
t_{plasma} (s)									
%R (after 8h)	80.6 ± 3.3	89.1 ± 2.0	87.9 ± 2.6	89.2 ± 1.0	87.0 ± 0.8	88.1 ± 1.4	89.7 ± 0.2	91.1 ± 0.8	
Released caffeine after 8h (mg/100 g PA66)	540.9 ± 22.1	514.7 ± 11.6	520.6 ± 15.4	496.6 ± 5.6	604.5 ± 5.6	570.9 ± 9.1	560.6 ± 1.2	620.4 ± 5.4	
n	1.03	1.04	1.06	1.06	1.06	1.03	1.07	1.07	
Korsmeyer-Peppas	k	34.24	41.26	42.67	40.49	46.35	47.26	47.53	44.32
	R ²	0.999	0.998	0.999	0.999	0.999	0.991	0.999	0.999

As reflected in Table 20, R² was very good for all samples, which all presented an exponent n very close to 1. Assuming that the geometry of our fabric samples can be regarded like a film, for the sake of simplification, this value of the exponent corresponds to a Zero-order release mechanism meaning that the drug is released at a constant rate over time. This kind of release is desirable in case of drugs that are rapidly absorbed and rapidly eliminated because it minimizes potential drug concentration peaks and fluctuations in the blood (Siegel, 2012), which may lead to periods of underexposure or overexposure, and thus out of the therapeutic window.

As confirmed by the release profiles, the release mechanism is affected neither by the washing treatment nor by the corona plasma treatment. From the k values it can be inferred that the initial caffeine release rate of IF-PA66 samples is increased by the plasma treatment.

Korsmeyer-Peppas fitting of the caffeine release curves of untreated and corona plasma-treated PA66 revealed zero order release mechanism in both cases, showing that the treatment did not alter the release mechanism.

Finally, the overall contribution of the corona plasma on the loading and release of caffeine from the W-PA66 fiber is summarized in Figure 64.

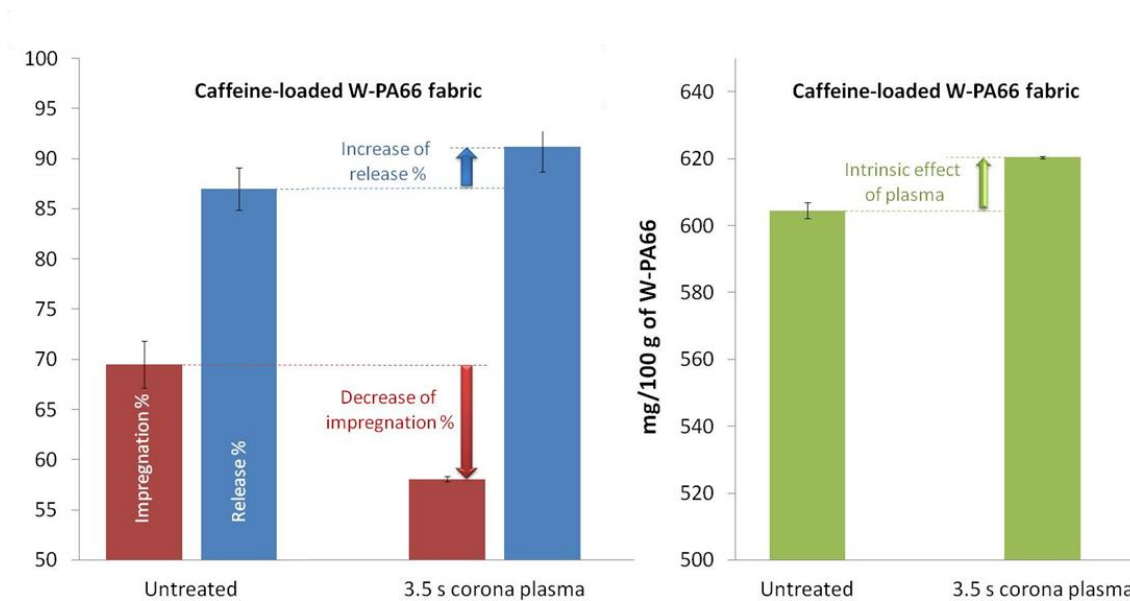


Figure 64: Global effects of the low pressure plasma treatment on the loading and the release of caffeine from the W-PA66 fibres.

It is shown that the plasma treatment of W-PA66, on the one hand, leads to a decrease of the impregnation percentage of caffeine, and on the other hand, achieves an improvement of the release percentage. Regarding the overall set of

operations, it is shown that, through the plasma treatment, an equal or greater yield in the amount of caffeine release from the fiber is obtained (Table 18 and Figure 64).

Corona plasma treatment of the PA66 fabrics leads to achieve the desired topical therapeutic levels, with the advantage of allowing to save active principle with respect to the untreated PA66, since the lower caffeine impregnation of the corona plasma treated PA66 fabrics combined with the higher percentage released, allows similar amount of caffeine released from the PA66 fibres.

Low pressure plasma

Release experiments performed with low-pressure plasma treated PA66 fibres have only been performed with IF-PA66 and caffeine, focusing the research on the influence of the low-pressure plasma conditions (gas and time) on the release of the caffeine. In vitro release profiles of caffeine during 24 h from untreated and plasma treated IF-PA66 fabrics are shown in Figure 65. In this case, the release assays have been performed during 24 h, since the equilibrium of the drug delivery system was not been reached after 8-hour experiments.

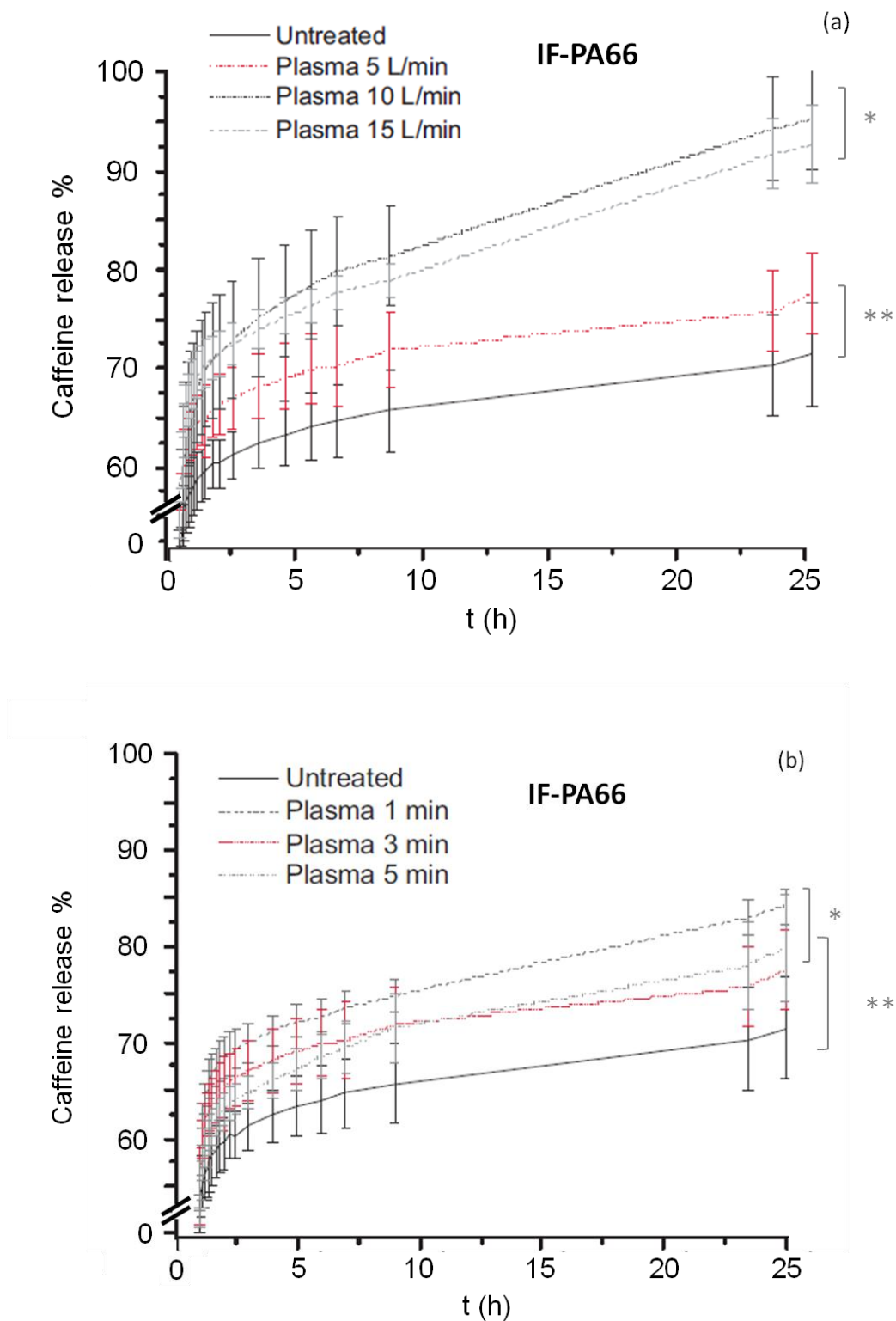


Figure 65: Influence of (a) gas flow rate into the plasma chamber (samples treated for 180 s) and (b) plasma treatment time (samples treated under 5 L/min of gas flow) on the caffeine release kinetics from IF-PA66 fabrics (*indicates no significant differences at $p < 0.05$).

Release kinetics of untreated PA66 shows a moderate burst release during the first hour of experiment, only up to 20%, due to the high solubility of caffeine in aqueous media. The effects of plasma on the release of caffeine from IF-PA66 fabrics can be clearly remarked, the increase of gas flow (air) in the chamber provoking a significant increase of caffeine release after 24 hours. Untreated IF-PA66 presents a maximum release value of 72% after 24 h, while plasma-treated fabrics under 15 L/min of air flow present a final caffeine release value close to 90%, with a constant increase of the percentage of caffeine released with the increasing of gas flow. However, as observed with caffeine loading, no significant difference is observed for the low-pressure plasma-treated IF-PA66 for 5 L/min with respect to the untreated fabric. Among plasma treated samples, increased gas flow improves wettability, as shown in section 4.1.1. This allows better contact between fabrics and release media, so plasma-treated fabrics can be more easily wetted by the aqueous receptor solution and therefore more easily release the drug.

When the effects of treatment time with air plasma were evaluated on the caffeine release from IF-PA66 fabrics, all plasma-treated samples displayed higher release percentages than the untreated ones. However, significant differences were observed among them. This may possibly be explained by the thinner polysiloxane layer on the surface of the fibers, facilitating diffusion of the drug to the release media.

It has been remarked that all curves display the same profile, which suggests that the plasma treatment does not alter the mechanism of release from knitted PA66 fabrics. Nevertheless, it can be noticed that caffeine release kinetics for plasma-treated fabrics, at high flows (10-15 L/min) and longer plasma treatment time (5 min), present a higher final slope than untreated fabrics, pointing out to a modification in the surface interactions. In addition, during the 24 hour experiment, the stationary state was not achieved, and the final slope of the release profile was higher in samples treated with plasma at high flow rate and longer treatment time, reflecting faster caffeine release. The effects of plasma gas flow on drug release have to be related with wetting properties of the materials, as well as with the thickness reduction of the outer PDMS

layer which facilitates the diffusion of the drug through the PDMS layer. All the results seem to indicate that hydrophilic properties of the PA66 fibers and thickness of the PDMS layer are the two main factors which affect the caffeine incorporation and release process from the PA66 fiber.

As for corona plasma treatment of the IF-PA66 and W-PA66, the release of caffeine enters in the topical therapeutical range of the active principle, since the quantity of caffeine loaded remains unchanged and the release percentages of caffeine from the fabrics are in the same range between both kinds of plasma treatment.

4.1.5.3. Methylxantines

4.1.5.3.1. Loading

As W-PA66 presents a better incorporation of caffeine than IF-PA66, only washed PA66 fabrics have been employed in this part of the study, focused on the influence of the corona plasma effect and the molecule polarity on the active principle loading. The corona plasma conditions yielding more clear effects (3.5 s) have been selected for the fundamental studies with the three methylxantines.

Table 21: Methylxantine weight percentage for untreated and 3.5 s corona plasma-treated W-PA66 fabrics.

Treatment time (s)	Caffeine	Theobromine	Pentoxifylline
0	69.47 ± 2.33	70.35 ± 2.34	69.86 ± 0.82
3.5	58.05 ± 0.28	61.62 ± 0.54	58.31 ± 0.42

Corona plasma treatment of PA66 fabrics for 3.5 s reduces the loading of the three methylxantines in the W-PA66 fibres as shown in Table 21. Caffeine, theobromine and pentoxifylline present an impregnation percentage decrease after 3.5 s corona plasma treatment of 11.4%, 8.7% and 11.5% respectively.

4.1.5.3.2. Release

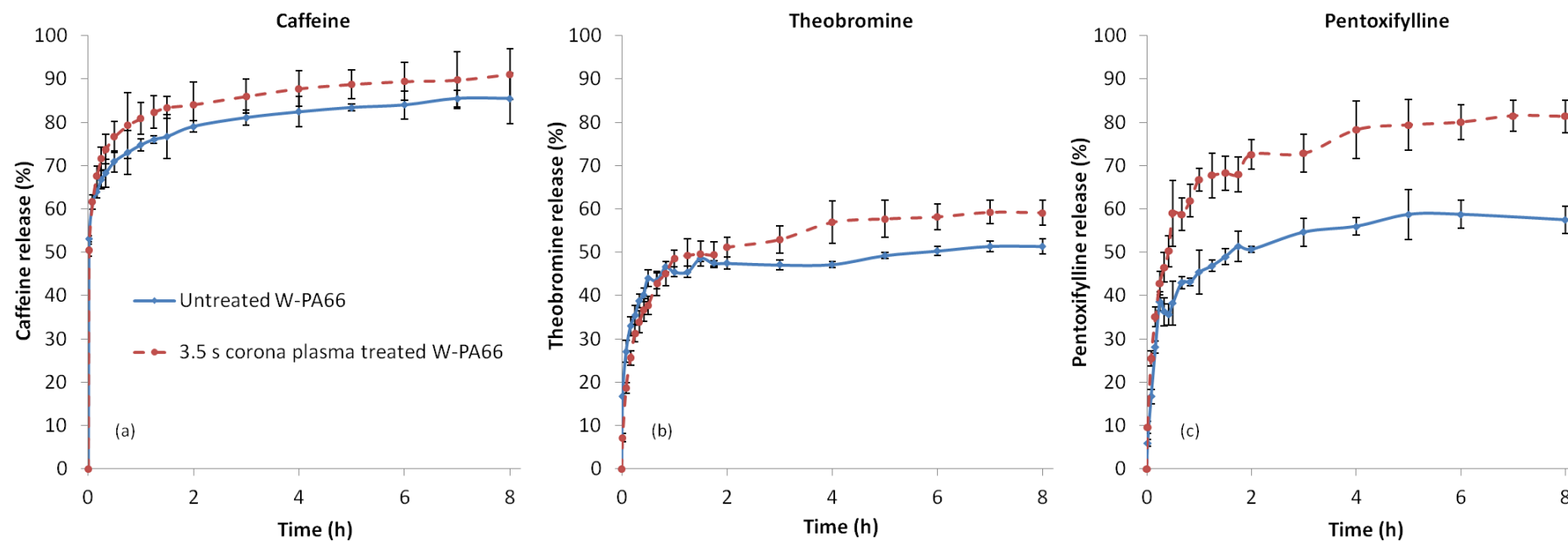
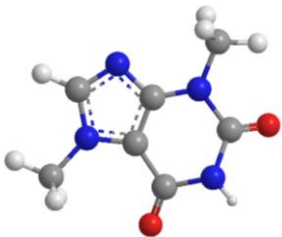
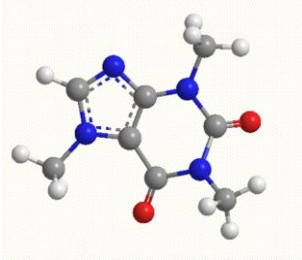
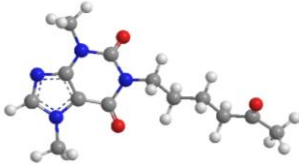


Figure 66: Caffeine (a), theobromine (b) and pentoxifylline (c) release percentage from W-PA66 fabrics. Influence of 3.5 s corona plasma treatment on the release kinetics of the methylxantine molecules.

Table 22: Relevant properties of the methylxantines used for the release study.

	Theobromine	Caffeine	Pentoxifylline
Molecular weight	180.164 g/mol	194.19 g/mol	278.31 g/mol
Formula	$C_7H_8N_4O_2$	$C_8H_{10}N_4O_2$	$C_{13}H_{18}N_4O_3$
			
Solubility in water	330 mg/L at 20 °C	2200 mg/L at 20 °C	517 mg/L at 20 °C
Polarizability	16.86	18.95	29.27
Polar surface area	67.23	58.44	75.51

While the impregnation percentages remain unchanged between all kinds of methylxantines loaded for the untreated W-PA66 and 3.5 s corona plasma treated W-PA66 (Table 21), the increase of the release percentages vary as function of the kind of methylxantines due to the effect of plasma treatment, in the following order:



To assist in the understanding of this behavior, Table 22 summarizes some relevant properties of the methylxantines studied in this work.

As described before, plasma treatment of PA66 achieves the functionalization of the fibre surface by creating new reactive groups. As shown in Figure 67, **the polar surface area of the methylxantines determines the increase in release percentage due to the plasma treatment. It can be observed that when the molecule has higher polar surface area, a much higher percentage is released after the plasma treatment with respect to the untreated sample.**

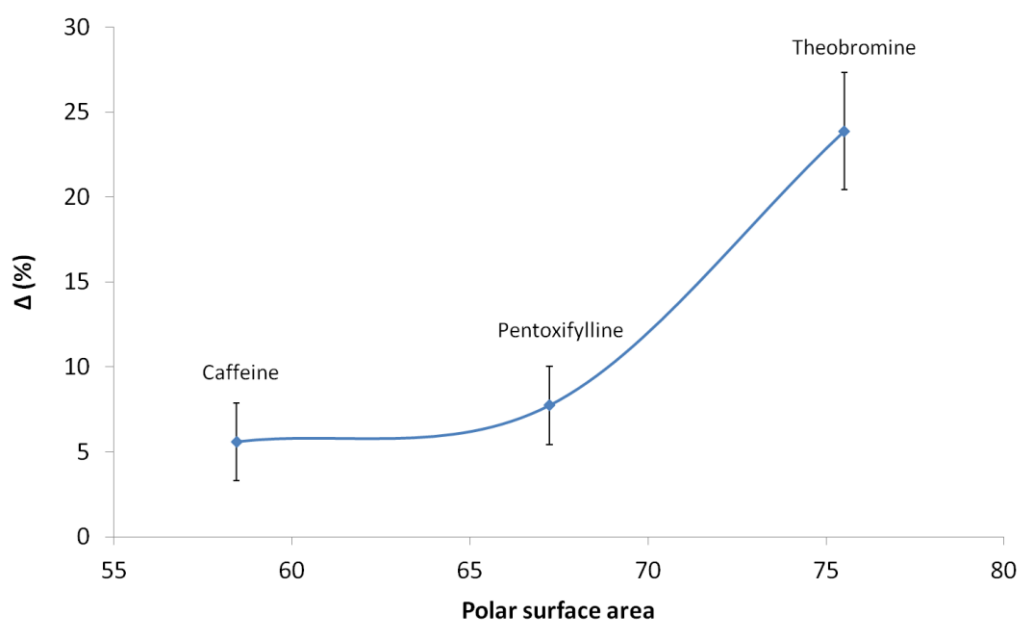


Figure 67: Increase of release percentage between untreated and 3.5 s corona plasma treated W-PA66 for pentoxifylline, theobromine and caffeine as a function of the polar surface area of each methylxantine.

This behavior can be explained through the interactions established between the drug and the surface of fibres. After plasma treatment the surface of PA66 is functionalized with O-containing polar groups which increase the electro-negativity of the fibre surface. In that case, the molecules with higher polar area (pentoxifylline) feel more repulsion from the higher electronegative surface of the plasma-treated samples, and thus show higher release percentages.

Loading of an active principle on the plasma-treated PA66 fibres and its subsequent release from such fibres not only depends on the modification of the surface chemistry and topography of the fibre due to plasma treatment but also on the polarity of the molecules loaded, since plasma treatment with air increases the electronegativity of the surface and thus modifies the electronic attraction/repulsion between the molecule and the polymer substrate.

4.2. Part II – Plasma-treated polypropylene meshes as drug-delivery body implants

This part of the PhD. Thesis is focused on the evaluation of the relevance of corona plasma and low temperature plasma as efficient tools to modify the incorporation and release of an antibiotic (ampicillin) from PP meshes aimed for body implant for abdominal hernia repair. The relevance of the loading of antibiotics on PP surgical meshes rests upon the need to treat and alleviate post surgical infections using the mesh as drug-delivery system, conferring it a functional added value to its main body tissue support function.

First, surface characterization of PP meshes has been performed to study the effects of corona plasma and low-pressure plasma treatments on the surface properties of the fiber. Both plasmas used air as gas for plasma generation. In the following sections, like in the previous part, the results obtained with both types of plasma are presented, beginning with corona plasma results, and followed by those obtained with low-pressure plasma. Taking into account the biomedical applications of the PP meshes, the studies have always been done with washed PP fabrics.

Second, a process based on plasma polymerization of PEG, using tetraglyme as precursor, has been designed for the deposition of a thin biocompatible film on the ampicillin-loaded PP fibres to evaluate the possibility of slowing down the release kinetics of ampicillin, acting as a retention membrane.

4.2.1. Influence of plasma treatment on wetting properties

Given the open structure of the knitted PP mesh selected for this study, not allowing deposition of a water droplet, the static contact angle (θ_s) has been studied by using a PP film as a model. Figure 68 shows the static contact angle of a water droplet on the untreated and plasma-treated PP film. It can be observed that the surface of the

untreated PP film, with a contact angle of 124.4° , has a clear hydrophobic character. However, when this polypropylene surface is treated by plasma, under any of the experimental conditions tested, it acquires hydrophilic properties, showing a contact angle below 90° (Figure 69).

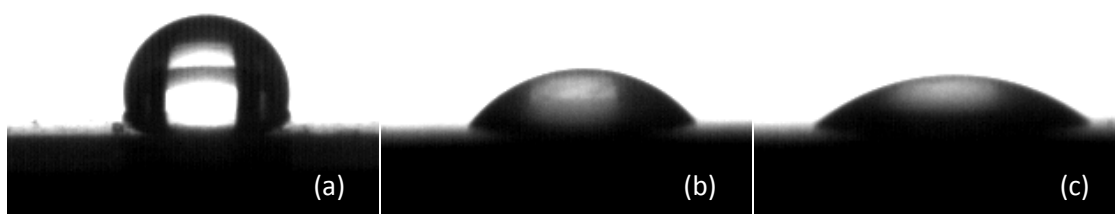


Figure 68: Profile shape of a $10\ \mu\text{L}$ H_2O droplet on the untreated (a), 0.35 s corona plasma-treated (b) and 30 s low pressure plasma-treated PP film for 30 L/min gas flow and 100 W power supply.

Corona plasma

As shown in Figure 69a, at the shortest corona plasma treatment time, corresponding to 0.35 s, PP film shows a static contact angle of $52.4 \pm 2.3^\circ$. With the increase of the plasma treatment time, corona plasma-treated PP film shows a decrease of the contact angle value down to $23.1 \pm 2.8^\circ$ with 7.0 s corona plasma treatment time. It has also been observed that the static contact angle values do not show any significant statistical difference for treatment times longer than 7.0 s (not shown in the figure for clarity).

Low-pressure plasma

Static contact angle of low-pressure plasma treated PP surface was measured for 30, 60 and 180 s treatment time with air gas flow and power set at 30 L/min and 100 W, respectively, according to the results shown in the previous section using the plasma treatment conditions. As for corona plasma treatment, the same trend of exponential decrease of the contact angle value with the increase of plasma treatment time can be observed with low pressure plasma-treated PP film. The shortest low pressure plasma treatment time, corresponding to 30 s of treatment, reaches a static contact angle of

$35.8 \pm 3.4^\circ$, 3.5 times lower than the untreated PP. PP surfaces treated for 60 s and 180 s low-pressure plasma treatment show even better hydrophilic properties, with contact angles of $22.01 \pm 3.08^\circ$ and $18.08 \pm 3.88^\circ$ respectively, which are values similar to a corona plasma treatment of 7.0 s. However, no significant difference was observed between low-pressure plasma treatment for 60 s and 180 s, allowing concluding that plasma treatments longer than 60 seconds do not further enhance the wetting properties of the PP surface.

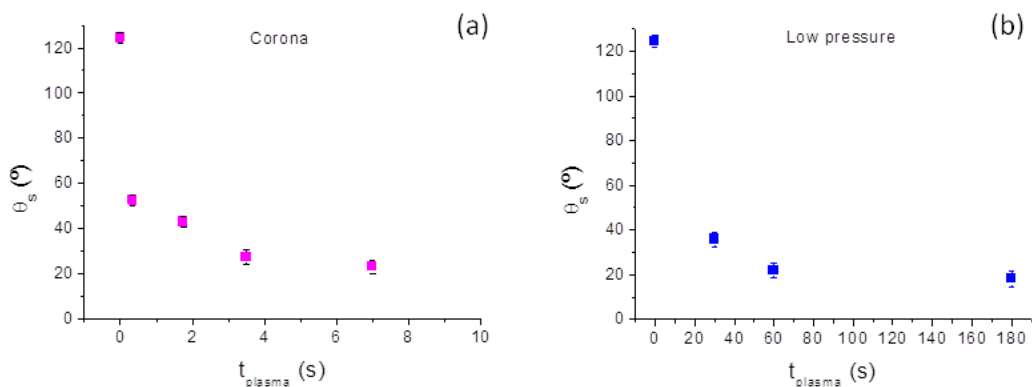


Figure 69: Water static contact angle as a function of the plasma treatment source and plasma treatment time. Comparison of corona plasma treatment (a) and low pressure plasma treatment at 30 L/min gas flow and 100 W power supply (b).

In both corona and low pressure plasma treatments it can be observed that the wetting properties show an exponential decrease as a function of treatment time. A plateau is reached in corona plasma after 3.5 s of treatment at around 25° , while longer times of 60 s are required in low pressure plasma treatment to get close to the plateau region, with contact angles around 20° .

4.2.2. Influence of plasma treatment on surface chemistry

Corona and low-pressure plasma

The relationship of the wettability improvement with the chemical modifications of the surface was evaluated through XPS, and the general spectra are shown in Figure 70 for untreated, 1.75 s and 3.5 s corona plasma treated, and for 60 s low-pressure plasma treated PP meshes. The plasma treatment times have been selected for XPS analysis from the static contact angle results presented in section 4.2.1, since longer plasma treatment times did not further improve of the wetting properties of PP meshes.

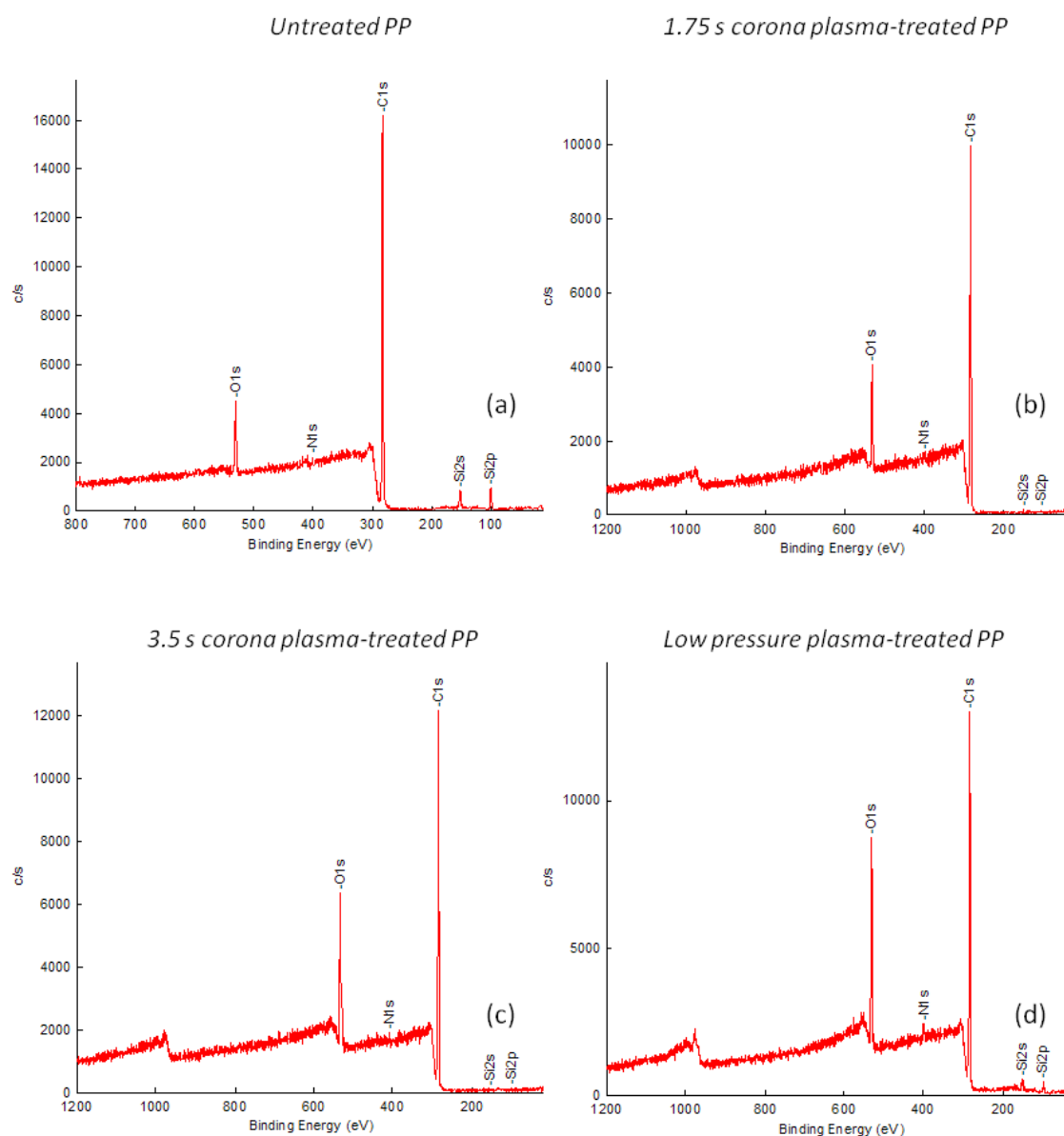


Figure 70: XPS general spectra of untreated (a), corona plasma-treated for 1.75 s (b) and 3.5 s (c), and low-pressure plasma treated PP meshes for 60 s with power supply and gas flow set at 100 W and 30 L/min respectively (d).

It can be observed that C_{1s} and O_{1s} are the main species, which is according to the chemical structure of polypropylene. It can also be observed the presence of Si in the untreated mesh even though the samples have been washed/prepared prior to their use, as well as the grafting of N atoms on the fibre surface with the low pressure plasma treatment. The quantification and the evolution of the surface chemistry with plasma treatment on the surface of PP meshes is reported in Table 23.

Table 23: Surface elemental composition and atomic ratios of untreated and plasma-treated PP meshes.

t_{plasma} (s)	Chemical composition (%)				Atomic ratios	
	C_{1s}	N_{1s}	O_{1s}	Si_{2p}	O/C	N/C
Untreated	84.0	0.3	10.0	5.8	0.12	0.004
1.75 s corona	84.2	0.1	13.4	2.3	0.16	0.001
3.5 s corona	79.7	0.7	18.5	1.1	0.23	0.009
60 s low-pressure	75.4	2.7	20.9	1.1	0.28	0.036

Table 23 reports the elemental relative composition of the fiber surface of untreated, corona plasma-treated and low pressure plasma-treated PP fibers. Untreated PP mesh presents a surface composition with 84% of C_{1s} and 10% of O_{1s} . Since the polypropylene structure does not include oxygen atoms in its formula ($CH_2=CH-CH_3$), and even if the meshes have been previously washed by the provider as well as in our laboratory, it can be observed that in untreated PP meshes a small percentage of Si is present on the fiber surface. Thus, it can be deduced that the fiber surface of the untreated mesh contains some contamination with silicone-based compounds that can justify the presence of oxygen.

For both types of plasma, the results observed after the treatment of the PP fabrics with air as gas for plasma generation show a progressive increase of oxygen groups

combined with a reduction of silicon. As described in the preceding part of this PhD. Thesis for polyamide 66, the increase of oxygen moieties comes from the functionalization of the fibre surface, while the reduction of silicon comes from the elimination of the remaining of finishing products that have not been removed by the initial washing of the PP fabrics, or rests of some surfactants in the fibre surface.

In the case of low pressure plasma treatment it has been observed an apparition of nitrogen groups in surface of the fibers of 2.7% for a plasma treatment of 60 s. This introduction of nitrogen can be attributed exclusively to a functionalization process by N_2 molecules coming from the air plasma studied. For low-pressure plasma, only the sample treated for 60 s was selected, taking into consideration the contact angle results shown in Figure 69, as the hydrophilic properties are much improved in these conditions and longer treatment times do not lead to significant improvements.

Figure 71 shows the C_{1s} high resolution XPS spectra of the untreated, corona plasma-treated and low pressure plasma-treated PP meshes. The surfaces of untreated and plasma-treated PP fibers show two distinct peaks at 284.73 eV and 286.21 eV, corresponding, respectively, to (-C-C, -C-H) and (-C-N, -C-O) groups. Relative functional groups on the fibre surface, calculated from the relative area of each peak, are reported in Table 24.

It can be observed that the C-C and C-H bonds are predominant for the untreated PP mesh (97.7%) since the structure of PP includes only these atoms and type of bonding. Submitted to corona plasma treatment, the PP fibres undergo a progressive functionalization process of the fibre surface by O and N atoms with the plasma treatment time up to 6.8% for 3.5 s of corona plasma treatment. Regarding the results in Table 23 of the surface elemental composition of the untreated and corona plasma treated PP meshes, with a ratio of N atoms < 1 in all cases, it can be concluded that the predominant bonding due to the functionalization by corona plasma is the C-O bonding.

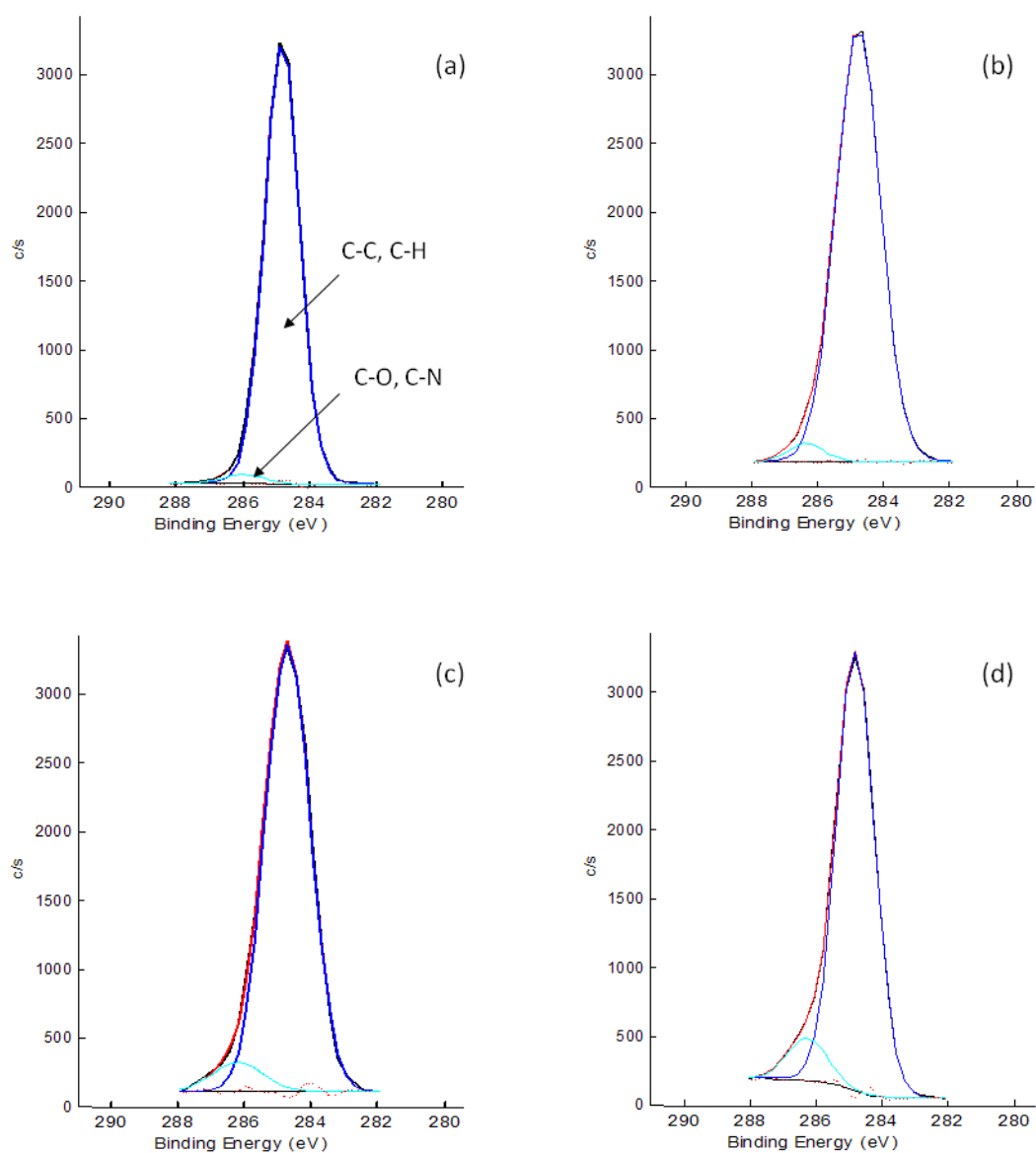


Figure 71: C_{1s} high-resolution XPS spectra of the untreated (a), corona plasma-treated (b, c) and low pressure plasma-treated (d) PP fabrics.

Table 24: Fraction of carbon functional groups from high-resolution C_{1s} XPS peaks for untreated, corona plasma-treated and low-pressure plasma-treated PP meshes.

Sample	Relative functional groups (%)	
	284.73 eV C-C, C-H	286.21 eV C-O, C-N
Untreated	97.72	2.28
1.75 s corona	96.74	3.26
3.5 s corona	93.20	6.80
60 s LPP	91.02	8.98

Low pressure plasma treatment for 60 s (100 W, 30 L/min, 300 mT) maximized the increase in C-O, C-N groups on the PP surface to 9.0%. While corona plasma treatment carries out the functionalization of the PP surface by grafting mainly oxygen atoms by covalent bonding with carbon atom of the PP fibres, low-pressure plasma treatment also increases the attachment of N atoms with the macromolecular chain of PP and achieves a functionalization with O and N atoms, as reflected by the increase of N in Table 23.

4.2.3. Influence of plasma treatment on PP fiber topography

Corona plasma

In this section, the topographic surface modifications introduced by different corona plasma treatment times are investigated by Scanning Electron Microscopy (SEM) and by Atomic Force Microscopy (AFM).

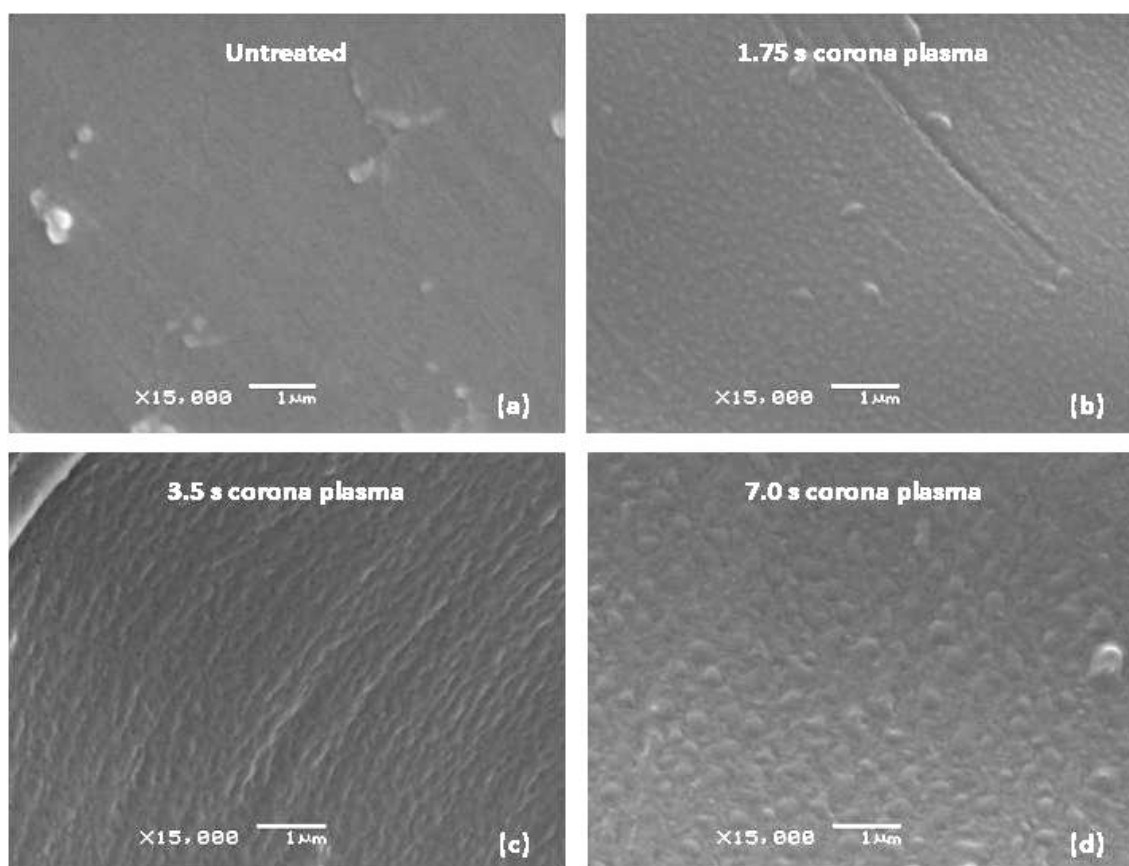


Figure 72: SEM images for untreated (a) and corona plasma-treated PP mesh for 1.75 s (b), 3.5 s (c) and 7.0 s (d).

The SEM micrographs of the untreated PP mesh presented in Figure 72a and the AFM morphology presented in Figure 73 reveal that the surface is mainly flat showing a limited nanometric roughness, with an average roughness (R_{RMS}) of 5.8 nm (Table 25). In general, untreated PP meshes present a smooth surface, as also shown in previous works, in which AFM has been used to characterize PP surfaces (Wei, 2006; Gomathi, 2009).

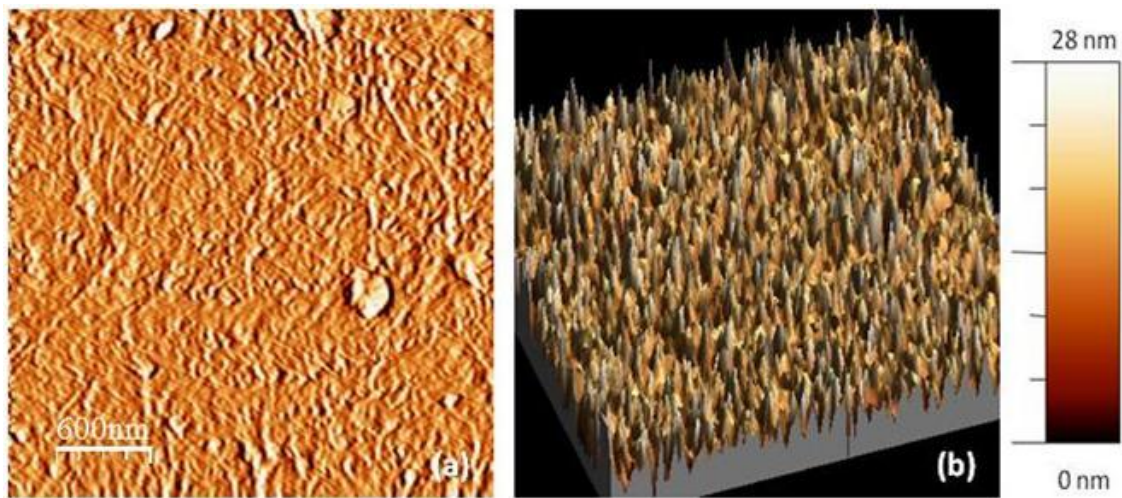


Figure 73: AFM topography of untreated PP meshes (a), with 3D reconstitution image (b).

Figure 74 shows the AFM topography of corona plasma-treated PP meshes with the 3D reconstruction images for 0.35 s, 1.75 and 3.5 s plasma treatment time.

In the case of corona plasma treatment, important changes in roughness are observed with the longer plasma treatment time studied. While short plasma treatment times (0.35 s) do not affect significantly the roughness regarding the untreated sample, the value of mean roughness (R_{RSM}) increased from $R_{RSM} = 5.8$ nm for the untreated PP mesh to $R_{RSM} = 20.3$ nm for the sample treated for 1.75 s with corona plasma and $R_{RSM} = 18.3$ nm for the 3.5 s corona plasma treatment. As observed in previous sections, this plasma treatment condition is the one showing the major changes in surface chemistry. Quantification of the evolution of the average roughness with the plasma

treatment is reported in Table 25 with the maximum roughness values for each plasma treatment condition studied.

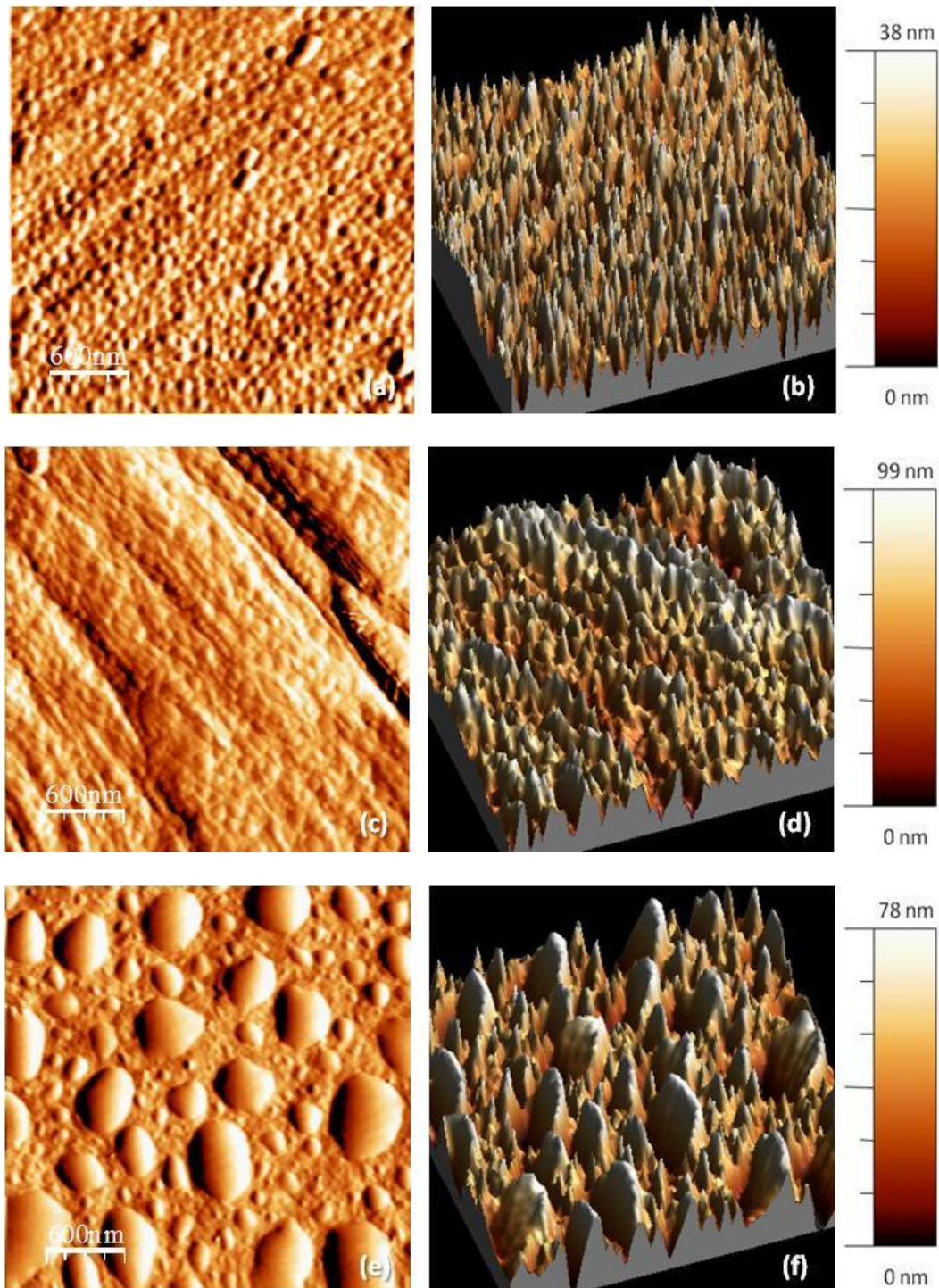


Figure 74: AFM topography with the corresponding 3D reconstitution images of 0.35 s (a, b), 1.75 s (c, d) and 3.5 s (e, f) corona plasma-treated PP meshes.

This change of surface topography results in a pattern of peaks and valleys on the polypropylene fibre surface. In fact, as shown in previous works (F. Poncin-Epaillard, 1997; Médard, 2002; Fresnais, 2006), different mechanisms are taking place. Combined etching processes, photo oxidation and thermal oxidation are taking place on the amorphous regions of the polymer. The energy transferred to the polymer thermally and from UV-VIS by the corona (which is characterized by the presence of highly energetic sparks) acts as a reaction initiator on the weakest regions of the polymer (i.e. amorphous regions in between spherulites) which is then continued and enhanced by the presence of O and N radicals, as well as by the highly reactive O₃ also present in the plasma, that results in the apparition of the peaks/spherulites on the surface of PP fibres.

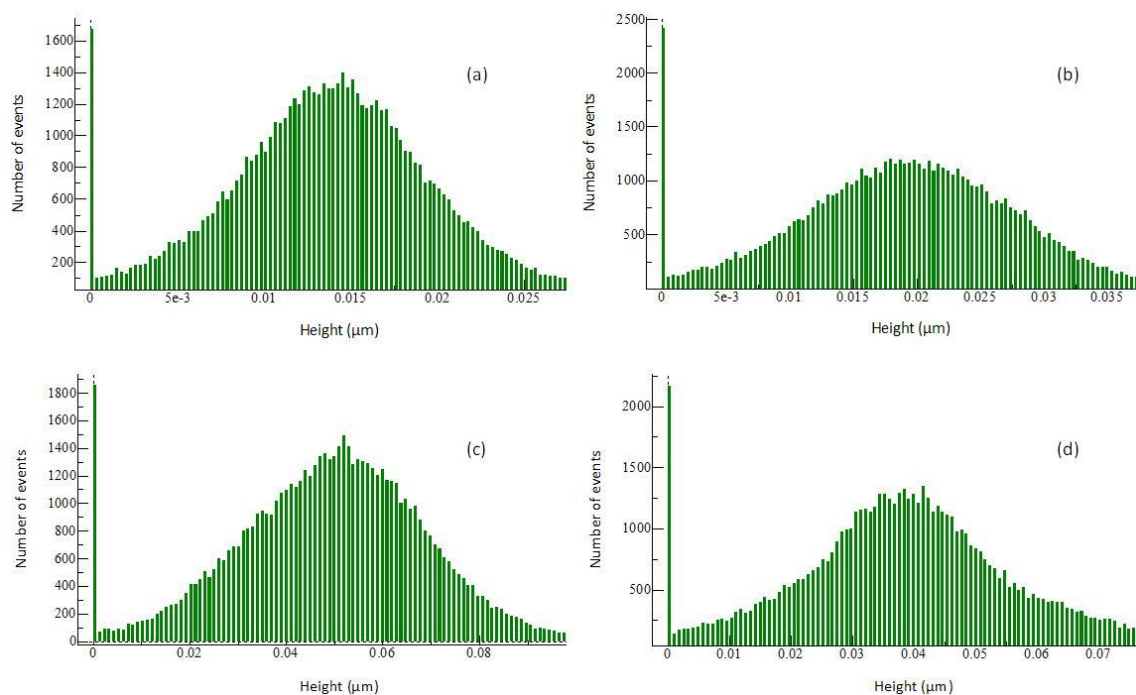


Figure 75: Roughness analysis of untreated (a) and corona plasma-treated PP meshes for 0.35 s (b), 1.75 s (c) and 3.5 s (d). Relative repartition of height of the analyzed surface from (600×600) nm AFM pictures.

Table 25: Average (R_{rms}) and maximum roughness (R_{max}) of untreated and plasma-treated PP meshes, computed from (600×600) nm AFM images.

Roughness of untreated and plasma-treated PP fibres			
	R_{rms} (nm)	R_{max} (nm)	Average height (nm)
Untreated PP	5.8	27.8	14.0
0.35 s corona plasma-treated PP	8.7	37.9	19.1
1.75 s corona plasma-treated PP*	20.3	99.3	49.9
3.5 s corona plasma-treated PP	18.3	77.9	39.0
60 s low pressure-treated PP	6.6	30.3	15.0

* Highest roughness achieved by plasma treatment

The change observed on the surface topography of the PP fibre after corona plasma treatment has also been described in a previous study on the modification of surface properties of polypropylene (PP) film using glow discharge air plasma (Pandiyaraj, 2009). Like the apparition of roughness on the PP surface observed in this PhD. Thesis with corona plasma treatment, untreated PP surface is described as smooth one (Pandiyaraj, 2009), and the surface roughness of the PP film increased after the glow discharge plasma treatment even for shorter exposure time (2–10 min). The etching effect produced by the plasma treatment results in protrusions, with similar shape as observed in this work. For longer treatment time, from 10 min to 20 min, protruding spikes get flattened due to continued etching. This behavior supports the use of short plasma treatment times to achieve higher roughness, and therefore a larger apparent surface of the PP fibre to attach molecules. A major apparent surface implies a higher availability of bonding sites regarding the loading of the drug, in this case ampicillin.

Low pressure

The surface topography of PP meshes treated by low-pressure plasma for 60 s at 30 L/min of gas flow inside the chamber has been studied by SEM and AFM, and the respective micrographs are shown in Figure 76 and Figure 77.

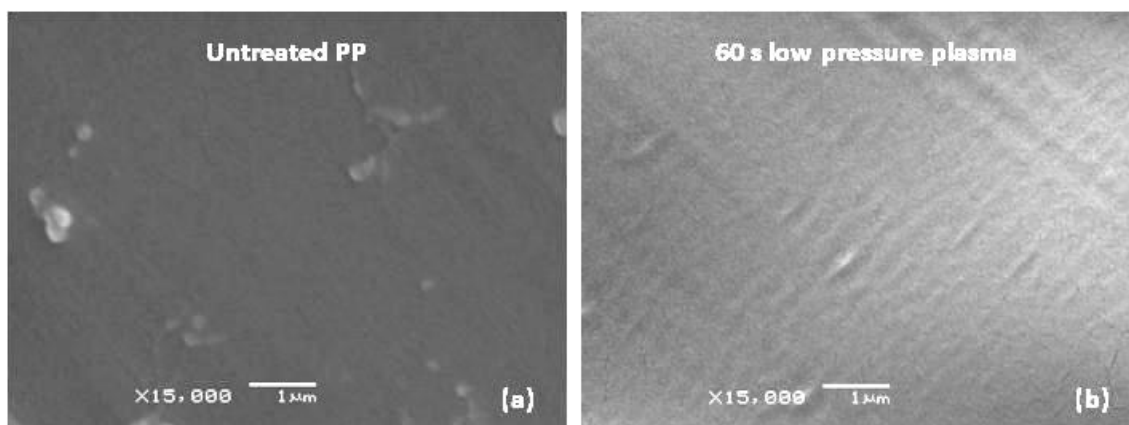


Figure 76: Scanning Electron Micrographs of untreated (a) and low pressure plasma-treated PP fabrics for 60 s, 100 W, 30 L/min (b).

The roughness of the low-pressure plasma-treated PP mesh ($R_{\text{RMS}} = 6.6 \text{ nm}$) is not significantly increased with respect to the untreated PP mesh, even if a wave-shaped pattern can be distinguished in the parallel direction of the fibre spinning, as observed in the SEM micrograph.

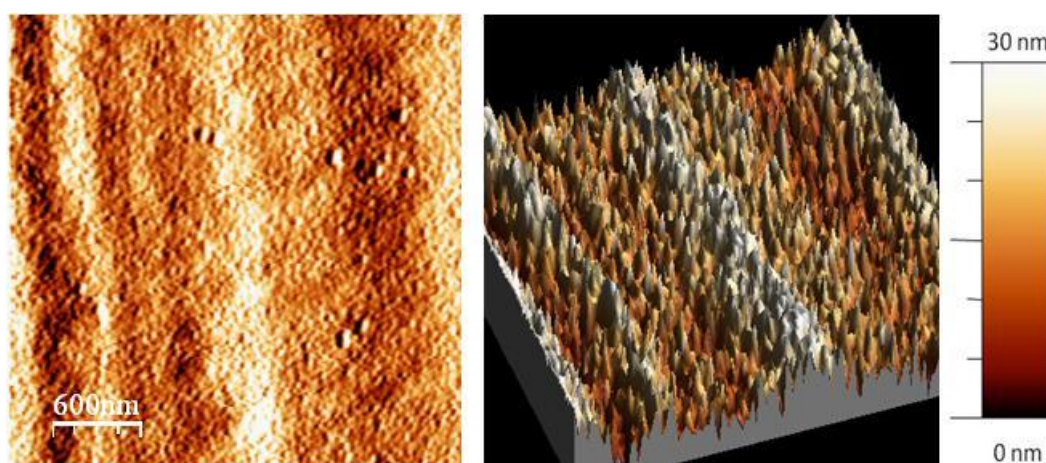


Figure 77: AFM morphology of low pressure plasma-treated PP meshes for 60 s, 100 W and 30 L/min plasma conditions (a), with 3D reconstitution image (b).

While untreated PP fibres present a smooth surface, the surface roughness of the polymer is clearly enhanced with corona plasma treatment times of 1.75 seconds and longer. The surface topography of the corona-plasma treated PP mesh presents a pattern of peaks and valleys, resulting from the combined effect of different mechanisms such as etching processes, photo oxidation and thermal oxidation that are taking place on the amorphous regions of the polymer. Low-pressure plasma treatment is milder and does not produce significant modifications on the surface topography of the PP fibres.

4.2.4. Influence of plasma treatment on the ampicillin loading

Once characterized the surface effects of corona plasma and low pressure plasma treatments on the PP mesh, in this section their influence on the loading of ampicillin is analyzed. Loading of ampicillin from an aqueous solution at 4% (c.f. section 3.3.3.2) in the PP mesh has been studied in views of designing an antibiotic-loaded surgical mesh to avoid post-surgical infections.

Corona plasma

In this section the effects of corona plasma are investigated with regard to the impregnation of ampicillin.

Table 26: Evolution of ampicillin impregnation percentage of the PP meshes as a function of corona plasma treatment time. Power supply at 100 W.

	t (s)				
	0	0.35	1.75	3.5	7.0
Impregnation (%)	20.8 ± 2.9	38.0 ± 4.1	44.9 ± 2.2	59.5 ± 2.9	59.2 ± 5.8

Evolution of ampicillin impregnation percentage of corona plasma-treated PP meshes at different plasma treatment time is presented in Table 26. **Untreated PP presents a low impregnation percentage of 20.8%. With the increase of corona plasma treatment time, a better impregnation is achieved until a 59.5% for a plasma treatment time of 3.5 s, which corresponds to an ampicillin quantity loaded in the PP fibres 2.9 times higher than the untreated ones.** The creation of C-O and C-N groups, mainly C-O groups, in the surface of PP fibres, observed by XPS in section 4.2.2, leads to an increase of the bonding sites for the ampicillin sodium salt in anionic form in the impregnation solution.

Longer corona plasma treatment time (7.0 s) does not lead to a significant improvement of the ampicillin loading, the same way that 7.0 s corona plasma treatment did not lead to an improvement of the wetting properties with respect to 3.5 s plasma treatment as observed with the static contact angle in section 4.2.1, neither leads to an improvement of surface roughness, as observed by SEM and AFM in section 4.2.3. Therefore, for further studies related with the wetting properties, the surface topography and the impregnation percentage of ampicillin, 3.5 s corona plasma treatment will be considered as the optimal condition of corona plasma treatment to enhance such properties.

This high impregnation can be related to the improved wettability of the materials. To study the relationship between the wetting properties of corona plasma-treated PP meshes and the loading of ampicillin in the PP fibres, ampicillin impregnation percentage has been represented as a function of the static contact angle of the corresponding corona plasma-treated mesh in Figure 78.

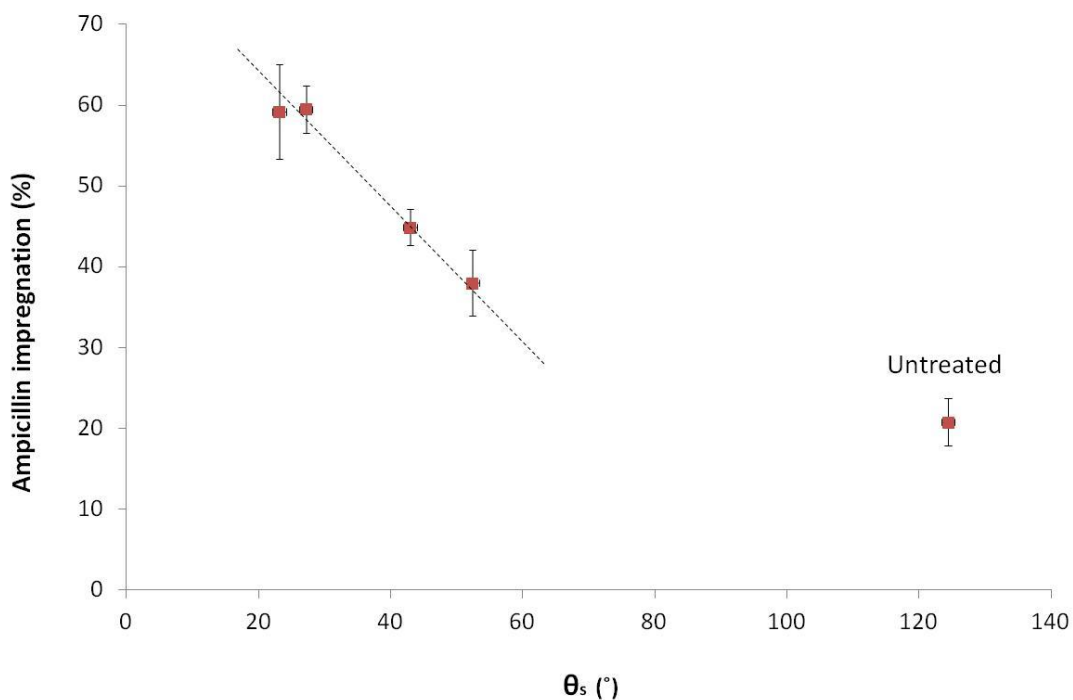


Figure 78: Ampicillin impregnation percentage as function of the static contact angle of PP surface due to the corona plasma treatment.

Figure 78 shows a **linear increase of the ampicillin impregnation percentage with the decrease of the static contact angle, corresponding to longer corona plasma treatment times. For the corona plasma conditions studied, this trend results in a linear fit for all plasma-treated samples.**

So, beside the increase of the specific area of the PP fibres achieved by corona plasma treatment, as observed by SEM and AFM in section 4.2.3, this comparative study between the evolution of the wetting properties and the impregnation percentage of the antibiotics reveals the importance and the predominance of the influence of the modified-surface chemistry on the improvement of the ampicillin impregnation.

Low pressure plasma

Different low pressure plasma conditions, varying plasma treatment time and gas flow, were tested with regard to ampicillin loading. Higher gas flow in plasma treatment could be related with higher density of reactive species in the plasma treatment, while higher plasma treatment time is related with a higher exposition time to such reactive species, and both parameters seem relevant since they could influence the impregnation percentage of the low-pressure plasma-treated PP meshes.

To study the influence of the plasma treatment time on the loading of ampicillin in the fibre, gas flow (air) has been set at 10 L/min and plasma treatment time has been studied for 30, 60 and 180 seconds, while to study the influence of gas flow inside the chamber during the low-pressure plasma treatment, plasma treatment time has been set at 60 s and air flow has been studied for 10, 30 and 50 L/min as reported in Table 27 and represented in 3D in Figure 79.

Table 27: Evolution of ampicillin impregnation percentage of the PP mesh with low pressure plasma treatment. Influence of plasma treatment time and gas flow (air) inside the chamber. Power supply fixed at 100 W.

		Treatment time (s)		
		30	60	180
Gas flow (L/min)	10	46.0 ± 1.1	69.0 ± 1.1	69.6 ± 5.0
	30	-	69.3 ± 7.1	-
	50	-	72.7 ± 0.1	-

Ampicillin impregnation percentages of low-pressure plasma treated PP meshes show an improved impregnation for all the studied conditions regarding the untreated PP mesh (that presents a 20.8% ampicillin impregnation). While the variation of gas flow inside the chamber during the low-pressure plasma treatment of the samples does not lead to relevant differences in the loading of ampicillin in the fibres, it can be observed that the plasma treatment time has greater influence on the impregnation percentage of the antibiotic. For 30 s low-pressure plasma treatment, PP meshes show an ampicillin impregnation of 46.0%, increasing until 69.6 for 60 s plasma treatment that is to say 3.3 times more than the untreated mesh.

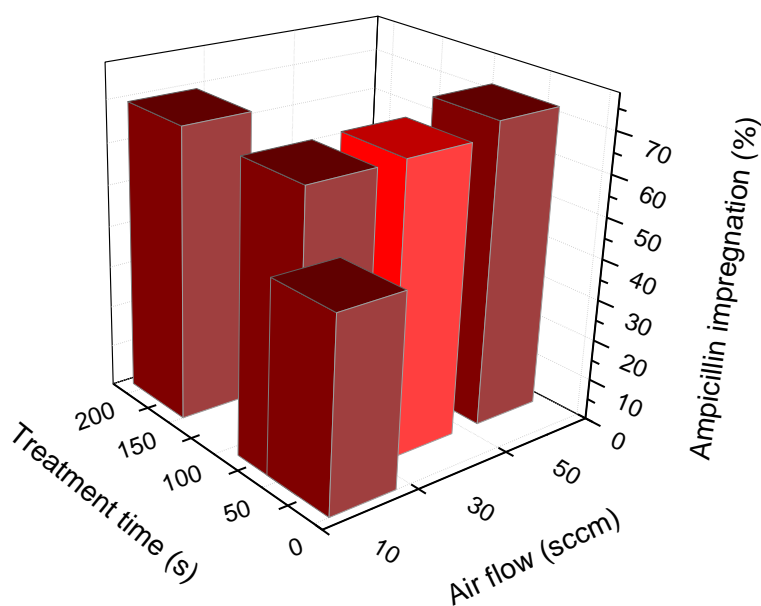


Figure 79: Evolution of ampicillin impregnation percentage of the PP mesh with low pressure plasma treatment. Error bars in Table 27.

Longer plasma treatment times (180 s or 300 s) do not further improve the loading of the antibiotic in the PP fibres, in parallel to the observations regarding the wetting properties shown in section 4.2.1.

Low-pressure plasma treatment leads to an increase of the ampicillin impregnation percentage of the PP meshes. The improvement of the ampicillin loading depends on the plasma treatment time of the PP fibres, until 60 s plasma treatment, a condition in which ampicillin impregnation percentage is 3.3 times higher than that of untreated PP mesh.

4.2.5. Influence of plasma treatment on the release of ampicillin from PP meshes

In order to determine if the amount of ampicillin released from PP meshes could be modified by plasma treatment, release experiments were performed from untreated, corona plasma-treated and low-pressure plasma-treated PP meshes.

Corona plasma

The influence of the corona plasma treatment time on the release of ampicillin from PP meshes to an isotonic liquid media has been studied by means of “in vitro” release assays of 4 hours, following the protocol described in section 3.3.4. Ampicillin release from the PP mesh has been studied for PP meshes treated with corona plasma using air as gas for plasma generation during 0, 0.35, 1.75, 3.5 and 7.0 seconds.

Figure 80a shows the ampicillin release percentage during the 4-hour release assay from corona-plasma treated PP meshes. Untreated PP mesh presents an instant burst release to reach a 74.0% of ampicillin released after one minute experiment, followed

by a stabilization, as the release after 4 hours achieves a 74.7% at the end of the release assay.

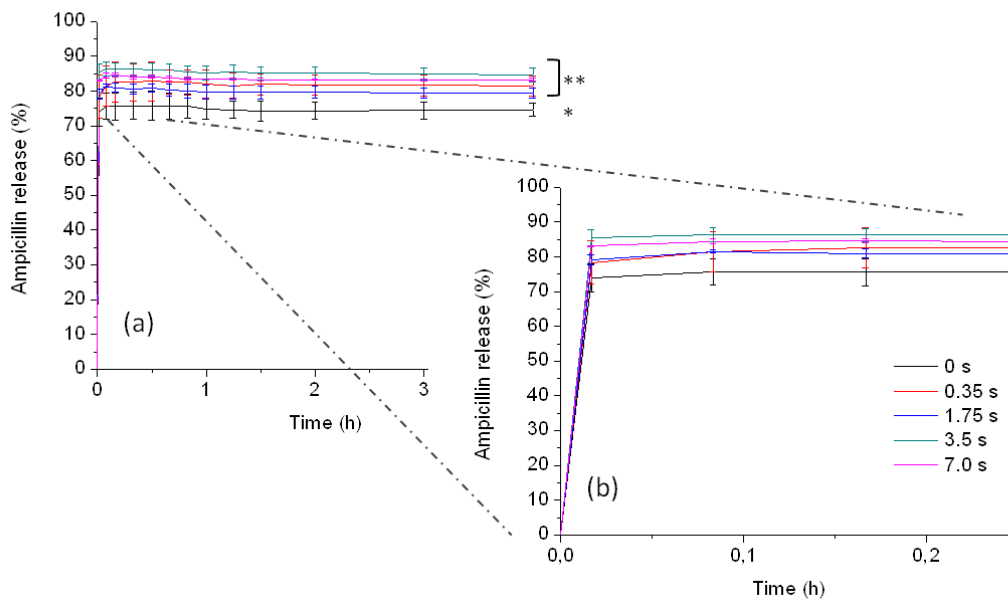


Figure 80: Ampicillin release percentage during the 4-hour release assay from untreated and corona-plasma treated PP meshes at different treatment times (a). Enlargement of the ampicillin release percentage during the first 15 minutes of the 4-hour release assay (b).

Corona plasma-treated PP meshes show the same behavior, with burst release within the first minute of release as can also be observed in the enlargement of release kinetics profile in Figure 80b. However, the results of plasma-treated PP fibres show slightly higher ampicillin release from the PP meshes, reaching values of 84.6% for 3.5 s corona plasma-treated PP fibres at the end of the assay, so about 10% above the untreated ones. Even if the improvement of the ampicillin release from the PP meshes seems to increase with plasma treatment time, the differences are not statistically significant.

Figure 81 presents the accumulated release of ampicillin from the PP fibres to the isotonic liquid media at the end of the 4-hour release assay.

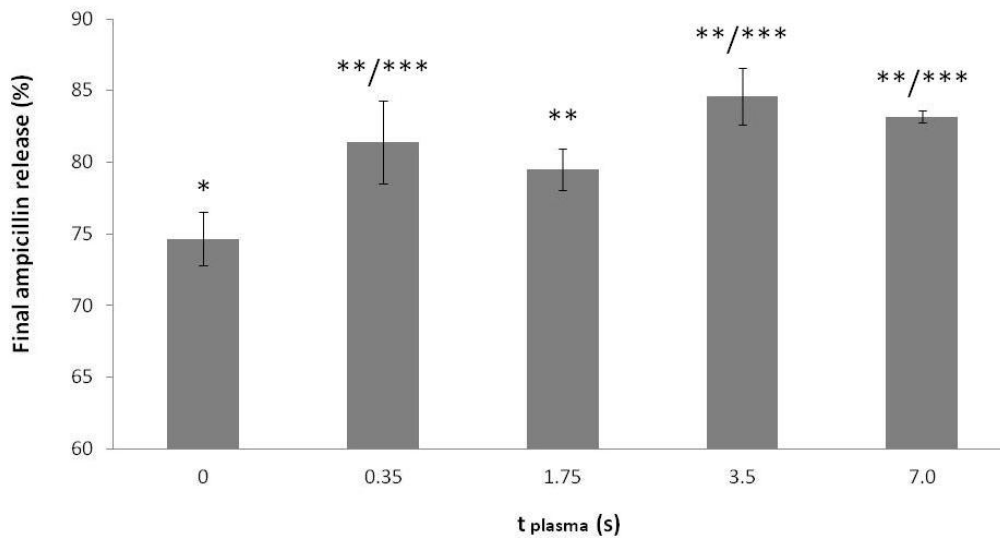


Figure 81: Maximum release percentage of ampicillin from corona plasma-treated PP meshes after 4-hour experiment.

It has been observed that both untreated and corona plasma-treated PP meshes present a burst ampicillin release in the first minutes of the assay. Anyhow, the corona plasma treatment improves the ampicillin release from the PP fibres, with an ampicillin release percentage of 74.7% for untreated PP fibres while for 3.5 s corona plasma-treated PP fibres it is of 84.6%, probably due to the improved contact with the receptor media due to 2 factors: a higher specific surface area and a better wettability. From these results, it can be concluded that corona plasma treatment has an influence on the ampicillin released amount. Nevertheless, corona plasma treatment of the PP mesh does not influence the release kinetics of the ampicillin with time, and does not slow down the burst release of ampicillin presented by the untreated mesh.

Unfortunately, the new interactions generated with the plasma are not strong enough so as to significantly reduce the burst release observed. Thus, other strategies have been investigated to try controlling this pattern (see next section).

Low pressure plasma

Figure 82 presents the influence of the gas flow during the low-pressure plasma treatment of the PP meshes on the release of ampicillin from such PP fibres. Ampicillin release percentage is represented for untreated PP meshes as well as for low-pressure plasma treated PP meshes at 10, 30 and 50 L/min of gas flow (air) during 60 seconds, with power supply set at 100 W.

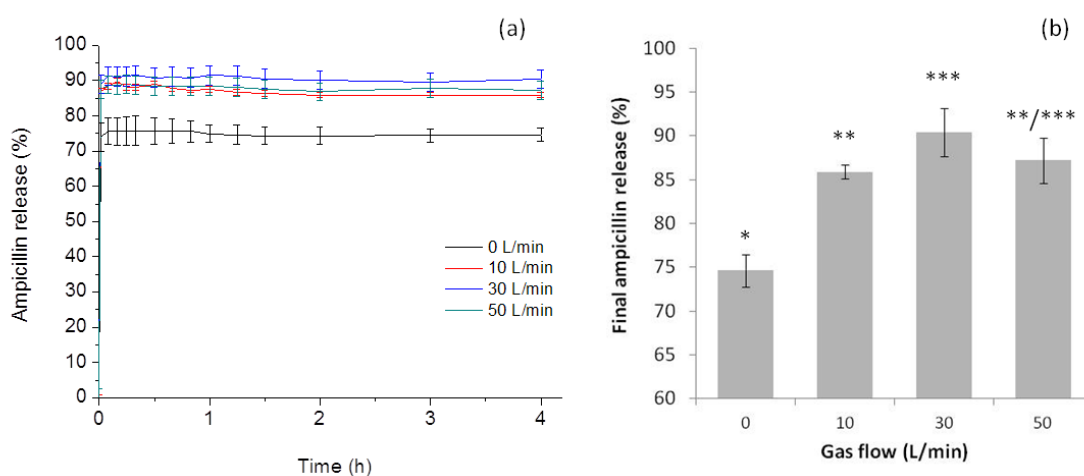


Figure 82: Influence of the gas flow during the low-pressure plasma treatment on the ampicillin release percentage from the PP meshes. Release kinetics of the 4-hour release assay of the antibiotic for untreated PP mesh and low-pressure plasma-treated meshes for 10, 30 and 50 L/min (a), with the cumulative release percentage of ampicillin from the meshes at the end of the release experiment. Plasma treatment time set at 60 seconds and power supply at 100 W.

The untreated PP mesh presents an ampicillin release of 74.7% after 4 hours. Low pressure plasma treatment leads to a significant increase of the ampicillin release for the three gas flows studied. Final ampicillin percentage released improves progressively with gas flow. **The major difference is reached for a plasma treatment with gas flow of 30 L/min, presenting an increase of + 15.8% of ampicillin release with respect to the untreated PP mesh.** Above this value, no statistically significant differences could be recorded.

The influence of the plasma treatment time has also been studied on such release, setting gas flow at 10 L/min and power supply at 100 W. Low-pressure plasma has been studied for plasma treatment times of 30, 60 and 180 seconds and the results are reported in Figure 83. As in the previous cases, release follows a burst profile.

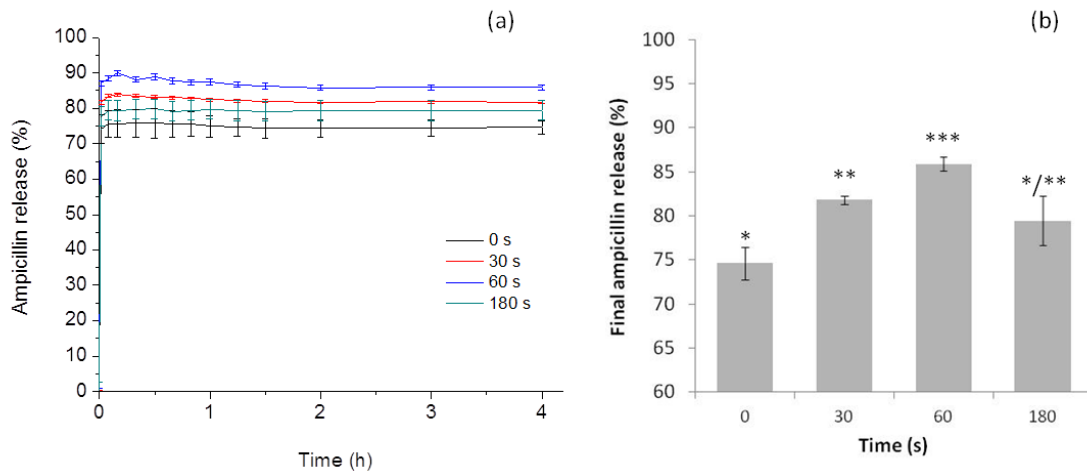


Figure 83: Influence of the low-pressure plasma treatment time on the ampicillin release percentage from the PP meshes at 30 s, 60 s and 180 s (a). Accumulated release percentage of ampicillin from the meshes at the end of the release experiment. Gas flow set at 10 L/min and power supply at 100 W.

Low pressure plasma treatment leads an increase of the ampicillin release with the plasma treatment time up to 85.9% until low-pressure plasma treatment time of 60 s, presenting a difference of +11.2% of ampicillin release from the plasma-treated PP mesh respect to the untreated one. However, longer plasma treatment times (180 s) show lower ampicillin release than plasma treatment times of 30 s and 60 s, even if the value of ampicillin release for this condition remains improved respect to the untreated PP mesh.

As observed with both types of plasma, plasma treatments only influence the amount of ampicillin released from the PP fibres, without affecting the release kinetics profile.

The improved behavior of both ampicillin impregnation and ampicillin release percentage from the PP fibres with plasma treatment could be explained by two factors:

- Wettability
- Interactions drugs-functional groups

Plasma treatment leads to the creation of new oxygen and nitrogen-containing functional groups on the propylene surface, increasing the wettability as well as the availability and the variety of bonding sites for the ampicillin molecule with the polypropylene fibres. The presence of mainly C-O and C-N groups on the surface of the plasma-treated PP fibres allows increasing the possibility of interactions with the ampicillin since the two methyl groups of the ampicillin could establish hydrogen bonds with N or O atoms on the PP surface (Figure 84).

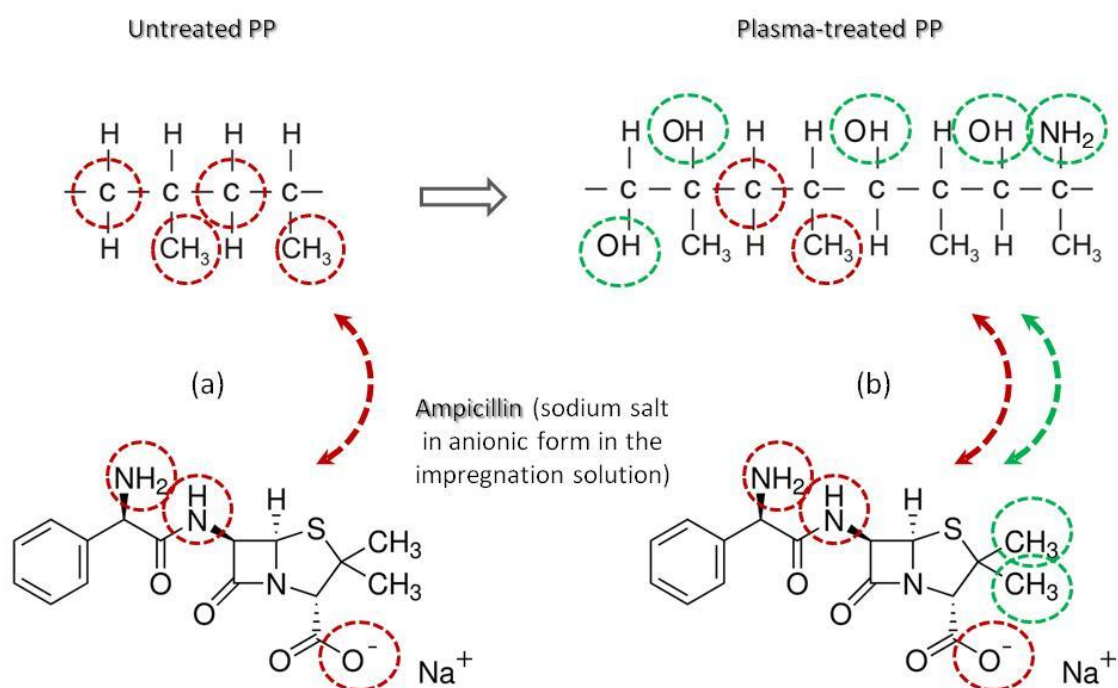


Figure 84: Proposed interactions by H-bonds of ampicillin on the PP fibre surface for untreated PP (a) and plasma-treated PP meshes (b).

On the one hand, both plasma treatments lead to the increase of the availability of the bonding sites with the incorporation of new grafted moieties on the fibre surface with

combined with the improved wettability lead to higher drug loadings. On the other hand, the bonds between the functional groups created on the polymer surface and the ampicillin are weaker than the interactions of the antibiotic directly with the macromolecular chain of carbon of the polymer, so with the improved contact with the release media derived from the better wettability, plasma-treated PP meshes have a lower ability to retain ampicillin in the PP fibre in the release assays.

Air plasma treatment of the polypropylene fibres leads to the functionalization of the PP surface of new O and N-containing groups, improving the wettability, which is reflected by an improvement of the ampicillin loading in the plasma-treated PP meshes, for both corona and low-pressure plasma treatments. However, the new chemical bonds in the surface of the polymer and the bonding between ampicillin and polypropylene resulting from this modification of the surface chemistry are not sufficient to retain the drug, and the improved wettability leads to a higher ampicillin release from the fibres to the receiving isotonic liquid receptor.

It has been shown that plasma-treated PP meshes can achieve a better released amount of drug than untreated PP meshes, and that much higher loadings can be obtained. However, in the development of biomaterial-based drug delivery systems, a great part of the attention is focused on slow- or controlled delivery systems in order to achieve an optimal therapeutic effect on a determined period of time.

The release kinetics profile, that remains unchanged for both untreated and plasma-treated PP meshes, needs to be modified to design an effective drug delivery system using this PP fibres as drug support. One potential strategy to delay drug release could be to create a biocompatible plasma polymer coating on the ampicillin-loaded PP fibres, with the aim that it may act as a membrane by limiting the diffusion of the antibiotic.

In implantable materials, cell adhesion is a highly relevant parameters towards the response of the host tissue to the implant. It has been shown in the previous sections that plasma treatments, improved the wettability and the roughness – and therefore the adhesion – of the PP meshes. To keep unaltered the biological response to the materials, the creation of an antifouling layer could be of great interest, and plasma polymerization a mean to obtain such coating of the PP fibres.

4.2.6. Plasma polymerization of PP meshes

The purpose for the use of plasma polymerization is twofold:

1. To create a thin biocompatible film on the ampicillin-loaded PP fibres which can slow down the release kinetics of ampicillin, acting as a retention membrane to avoid a quick release of the drug in the first minutes of the assay.
2. To create an antifouling layer on the polymer surface to keep cell adhesion unaltered with respect to the untreated PP meshes which are widely used in clinics with success.

The use of plasma polymerization to achieve this coating is justified for three main reasons:

- To continue having a complete dry process, using environmentally friendly technique.
- To prevent that the active principle previously loaded into the fiber is released as it could happen via a wet process.
- To prevent degradation of the drug using wet chemical processes.

For further *in vivo* and *in vitro* studies and applications, a low immune response in tissue (histocompatibility) and good blood compatibility (hemocompatibility) are the most important properties for biocompatible materials (Goddard, 2007; Ratner, 2007; Williams, 2008). Poly(ethylene glycol) (PEG) polymer is a well-known coating material in biomedical applications that acts as an effective repellent against proteins and cell

adsorption, offering sufficient biocompatibility (Choi, 2013b). As such, the Food and Drug Administration (FDA) has approved the PEG polymer for human use. Deposition of PEG plasma coating on different substrates has been carried out by plasma polymerization using tetraethylene glycol dimethyl ether (tetraglyme) as precursor (Goessl, 2001a; Goessl, 2001b; Choi 2013), but there are no precedents of using it on PP meshes as barrier layer for drug release.

In this PhD. Thesis, to study the effect of the deposited coating on the release of the antibiotic from the PP fibres and observe if such deposited biocompatible coating is able to slow down the release kinetics previously observed from the PP surgical meshes, PEG coating by plasma polymerization of ampicillin-loaded PP meshes has been carried out for untreated and 3.5 s corona plasma treated PP meshes (Figure 85).

Plasma polymerization of PEG from tetraglyme as precursor has been performed during 1 hour after a surface activation of the fibres by argon plasma, as described in section 3.3.2.3. The choice of these two ampicillin-loaded PP meshes for this study not only rests upon the results achieved by 3.5 s corona plasma treatment on the surface chemistry but also on the topography of the sample. Indeed, while the untreated PP mesh presents a relative flat surface ($R_{\text{RMS}} = 5.8 \text{ nm}$), 3.5 s corona plasma treated PP meshes presents a higher roughness with the apparition of protrusions until 77.9 nm height, and both types of PP samples could be interesting regarding the deposition of PEG coating in surface of the fibres since the topography could affect the uniformity of the deposition of the biocompatible polymer.

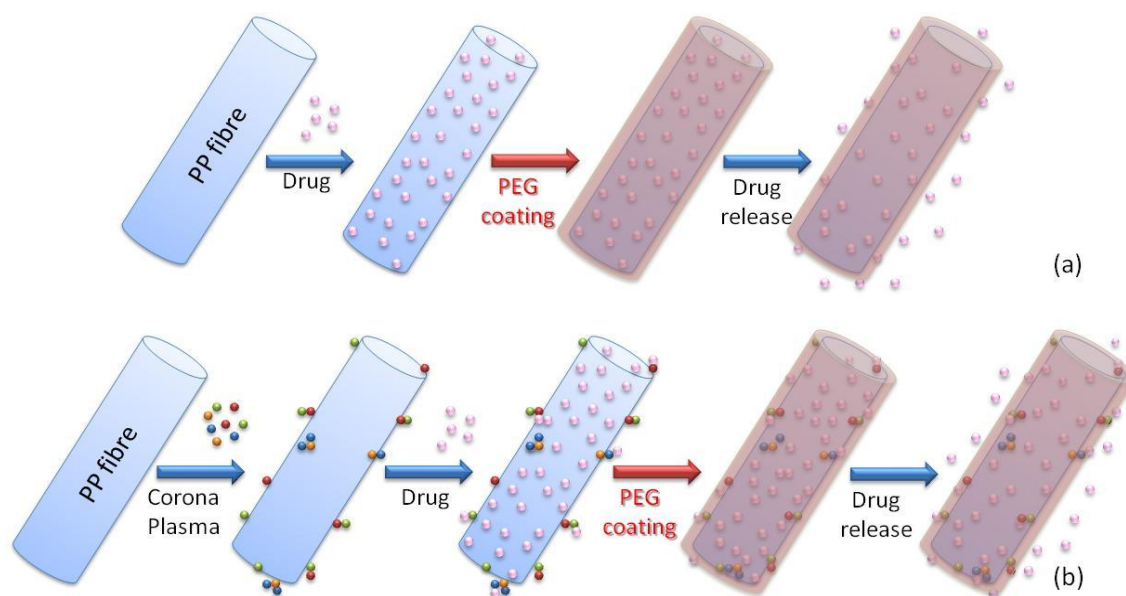


Figure 85: Concept beyond the PEG coating of the ampicillin-loaded PP meshes proposed in views of creating a retention membrane allowing slowing down the release kinetics of ampicillin from the fibres. Stages of the designed of the textile-based antibiotic delivery for untreated PP (a) and corona plasma-treated PP surgical meshes (b).

As in previous section, wetting properties of the PEG-coated PP material has been evaluated on PP film due to the open structure of the surgical mesh. The measurements of the static contact angles on uncoated and plasma-coated PP films are reported in Table 28.

Table 28: Comparison of the static contact angles of untreated and 3.5 s corona plasma-coated PP film PEG-coated with the uncoated ones.

PP film	t_{plasma} (s)	θ_s (°)	
		0 s	3.5 s
Uncoated		124.38 ± 2.51	27.17 ± 3.19
PEG-coated		77.92 ± 3.42	≈ 0

The decrease of the static contact angle of - 46.5% between the untreated PP film and the untreated PP film PEG-coated reflects a change in the surface chemistry of the PP material, maybe due to the deposition of the PEG coating on the surface of the PP

material. To quantify this modification of the surface chemistry, XPS analysis has been performed.

Figure 86 shows the general spectra of the untreated PP mesh PEG-coated and 3.5 s corona plasma-treated PP mesh PEG-coated during 1 hour.

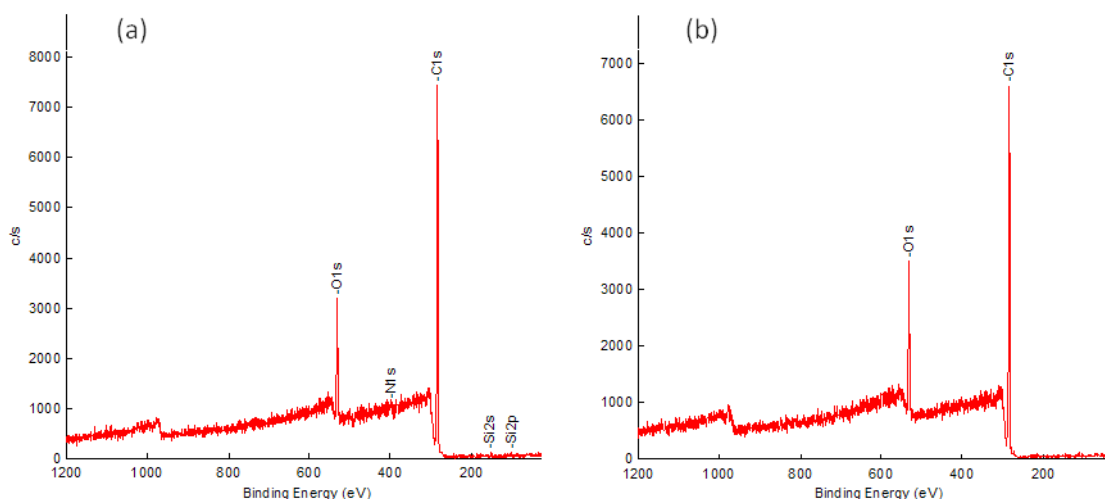


Figure 86: General XPS spectra of untreated PP mesh PEG-coated (a) and 3.5 s corona plasma-treated PP mesh PEG-coated (b).

Surface elemental composition computed from the general spectra and atomic ratios are reported in Table 29 for uncoated or PEG-coated samples either untreated or previously treated with corona plasma for 3.5 s.

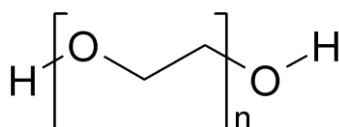


Figure 87: Polyethylene glycol (PEG) chemical structure.

While surface chemistry should show a theoretical percentage of carbon and oxygen of 66.6% / 33.3% for a homogenous deposition of PEG coating in the surface of the PP mesh, surface chemistry of the untreated PP mesh submitted to plasma polymerization shows percentages of 83.8% / 15.5%.

Table 29: Surface elemental composition and atomic ratios of untreated and plasma-treated PP meshes PEG-coated.

Sample	Chemical composition (%)				Atomic ratios
	C _{1s}	N _{1s}	O _{1s}	Si _{2p}	O/C
Untreated	84.0	0.3	10.0	5.8	0.12
3.5 s corona plasma-treated	79.7	0.7	18.5	1.1	0.23
Untreated + PEG	83.8	0.1	15.5	0.6	0.18
3.5 s corona plasma + PEG	81.2	<0.1	18.8	<0.1	0.23

Surface chemistry of plasma treated PP mesh PEG-coated presents a similar relationship in its atomic composition with the uncoated ones. This behavior indicates that the conditions used for plasma polymerization possibly lead to the deposition of a very thin PEG film, below the depth of detection of the XPS technique, which analyzes the first 10 nm of the surface, so the measurement is also taking into account C atoms proceeding from the PP fibre. However, the decrease observed for the Si compounds on the surface of the mesh from 5.8% for the untreated PP mesh to 0.6% for untreated PP mesh PEG-coated could indicate either the deposition of a thin film on the surface of the polymer, or an etching effect by Ar radicals during plasma polymerization. Also, the O/C ratio of plasma-polymerized PP meshes points out to the deposition of a PEG-like film, since its value (O/C = 0.2) is comparable with other works related with surface characterization of plasma-polymerized polyethylene glycol thin film on a PP film (Choi, 2013a; Choi, 2013b).

Modification of the carbon functional groups present in surface of the PP fibres with the plasma polymerization has been studied from the deconvolution of the C_{1s} high resolution XPS spectra of the untreated and 3.5 s corona plasma-treated PP meshes PEG-coated for 1 hour plasma polymerization, as presented in Figure 88.

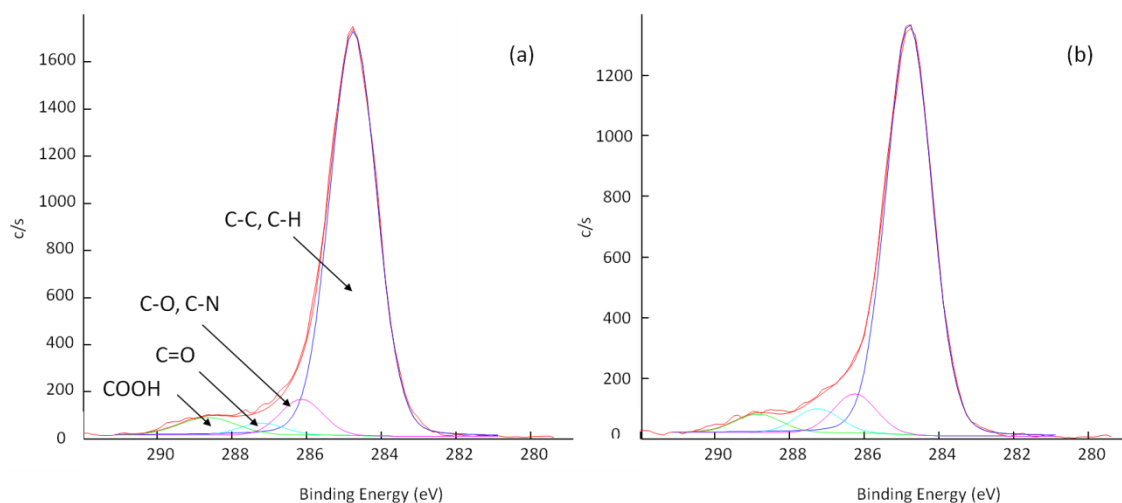


Figure 88: C_{1s} high-resolution XPS spectra of the untreated (a) and 3.5 s corona plasma-treated (b) meshes PEG-coated for 1 hour plasma polymerization.

It can be observed that the deconvolution of C_{1s} peak results in 4 sub-peaks (Figure 88), while the uncoated PP meshes presented only 2 peaks (Figure 71) issues from the deconvolution corresponding to C-C, C-H and C-O, C-N functional groups, respectively centered in bonding energies of 284.8 eV and 286.16 eV. For PEG-coated PP fibres, both sub-peaks still appear in major proportion with 2 new peaks centered in bonding energies of 287.22 eV and 288.66 eV, corresponding to bonding energies of C=O and COOH groups, respectively. Relative quantification of these carbon functional groups in the surface of the PEG-coated PP meshes is presented in Table 30.

Table 30: Fraction of carbon functional groups from high-resolution C_{1s} XPS peaks for untreated and 3.5 s corona plasma-treated PP meshes PEG-coated for 1 hour plasma polymerization.

Sample	Relative chemical bonds (%)			
	284.76 eV C-C, C-H	286.16 eV C-O, C-N	287.22 eV C=O	288.66 eV COOH
Untreated + PEG	86.80	6.64	2.29	4.27
3.5 s corona plasma + PEG	84.66	7.14	4.56	3.64

While the untreated PP mesh presented a relation between C-C, C-H groups and C-O, C-N groups of 97.72 % / 2.28 % and the 3.5 s corona plasma treated-PP mesh of 93.2%

/ 6.80% (Table 24), the PEG-coated meshes present a lower proportion of C-C, C-H groups, which could result from the deposition of new material combined with the coating on the PP fibres that “hides” the C-C and C-H groups of the macromolecular chain of the polymer. The presence of this coating of the surface of the PP textile material as consequence of the plasma polymerization is also supported by the apparition of the C=O and COOH groups in similar proportion, as also observed in other works on PEG-like coating by plasma polymerization (Choi, 2013a; Menzies, 2011).

As for uncoated PP surgical meshes, AFM and SEM techniques have been used to study the changes in morphology of the PP fibres resulting from the PEG coating by plasma polymerization, as it can be seen in Figure 89 and Figure 90. Determination of the average surface roughness, maximum surface roughness and average height of the PP fibre has been done from AFM analysis by a statistical analysis of 10 000 points computing from the surface (Figure 93a), and results are reported in Table 31.

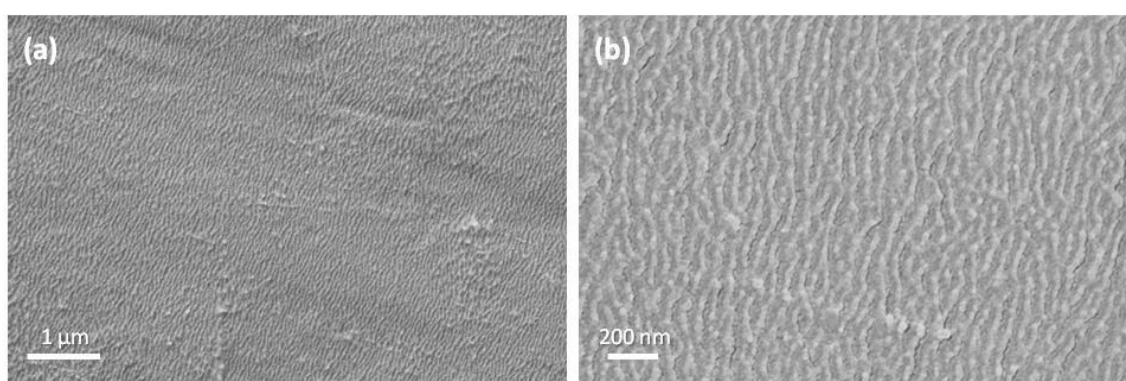


Figure 89: Scanning Electron Micrographs of untreated PP mesh PEG-coated.

Untreated PP meshes PEG-coated by plasma polymerization presents an average roughness of the fibre surface similar to the untreated PP mesh observed in section 4.2.3. The untreated PP mesh PEG-coated presents a R_{rms} value of 6.6 nm while the uncoated PP mesh presented a R_{rms} value of 5.8 nm. However, the surface of the coated fibre is not as flat as the untreated one and presents a surface morphology with a pattern comparable with the effects of the treatment of the PP fibres with low-

pressure plasma treatment. Plasma polymerization, carried out in a low-pressure reactor, leads to a wave-shaped surface of the PP fibres.

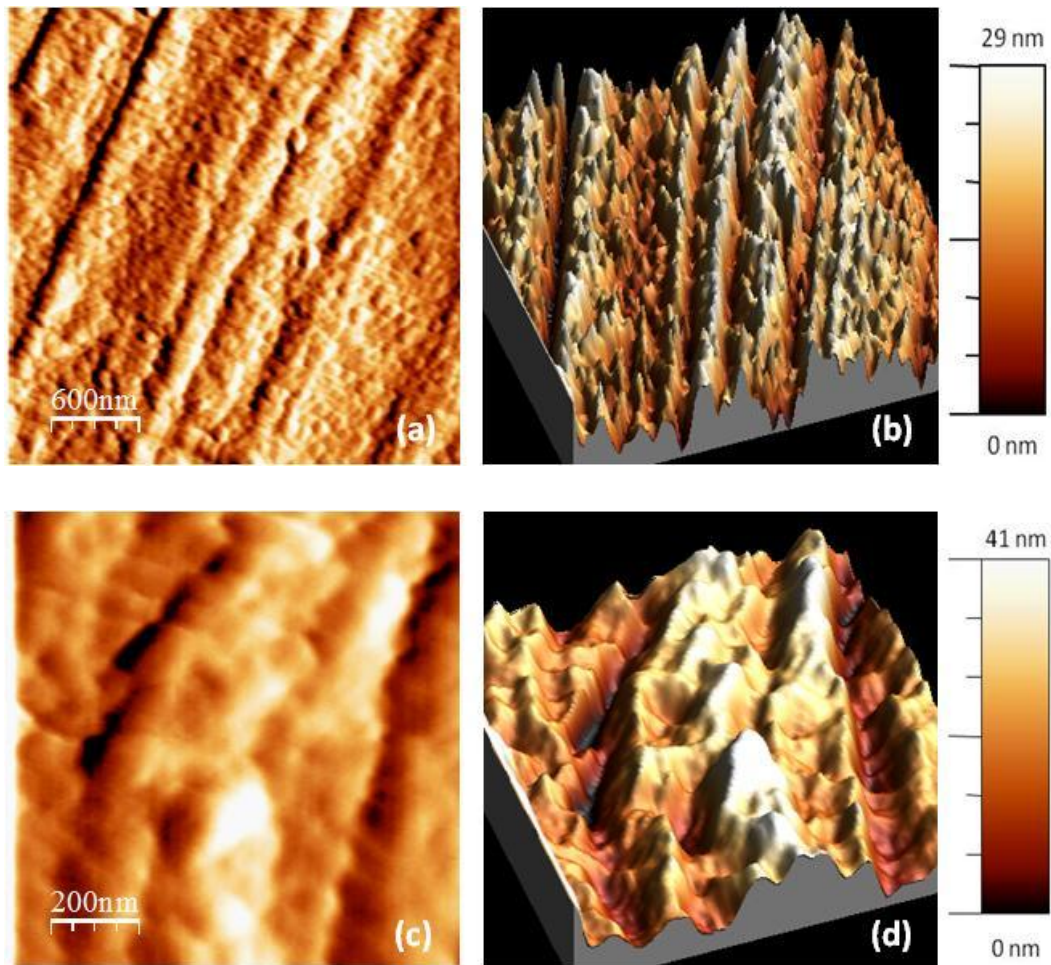


Figure 90: AFM pictures of PEG-coated untreated PP mesh with its 3D reconstitution for (600×600) nm (a)(b), with (600×600) nm enlargements (c)(d) .

Otherwise, the absence of agglomerates in the fibre surface indicates, if the PEG coating has been deposited as desired, that the deposition of such coating of the PP mesh has been done in a homogeneous way.

Figure 89 and Figure 90 present the surface topography of 3.5 s corona plasma-treated PP mesh PEG-coated observed respectively by SEM and AFM. As done for untreated PP mesh, determination of the average surface roughness, maximum surface roughness and average height of the PP fibre has been done from AFM analysis by a statistical

analysis of 10 000 points computing from the surface (Figure 93b), and results are reported in Table 31.

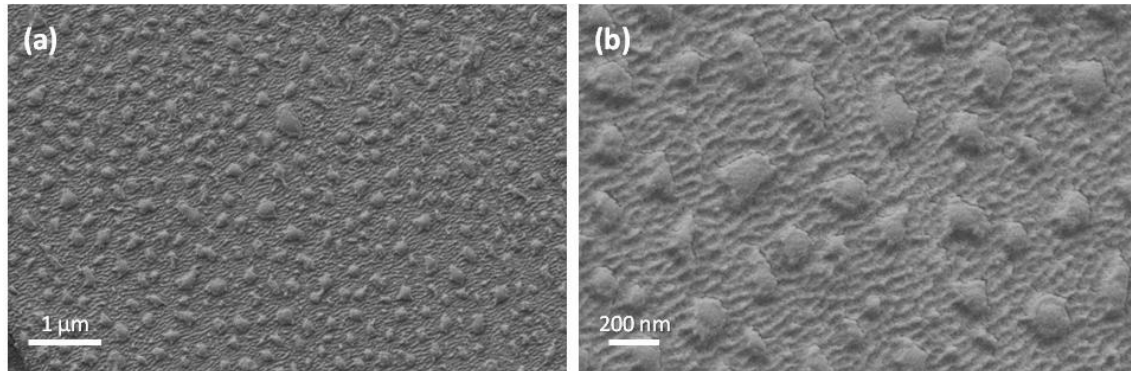


Figure 91: Scanning Electron Micrographs of PEG-coated 3.5 s corona plasma-treated PP mesh.

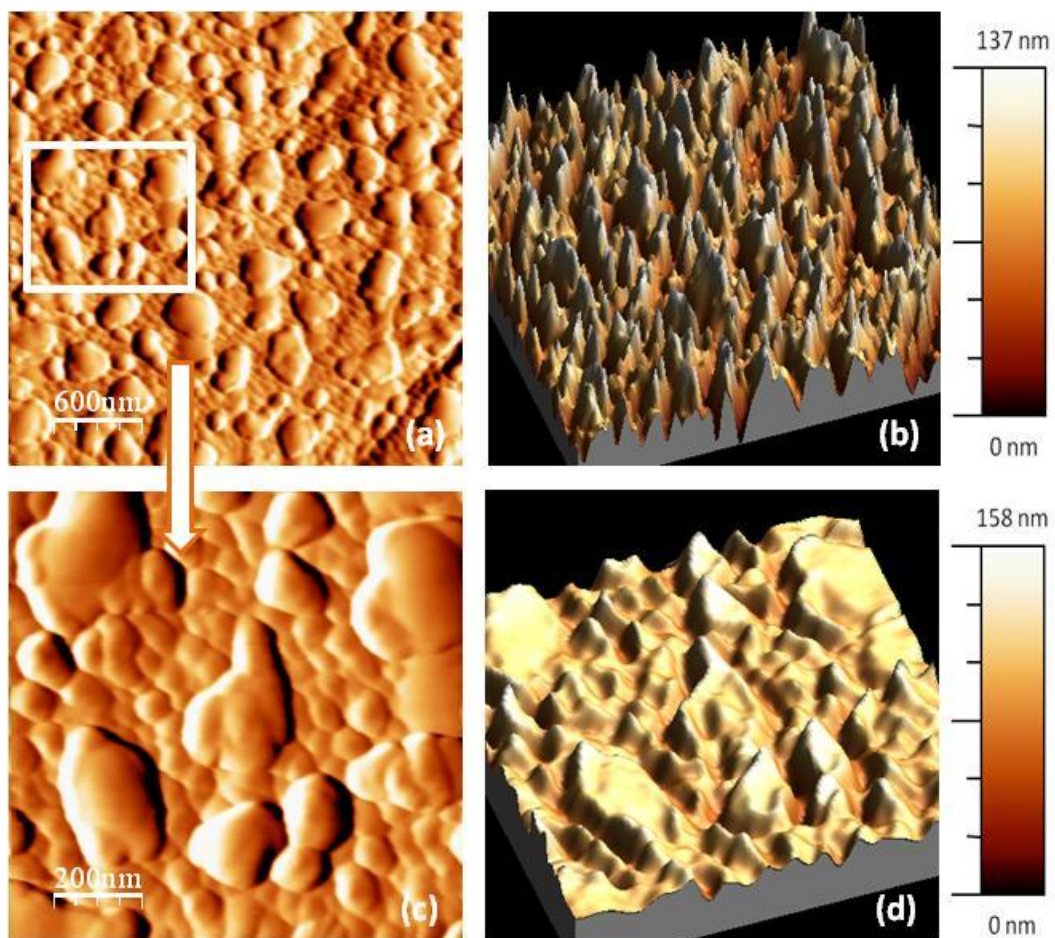


Figure 92: AFM pictures of 3.5 s corona plasma-treated PP mesh PEG-coated with its 3D reconstitution for (600×600) nm (a)(b), and (200×200) nm enlargements (c)(d).

Corona plasma-treated PP meshes PEG-coated show a pattern similar to the uncoated corona plasma-treated samples, with peaks and valleys resulting from the apparition of protrusions in the corona plasma treatment of the PP meshes due to the sparks of the corona plasma. The observation of these protrusions suggests that the low pressure plasma polymerization does not affect the surface morphology. However, the increased of the roughness observed by AFM, from $R_{\text{RMS}} = 18.3 \text{ nm}$ to $R_{\text{RMS}} = 30.2 \text{ nm}$ between uncoated and PEG-coated PP mesh, as well the wave-shaped pattern distinguished in the valleys as observed by SEM (Figure 91), indicate that plasma polymerization affects the morphology of the surface of the PP fibres and result in a combined effect of the previous corona plasma treatment of the surgical mesh and of a low pressure plasma treatment. All these topographical effects can be attributed to etching by the Ar species of the carrier gas, which, after such a long treatment, produce very significant effects.

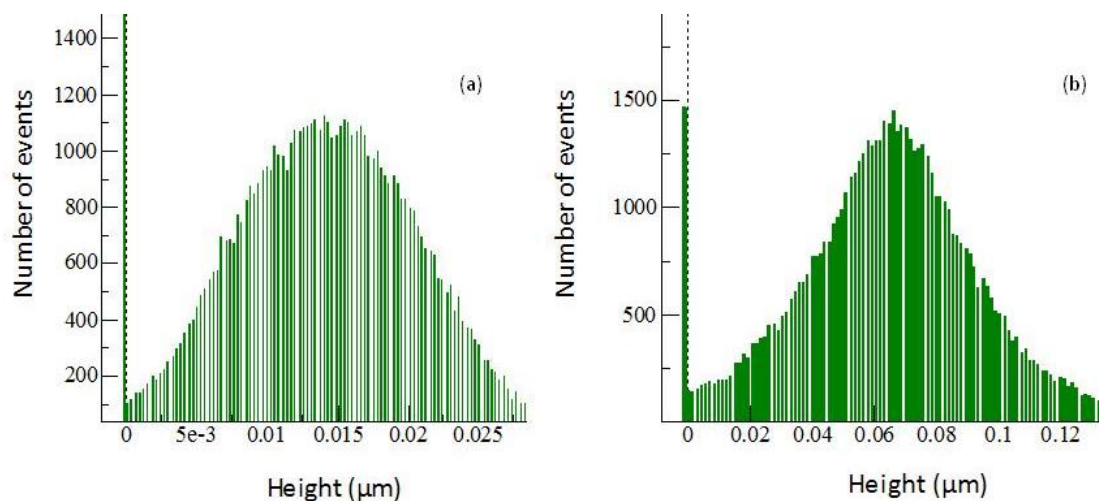


Figure 93: Roughness analysis of PEG-coated untreated PP mesh (a) and PEG-coated 3.5 s corona plasma-treated PP mesh (b). Relative repartition of height of the analyzed surface from (600×600) nm AFM pictures.

Table 31: Average (R_{rms}) and maximum roughness (R_{max}) for PEG-coated untreated PP mesh and 3.5 s corona plasma-treated PP mesh from (600×600) nm images.

	Roughness of PEG-coated PP fibres (nm)		
	R_{rms} (nm)	R_{max} (nm)	Average height (nm)
Untreated PP	5.8	27.8	14.0
3.5 s plasma treated PP	18.3	77.9	39.0
Untreated PP PEG-coated	6.6	29.1	14.5
3.5 s plasma treated PP PEG-coated	30.2	137.4	68.1

Low-pressure plasma polymerization of the PP meshes leads to a pattern of surface morphology that combines the surface morphology of the uncoated PP mesh with the pattern observed for low-pressure plasma treatment of the polymer material. This results in a wave-shaped pattern for untreated PP mesh PEG-coated, and in a peaks and valleys pattern, with wave-shaped topography in the valleys, for 3.5 s corona plasma-treated PP mesh PEG-coated by plasma polymerization for 1 hour. Regarding the roughness, while plasma polymerization does not achieve significant difference for untreated PP mesh, average and maximum roughness are increased 1.7 times for corona-plasma treated PP meshes.

Subsequently, ampicillin release kinetics of PEG-coated PP meshes have been performed with untreated and 3.5 s corona plasma-treated PP mesh loaded with ampicillin following the impregnation process described in section 3.3.3.2. The stability of the ampicillin has been checked by means of spectrophotometry technique to observe if the polymerization of the ampicillin-loaded PP meshes affects the molecule of the antibiotic. The general spectrum of the ampicillin released to the isotonic medium (pH 7.4) from impregnated PP fibers has been compared with those of the ampicillin released from impregnated PP fibres and PEG-coated by plasma polymerization (Figure

94). The overlapping of the two spectra shows there is no difference in the released ampicillin after PEG coating by plasma polymerization.

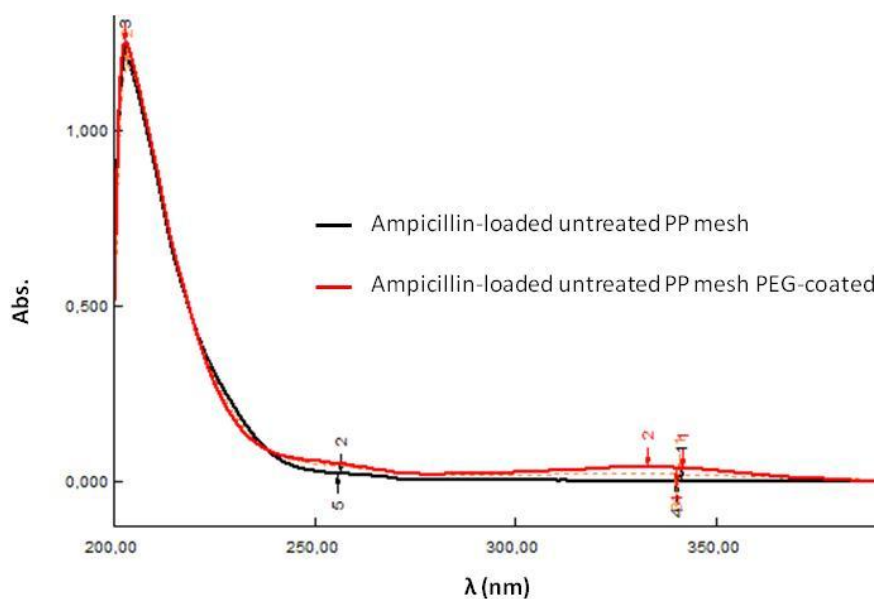


Figure 94: Study of the stability of the ampicillin by UV-spectrophotometry. Comparison of the general spectra of ampicillin released from untreated PP mesh PEG-coated by plasma polymerization with those released from untreated PP mesh.

Figure 95 presents the release kinetics of ampicillin from untreated PP mesh and PEG-coated untreated PP mesh, submitted to a plasma polymerization during 1 hour. The general spectra of the ampicillin released from the untreated PP mesh fits the spectra of the ampicillin molecule in aqueous solution, indicating that the ampicillin loaded to the PP mesh has not been altered in the loading process. Ampicillin release kinetics from the PEG-coated untreated PP mesh presents the same shape regarding the release kinetics profile than the uncoated one, revealing a similar release mechanism between both samples.

As for the uncoated PP fibres, PEG-coated PP meshes show a burst release of ampicillin in the first minute of the release assay, pointing that plasma polymerization of PP fibres during 1 hour does not achieve slowing down the release kinetics as the designed process had been aimed for.

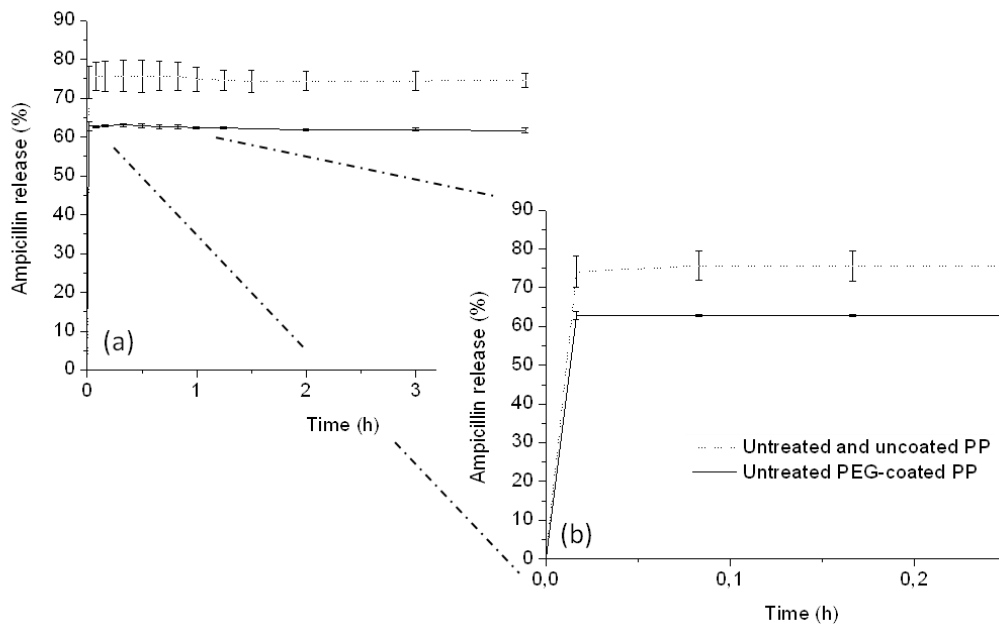


Figure 95: Ampicillin release percentage during the 4-hour release assay from untreated PP mesh and untreated PEG-coated PP mesh (a) with the enlargement of the ampicillin release percentage during the first 15 minutes of the release assay (b).

However, the maximum release percentage after 4 hours of release assay decreases slightly for PEG-coated PP meshes, presenting a value of 61.8% while the uncoated one presented a final value of 74.7%.

Results of ampicillin release percentage from the 3.5 s corona plasma-treated PP meshes PEG-coated for 1 hour are presented in Figure 96. Just as for untreated PP mesh PEG coated, plasma polymerization for 1 hour of the 3.5 s corona plasma-treated PP mesh loaded with ampicillin leads to a decrease of the ampicillin release from 84.6% for the uncoated PP mesh to 68.5% for the PEG-coated PP mesh at the end of the release assay. This decrease of ampicillin release percentage after plasma polymerization of the PP meshes is even higher for corona-plasma treated PP fibres (-16.1%) than the untreated PP fibres (-12.9%).

Plasma polymerization of the untreated and corona plasma treated-PP meshes has also been performed during 2 hours has also been performed and it has been check

that this longer plasma polymerization neither slows down the ampicillin release kinetics.

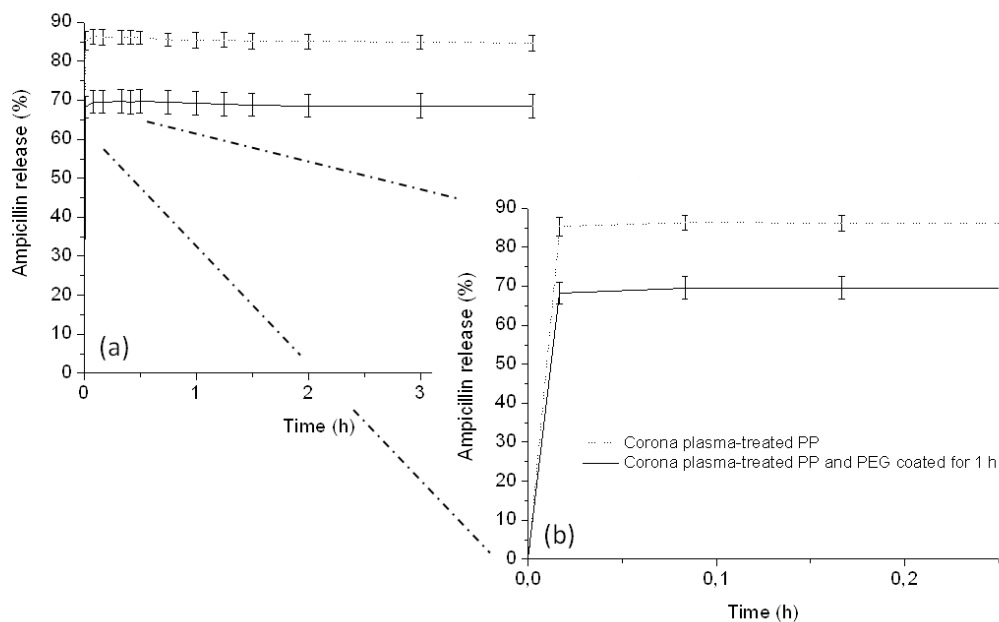


Figure 96: Ampicillin release percentage during the 4-hour release assay from 3.5 s corona plasma-treated PP mesh and 3.5 corona plasma-treated PP mesh PEG-coated (a) with the enlargement of the ampicillin release percentage during the first 15 minutes of the release assay (b).

Two interpretations of this behavior can be done:

- The coating created by the deposition of PEG by plasma polymerization retains a part of the ampicillin, like a membrane.
- A part of the ampicillin has been removed by etching reactions with Ar species during the plasma polymerization process

Beyond these interpretations regarding the decrease of ampicillin release percentage with the plasma polymerization, the unsolved problem to slow-down down the release kinetics of the ampicillin from the PP mesh and avoid the burst release effects also leads to three possible causes to explain the unchanged release kinetics. It could be come from the fact that:

- No polymer layer has been deposited in surface of the fibre.
- The PEG-coating layer is very permeable.
- The PEG-coating layer quickly dissolved in the isotonic release media.

Crossing both analyses, with the results of surface chemistry by XPS, it can be concluded that plasma polymerization leads to the deposition of a very thin layer (below 4 nm). Focus Ion beam technique has also been used to try confirming the existence of the thin coating film of PEG by performing the cross-section of a plasma-polymerized PP mesh but no coating could be observed.

Regarding biocompatible polymeric coating of the PP mesh to slow down the burst release kinetics of antibiotics from the PP fibres, it has been described recently (Guillaume, 2012) how a commercially available polypropylene mesh was modified to minimize the risk of post-implantation infection, alike in this PhD. Thesis. This coating was composed of three layers containing ofloxacin and rifampicin dispersed in a degradable polymer layer made up of [poly(ϵ -caprolactone) (PCL) and poly(DL-lactic acid) (PLA)]. Drug release kinetics was managed by varying the structure of the degradable polymer and the multilayer coating. Sustained release of the two antibiotics from the coated mesh prevented mesh contamination for at least 72 h. Before optimized the antibiotics release system to obtain a sustained release of 72 hours, a simple layer coating of PCL had been designed and the coated mesh no longer released significant amounts of antibacterial drugs after 24 hours.

Solvent free low pressure plasma polymerization strategy was also recently used to develop multilayer biodegradable nanometric PCL-co-PEG (poly (ϵ -caprolactone)-poly (ethylene glycol) copolymer) coatings for the controlled delivery of cisplatin, an anticancer drug (Bhatt, 2013). The resulting multilayer PCL-co-PEG coatings drug delivery device, built on a model surface (silicon wafer), can be tailored in such a way to have controlled cell-surface interactions and barrier layer dependent release. Methylene Blue (MB) was used as a model to simulate the drug release kinetics and the nature of which was examined by using the Korsmeyer-Peppas model for polymer coatings to optimize the system. Barrier layer dependent release was investigated by varying the deposition time from 5 to 50 min. The results show that by gradually increasing the barrier layer thickness with deposition time, the MB released was slowed down.

These other works (Guillaume, 2012; Bhatt, 2013), using wet processes produce thick polymer layers able to slow down the release of antibiotics (rifampicin and ofloxacin) from PP fibres, in which antibiotics are contained in a biodegradable polymer layer acting as a matrix for the antibiotics. Thus, the strategy proposed in this work is adequate but being focused only in dry plasma processes, would require further improvement/optimization of the thickness of the polymer layer produced.

4.2.7. Influence of plasma treatment on antibacterial effect of PP mesh

The application of antibiotics to some medical materials, like the surgical PP meshes for abdominal hernia repair used in this case, requires checking the conservation of the activity of the drug to study whether the previous plasma treatment of the mesh affects its antibacterial activity. The following section presents the *in vitro* evaluation of the antibacterial activity of the plasma-treated PP materials.

Corona plasma

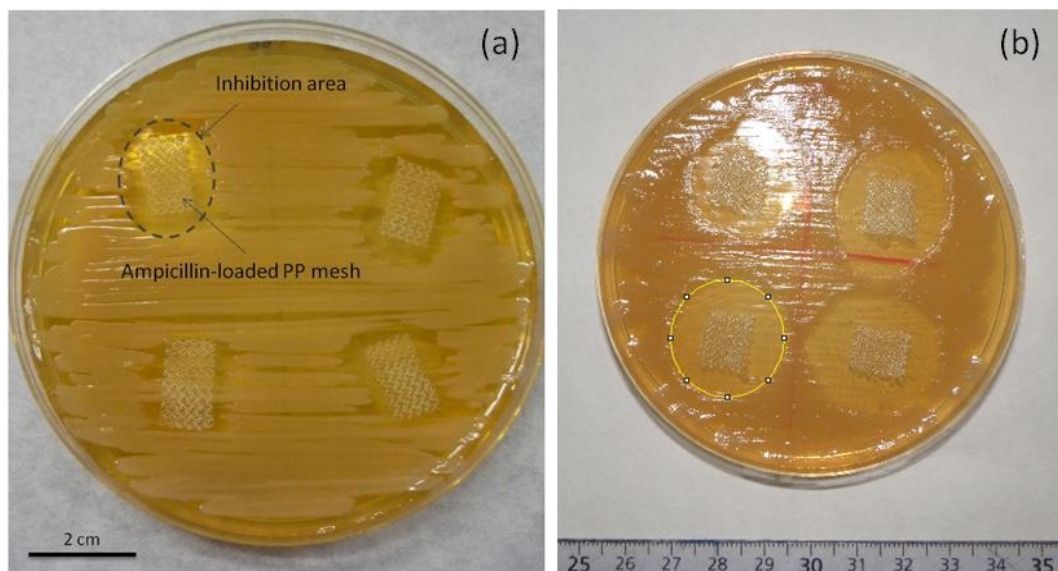


Figure 97: Images of the inhibition area of ampicillin-loaded PP meshes *Staphylococcus Aureus* (a) and *E. Coli* (b).

To evaluate the evolution of the antibacterial activity with the plasma treatment, the inhibition areas tested for *Staphylococcus Aureus* and *Escherichia Coli* for corona plasma-treated PP meshes loaded with ampicillin are respectively presented in Figure 98 and Figure 99. It has been verified using control samples that there is no inhibition area for untreated and plasma-treated PP meshes without ampicillin. The values presented are the average of at least 3 replicates. It has been verified using control samples that there is no inhibition area for untreated and plasma-treated PP meshes without ampicillin.

Untreated PP mesh presents an inhibition area of $45.03 \pm 8.29 \text{ mm}^2$. Even if at short corona plasma treatment times (0.35 s and 1.75 s) there seems to be a decrease of the inhibition area with respect to the untreated PP mesh with ampicillin, there is not statistical significant difference between these three samples, confirming that antibacterial activity has been preserved after corona plasma treatment.

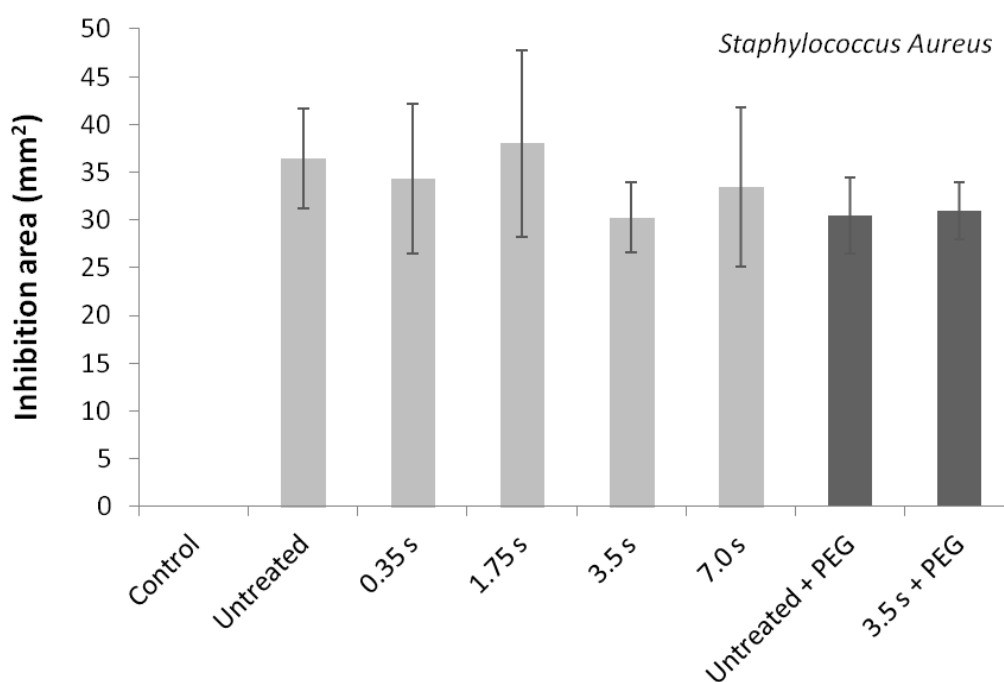


Figure 98: Inhibition areas for corona plasma-treated PP meshes loaded with ampicillin, tested for *Staphylococcus Aureus*. Influence of plasma treatment time and subsequent plasma polymerization.

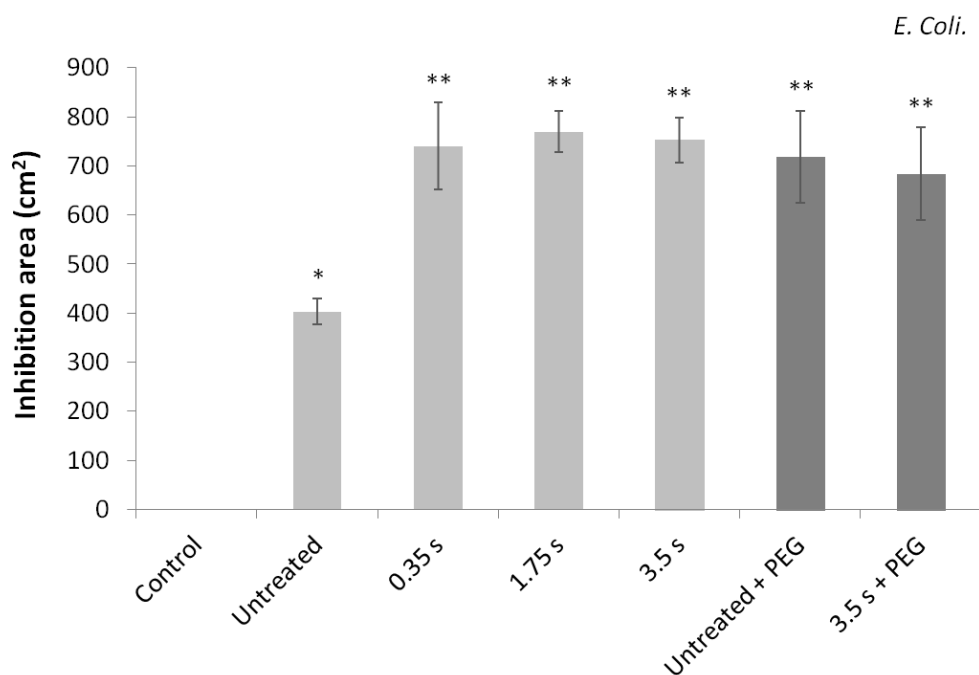


Figure 99: Inhibition areas for corona plasma-treated PP meshes loaded with ampicillin, tested for *Escherichia Coli*. Influence of plasma treatment time and subsequent plasma polymerization.

However, antibacterial activity of the ampicillin-loaded PP meshes tested for *E. Coli* shows an increase of the inhibition area for the corona plasma-treated PP meshes with respect to the untreated mesh, from $402.6 \pm 26.4 \text{ mm}^2$ for untreated mesh to $752.4 \pm 45.4 \text{ mm}^2$ for 3.5 s corona plasma treatment. This behavior can be related with the increased loading of ampicillin of the PP meshes obtained after corona plasma treatment. Including after PEG-based plasma polymerization of the corona-plasma treated PP meshes, this increased activity against *E. Coli* is conserved. Even if ampicillin has a broad spectrum of activity and is able to penetrate gram-positive and some gram-negative bacteria, the higher resistance of *Staphylococcus Aureus* against ampicillin could be explained that no difference has been recorded between untreated and corona plasma-treated PP meshes.

Low pressure plasma

Antibacterial activity has only been tested for *Staphylococcus Aureus* for low-pressure plasma-treated PP meshes loaded with ampicillin, and results are presented in Figure 100, where the evolution of the inhibition areas have been studied as a function of the plasma treatment time and the gas flow (air) inside the chamber during the plasma treatment.

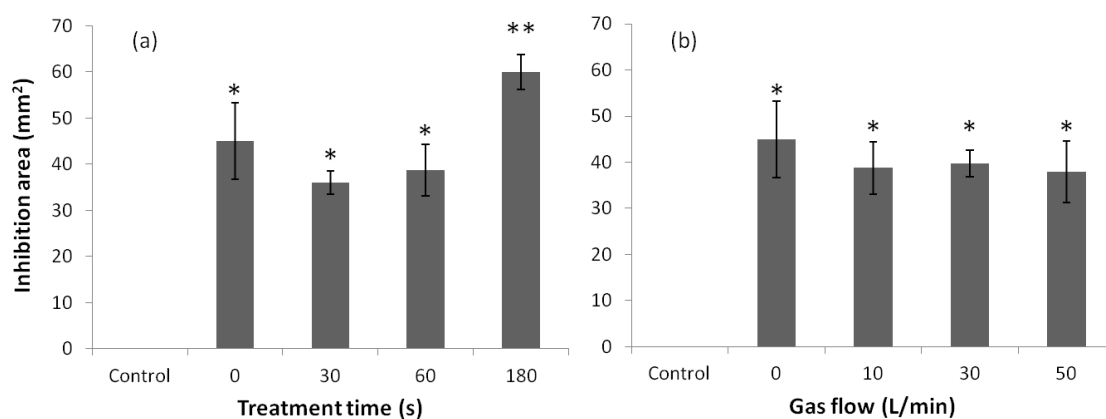


Figure 100: Inhibition areas for low pressure plasma-treated PP meshes loaded with ampicillin, tested for *Staphylococcus Aureus*. Influence of plasma treatment time (a) and gas flow in the reactor (b).

For low pressure plasma treatment, it has been checked that the gas flow in the reactor during plasma treatment does not affect the antibacterial activity against *Staphylococcus Aureus* (Figure 100b). The same trend is observed with the plasma treatment times, with only one significant difference observed for the longest plasma treatment time probed corresponding to 180 s (Figure 100a), since the plasma-treated mesh present a bigger inhibition area with respect to the other ones.

As determined by bacterial assays, the biological activity of the antibiotic against *E.Coli* and *Staphylococcus Aureus* was conserved after the different plasma treatments performed on the surgical PP meshes, and it has even been improved against *E.Coli* with corona-plasma treated PP meshes.

4.2.8. Influence of plasma treatment on cell adhesion

Cell adhesion plays a role in tissue and organ formation, in the generation of traction for the migration of cells, and it also important in determining the biocompatibility of synthetic implant materials. For example, the adhesion of microbial cells to surfaces is believed to be critical step in the pathogenesis of device-centered infections (Lamba, 1998) and designing materials with controlled surface properties is a key element in basic and biomedicine applied research (Antonini, 2014).

One of the aims of the present work is designing materials with controlled surface properties that are fundamentals in basic and biomedicine applied research, mostly using surgical mesh aimed for implants. In this respect, the surface chemistry and topography are the two major elements found to affect the cell adhesion to the biomaterial surface (Sardella, 2008). A lot of studies are done to separate the relative importance of these two factors with the help of pre formed structures to check the intrinsic effects of surface topography and the presence of a well defined chemistry. It was demonstrated that the surface roughness induces beneficial effects on cell proliferation (Pistillo, 2009). As for the chemistry, it is known that it influences the hydrophilic/hydrophobic character of the substrate. It is generally assumed that hydrophilic surfaces stimulate cell adhesion (Altankov, 2000; Antonini, 2014). Therefore, the study of the cell adhesion on the plasma-modified surgical PP meshes is necessary with views on the use of such meshes as implants.

The following preliminary results have been performed by the research group “Grup de Recerca en Cirurgia General – Vall d’Hebron Institut de Recerca” through an ongoing collaboration. Therefore, the following section does not present the results exhaustively, but only the main effects are shown as an indication of the performance of the materials developed.

Initially, THP1 cells were seeded on the sterilized (Gamma radiation, 25KGy) PP materials with corona plasma treatment, with or without ampicillin loading, and after low pressure plasma polymerization treatments. Cell concentration and viability of the cell suspension were determined at different times (1, 2, 3, 4, 7 days). It has been

observed that cell morphology is not altered during incubation (confocal microscopy). In general, cells grow on all the materials studied and cell viability is maintained in all the meshes studied, so the plasma treated materials are non toxic for the cells.

To evaluate cell adhesion on the PP fibres, 3T3 rat fibroblasts were seeded onto the sterilized PP meshes with the different treatments. After culturing for 5 days, staining was performed with Violet crystal and the cells were imaged (Figure 101).

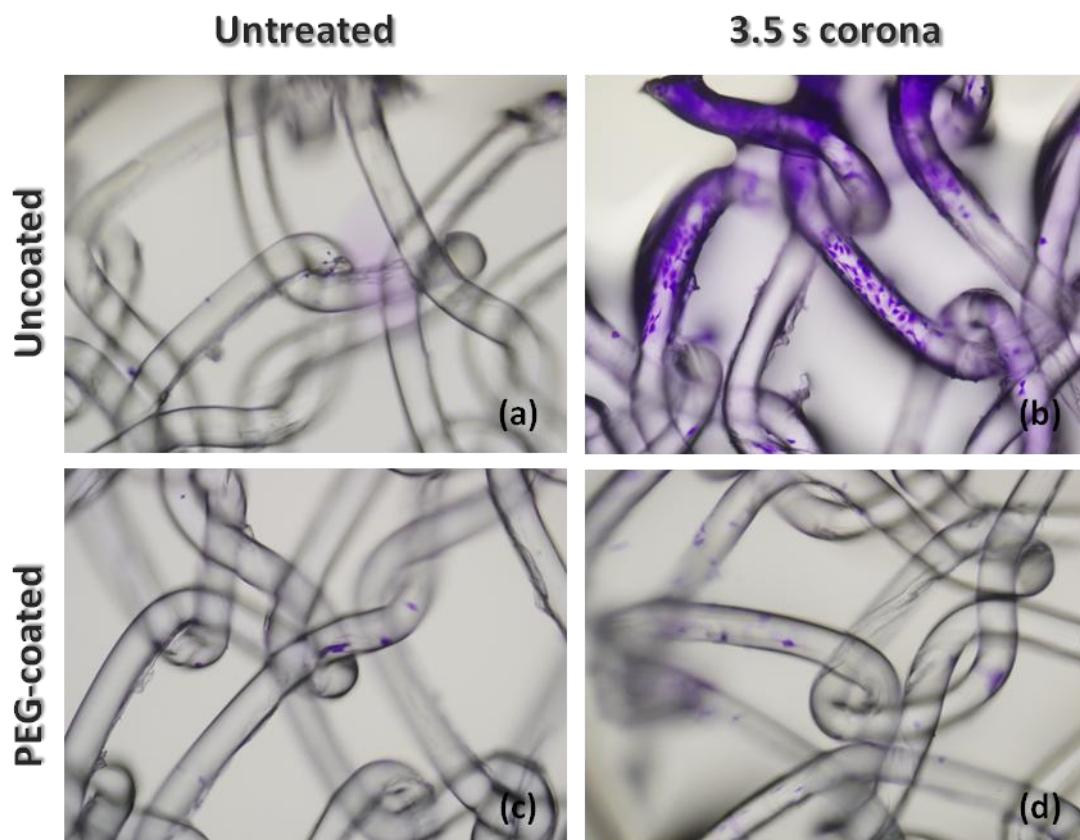


Figure 101: Cell adhesion to the PP fibres for untreated (a) and corona plasma treated for 3.5 s (b) meshes previously loaded with ampicillin. PEG-coating of the respective meshes (c) (d).

While untreated PP fibers present a low cell adhesion (Figure 101a), corona plasma treatment of the PP mesh shows high fibroblast adhesion to the fibres (Figure 101b), which can be attributed both to the improved wettability and to the higher roughness of the fibre surface. Figure 101c and Figure 101d show the adhesion of fibroblasts to the PEG-plasma coated meshes, either untreated or 3.5 s corona plasma-treated PP meshes and loaded with ampicillin. As shown in the images, the plasma coating of the

PP fibres with a PEG-like biocompatible thin film turns the cell adhesion back to the original level observed with the untreated mesh.

Thus, it has been shown that the surface chemistry and topography have significant effects on the cell biological functions, such as adhesion and proliferation, as observed in previous works (Keselowsky, 2003; Keselowsky, 2004). Besides, it has been demonstrated that plasma polymerization of a PEG-like film on the PP meshes can be a technique a means to obtain fibre surfaces with controlled functionalities able to regulate cell adhesion.

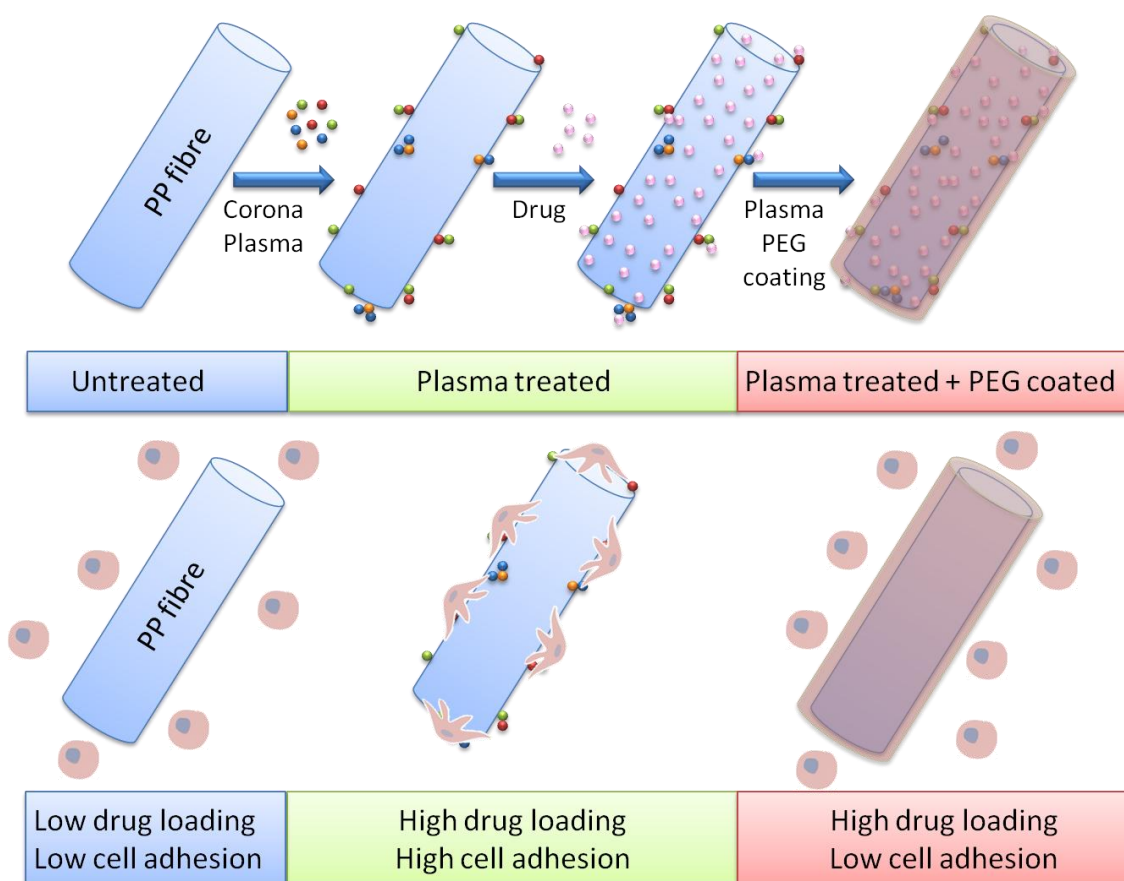


Figure 102: Effects of both (non- and polymerizing) plasma treatments on the antibiotic loading and the cell adhesion on the plasma-modified PP meshes.

As shown in the previous section, this PEG coating does not affect the ampicillin loading and release from the PP fibres, and plasma-treated PP meshes still show an improved release to the isotonic liquid media respect to the untreated PP mesh.

Moreover, cultures with *Staphylococcus Aureus* and *Escherichia Coli* confirmed that the antibiotic activity was preserved, since the inhibition areas presented by the untreated and corona plasma-treated PP meshes coated by plasma polymerization do not show statistical significant differences respected to the uncoated PP meshes.

Thus, the requirement of the subsequent PEG-like coating by plasma polymerization is completely justified since it does not affect the improved properties conferred by the first plasma treatment, and leads to obtaining a finished PP mesh those cell adhesion is low enough to allow its use as an implant avoiding cell proliferation on the textile material. The importance of both kinds of plasma treatments (non- and polymerizing) is summarized schematically in Figure 102.

Thus, both kinds of plasmas, non- and polymerizing plasma treatments, are justified in the design of the finished product. The first plasma process improves the loading of the antibiotic in the PP mesh through surface functionalization and etching, while the second one allows maintaining a low cell adhesion to the PP fibres through deposition of a nanometric antifouling PEG-like layer.

REFERENCES

- E. Adams, D. Coosmans, J. Smeyers-Verbeke, D. L. Massart, Nonlinear mixed effects models for the evaluation of dissolution profiles, *Int. J. Pharm.*, **2002**, 240, 37.
- G. Altankov, V. Thom, T. Groth, K. Jankova, G. Jonsson, M. Ulbricht, Modulating the biocompatibility of polymer surfaces with poly(ethylene glycol): Effect of fibronectin, *J. Biomed. Mater. Res.*, 52, **2000**, 219.
- V. Antonini, S. Torrenco; L. Marocchi, L. Minati, M. Dalla Serra, G. Bao, G. Speranza, Combinatorial plasma polymerization approach to produce thin films for testing cell proliferation, *Colloids Surface B*, 113, **2014**, 320.
- J. C. Berg, *Wettability*. M. Dekker Inc., New York, USA, **1993**.
- N. V. Bhat, D. J. Upadhyay, R. R. Deshmukh, S. K. Gupta, Investigation of plasma-induced photochemical reaction on a polypropylene surface, *J. Phys. Chem. B*, **2003**, 107, 4550.
- G. Borcia, C. A. Anderson, N. M. D. Brown, The surface oxidation of selected polymers using an atmospheric pressure air dielectric barrier discharge. Part II, *Appl. Surf. Sci.*, **2004**, 225, 186.
- R. D. Boyd, A. M. Kenwright, J. P. S. Badyal, D. Briggs, Atmospheric nonequilibrium plasma treatment of biaxially oriented polypropylene, *Macromolecules*, **1997**, 30, 5429.
- C. Canal, R. Molina, E. Bertran, P. Erra, *Wettability, ageing and recovery process of plasma treated polyamide 6*, *J. Adhes. Sci. Technol.*, **2004**, 18, 1077.
- C. Canal, F. Gaboriau, R. Molina, P. Erra, A. Ricard, Role of the active species of plasmas involved in the modification of textile materials, *Plasma Process. Polym.*, **2007a**, 4, 445.
- C. Canal, P. Erra, R. Molina, E. Bertran, Regulation of surface hydrophilicity of plasma treated wool fabrics, *Text. Res. J.*, **2007b**, 77 (8), 559.

- C. Canal, R. Molina, E. Bertran, P. Erra, Polysiloxane softener coatings on plasma-treated wool: Study of the surface interactions, *Macromol. Mater. Eng.*, **2007c**, 292, 817.
- C. Canal, R. Molina, E. Bertran, A. Navarro, P. Erra, Effects of low temperature plasma on wool and wool/nylon blend dyed fabrics, *Fiber. Polym.*, **2008**, 9 (3), 293.
- C. Choi, K. O. Choi, D. Jung, D. W. Moon, T. G. Lee, Surface characterization of plasma-polymerized polyethylene glycol thin film modified by plasma treatment, *Surf. Interface Anal.*, **2013a**, 45, 220.
- C. Choi, I. Hwang, Y.-L. Cho, S. Y. Han, D. H. Jo, D. Jung, D. W. Moon, E. J. Kim, C. S. Jeon, J. H. Kim, T. D. Chung, T. G. Lee, Fabrication and characterization of plasma-polymerized poly(ethylene glycol) film with superior biocompatibility, *ACS Appl. Mater. Interfaces*, **2013b**, 5, 697.
- P. Costa, J. M. Sousa, Modeling and comparison of dissolution profiles, *Eur. J. Pharm. Sci.*, **2001a**, 13, 123.
- P. Costa, J. M. Sousa, Influence of dissolution medium agitation on release profiles of sustained-release tablets, *Drug Dev. Ind. Pharm.*, **2001b**, 27, 811.
- U. Cvelbar, N. Krstulović, S. Milošević, M. Mozetič, Inductively coupled RF oxygen plasma characterization by optical emission spectroscopy, *Vacuum*, **2008**, 82, 224.
- Z. Elkoshi, On the variability of dissolution data, *Pharm. Res.*, **1997**, 14, 1355.
- J. Fresnais, J. P. Chapel, F. Poncin-Epaillard, Synthesis of transparent superhydrophobic polyethylene surfaces, *Surf. Coat. Tech.*, **2006**, 200, 5296.
- J. Friedrich, *The plasma chemistry of polymer surfaces: Advanced techniques for surface design*, Wiley-VCH Verlag & Co., Germany, **2012**.
- M. Gibaldi, S. Feldman, Establishment of sink conditions in dissolution rate determinations. Theoretical considerations and application to nondisintegrating dosage forms, *J. Pharm. Sci.*, **1967**, 56, 1238.

- J. M. Goddard, J. H. Hotchkiss, Polymer surface modification for the attachment of bioactive compounds, *Prog. Polym. Sci.*, **2007**, 32, 698.
- A. Goessl, M. D. Garrison, J. B. Lhoest, A. S. Hoffman, Plasma lithography - Thin-film patterning of polymeric biomaterials by RF plasma polymerization I: Surface preparation and analysis, *J. Biomater. Sci. Polym.*, **2001a**, 12, 721.
- A. Goessl, S. L. Golledge, A. S. Hoffman, Plasma lithography - Thin-film patterning of polymers by RF plasma polymerization II: Study of differential binding using adsorption probes, *J. Biomater. Sci. Polym.*, **2001b**, 12, 739.
- J. A. Goldsmith, N. Randall, S. D. Ross, On methods of expressing dissolution rate data, *J. Pharm. Pharmacol.*, **1978**, 30, 347.
- N. Gomathi, S. Neogi, Surface modification of polypropylene using argon plasma: Statistical optimization of the process variables, *Appl. Surf. Sci.*, **2009**, 255, 7590.
- T. Higuchi, Rate of release of medicaments from ointment bases containing drugs in suspension, *J. Pharm. Sci.*, **1961**, 50, 874.
- T. Higuchi, Mechanism of sustained action medication theoretical analysis of rate of release of solid drugs dispersed in solid matrices, *J. Pharm. Sci.*, **1963**, 52, 1145.
- A. W. Hixon, J. H. Crowell, Dependence of reaction velocity upon surface and agitation (I) theoretical consideration, *Ind. Eng. Chem.*, **1931**, 23, 923.
- B. G. Keselowsky, D. M. Collard, A. J. Garcia, Surface chemistry modulates fibronectin conformation and directs integrin binding and specificity to control cell adhesion, *J. Biomed. Mater. Res.*, **2003**, 66A, 247.
- B. G. Keselowsky, D. M. Collard, A. J. Garcia, Surface chemistry modulates focal adhesion composition and signaling through changes in integrin binding, *Biomaterials*, **2004**, 25, 5947.
- L. S. Koester, G. G. Ortega, P. Mayorga, V. L. Bassani, Mathematical evaluation of in vitro release profiles of hydroxypropylmethylcellulose matrix tablets containing carbamazepine associated to β -cyclodextrin, *Eur. J. Pharm.*, **2004**, 58, 177.

R. W. Korsmeyer, S. R. Lustig, N. A. Peppas, Solute and penetrant diffusion in swellable polymers. I. Mathematical modeling, *J. Polym. Sci. Polym. Phys.*, **1986a**, 24, 395.

R. W. Korsmeyer, E. von Meerwall, N. A. Peppas, Solute and penetrant diffusion in swellable polymers. II. Verification of theoretical models, *J. Polym. Sci. Polym. Phys.*, **1986b**, 24, 409.

K. Kosmidis, E. Rinaki, P. Argyrakis, P. Macheras, Analysis of Case II drug transport with radial and axial release from cylinders, *Int. J. Pharm*, **2003a**, 254, 183.

K. Kosmidis, P. Argyrakis, P. Macheras, A reappraisal of drug release laws using Monte Carlo simulations: the prevalence of the Weibull function, *Pharm. Res.*, **2003b**, 988.

K. Kosmidis, P. Argyrakis, P. Macheras, Fractal kinetics in drug release from finite fractal matrices, *J. Chem. Phys.*, **2003c**, 119, 6373.

H. Krump, M. Simor, I. Hudec, M Jasso, A. S. Luyt, Adhesion strength study between plasma treated polyester fibers and a rubber matrix, *Appl. Surf. Sci.*, **2005**, 240, 268.

N. M. K. Lamba, Cell-synthetic surface interaction in: *Frontiers in tissue engineering*, C. W. Patrick Jr. et al. Eds, Pergamon, Houston, Texas, USA, **1998**.

F. Langenbucker, Linearization of dissolution rate curves by the Weibull distribution, *J. Pharm. Pharmacol.* **1972**, 24, 979.

P. Lansky, M. Weiss, Classification of dissolution profiles in terms of fractional dissolution rate and a novel measure of heterogeneity, *J. Pharm. Sci.*, **2003**, 92, 1632.

P. Macheras, A. Dokoumetzides, On the heterogeneity of drug dissolution rate and release, *Pharm. Res.*, **2000**, 17, 108.

N. Médard, J.-C. Soutif, F. Poncin-Epaillard, Characterization of CO₂ plasma-treated polyethylene surface bearing carboxylic groups, *Surf. Coat. Tech.*, **2002**, 160, 197.

D. J. Menzies, A. Nelson, H.-H. Shen, K. M. McLean, J. S. Forsythe, T. Gengenbach, C. Fong, B. W. Muir, An X-ray and neutron reflectometry study of 'PEG-like' plasma polymer films, *J. R. Soc. Interface*, **2011**.

- R. Molina, P. Jovancic, F. Comelles, E. Bertran, P. Erra, Shrink-resistance and wetting properties of keratin fibres treated by glow discharge, *J. Adhes. Sci. Technol.*, **2002**, 16, 1469.
- R. Molina, P. Jovancic, D. Jovic, E. Bertran, P. Erra, Surface characterization of keratin fibres treated by water vapour plasma, *Surf. Interface Anal.*, **2003**, 35, 128.
- R. Morent, N. De Geyter, J. Verschuren, K. De Clerck, P. Kiekens, C. Leys, Non-thermal plasma treatment of textiles, *Surf. Coat. Tech.*, **2008**, 202, 3427.
- M. Morra, E. Occhiello, F. Garbassi, Contact angle hysteresis on oxygen plasma treated polypropylene surfaces, *J. Colloid Interface Sci.*, **1989**, 132, 504.
- J. Nakamatsu, L. F. Delgado-Aparicio, R. Da Silva, F. Soberón, Ageing of plasma-treated poly(tetrafluoroethylene) surfaces, *J. Adhes. Sci. Technol.*, **1999**, 13, 753.
- I. Novák, Š. Florián, Effect of aging on adhesion behavior of discharge plasma-treated biaxially oriented polypropylene, *J. Mater. Sci. Lett.*, **1999**, 18, 1055.
- I. Novák, Š. Florián, Investigation of hydrophilicity of polyethylene modified by electric discharge in the course of aging, *J. Mater. Sci. Lett.*, **2001**, 20, 1289.
- K. N.Pandiyaraj, V. Selvarajan, R. R. Deshmukh, C. Gao, Modification of surface properties of polypropylene (PP) film using DC glow discharge air plasma, *Appl. Surf. Sci.*, **2009**, 255, 3965.
- V. Papadopoulou, K. Kosmidis, M. Vlachou, P. Macheras, On the use of the Weibull function for the discernment of drug release mechanisms, *Int. J. Pharm.*, **2006**, 309, 44.
- N. A. Peppas, Mathematical modeling of diffusion processes in drug delivery polymeric systems. In: "Controlled drug bioavailability", V. F. Smolen, L. Ball (Eds.), Vol. 1, John Wiley & Sons, New York, pp. 203–237, **1984**.
- N. A. Peppas, Analysis of Fickian and non-Fickian drug release from polymers, *Pharm. Acta Helv.*, **1985**, 60, 110.

B. R. Pistillo, R. Pristina, E. Sardella, S. Lovascio, P. Favia, M. Nardulli, R. d'Agostino, Plasma processes combined with colloidal lithography to produce nanostructured surfaces for cell-adhesion, *Plasma Proc. Polym.*, **2009**, 6, S61.

F. Poncin-Epaillard, J. C. Brosse, T. Falher, Cold plasma treatment: Surface or bulk modification of polymer films?, *Macromolecules*, **1997**, 30, 4415.

B. D. Ratner, The catastrophe revisited: Blood compatibility in the 21st century, *Biomaterials*, **2007**, 28, 5144.

P. L. Ritger, N. A. Peppas, A simple equation for description of solute release. I. Fickian and non-Fickian release from non-swelling devices in the form of slabs, spheres, cylinders or discs, *J. Control. Release*, **1987**, 5, 23.

E. Sardella, L. De Tomaso, R. Gristina, G. S. Senesi, H. Agheli, D. S. Sutherland, R. d'Agostino, P. Favia, Nanostructured cell-adhesive and cell-repulsive plasma deposited coatings: Chemical and topographical effects on keratinocyte adhesion, *Plasma Proc. Polym.*, **2008**, 5, 540.

R. A. Siegel, M. J. Rathbone, Controlled release mechanisms. In: "Fundamentals and applications of controlled release drug delivery, *Advances in delivery science and technology*", J. Siepmann et al., Eds., Controlled Release Society, **2012**.

J. Siepmann, N. A. Peppas, Modeling of drug release from delivery systems based on hydroxypropyl methylcellulose, *Adv. Drug Deliv. Rev.*, **2001**, 48, 139.

L. Van Vooren, G. Krikilion, J. Rosier, B. De Spiegeleer, A novel bending point criterion for dissolution profile interpretation, *Drug Dev. Ind. Pharm.*, **2001**, 27, 855.

M. J. S. Varma, A. M. Kaushal, S. Garg, Influence of microenvironmental pH on the gel layer behavior and release of basic drug from various hydrophilic matrices, *J. Control. Release*, **2005**, 103, 499.

J. G. Wagner, Interpretation of percent dissolved-time plots derived from in vitro testing of conventional tablets and capsules, *J. Pharm. Sci.*, **1969**, 58, 1253.

C. Wang, X. He, Polypropylene surface modification model in atmospheric pressure dielectric barrier discharge, *Surf. Coat. Technol.*, **2006**, 201, 3377.

Q. Wei, Y. Wang, X. Wang, F. Huang S. Yang, Surface nanostructure evolution of functionalized polypropylene fibers, *J. Appl. Polym. Sci.*, **2007**, 106, 1243.

D. F. Williams, On the mechanisms of biocompatibility, *Biomaterials*, **2008**, 29, 2941.

CONCLUSIONS

5. CONCLUSIONS

General conclusions

Plasma treatments (either non- or polymerizing) can be considered as a relevant tool to confer an added value to textile materials for biomedical applications, as has been shown in this PhD. Thesis and is summarized in the following general conclusions:

- Atmospheric and low-pressure plasma treatments with air of polymer fibres (PA66 and PP) lead to the modification of the surface chemistry and topography due to combined effects of surface functionalization and etching processes.
- Functionalization of the polymer fibre surface mainly takes place through the introduction of O-containing groups, mostly C-O and C=O groups, which is related to an improved wettability of the textile material and provides more bonding sites for the attachment of an active molecule.
- The modification of the surface topography of the polymer fibre results generally in the increase of the surface roughness, with the observation of distinct patterns as function of the kind of plasma treatment employed.
- Since atmospheric and low-pressure plasmas present different energy transfers, modification of the topography and the surface chemistry greatly depends on the kind of plasma used for the treatment of the fibres, and the selection of one of them rests upon the compromise between the conferred properties, the improvement of specific properties and the application for which the textile material is aimed for.
- The loading of an active molecule on the plasma-treated fibres varies as consequence of the modification of the physical and chemical properties of the fibre surface. The polarity of the desired active principle conditions the increase or the decrease of the loading of such molecule on the polymer fibre.
- Both atmospheric and low-pressure plasma treatments, in optimized conditions, lead to a moderate modification of the release amount of the active

molecules from the textile materials, without affecting the mechanisms of the release kinetics.

- Plasma polymerization of the drug-loaded fibres with a nanometric PEG-like coating allows switching down the increased cell adhesion observed with plasma-treated textile materials.
- Combination of functionalization of the polymeric fibres by plasma treatment with plasma polymerization of biocompatible coating allows designing textile-based biomaterials with improved properties, such as high drug loading and low cell adhesion.

These general conclusions can be divided into two parts according to the textile material used and the application for which they are aimed for.

Polyamide as textile support for topical applications

- Untreated IF-PA66 presents a hydrophobic behavior in nature. The washing of the IF-PA66 fabrics greatly improves the wetting properties of the PA66 fabrics, with a decrease of 34.0 ° observed in static contact angle measurements. Corona plasma treatment also achieves an improvement of the hydrophilic behavior of the IF-PA66, with a decrease of 21.8 ° of the contact angle with short plasma treatment of 3.5 s. Moreover, when plasma treatment is combined with a previous washing of the polyamide fabrics, synergy is observed between both treatments, producing a further improvement of the wettability of PA66 fibres.
- This improvement of wettability has been related with the modification of the surface chemistry and the introduction of new oxygenated groups grafted on the surface with both types of plasmas, with the most significant increase registered being in C=O groups, reflecting the functionalization process of PA66 fibers by carbonyl groups.

- The presence of silicone-based finishing agents on the surface of the IF-PA66 leads to significant differences between both kinds of plasma treatments. While low-pressure plasma treatment of IF-PA66 causes surface etching, removing the PDMS present in the fibre surface, corona plasma treatment of IF-PA66 promotes the thermomigration of these Si-based compounds from the bulk to the surface of the PA66 fibre, mainly due to higher local surface temperatures reached by the sparks of the corona plasma. Anyway, it has been shown by XPS for both types of plasmas that PDMS were etched by the plasma treatment, although they were not completely removed from the fiber surface.
- Corona plasma treatment improved homogeneity of the surface topography by removal of the aggregates of the silicone-finishes present on untreated IF-PA66 fibers. While no relevant topographic modifications at short plasma treatment times were detected in the W-PA66 fabrics, for both kinds of samples (IF-PA66 and W-PA66), at the longest corona plasma exposure studied (3.5 s plasma treatment), some melt polymer and localized creasing of the fibres can be randomly observed on some isolate regions of the surface due to the sparks of the corona plasma. Low pressure plasma treatment did not produce remarkable changes on the topography of PA66 which, after any of the treatments evaluated under different gas flow rate conditions. Regarding the cleaning of the PDMS, it can be also underlined that the increase of gas flow or treatment time allows a more effective elimination of these products.
- Corona plasma treatment of the IF-PA66 fabrics leads to an increase of the ketoprofen loading in the fibres, as well as an increase of the ketoprofen released.
- Atmospheric plasma treatment leads to an increase of 10% of the ketoprofen release percentage after 24 h, which can be attributed to a better wettability of the textile material that allows improved exchange with the release media.
- For both caffeine-loaded IF-PA66 and W-PA66 materials, corona plasma-treated samples show higher release percentages, with no significant differences between the two different corona plasma treatment times evaluated. In all cases, burst release is recorded, up to 70% and 83% in the first hour for untreated and plasma-treated materials, respectively. This stage is

followed by a slower release up to 8 hours, without reaching the stationary stage in any of the samples, and thus, with potential for longer release.

- Low pressure plasma treatment of IF-PA66 shows an increase of the caffeine release with the increase of gas flow. This behavior has to be related with the improvement of the wettability observed between plasma treated samples with increasing gas flow.
- In general, plasma treatment of PA66 fabrics reduces the loading of caffeine and the other methylxantines, which may be related to the low polarity of the active principles and the increased electronegativity of the plasma treated PA66 surface.
- The fundamental study with methylxantines showed that the polar surface of the methylxantines determines the increase in release percentage due to the plasma treatment. It can be observed that when the molecule has higher polar surface area, a much higher percentage is released after the plasma treatment with respect to the untreated sample due to the modified polarity of the fiber surface.
- The implementation of the drug loading process directly to the industrial chain employing finished fabrics such as IF-PA66 can be considered viable for the loading of cosmetic active principles such as caffeine.

Polypropylene as textile support for implantable drug delivery systems

- Corona plasma and low pressure plasma have been used to modify PP meshes. Both plasma treatments can greatly change the surface chemistry of the PP fibre, as well as on its topographic morphology in the case of corona plasma treatment. The polar functional groups generated due to plasma treatment on the surface of polypropylene lead to increased wettability.
- For both types of plasma treatments, analysis of XPS spectra of plasma-treated PP fibres with air revealed an increase of O atoms and O-based functional groups. However, while corona plasma treatment carries out the

functionalization of the PP surface by grafting mainly oxygen atoms by covalent bonding with carbon atom of the PP fibres, low-pressure plasma treatment also increases the attachment of N atoms with the macromolecular chain of PP and achieves a functionalization with O and N atoms. Low pressure plasma treatment for 60 s (100 W, 30 L/min, 300 mT) maximized the increase in C-O, C-N groups on the PP surface to 9.0%.

- While untreated PP fibres present a smooth surface, the surface roughness of the polymer is clearly enhanced with corona plasma treatment times of 1.75 seconds and longer. The surface topography of the corona-plasma treated PP mesh presents a pattern of peaks and valleys, resulting from the combined effect of different mechanisms such as etching processes, photo oxidation and thermal oxidation that are taking place preferentially on the amorphous regions of the polymer. Low-pressure plasma treatment is milder and does not produce significant modifications on the surface topography of the PP fibres.
- The chemical and morphological changes made on surface of PP fibres lead to increase the hydrophilic properties and the apparent surface of the PP fibre, and allowing a better availability of bonding sites for subsequent attachment of molecules.
- Untreated PP presents a low impregnation percentage of 20.8%. With the corona plasma at increasing treatment times, impregnation is progressively improved up to 59.5% for a plasma treatment time of 3.5 s, which corresponds to a 2.9 times higher ampicillin quantity loaded in the PP fibres than in the untreated ones. Low-pressure plasma treatment also leads to an increase of the ampicillin impregnation percentage of the PP meshes with treatment time up to 60 s, condition for which ampicillin impregnation percentage is 3.3 times higher than those of untreated PP meshes.
- Both untreated and corona plasma-treated PP meshes present a burst ampicillin release in the first minutes of the assay. Anyhow, the corona plasma treatment improves around 10% the ampicillin release from the PP fibres, reaching 84.6% for 3.5 s corona plasma-treated PP meshes, probably due to the improved contact with the receptor media due to 2 factors: a higher specific surface area and a better wettability. Thus, corona plasma treatment has an

influence on the ampicillin release amount although it does not influence the release kinetics of the ampicillin with time, nor slows down the burst release of ampicillin presented by the untreated mesh. Low pressure plasma treatment also leads to a significant increase of the ampicillin release with the different conditions studied, up to an increase of + 15.8% with gas flow rates of 30 L/min with respect to the untreated PP meshes.

- Low-pressure plasma polymerization of the PP meshes with Tegradyne leads to very high wettabilities, and also a highly modified surface topography with complex patterns combining the different etching effects observed both for the corona plasma treatment and for the plasma polymerization treatment.
- The PEG-coated PP meshes display a burst release of ampicillin, combined with a decrease of the percentage released which may indicate that the coating created by the deposition of PEG by plasma polymerization retains a part of the ampicillin, like a membrane, or that a part of loaded-ampicillin has been removed during the plasma polymerization process. Further research needs to be done in order to increase the thickness of the layer and achieve slowing down the release of the antibiotic from the PP fibres.
- As determined by bacterial assays, the biological activity of the antibiotic loaded in the surgical PP mesh was conserved after the different plasma treatments performed on the fabrics.
- The increased surface energy of plasma treated PP leads to high cellular adhesion which may not be adequate for in vivo use. The plasma polymerization treatment performed has been shown to produce low cell adhesive PP surfaces.
- Thus, the combination of surface functionalization with subsequent plasma polymerization can be a means of obtaining PP meshes with improved antibiotic loading in the PP mesh, while maintaining low cell adhesion to the surface of PP fibres.

6. FURTHER INVESTIGATION LINES

In view of the results of this work, some recommendations are proposed for possible future research:

Polyamide as textile support for topical application

- The studies on the modification of the fibre surface of the PA66 fabrics and its relevance on the loading of active molecules and their posterior release from such fibres can be **extended by using other plasma gases or mixtures of gas**, even other plasma reactors, to evaluate the kind of functionalization and determine if further improved conditions for the attachment of active molecules can be achieved.
- Regarding the study of the release kinetics, the next step for the in vitro release experiments of the active principle from the PA66 fabrics could be the **introduction of a synthetic membrane or skin in the design the release experiment**, as a membrane between the fabric and the receptor isotonic liquid media.
- Deeper and applied studies on the evaluation of the influence of environmental effects of the PA66 fabrics and the active principle stability, degradation and release such as sweat, temperature, humidity, etc. could be one approach to broaden the research. In this way, it could be designed release studies of ketoprofen or caffeine on animals.

Polypropylene as textile for implantable drug delivery system

- As for the PA66 fabrics, study of the modification of the fibre surface of the surgical PP mesh and its relevance on the loading of an antibiotic and its release from such fibres could be **extended by using other gas for the plasma treatment or gas mixtures**, to evaluate the kind of functionalization and determine if further improved conditions for the attachment of the antibiotic can be found.

- Evaluation of other antibiotics, other plasma reactors or other biocompatible coatings to compare with the results obtained in this work can be one approach to enlarge the study.
- In this PhD. Thesis, the importance of the plasma polymerization of a PEG-like thin film on the PP fibres to maintain a low cell adhesion on the surface of the corona plasma-treated fibres has been demonstrated. However, working on the optimization of the plasma conditions of the plasma polymerization (type of plasma, power, time, flow, pressure...) to **obtain a polymerized film with desired thickness and permeability** for the path of the antibiotic, this coating could be also exploited in the modulation of the release kinetics to slow down the release of the antibiotic. Even if it has been described in other works that biocompatible coating of polymeric fibres can be obtained by chemical way to act as a membrane to retain active principles, if the implementation of plasma polymerization could be carried out, it will allow obtaining a final product achieved only by dry processes.
- **Slowing down the release kinetics remains the main challenge to be solved to contemplate further pre-clinical and clinical studies.** Release kinetics of the ampicillin on longer periods would have to be achieved to fulfill the specification of such polymeric surgical mesh regarding its role on the prevention and the contention of post-surgical infections and neusocomial diseases.
- Regarding the biological aspect, **complementary experiments regarding biological response and cell adhesion** would have to be performed respectively with other kinds of cells, to have a more complete overview.

PUBLICATIONS AND ACTIVITIES

7. PUBLICATIONS AND ACTIVITIES DERIVED FROM THE PHD. THESIS

7.1. Papers published in JCR Journals

AUTHORS: **C. Labay**, J. M. Canal, A. Navarro, C. Canal

TITLE: Corona plasma modification of polyamide 66 for the design of textile delivery systems for cosmetic therapy.

JOURNAL/BOOK REF.: Applied Surface Science (2013).

KEY: A

PUBLICATION DATE: *Under revision- Sent on January 2014.*

AREA OF KNOWLEDGE OF THE JOURNAL: Material Science, Coating and Films

Publication in the 25% higher impact factor in the area of expertise

IMPACT FACTOR: 2.112 (Q1)

AUTHORS: **C. Labay**, C. Canal, C. Rodríguez, G. Caballero, J. M. Canal

TITLE: Plasma surface functionalization and dyeing kinetics of PAN-PMMA copolymers.

JOURNAL/BOOK REF.: Applied Surface Science (2013) 283: 269–275.

KEY: A

PUBLICATION DATE: October, 2013.

AREA OF KNOWLEDGE OF THE JOURNAL: Material Science, Coating and Films

Publication in the 25% higher impact factor in the area of expertise

IMPACT FACTOR: 2.112 (Q1)

AUTHORS: **C. Labay**, J. M. Canal, C. Canal

TITLE: Relevance of surface modification of PA 6.6 fibers by air plasma treatment on the release of caffeine.

JOURNAL/BOOK REF.: Plasma Processes and Polymers (2012) 9:165-173.

KEY: A

PUBLICATION DATE: February, 2012

AREA OF KNOWLEDGE OF THE JOURNAL: Polymer Science and Technology

Publication in the 25% higher impact factor in the area of expertise

IMPACT FACTOR: 4.037 (Q1)

AUTHORS: **C. Labay**, C. Canal, M. J. García-Celma

TITLE: Influence of corona treatment on plasma PP and PA 6.6 on the release of a model drug.

JOURNAL/BOOK REF.: Plasma Chemistry and Plasma Processing (2010) 30:885-896.

POSITION IN THE AREA OF KNOWLEDGE: 26/126

KEY: A

AREA OF KNOWLEDGE OF THE JOURNAL: Engineering, Chemical

PUBLICATION DATE: October, 2010

Publication in the 25% higher impact factor in the area of expertise

IMPACT FACTOR: 2.039 (Q1)

AUTHORS: **C. Labay**, J. M. Canal, F. X. Gil, M. Modic, U. Cvelbar, M. Quiles, M. A. Arbos Via, C. Canal

TITLE: Modification of PP fibre surface by atmospheric and low-pressure plasma treatments for the design of an antibiotic-loaded surgical mesh.

PUBLICATION DATE: *In preparation.*

KEY: A

7.2. Communications in International Congresses

AUTHORS: **C. Labay**, J. M. Canal, M. Modic, U. Cvelbar, C. Canal

TITLE: Modification of PP surgical meshes by atmospheric plasma treatment for the loading and the release of ampicillin.

TYPE OF PARTICIPATION: Oral communication

CONGRESS: Workshop on Atmospheric Plasma Processes and Sources for Functional Coating on Biomaterial Surfaces.

PLACE: Bohinjka Bistrica (Slovenia)

DATE: January 22nd-23rd, 2014

AUTHORS: **C. Labay**, I. X. Mojica, C. Canal, C. Rodriguez, G. Caballero, J. M. Canal

TITLE: Corona plasma surface effects on dyeing kinetics of acrylic fibre under glass transition temperature.

TYPE OF PARTICIPATION: Plenary oral contribution – Inaugural conference

CONGRESS: 23rd Congress of the International Federation of Associations of Textile Chemists and Colourists

PLACE: Budapest (Hungary)

DATE: May 8th-10th, 2013

AUTHORS: C. Canal, **C. Labay**, A. Navarro, M. Modic, U. Cvelbar, M. P. Ginebra, J. M. Canal

TITLE: Plasmas in organic biomaterials: a case study of polypropylene meshes for soft tissue repair.

TYPE OF PARTICIPATION: Invited lecture

CONGRESS: 69th International Union for Vacuum Science, Technique and Applications Workshop - IUVESTA

PLACE: Cerklje na Gorenškem (Slovenia)

DATE: December 9th-12th, 2012

AUTHORS: **C. Labay**, J. M. Canal, C. Canal, A. Navarro

TITLE: Comparison of the effects of corona and low pressure plasma on the release of caffeine from PA66 filaments.

TYPE OF PARTICIPATION: Oral communication

CONGRESS: 51st Dornbirn Man-Made Fibers Congress

PLACE: Dornbirn (Austria)

DATE: September 19th-21st, 2012

AUTHORS: **C. Labay**, J. M. Canal, C. Canal

TITLE: Modification of textile fibers by plasma treatment for biomedical applications - Textile as drug delivery system.

TYPE OF PARTICIPATION: Oral communication

CONGRESS: 4th Summer School on Medicines

PLACE: Montreal, Quebec (Canada)

DATE: July 2nd-13th, 2012

AUTHORS: **C. Labay**, J. M. Canal, C. Canal

TITLE: Modification of the release properties of a cosmetic active principle from a knitted polyamide 66 fabric by low temperature plasma treatment.

TYPE OF PARTICIPATION: Poster

CONGRESS: 12th Mediterranean Congress of Chemical Engineering

PLACE: Barcelona (Spain)

DATE: November 15th-18th, 2011

AUTHORS: C. Canal, **C. Labay**, A. Navarro, J. M. Canal

TITLE: Opportunities of low temperature plasma for controlled drug delivery from polymer substrates.

TYPE OF PARTICIPATION: Invited lecture

CONFERENCE: 4th International Conference on Advanced Plasma Technologies

PLACE: Strunjan (Slovenia)

DATE: September 11th-12th, 2011

AUTHORS: **C. Labay**, J. M. Canal, C. Canal

TITLE: Modificación de las propiedades de liberación de un principio activo cosmético por tratamiento de plasma en tejidos de punto de poliamida 66.

TYPE OF PARTICIPATION: Oral communication

CONGRESS: 37th AEQCT Symposium (Spanish Association of Textile Chemists and Colorists)

PLACE: Barcelona (Spain)

DATE: April 6th-7th, 2011

AUTHORS: **C. Labay**, C. Canal, M. J. Garcia-Celma

TITLE: Low temperature plasma treatment of PA and PP for release of a model drug.

TYPE OF PARTICIPATION: Oral communication

CONFERENCE: 22nd International Congress IFATCC

PUBLICATION: Abstracts CD ISBN 9788896679005

PLACE: Stresa (Italy)

DATE: May 5th-7th, 2010

7.3. Scientific awards and honors

AUTHOR: C. Labay

TITLE: 24th Prize of the Spanish Association of Textile Chemists and Colorists for the "Best study in textile chemistry for textile applications in industry."

DATE OF RECEIPT: April 2011

7.4. Non-indexed JCR publications

AUTHORS: J. M. Canal, **C. Labay**, A. Navarro, C. Canal

TITLE: Comparison of the effects of corona and low pressure plasma on the release of caffeine from PA66 filaments.

JOURNAL/BOOK REF.: Chemical Fibers International (2012) 62(4):182.

TYPE OF PUBLICATION: Short communication

PUBLICATION DATE: December, 2012

ISSN: 0340-3343

AUTHORS: **C. Labay**, J. M. Canal, C. Canal

TITLE: Effects of air plasma in the release of caffeine from knitted fabrics PA 6.6.

JOURNAL/BOOK REF.: Revista Química Textil (2011) 210:14-28.

KEY: A

PUBLICATION DATE: March, 2011

7.5. Research stages

TYPE: Research stay as part of the doctoral thesis

CENTER: Plasma laboratory, Jožef Stefan Institute (IJS), Ljubljana, Slovenia

DURATION: From September 9th, 2012 to September 23rd, 2012

RESEARCH RESPONSIBLE: Uroš Cvelbar

APPENDIX

8. APPENDIX

8.1. List of abbreviations

AFM	Atomic Force Microscopy
CCD	Camera-Coupled Device
DDS	Drug Delivery System
FDA	Food and Drug Administration
FIB	Focus Ion Beam
HPLC	High-Pressure Liquid Chromatography
IF-PA66	Industrially-finished Polyamide 6.6
ISO	International Standard Organization
KP	Ketoprofen
LPP	Low Pressure Plasma
LSV	Liquid-Solid-Vapor
MB	Methylene Blue
MEDTECH	Medical Textiles
MD/CMD	Machine Direction (MD)/ Cross Machine Direction (CMD)
NSAID	Non-Steroidal Anti-Inflammatory Drug
OES	Optical Emission Spectroscopy
PA66	Polyamide 6.6
PBS	Phosphate Buffer Saline
PCL	Poly(ϵ -caprolactone)
PCM	Phase Change Materials
PEG	Polyethylene glycol
PES	Polyester
PDMS	Poly-dimethylsiloxanes
PLA	Poly(-lactic acid)
PP	Polypropylene
PTFE	Polytetrafluoroethylene
R&D	Research and Development
SEM	Scanning Electron Microscopy
UV	Ultra-Violet
XPS	X-Ray Photospectroscopy
W-PA66	Washed Polyamide 6.6

8.2. Index of figures

Figure 1: Proposed modulation of the drug release kinetics from synthetic fibers to an isotonic media using plasma treatment to modify chemical and topographical properties of the fibre surface previous to loading of active principles in the fibres.....	10
Figure 2: Textile materials and products include non-implantable materials (a), implantable materials (b) and healthcare and hygiene products (c).	26
Figure 3: Medical textiles industry trends from the EvaluateMedTech™ World Preview 2018 report.	27
Figure 4: Cross-section representation of skin layers.	37
Figure 5: Conceptual design of transdermal commercial delivery patches based on (a) Skin permeability control and (b) membrane control adapted from Siegel, 2012.	39
Figure 6: A schematic presentation of the normal anatomy of the abdominal wall (a), the mechanism of an abdominal wall defect (b) and the possibility of open (c) and laparoscopic (d) implantation of a surgical mesh. (Adapted from Engelsman, 2007)	44
Figure 7: Protrusion formation to an elevate intra-abdominal pressure in case of a midline abdominal wall defect.....	45
Figure 8: Multifilament PP meshes currently used in hernia repair.	47
Figure 9: Cross-section of abdominal wall with classification of surgical site of infection (Adapted from Horan, 1992) with positioning of the surgical mesh in case of and of open implantation (*) and laparoscopic abdominal repair (**).....	49
Figure 10: General polyamide polycondensation reaction.	53
Figure 11: Chemical structure of polyamide 6.6.....	53
Figure 12: Chemical structure of polypropylene in isotactic configuration.	55
Figure 13: Classification of plasmas in nature as a function of generation temperature and electron number density.	66
Figure 14: General classification of plasmas.	67
Figure 15: Scheme of a low-pressure plasma reactor.....	69
Figure 16: Scheme of an atmospheric plasma reactor: corona system of potential use in the textile industry.....	70
Figure 17: Scheme of plasma etching of materials from the polymer surface.	74
Figure 18: Activation step in the case of the polyethylene giving rise to alkyl radicals.....	75
Figure 19: Concept of specific functionalization and unspecific functionalization of a polymeric surface by plasma treatment.	76
Figure 20: Scheme of polymer surface functionalization by plasma processes using air as gas for plasma generation.	77
Figure 21: Scheme of plasma polymerization process.....	79
Figure 22: Structure of the PhD. Thesis.....	112
Figure 23: PA66 elastic-compressive knitted fabric (a) macroscopic image and (b) SEM image used as textile supports in this PhD. Thesis.	116

Figure 24: (a) PP mesh macroscopic image and (b) Scanning Electron Micrograph of the structure of the PP mesh.....	117
Figure 25: Chemical structure of ketoprofen.	118
Figure 26: Chemical structure of caffeine.	119
Figure 27: Chemical structure of pentoxifylline.	120
Figure 28: Chemical structure of theobromine.	120
Figure 29: Chemical structure of ampicillin sodium salt.	121
Figure 30: Experimental scheme followed for (a) ketoprofen loading of industrially-finished PA66 knitted fabrics for pharmaceutical topical applications, (b) for the study of the influence of plasma treatment and initial preparation of the PA66 fabrics on the loading and the release of methylxantines, and (c) for obtaining plasma-treated ampicillin-loaded PP meshes to study of the influence of the plasma on the PP meshes for the loading and the release of ampicillin from the PP fibers.	123
Figure 31: Storage of PP fabrics in a desiccator to avoid humidity absorption.	124
Figure 32: (a) Scheme of the corona plasma used to treat the textile samples. (b) Scheme of different reactive species present in the plasma generation zone.	125
Figure 33: Plasma generation with ambient air using an <i>Ahlbrandt FG-2</i> corona plasma equipment.	126
Figure 34: <i>Europlasma Junior Advanced PLC</i> low-pressure plasma equipment using with air as gas for plasma generation (a). Focus of the panel control screen (b) and the inside of the chamber (c).....	127
Figure 35: Picture of the low pressure plasma reactor used in this PhD. Thesis for the treatment of PA66 (a) and PP (b) fabrics with air as plasma generation gas.....	127
Figure 36: Standard pulsed-plasma equipment used for polymerization (a). Schematic cross-section of the reactor (b).	128
Figure 37: Tetraglyme molecule used as precursor for plasma polymerization.	129
Figure 38: Padding equipment used for homogenization of the active principle on the PA or PP sample after impregnation process.	132
Figure 39: Active principle release experiment.	134
Figure 40: (a) <i>Jeol JSM-5000/5610</i> SEM Field-Emission Scanning Electron Microscopy. (b) Au-coated PP mesh fabrics prior to SEM observation (UPC, Terrassa, Spain).....	138
Figure 41: Schematic functioning principle of an Atomic Force Microscope (a). Picture of the <i>Solver Pro NT-MDT</i> Atomic Force Microscope used in this work (IJS Center, Ljubljana, Slovenia) (b).....	140
Figure 42: PHI ESCA-5500 Multitechnique System (<i>Physical Electronics</i>) equipment (IJS Center, Ljubljana, Slovenia).	142
Figure 43: Schematic representation of the contact angle of a liquid drop on a solid surface.	144
Figure 44: <i>Krüss DSA100</i> goniometer (a) with detail of the sample support and the needle for deposition of the droplets (b).....	145
Figure 45: Schematic of the working principle of a double beam UV-visible spectrophotometer.	147
Figure 46: <i>Agilent 1100 series</i> HPLC equipment used in this PhD. Thesis.....	148
Figure 47: Antibacterial assays. (a) Preparation of the <i>Staphilococcus aureus</i> culture media. (b) Placement of treated textile materials. (c) Measurement of the inhibition areas.....	150
Figure 48: XPS general spectra of untreated IF-PA66 (a) and W-PA66 (b).....	166

Figure 49: XPS general spectra of 1.75 s corona plasma-treated (a) and 3.5 s corona plasma-treated IF-PA66 (b).....	166
Figure 50: XPS general spectra of 1.75 s corona plasma-treated (a) and 3.5 s corona plasma-treated W-PA66 (b).....	168
Figure 51: XPS general spectra of of untreated and low pressure plasma treated IF-PA66 for 5, 10 and 15 L/min as gas flow.	171
Figure 52: Deconvolution of C _{1s} peaks for untreated IF-PA66 sample (a) and plasma-treated PA66 under 5 (b), 10 (c) and 15 (d) L/min gas flow rate.	174
Figure 53: SEM micrographs of untreated IF-PA66 (a) and W-PA66 (b) fabrics.	175
Figure 54: Influence of plasma treatment on PA66 fiber topography. SEM micrographs of 1.05 s corona plasma-treated IF-PA66 (a) and W-PA66 (b) fabrics, and 3.5 s corona plasma-treated IF-PA66 (c) and W-PA66 (d) fabrics.....	176
Figure 55: SEM images for (a) untreated IF-PA66 fibers and (b) low pressure plasma-treated PA66 fibers at 100 W, 180 s, 10 L/min.....	177
Figure 56: SEM images for untreated (a) and plasma-treated IF-PA66 fabrics with various treatment times and gas flow conditions at 1.33 mbar pressure and 100 W power supply as fixed working parameters. Effect of 60 s (b) and 300 s (c) minutes plasma treatment time on fiber topography for 5 L/min gas flow rate and effect of 5 (d), 10 (e), 15 (f) L/min gas flow on PA66 topography for 180 s plasma treatment time.	177
Figure 57: Evolution of water absorption time of 3.5 s corona-plasma treated IF-PA66 fabrics as a function of storage time, during 9 days.	179
Figure 58: Ketoprofen impregnation for corona plasma-treated IF-PA66 for 1.75 s and 3.5 s plasma treatment. Weight of ketoprofen loaded in the IF-PA66 for 1 g of IF-PA66 fabric.	182
Figure 59: Accumulated ketoprofen release percentage from untreated, 1.75 s and 3.5 s corona plasma-treated IF-PA66 fabrics.....	183
Figure 60: Caffeine impregnation percentage for IF-PA66 and W-PA66 fabrics as a function of corona plasma treatment time.....	185
Figure 61: Proposed mechanism of PDMS layer reduction with the increase of gas flow in plasma treatment and its relationship with caffeine incorporation to the fibre.	187
Figure 62: Accumulated caffeine release percentage from W-PA66 (a) and IF-PA66 (b) fabrics. Influence of corona plasma treatment on caffeine release kinetics.* and ** indicate statistically significant differences.	188
Figure 63: Caffeine release percentages at the end of 8 hour release assay, for untreated, 1.75 s and 3.5 s corona plasma-treated IF-PA66 and W-PA66 fabrics, with details of the dominant plasma contribution.....	189
Figure 64: Global effects of the low pressure plasma treatment on the loading and the release of caffeine from the W-PA66 fibres.	196
Figure 65: Influence of (a) gas flow rate into the plasma chamber (samples treated for 180 s) and (b) plasma treatment time (samples treated under 5 L/min of gas flow) on the caffeine release kinetics from IF-PA66 fabrics (*indicates no significant differences at p < 0.05).	198
Figure 66: Caffeine (a), theobromine (b) and pentoxifylline (c) release percentage from W-PA66 fabrics. Influence of 3.5 s corona plasma treatment on the release kinetics of the methylxantine molecules.	201

Figure 67: Increase of release percentage between untreated and 3.5 s corona plasma treated W-PA66 for pentoxifylline, theobromine and caffeine as a function of the polar surface area of each methylxantine.	203
Figure 68: Profile shape of a 10 μ L H ₂ O droplet on the untreated (a), 0.35 s corona plasma-treated (b) and 30 s low pressure plasma-treated PP film for 30 L/min gas flow and 100 W power supply.	205
Figure 69: Water static contact angle as a function of the plasma treatment source and plasma treatment time. Comparison of corona plasma treatment (a) and low pressure plasma treatment at 30 L/min gas flow and 100 W power supply (b).	206
Figure 70: XPS general spectra of untreated (a), corona plasma-treated for 1.75 s (b) and 3.5 s (c), and low-pressure plasma treated PP meshes for 60 s with power supply and gas flow set at 100 W and 30 L/min respectively (d).	207
Figure 71: C _{1s} high-resolution XPS spectra of the untreated (a), corona plasma-treated (b, c) and low pressure plasma-treated (d) PP fabrics.	210
Figure 72: SEM images for untreated (a) and corona plasma-treated PP mesh for 1.75 s (b), 3.5 s (c) and 7.0 s (d).	211
Figure 73: AFM topography of untreated PP meshes (a), with 3D reconstitution image (b).	212
Figure 74: AFM topography with the corresponding 3D reconstitution images of 0.35 s (a, b), 1.75 s (c, d) and 3.5 s (e, f) corona plasma-treated PP meshes.	213
Figure 75: Roughness analysis of untreated (a) and corona plasma-treated PP meshes for 0.35 s (b), 1.75 s (c) and 3.5 s (d). Relative repartition of height of the analyzed surface from (600 \times 600) nm AFM pictures.	214
Figure 76: Scanning Electron Micrographs of untreated (a) and low pressure plasma-treated PP fabrics for 60 s, 100 W, 30 L/min (b).	216
Figure 77: AFM morphology of low pressure plasma-treated PP meshes for 60 s, 100 W and 30 L/min plasma conditions (a), with 3D reconstitution image (b).	216
Figure 78: Ampicillin impregnation percentage as function of the static contact angle of PP surface due to the corona plasma treatment.	218
Figure 79: Evolution of ampicillin impregnation percentage of the PP mesh with low pressure plasma treatment. Error bars in Table 27.	220
Figure 80: Ampicillin release percentage during the 4-hour release assay from untreated and corona-plasma treated PP meshes at different treatment times (a). Enlargement of the ampicillin release percentage during the first 15 minutes of the 4-hour release assay (b).	222
Figure 81: Maximum release percentage of ampicillin from corona plasma-treated PP meshes after 4-hour experiment.	223
Figure 82: Influence of the gas flow during the low-pressure plasma treatment on the ampicillin release percentage from the PP meshes. Release kinetics of the 4-hour release assay of the antibiotic for untreated PP mesh and low-pressure plasma-treated meshes for 10, 30 and 50 L/min (a), with the cumulative release percentage of ampicillin from the meshes at the end of the release experiment. Plasma treatment time set at 60 seconds and power supply at 100 W.	224
Figure 83: Influence of the low-pressure plasma treatment time on the ampicillin release percentage from the PP meshes at 30 s, 60 s and 180 s (a). Accumulated release percentage of ampicillin from the meshes at the end of the release experiment. Gas flow set at 10 L/min and power supply at 100 W.	225

Figure 84: Proposed interactions by H-bonds of ampicillin on the PP fibre surface for untreated PP (a) and plasma-treated PP meshes (b).	226
Figure 85: Concept beyond the PEG coating of the ampicillin-loaded PP meshes proposed in views of creating a retention membrane allowing slowing down the release kinetics of ampicillin from the fibres. Stages of the designed of the textile-based antibiotic delivery for untreated PP (a) and corona plasma-treated PP surgical meshes (b).	230
Figure 86: General XPS spectra of untreated PP mesh PEG-coated (a) and 3.5 s corona plasma-treated PP mesh PEG-coated (b).	231
Figure 87: Polyethylene glycol (PEG) chemical structure.....	231
Figure 88: C _{1s} high-resolution XPS spectra of the untreated (a) and 3.5 s corona plasma-treated (b) meshes PEG-coated for 1 hour plasma polymerization.....	233
Figure 89: Scanning Electron Micrographs of untreated PP mesh PEG-coated.	234
Figure 90: AFM pictures of PEG-coated untreated PP mesh with its 3D reconstitution for (600×600) nm (a)(b), with (600×600) nm enlargements (c)(d)	235
Figure 91: Scanning Electron Micrographs of PEG-coated 3.5 s corona plasma-treated PP mesh.	236
Figure 92: AFM pictures of 3.5 s corona plasma-treated PP mesh PEG-coated with its 3D reconstitution for (600×600) nm (a)(b), and (200×200) nm enlargements (c)(d).	236
Figure 93: Roughness analysis of PEG-coated untreated PP mesh (a) and PEG-coated 3.5 s corona plasma-treated PP mesh (b). Relative repartition of height of the analyzed surface from (600×600) nm AFM pictures.	237
Figure 94: Study of the stability of the ampicillin by UV-spectrophotometry. Comparison of the general spectra of ampicillin released from untreated PP mesh PEG-coated by plasma polymerization with those released from untreated PP mesh.	239
Figure 95: Ampicillin release percentage during the 4-hour release assay from untreated PP mesh and untreated PEG-coated PP mesh (a) with the enlargement of the ampicillin release percentage during the first 15 minutes of the release assay (b).....	240
Figure 96: Ampicillin release percentage during the 4-hour release assay from 3.5 s corona plasma-treated PP mesh and 3.5 corona plasma-treated PP mesh PEG-coated (a) with the enlargement of the ampicillin release percentage during the first 15 minutes of the release assay (b).....	241
Figure 97: Images of the inhibition area of ampicillin-loaded PP meshes <i>Staphylococcus Aureus</i> (a) and <i>E. Coli</i> (b).....	243
Figure 98: Inhibition areas for corona plasma-treated PP meshes loaded with ampicillin, tested for <i>Staphylococcus Aureus</i> . Influence of plasma treatment time and subsequent plasma polymerization.....	244
Figure 99: Inhibition areas for corona plasma-treated PP meshes loaded with ampicillin, tested for <i>EEscherichia Coli</i> . Influence of plasma treatment time and subsequent plasma polymerization.....	245
Figure 100: Inhibition areas for low pressure plasma-treated PP meshes loaded with ampicillin, tested for <i>Staphylococcus Aureus</i> . Influence of plasma treatment time (a) and gas flow in the reactor (b).....	246
Figure 101: Cell adhesion to the PP fibres for untreated (a) and corona plasma treated for 3.5 s (b) meshes previously loaded with ampicillin. PEG-coating of the respective meshes (c) (d)..	248

Figure 102: Effects of both (non- and polymerizing) plasma treatments on the antibiotic loading and the cell adhesion on the plasma-modified PP meshes.249

8.3. Index of tables

Table 1: Non-implantable medical textiles. Examples of non-implantable textiles, type of fiber and manufacture system (adapted from Bektaş, 2010).	34
Table 2: Benefits and limitations associated with cutaneous release.	41
Table 3: Implantable medical textiles. Examples of implantable textiles, type of fiber and manufacture system.	43
Table 4: Topical therapies for cellulite based on the proposed mechanism of action, from Hexsler, 2006.	60
Table 5: Classification of the active principles used with their corresponding textile fabrics as used in this PhD. Thesis.	130
Table 6: Experimental techniques used for the physical characterization and the surface chemistry analysis of the elastic-compressive PA66 fabrics knitted fabric and the PP mesh...	137
Table 7: Water static contact angle of corona plasma-treated PA66 fabrics.....	160
Table 8: Water absorption time of corona plasma-treated PA66 fabrics as a function of plasma treatment time.	161
Table 9: Absorption time (t_{abs}) of a 10 μ L water droplet (in seconds) of low pressure plasma-treated IF-PA66 as a function of plasma power supply. Plasma treatment time of 180 s and gas flow rate of 5 L/min.	163
Table 10: Absorption time (t_{abs}) of a 10 μ L water droplet (in seconds) of low pressure plasma-treated IF-PA66 as a function of plasma treatment time and gas flow rate (air). Power supply of 100 W.	164
Table 11: Surface elemental composition and atomic ratios of untreated and corona-plasma treated IF-PA66 fabrics.....	167
Table 12: Surface elemental composition and atomic ratios of of untreated and corona-plasma treated W-PA66 fabrics.	169
Table 13: Fraction of carbon functional groups from high-resolution C _{1s} XPS peaks of corona plasma treated IF-PA66 fabrics.....	170
Table 14: Fraction of carbon functional groups from high-resolution C _{1s} XPS peaks of corona plasma treated W-PA66 fabrics.	170
Table 15: Surface elemental composition and atomic ratios of low pressure plasma treated IF-PA66 as a function of gas flow.....	172
Table 16: Fraction of carbon functional groups from high-resolution C _{1s} XPS peaks.	173
Table 17: Caffeine impregnation percentage of untreated and low-pressure plasma-treated IF-PA66 fabrics as a function of the gas flow (air) and treatment time.	187
Table 18: Effect of low-pressure plasma treatment time on the release percentage of caffeine and the released quantity of caffeine from IF-PA66 and W-PA66 fabrics.	190
Table 19: Ritger-Peppas diffusion exponent and mechanism of diffusional release from various non-swellable controlled release systems.	193
Table 20: Impregnated and released caffeine (in mg) from 100 g of corona plasma treated PA66 fabrics.	195
Table 21: Methylxantine weight percentage for untreated and 3.5 s corona plasma-treated W-PA66 fabrics.	200

Table 22: Relevant properties of the methylxantines used for the release study.	202
Table 23: Surface elemental composition and atomic ratios of untreated and plasma-treated PP meshes.	208
Table 24: Fraction of carbon functional groups from high-resolution C _{1s} XPS peaks for untreated, corona plasma-treated and low-pressure plasma-treated PP meshes.	210
Table 25: Average (R_{rms}) and maximum roughness (R_{max}) of untreated and plasma-treated PP meshes, computed from (600×600) nm AFM images.....	215
Table 26: Evolution of ampicillin impregnation percentage of the PP meshes as a function of corona plasma treatment time. Power supply at 100 W.	217
Table 27: Evolution of ampicillin impregnation percentage of the PP mesh with low pressure plasma treatment. Influence of plasma treatment time and gas flow (air) inside the chamber. Power supply fixed at 100 W.....	220
Table 28: Comparison of the static contact angles of untreated and 3.5 s corona plasma-coated PP film PEG-coated with the uncoated ones.	230
Table 29: Surface elemental composition and atomic ratios of untreated and plasma-treated PP meshes PEG-coated.....	232
Table 30: Fraction of carbon functional groups from high-resolution C _{1s} XPS peaks for untreated and 3.5 s corona plasma-treated PP meshes PEG-coated for 1 hour plasma polymerization. .	233
Table 31: Average (R_{rms}) and maximum roughness (R_{max}) for PEG-coated untreated PP mesh and 3.5 s corona plasma-treated PP mesh from (600×600) nm images.	238

8.4. List of techniques used in this PhD. Thesis

- Drop test
- Goniometry: Static contact angle
- Scanning Electron Microscopy (SEM)
- Atomic Force Microscopy (AFM)
- X-rays Photoelectron Spectroscopy (XPS)
- Drug release experiments
- UV-visible spectrophotometry
- High-Pressure Liquid Chromatography (HPLC)
- Antibacterial assays

8.5. Glossary

Adhesion: Joining of two different materials.

Adsorption: Physical attachment of foreign material on a surface.

Anti-inflammatory: Substance or treatment that reduces inflammation. Anti-inflammatory drugs make up about half of analgesics, remedying pain by reducing inflammation as opposed to opioids, which affect the central nervous system.

Antibiotics: Types of medications that destroy or slow down the growth of bacteria and are used to treat infections caused by bacteria.

Antibiotic prophylaxis: Prevention of infection complications using antimicrobial therapy (most commonly antibiotics).

Atmospheric pressure plasmas: Typical atmospheric pressure plasma systems regroup corona discharges, dielectric barrier discharges (DBD) and plasma torches.

Biomaterial: Synthetic material used to replace part of living system or to function in intimate contact with living tissue (to improve its condition).

Biocompatibility: Acceptance of an artificial implant by the surrounding tissues and by the body as whole. Ability of a biomaterial to perform its designed function with respect to a medical therapy, without eliciting any undesirable local or systemic effects in the host body and generating the most appropriate beneficial cellular or tissue response and optimizing the clinical relevant performance of the therapy. The biomaterial must not be degraded by the body environment, and its presence must not harm tissues, organs, or systems. If the biomaterial is designed to be degraded, then the products of degradation should not harm the tissues and organs.

Burst release: Rapid release of drug.

Cellulite: Unsightly skin dimpling that is frequently found on the thighs and buttocks of women.

Cold plasmas: Cold plasmas are divided in thermal plasmas, which regroup arc plasmas or plasma torches, and non-thermal plasmas, which include laboratory plasmas such as corona plasma, glow discharge, dielectric barrier discharge, low-pressure plasmas, etc.

Contact angle (θ): Angle made when a drop of liquid spreads over a solid surface. It is governed by the balance of surface tension at various interfaces.

Corona plasma: Corona discharge is characterized by bright filaments extending from a sharp, due to the high-voltage between two electrodes towards the substrate.

Cosmetics: Care substances used to enhance the appearance or odor of the human body. They are generally mixtures of chemical compounds, some being derived from natural sources, many being synthetic.

Cosmetotextiles: A cosmetotextile is a textile containing a substance or preparation intended to be released permanently on different parts of the epidermis and claiming one (or several) special property(ies) such as cleaning, fragrance, change in appearance, protection, upkeep or correcting body odors.

Covalent bonding: Bonding of atoms or molecules by sharing valence electrons.

Cream: Semisolid dosage forms that contain one or more drug substances dissolved or dispersed in a suitable base. This term traditionally has been applied to semisolids that possess a relatively soft, spreadable consistency formulated as either water-in-oil or oil-in-water emulsions. However, more recently the term has been restricted to products consisting of oil-in-water emulsions or aqueous microcrystalline dispersions of long-chain fatty acids or alcohols that are water washable and more cosmetically and aesthetically acceptable.

Drug delivery system: A drug delivery system (DDS) is defined as a formulation or a device that enables the introduction of a therapeutic substance in the body and improves its efficacy and safety by controlling the rate, the time, and the place of release of drugs in the body. This process includes the administration of the therapeutic product, the release of the active ingredient, and the subsequent

transport of the active ingredients across the biological membranes to the site of action.

Elastic-compressive stockings: Specific compressive hosiery designed to prevent the occurrence of venous disorders in the leg region and guard against their further progression.

Etching (ablation): Action to remove material from a surface.

Fibres: Materials characterised by high ratio of length to thickness. Fibres can be natural or man-made.

Filament: Single strand of a natural or synthetic fibre.

FDA (Food and Drug Administration): Government agency regulating testing, production, and marketing of food and drugs including medical devices within the United States.

Foam: Emulsified systems packaged in pressurized containers or special dispensing devices that contain dispersed gas bubbles, usually in a liquid continuous phase, that when dispensed has a fluffy, semisolid consistency.

Gel: Semisolid systems consisting of either suspensions composed of small inorganic particles or large organic molecules interpenetrated by a liquid.

Hernia: Protrusion of an organ or the fascia of an organ through the wall of the cavity that normally contains it from within. As example, an abdominal hernia is a protrusion of the abdominal-cavity contents due to tissue that bulges out of a weak spot in the abdominal wall.

Infection: Invasion by and multiplication of pathogenic microorganisms in a bodily part or tissue, which may cause disease and produce subsequent tissue injury and progress to overt disease through a variety of cellular or toxic mechanisms. Infections are caused by infectious agents such as viruses, viroids, and prions, microorganisms such as bacteria, nematodes, arthropods, fungi, and other macroparasites.

Inguinal hernia repair: Surgical operation for the correction of an inguinal hernia.

Knitted fabric: Textile structure created by interlocking yarns by means of needles.

Laparoscopic hernia repair: Consists in a small cut (incision) made in or just below the navel. The abdomen is inflated with air so that the surgeon can see the abdominal organs. A thin, lighted scope called a laparoscope is inserted through the incision. The instruments to repair the hernia are inserted through other small incisions in the lower abdomen. Mesh is then placed over the defect to reinforce the abdominal wall.

Lotion: Although the term lotion may be applied to a solution, lotions usually are fluid, somewhat viscid emulsion dosage forms for external application to the skin. Lotions share many characteristics with creams.

Low pressure plasmas: Class of plasmas generated under atmospheric pressure.

Medical textiles (MEDTECHs): Textile products for medical applications and hygiene.

Mesh: Interlaced structure / material made of a network of wire or thread.

Nanotechnology: Branch of technology that deals with dimensions and tolerances of less than 100 nanometers.

Non-wovens: Fabrics made from webs of fibres held together and then bonded by some method.

Non-steroidal anti-inflammatory drugs (NSAIDs): Class of drugs that provides analgesic and antipyretic (fever-reducing) effects, and, in higher doses, anti-inflammatory effects. The term *nonsteroidal* distinguishes these drugs from steroids, which, among a broad range of other effects, have depressing effects.

Ointment: Ointments are semisolids intended for external application to the skin or mucous membranes. They usually contain less than 20% water and volatiles and more than 50% hydrocarbons, waxes, or polyols as the vehicle. Ointment bases recognized for use as vehicles fall into four general classes: hydrocarbon bases, absorption bases, water-removable bases, and water-soluble bases. Each therapeutic ointment possesses as its base one of these four general classes.

Open hernia surgery: Consists in a single long incision is made in the groin. If the hernia is bulging out of the abdominal wall (a direct hernia), the bulge is pushed back into place. If the hernia is going down the inguinal canal (indirect), the hernia sac is either pushed back or tied off and removed. After reducing the hernial sac into the abdominal cavity the defect is covered with a surgical mesh.

Plasma polymerization: Coating by plasma polymerization is defined as the formation of polymer materials, on a surface, under the influence of plasma conditions.

Polymer surface functionalization: Addition of chemical groups, small moieties, oligomers, and even other polymers (grafting copolymers) onto the surface or interface of a polymeric material.

Polypropylene fibres: Polypropylene (PP) is the generic name of fibres constituted by linear macromolecules of saturated alifatic hydrocarbons, in which one of every two atoms has a methyl ramification, usually in isotactic configuration $(-\text{CH}_2-\text{CH}(\text{CH}_3)-)_n$.

Polyamide fibres (nylon): Chemical fibres formed from a polymer of synthetic linear macromolecules in which the chain is a succession of amide groups, with a minimum of 85% of them linked to alifatic or cycloalifatic groups.

Powders: Solids or mixture of solids in a dry, finely divided state for external (or internal) use.

Pressure: Ratio of force to the area over which that force is distributed. (1 Pa = 0.01 mbar).

Repeating unit: Basic molecular unit that can represent a polymer backbone chain. The average number of repeating unit is called the degree of polymerization.

Route of administration: The path by which a substance / a drug may be administered into the body, such as intradermally, intrathecally, intramuscularly, intranasally, intravenously, orally, rectally, subcutaneously, sublingually, topically, or vaginally.

Spark: Refers to the luminous phenomenon resulting from a disruptive discharge through an insulating material or to the discharge itself.

Spray: Products formed by the generation of droplets of solution containing dissolved drug for application to the skin or mucous membranes. The droplets may be formed in a variety of ways but generally result from forcing the liquid through a specially designed nozzle assembly.

Stratum corneum: The stratum corneum is the outermost layer of skin that forms the main barrier for diffusion of the permeants through the skin.

Surface tension (surface energy): Amount of free energy exhibited at the surface of a material.

Surface activation: Modification of the surface of a polymer by attaching polar or functional groups to it.

Surface roughness: The roughness is a measure of the texture of a surface. It is quantified by the vertical deviations of a real surface from its ideal form. If these deviations are large, the surface is rough; if they are small the surface is smooth.

Suture: Material used in closing a wound with stitches.

Topical drug delivery (or topical application): Topical drug delivery is the term used for localized treatment of dermatological condition where the medication is not targeted for systemic delivery.

Topical aerosols: Products that are packaged under pressure. The active ingredients are released in the form of fine liquid droplets or fine powder particles upon activation of an appropriate valve system. A special form is a metered-dose aerosol that delivers an exact volume (dose) per each actuation.

Topical solutions: Liquid preparations, that usually are aqueous but often contain other solvents such as alcohol and polyols that contain one or more dissolved chemical substances intended for topical application to the skin.

Topical suspensions: Liquid preparations that contain solid particles dispersed in a liquid vehicle intended for application to the skin.

Transdermal drug delivery (or transdermal administration): Transdermal delivery is the term that is confined to a situation in which the drug diffuses through different layers of the skin into systemic circulation to elicit the therapeutic response.

Transdermal delivery system: Transdermal delivery systems (TDS) are self-contained, discrete dosage forms that, when applied to intact skin, are designed to deliver the drug(s) through the skin to the systemic circulation. Systems typically comprise an outer covering (barrier), a drug reservoir that may have a drug release–controlling membrane, a contact adhesive applied to some or all parts of the system and the system/skin interface, and a protective liner that is removed before the patient applies the system. The dose of these systems is defined in terms of the release rate of the drug(s) from the system and surface area of the patch and is expressed as mass per unit time for a given surface area. With these drug products, the skin typically is the rate-controlling membrane for the drug input into the body. The total duration of drug release from the system and system surface area may also be stated.

Wound dressings: Any material used for covering and protecting a wound.

Wound healing: Intricate process whereby the skin (or another organ-tissue) repairs itself after injury.

Woven fabrics: Fabrics that consist of two sets of threads, the warp and weft, which are interlaced at right angles to each other.